Investigation into the relationship between PARPs in DNA repair and synthetic lethality with homologous recombination deficiency

George Ronson

Exeter College

A thesis submitted for the award of D.Phil in Chromosome and Developmental Biology

Trinity term 2017

42,377 words

Abstract

The genome of each cell is under constant threat from various forms of DNA damage. In order to protect themselves from this danger, cells possess a number of pathways able to resolve DNA lesions. The addition of poly(ADP-ribose) is a post-translational modification produced by attaching successive ADP-ribose moieties to a protein acceptor, forming long chains. Enzymes called poly(ADP-ribose) polymerases (PARPs) catalyse the production of these modifications, and a number of different PARPs have been linked to the process of DNA repair, including PARP1, PARP2 and PARP3. How these enzymes might function together to facilitate the repair of different lesions is unclear. Furthermore, inhibitors that target these enzymes are in clinical use for their ability to kill homologous recombination deficient tumour cells, through a mechanism of synthetic lethality. Which subset of PARPs is necessary to inhibit to achieve maximum efficacy of these agents has not been assessed.

I use genome editing to generate cells disrupted for these PARPs in different combinations. Whilst loss of PARP1 compromises cellular tolerance to homologous recombination deficiency, this is independent of the status of PARP2 and PARP3, indicating the development of PARP1-specific inhibitors may hold therapeutic potential. In contrast to these observations, I uncover strong redundancy between PARP1 and PARP2 in the repair of damaged DNA bases through the base excision repair (BER) pathway. I also identify BER-independent roles of both PARP1 and PARP2 in resolving replication forks that have collided with BER-intermediates, through promoting the stability of Rad51

nucleofilaments via an Fbh1-dependent mechanism. Thus PARP1 and PARP2 perform two closely-linked functions in response to cellular base damage; promoting resolution of these lesions directly through BER, and stabilising replication forks which have encountered BER intermediates.

Acknowledgements

Firstly, I would like to thank my supervisor, Nick Lakin, for his help and guidance throughout my time in his laboratory. I would also like to thank others who have contributed to the work within this thesis; Peter McHugh, Anna Olsen, George Driscoll, Daniel Ebner and Stephanie Hatch. Without their efforts, the completion of this work would not have been possible. I also wish to thank Catherine Pears for her suggestions and patience during lab meetings. I am also indebted to the Wellcome Trust, and the Chromosome and Developmental Biology programme, for giving me the opportunity to study in Oxford.

I also owe thanks to my lab-mates, for their discussions and suggestions regarding scientific matters, but also their support, friendship and humour. Special thanks go to Alasdair Gunn, Lena Kolb, Florian Zobel, Fusheng Chang, Anna Montnenko and Li-Yao Huang. I would also like to acknowledge my Wellcome Trust course-mates, James Holder, Ben Kroeger, Anne Tuberfield and Tomek Dobrzycki, for making our time together on the programme so enjoyable.

I am also grateful to my family; to my parents, brother and sister for their love, support and encouragement during my studies. Finally, and most of all, I would like to thank Sophie. You have been there through every tough day, late night or failed experiment. Words cannot express how grateful and lucky I feel for having been able to share this journey with you.

Abbreviations

Alt-NHEJ – Alternative non-homologous end joining

ARTD – ADP-ribosyltransferase

BER – Base excision repair

BIR – Break Induced Replication

BRCT – BRCA1 C terminus

c-NHEJ – Classical non-homologous end joining

CRISPR – Clustered regularly-interspaced short palindromic repeats

DDR – DNA damage response

D-loop – Displacement loop

dNTP – Deoxynucleoside triphosphate

DSB – Double strand break

DSBR – Double strand break repair

EdU - 5-ethynyl-2’-deoxyuridine

EMA – European Medicines Agency

ER – Endoplasmic reticulum

FDA – Food and Drug Administration

gRNA – Guide RNA

HD – Helical subdomain

HR – Homologous recombination

HU – Hydroxyurea

MAR – Mono(ADP-ribose)

MMS – Methyl methanesulfonate

MRN – Mre11/Rad50/Nbs1

NAD^+ - Nicotinamide adenine dinucleotide

NHEJ – Non-homologous end joining

PAR – Poly(ADP-ribose)

PARG – Poly(ADP-ribose) glycohydrolase

PARP – Poly(ADP-ribose) polymerase

PARPi – PARP inhibitor

Pgp – P-glycoprotein 1

PIKK – Phosphatidylinositol 3-kinase-related kinase

PRR – Post-replication repair

PTM – Post-translational modification

ROS – Reactive oxygen species

RPA – Replication protein A

SDSA – Synthesis-dependent strand annealing

dHJ – Double Holliday junction

siRNA – Short interfering RNA

SSA – Single-strand annealing

SSB – Single strand break

SSBR – Single strand break repair

TLS – Translesion synthesis

UPR – Unfolded protein response

UV – Ultraviolet

Contents

Abstract i
Acknowledgements iii
Abbreviations iv
1. Introduction 1
1.1 PARPs and ADP-ribosylation 1
1.1.1 Signalling pathways and post-translational modifications 1
1.1.2 Enzymatic activity of PARPs 2
1.1.3 The PARP superfamily 3
1.1.4 Catalytic mechanism of PARPs 7
1.1.5 Activation of DNA-dependent PARPs 9
1.1.6 Turnover of ADP-ribose 10
1.2 PARPs and the DNA damage response 11
1.3 Repair of base damage and DNA SSBs 12
1.3.1 Sources of DNA SSBs 12
1.3.2 BER-processed SSBs 12
1.3.3 SSB repair 13
1.3.4 Roles of PARPs in SSBR 16
1.4 Repair of DNA DSBs 19
1.4.1 Sources of DNA DSBs 19
1.4.2 DNA DSBR pathways 20
1.4.3 Non-homologous end joining 20
1.4.4 Roles of PARPs in non-homologous end joining 23
1.4.5 Homologous recombination 24
1.4.6 Roles of PARPs in homologous recombination 29
1.4.7 Alternative-NHEJ 30
1.4.8 Roles of PARPs in alternative-NHEJ 32
1.5 Cellular response to replication stress 32
1.5.1 Sources of replication stress 32
1.5.2 Tolerance and resolution of replication stress 33
1.5.3 Roles of PARPs in the cellular response to replication stress 36
1.6 The synthetic lethal relationship between PARPs and HR 38
1.6.1 Discovery of synthetic lethality and mechanistic models 38
1.6.2 Mechanisms of resistance to PARPi 41

1.6.3 Specificity and further uses of PARPi 42
1.7 Aims 42
2. Materials and Methods 44
2.1 Materials 44
2.1.1 Buffers 44
2.2 Methods 47
2.2.1 Cell culture and generation of CRISPR-mediated parpΔ cells 47
2.2.2 Protein extract preparation and Western blotting 49
2.2.3 Clonogenic survival assays 51
2.2.4 Immunofluorescence 52
2.2.5 Alkaline comet assays 53
2.2.6 Screen to identify novel DDR factors that display a synthetic lethal relationship with PARP loss 53
2.2.7 Statistical analysis 54
3. Generation and characterisation of cell lines disrupted for DNA-dependent PARPs 55
3.1 Introduction 55
3.1.1 PARP1, PARP2 and PARP3 function in the DNA damage response 55
3.1.2 Additional members of the PARP superfamily function in the DNA damage response 56
3.1.3 Aims 58
3.2 Results 58
3.2.1 Generation and verification of parp1Δ, parp2Δ and parp3Δ cell lines 58
3.2.2 DNA damage sensitivity profiles of parp1Δ, parp2Δ and parp3Δ cell lines 65
3.2.3 Additional PARP(s) function in the absence of PARP1 in response to MMS 66
3.2.4 PARP1 and PARP2 share overlapping roles in response to base damage 68
3.2.5 PARP1 and PARP2 are redundant for their contribution to BER strand ligation rates 73
3.2.6 Redundancy between PARP1 and PARP2 does not extend to H_2O_2-induced SSBs 75
3.2.7 Loss of PARP3 does not affect cellular survival to MMS exposure 75
3.2.8 Understanding the contribution of the PARP superfamily to the cellular response to MMS in the absence of PARP1 and PARP2 81
3.3 Discussion 86
4. Understanding the roles of PARP1 and PARP2 in MMS-induced replication-associated damage 92
4.1 Introduction 92

4.1.1 Differences in the relationship between PARP1 and PARP2 in BER and SSBR 92
4.1.2 MMS-induced base methylations lead to an accumulation of S-phase associated damage 93
4.1.3 PARPs have been implicated in the resolution of replication-associated damage in other contexts 94
4.1.4 Aims 95
4.2 Results 96
4.2.1 MMS induces γH2AX phosphorylation in actively replicating cells 96
4.2.2 Resolution of MMS-induced γH2AX foci is compromised in the absence of PARP1 and PARP2 98
4.2.3 HR is engaged in response to MMS in U2OS cells 102
4.2.4 In the absence of PARP1 and PARP2, Rad51 nucleofilament formation is compromised 105
4.3 Discussion 109
5. PARP1 and PARP2 regulate Rad51 nucleofilament stability through an Fbh1-dependent mechanism 114
5.1 Introduction 114
5.1.1 Rad51 is a key player in the cellular response to replication stress 114
5.1.2 Regulation of homologous recombination and Rad51 filament assembly 115
5.1.3 Aims 117
5.2 Results 118
5.2.1 Resection is not compromised in the absence of PARP1 and PARP2 118
5.2.2 Recruitment of the BRCA2-PALB2 complex to chromatin after MMS exposure is not compromised by inhibition of PARP1 and PARP2 122
5.2.3 Rad52 does not contribute to the resolution of S-phase associated damage after MMS exposure 122
5.2.4 Depletion of Fbh1, but not BLM, is able to rescue Rad51 foci formation in parp1Δparp2Δ cells 126
5.3 Discussion 128
6. Understanding the roles of specific PARPs in the synthetic lethal relationship with HR disruption 136
6.1 Introduction 136
6.1.1 Multiple mechanisms have been proposed to explain the toxicity of PARP inhibitors to HR deficient cells 136
6.1.2 Efforts to expand the use of clinical PARPi beyond BRCA mutant breast and ovarian cancers 137
6.1.3 Aims 139
6.2 Results 139

6.2.1 Rad51 inhibitors can be used to chemically recapitulate synthetic lethality between PARPs and HR 139
6.2.2 Loss of PARP1 is the key driver of synthetic lethality with HR dysfunction 142
6.2.3 Synthetic lethality is not wholly driven by PARP trapping or disruption of SSBR or Rad52-depedndant repair pathways 145
6.2.4 A targeted screen of DDR factors to identify novel determinants of synthetic lethality with PARP loss 149
..... 150
6.2.5 Identification of novel factors that possess a synthetic lethal relationship with loss of PARP1 and/or PARP2 151
6.3 Discussion 153
7. General Discussion 164
8. References 175
9. Appendices 200
9.1 Oligonucleotide Sequences 200
9.1.1 gRNA sequences 200
9.1.2 PCR primer sequences 200
9.2 siRNA screen dataset 200

1. Introduction

1.1 PARPs and ADP-ribosylation

1.1.1 Signalling pathways and post-translational modifications

Cells must constantly respond and adapt to changes in their external environment or internal conditions. This is achieved through a range of signalling pathways, which communicate these changes within the cell and bring about an appropriate response. Post-translational modification (PTM), which involves chemically altering proteins after synthesis, lies at the heart of these signalling pathways. The rapidly reversible nature of these modifications, combined with their ability to fundamentally alter the structure and function of proteins, facilitates the effective and dynamic cellular response to stress. PTMs can take numerous forms, including phosphorylation, ubiquitination, acetylation and ADP-ribosylation. The addition of these PTMs is normally achieved by certain enzymes; in the case of ADP-ribosylation, this is performed by poly(ADP-ribose) polymerases (PARPs).

One variety of cellular stress is the formation and accumulation of DNA damage. If these lesions are not repaired in a timely fashion, they can cause mutations and genomic instability, which in turn can assist the development of cancer, or cause cell death (Jackson and Bartek, 2009). In order to protect themselves from these outcomes, cells have developed a network of pathways which facilitate the resolution of this DNA damage, collectively known as the DNA damage response (DDR). Whilst a wide variety of PTMs have been

identified to participate in these pathways, the focus of this thesis will be on the roles of PARPs in the DDR.

1.1.2 Enzymatic activity of PARPs

PARPs, also known as ADP-ribosyltransferases (ARTDs), are able to catalyse ADP-ribosylation reactions. They use NAD^+ as a substrate to add one or more ADP-ribose units to an acceptor, with the production of free nicotinamide. This acceptor is often a protein, although there are examples of modification of other biomolecules, for example the direct ADP-ribosylation of DNA (Jankevicius et al., 2016; Nakano et al., 2014). ADP-ribosylation can take the form of mono(ADP-ribose) (MAR), where a single ADP-ribose moiety is transferred to an acceptor, or poly(ADP-ribose) (PAR), where multiple ADP-ribose units are successively added to form linear or branched chains of up to 200 units in length (Alvarez-Gonzalez and Jacobson, 1987). Whilst some PARP enzymes can produce PAR, others are limited to the addition of MAR to their substrates (Vyas et al., 2014).

Numerous amino acid residues have been suggested to be able to accept ADP-ribose, including aspartic acid, glutamic acid (Zhang et al., 2013), lysine (Altmeyer et al., 2009), cysteine (Vyas et al., 2014) and serine (Bonfiglio et al., 2017). A clear consensus over which acceptors are most important *in vivo* is yet to emerge, but recent advances have highlighted the potential importance of serine ADP-ribosylation. This has centred around the discovery of the factor HPF1, which is able to bind PARP1 and PARP2 and modify their substrate specificity, as well as promote the modification of target serines (Bonfiglio et al., 2017; Gibbs-Seymour et al., 2016).

1.1.3 The PARP superfamily

In humans, there are presently seventeen members of the PARP superfamily, all of which possess a conserved PARP C-terminal catalytic domain (Figure 1.1). In contrast, the N-terminal domains of these PARPs are far more divergent, encoding a varied set of domains (Hottiger et al., 2010).

The best studied member of the superfamily is PARP1, which is capable of producing poly(ADP-ribose) chains, and has been implicated in diverse cellular processes including DNA repair, transcription, RNA processing, metabolism and telomere maintenance (Ambrose et al., 2009; Bai et al., 2011a; Erener et al., 2012; Gamble and Fisher, 2007; Di Giammartino et al., 2013; Gomez et al., 2006; Guetg et al., 2012; Ji and Tulin, 2009; Kotova et al., 2009; Masutani et al., 2000a; Ogino et al., 2007; Simbulan-Rosenthal et al., 2000). Consistent with its role as a sensor of DNA damage, PARP1 possess N-terminal zinc finger domains which can specifically bind to damaged DNA structures (Ikejima et al., 1990), as well as a BRCT domain, a catalytic domain and a WGR domain which is important in DNA-dependent PARP1 activation.

PARP2 is also capable of catalysing the formation of poly(ADP-ribose), and has also been implicated in DNA repair, along with other functions in the centromere, at telomeres and in metabolism (Amé et al., 1999; Bai et al., 2011b; Dantzer et al., 2004, 2006; Saxena et al., 2002; Szántó et al., 2014). PARP2 has a shorter N-terminus, which possesses the ability to bind certain damaged DNA structures, despite not containing any canonical DNA binding domains (Langelier et al., 2014). PARP3 has also been implicated in the DDR (Beck et al., 2014; Rulten et al., 2011), and can recognise damaged DNA

through its short N-terminus (Langelier et al., 2014). In contrast to PARP1 and PARP2, PARP3 catalyses the addition of mono(ADP-ribose) to its targets (Vyas et al., 2014).

PARP1, PARP2 and PARP3 make up the subclass of DNA-dependent PARPs, whose activity depends on binding to particular DNA structures. A number of other PARPs can be grouped into subclasses, whilst others are distinct and do not fit into any particular class. There are three members of the macroPARP subclass; PARP9, PARP14 and PARP15, so categorised due to the presence of a macrodomain in their N-terminus. They are all encoded on a 200 Kbp portion of chromosome 3, suggesting they may be co-ordinately regulated (Aguiar et al., 2005). Two of these macroPARPs have functions in DNA repair pathways; PARP9, which is catalytically inactive, and PARP14, which possesses mono(ADP-ribosyl)transferase activity (Nicolae et al., 2015; Yan et al., 2013). In contrast the third member of the subclass, PARP15, may have roles in transcriptional regulation (Aguiar et al., 2005).

A second subclass is the CCCH-PARPs, made up of PARP7, PARP12 and PARP13, all of which possess CCCH-type zinc fingers in their N-terminus. The catalytically inactive PARP13 has antiviral roles (Gao et al., 2002), and is able to bind viral RNA through its four zinc fingers (Chen et al., 2012a). It supports resistance to infection by a range of viruses by promoting the degradation of viral RNA through decapping and poly(A) tail shortening (Bick et al., 2003; Müller et al., 2007; Zhu et al., 2011b). PARP12 is closely related to PARP13 and may also have antiviral functions (Atasheva et al., 2012), although it co-localises with golgi markers (Vyas et al., 2013). In contrast, PARP7, or tiPARP (Ma et al., 2001), has roles in the arylhydrocarbon receptor signalling pathway

(MacPherson et al., 2013), and its expression is induced by progesterone receptor (Wright et al., 2012) and androgen receptor (Bolton et al., 2007) signalling.

PARP5a and PARP5b, or Tankyrase1 and 2, make up the tankyrase subclass of PARPs. These are the other PARPs capable of producing poly(ADP-ribose), and have roles in telomere maintenance, mitotic segregation and Wnt signalling (Chang et al., 2005a, 2005b; Cook et al., 2002; Smith et al., 1998; Yang et al., 2016).

The remaining PARPs do not fit into any particular subclass, and have diverse cellular functions. PARP4, also known as vPARP, is a component of vault particles (Kickhoefer et al., 1999), large ribonucleoprotein particles whose exact functions are poorly defined. The mono(ADP-ribosyl)transferase PARP10 functions in DNA repair by binding PCNA and facilitating translesion synthesis (Nicolae et al., 2014). PARP16 contains a transmembrane domain, and localises to the endoplasmic reticulum (ER) (Di Paola et al., 2012; Vyas et al., 2013) where it functions in the unfolded protein response (UPR). It is activated by ER-stress, and modifies and activates the key kinases PERK and IRE1α involved in the UPR (Jwa and Chang, 2012). PARP6 has been shown to negatively regulate cellular proliferation (Tuncel et al., 2012). Whilst PARP11 localises to centrosomes, PARP8 accumulates at both centrosomes and the nuclear envelope (Vyas et al., 2013), but the precise roles of these PARPs remain unknown. Overall, the PARP superfamily possesses diverse roles in a multitude of cellular processes, many of which are still coming to light.

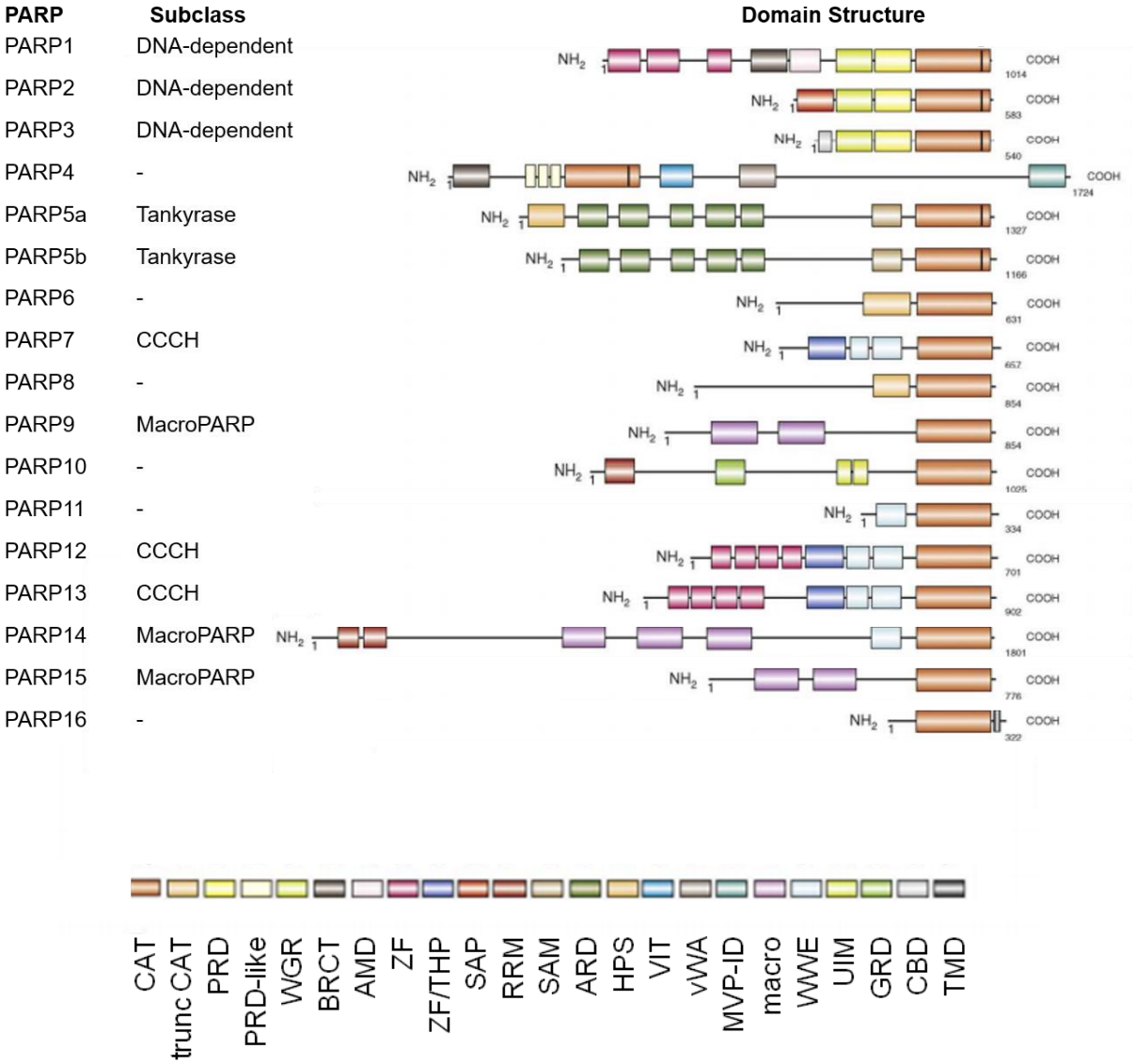


Figure 1.1: Domain configurations of the 17 members of the PARP superfamily. The CAT domain is the core catalytic PARP domain. The PARP regulatory domain (PRD) helps control catalytic activity. The WGR domain has a core W-G-R motif. The BRCT domain can bind phospho-proteins. The ZF domain is a zinc finger domain. The SAF/Acinus/PIAS-DNA-binding domain (SAP) is able to mediate DNA binding. The RRM is the RNA Recognition Motif. The Sterile Alpha Motif (SAM) can mediate protein dimerisation. The ankyrin repeat domains (ARD) also mediate protein-protein interactions. The Histidine-Proline-Serine (HPS) region contains homopolymeric runs of these amino acids. The vault protein inter-alpha-trypsin (VIT) and von Willebrand type A (vWA) domains mediate protein-protein interactions. The MVP-ID is the major-vault particle interaction domain. The macro domain is a module able to bind to ADP-ribose. The WWE domain is able to mediate specific protein-protein interactions. The UIM is the ubiquitin interaction motif. The GRD is a glycine-rich domain. The TMD is a transmembrane domain. Adapted from Hottiger et al 2010.

1.1.4 Catalytic mechanism of PARPs

All PARPs possess a PARP catalytic domain, which in PARP1 is made up of a donor site that binds the NAD^+ and an acceptor site that binds the protein or ADP-ribose chain to which the new ADP-ribose moiety will be attached (Figure 1.2). The donor site contains a conserved H-Y-E triad first identified in the Diphtheria Toxin ADP-ribosyltransferase (Bell and Eisenberg, 1996). Crystal structures show the side chains of these residues contact the NAD^+ within the active site, and their presence is important for catalysis. Human PARPs can be separated into those which contain a complete H-Y-E triad (PARP1, 2, 3, 4, 5a and 5b), and those that contain a variant third amino acid, either H-Y-I (PARP6, 7, 8, 10, 11, 12), H-Y-L (PARP14, 15) or H-Y-Y (PARP16) (Otto et al. 2005, Figure 1.3). The glutamate within the triad has been postulated to mediate elongation of ADP-ribose chains (Marsischky et al., 1995; Rolli et al., 1997), as it forms hydrogen bonds with the acceptor on the ADP-ribose chain, as well as with the donor NAD^+ (Ruf et al., 1996). These interactions polarise both positions, allowing nucelophillic attack of the acceptor onto the NAD^+ via an S_N2 reaction (Marsischky et al., 1995). The acidic residues able to accept ADP-ribose modifications are intrinsically polar, so may not need this glutamate interaction in order to act as nucleophiles (Kleine et al., 2008). This can potentially explain why PARP1, 2, 5a and 5b, all of which contain the glutamate within the H-Y-E triad, are able to form poly(ADP-ribose) chains. In contrast, all the PARPs lacking this glutamate have been identified to catalyse the addition of mono(ADP-ribose). However, the fact that PARP3 and PARP4 have been shown to possess only mono(ADP-

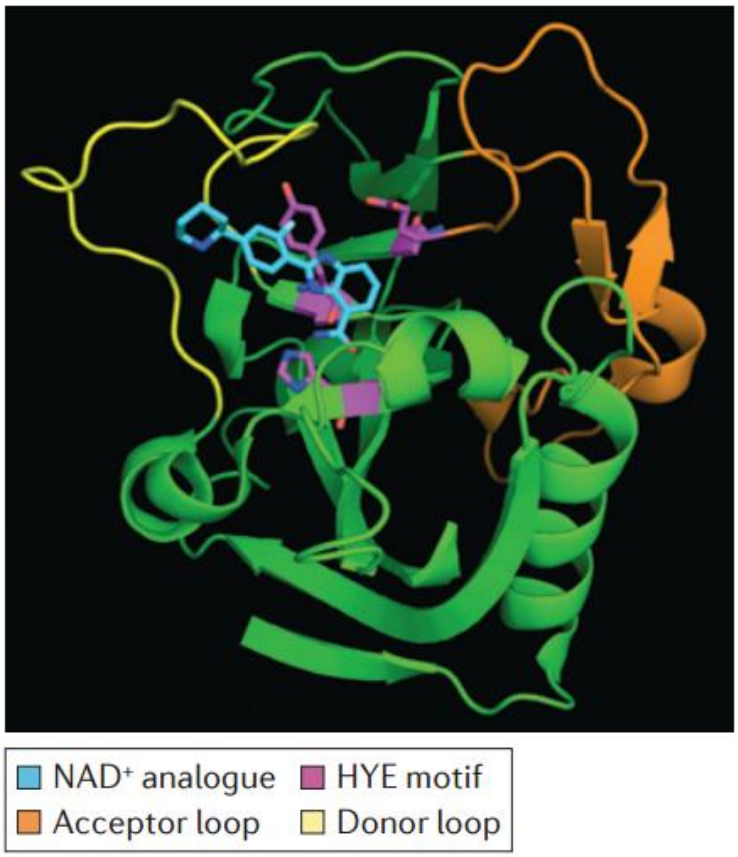


Figure 1.2: The crystal structure of the PARP1 catalytic domain, showing the key structural features (PDB ID: 3L3M). The acceptor loop is shown in orange and donor loop is shown in yellow. The H-Y-E catalytic triad is shown in purple. The co-crystallised NAD^+ analogue (A927929) is shown in blue. Adapted from Vyas and Chang 2014.

ribosyl)ation activity whilst possessing an intact H-Y-E triad indicates additional determinants of poly(ADP-ribosyl)ation likely exist, and these have been suggested to reside within the D-loop of the catalytic domain (Vyas et al., 2014).

It should be noted that two human PARPs harbour additional substitutions in the triad, either Q-Y-T (PARP9) or Y-Y-V (PARP13). Consistent with predictions that these mutations would disrupt the ability to bind NAD^+, no auto-modification activity can be detected for these proteins, indicating they are catalytically inactive (Vyas et al., 2014).

1.1.5 Activation of DNA-dependent PARPs

The mechanism of DNA-dependent activation of PARP1 has been elucidated through crystal structures of the minimal domains required for PARP activation bound to a DNA double strand break (DSB) (Langelier et al., 2012). The key domains involved are the zinc fingers Zn1 and Zn3, the WGR domain and the catalytic domain with its associated helical subdomain (HD). The Zn1, Zn3 and WGR domains directly contact the DNA, largely binding the DNA backbone, termini and exposed bases characteristic of DNA DSBs. Upon binding to DNA, conformational changes in these domains alter their interactions with the adjacent HD, causing it to distort as compared to structures of isolated catalytic domain. These distortions disrupt the hydrophobic core of the HD, destabilising it, and it is thought this destabilisation is the key to catalytic activation. Indeed, the introduction of mutations that decrease the stability of the HD are able to amplify DNA-independent ADP-ribosylation activity of PARP1. Whilst this distortion of the HD domain does not appear to influence NAD^+ or substrate

binding, it has been suggested to accelerate ADP-ribosylation activity through increasing protein dynamics of the catalytic domain.

Interestingly, PARP2 and PARP3 have very similar mechanisms of activation to PARP1, where upon binding damaged DNA, alterations in interdomain contacts lead to a destabilisation of the HD, ultimately resulting in an increase in ADP-ribosylation activity (Langelier et al., 2014). In contrast to PARP1, the short N-termini of PARP2 and PARP3 are not strictly required for DNA-dependent activation. Instead, both PARP2 and PARP3 rely heavily on their WGR domains for DNA binding and communication with the HD.

1.1.6 Turnover of ADP-ribose

Cellular ADP-ribosylation is a rapidly produced but transient signal; for example after DNA damage, PAR can be detected within seconds, and is quickly removed following resolution of the lesions (Alvarez-Gonzalez and Althaus, 1989). This necessitates factors capable of removing PAR and MAR from modified proteins, collectively called ADP-ribosyl hydrolases. Several such enzymes have been identified in humans, named PARG, ARH3, TARG1 and MACROD1/2. All contain a macrodomain fold, present in some proteins simply as a PAR-binding domain, but in these enzymes this motif also possesses ADP-ribosyl hydrolase activity.

The PARG macrodomain contains an additional PARG unique catalytic loop, bearing the key amino acids for ADP-ribosyl hydrolysis (Dunstan et al., 2012; Slade et al., 2011; Tucker et al., 2012). PARG is able to hydrolyse the glycosidic bonds between ADP-ribose moieties, but not those between the acceptor and first ADP-ribose unit, meaning PARG can essentially convert PAR

into MAR (Hatakeyama et al., 1986). The inability of PARG to remove terminal mono(ADP-ribose) may be due to steric hindrance encountered between the macro domain and terminal ADP-ribose. ARH3 is structurally unrelated to PARG but is also able to degrade poly(ADP-ribose) chains through an Mg^{2+}-dependent mechanism (Mueller-Dieckmann et al., 2006; Oka et al., 2006). TARG1and macroD1/2 are both able to remove mono(ADP-ribose) modifications from proteins, but utilise distinct catalytic mechanisms from both PARG and each other (Chen et al., 2011; Jankevicius et al., 2013; Peterson et al., 2011; Rosenthal et al., 2013; Sharifi et al., 2013). The importance of PAR turnover to cellular survival is highlighted by the fact disruption of the PARG gene results in accumulation of PAR and early embryonic lethality through apoptosis (Koh et al., 2004). Furthermore, depletion of PARG can potentiate the effects of DNA damaging agents (Zhou et al., 2010) and complicate DNA replication (Ray Chaudhuri et al., 2015).

1.2 PARPs and the DNA damage response

The genome is under constant assault from both endogenous and exogenous sources of DNA damage. This can result in a wide variety of lesions, including strand breaks, intra- and inter-strand crosslinks, chemical modifications and mismatched base pairs. A general theme of failing to resolve these forms of damage is genome instability, and ultimately tumorigenesis or cell death. Therefore cells have developed a diverse set of repair pathways to deal the different forms of DNA damage that can occur. These include single strand break repair (SSBR), double strand break repair (DSBR), inter-strand crosslink repair, base excision repair (BER), nucleotide excision repair and mismatch

repair. Numerous PARPs have been identified to function in a range of these repair pathways. I will discuss a number of repair pathways relevant to this thesis, and consider the current understanding of how PARPs influence these processes.

1.3 Repair of base damage and DNA SSBs

1.3.1 Sources of DNA SSBs

DNA single strand breaks (SSBs) are one of the most common lesions encountered by cells. These can arise directly, for example through cleavage of one strand of the DNA backbone by reactive oxygen species (ROS) or γ-irradiation (Pogozelski and Tullius, 1998). Alternatively, they can be produced during the normal functioning of the base excision repair pathway, which acts to resolve a diverse array of chemically modified DNA bases. This includes oxidised bases, for example 8-oxo-guanine, alkylated bases, for example 3-methyl-adenine, and deaminated bases, for example hypoxanthine.

1.3.2 BER-processed SSBs

SSBs can be generated from chemically damaged bases through a series of enzymatic reactions within the BER pathway. BER is able to recognise and repair a wide range of damaged bases. Enzymes called glycosylases are the sensors of the damaged bases and an array of different glycosylases exist to recognise diverse forms of base damage. For example, the enzyme OGG1 (Radicella et al., 1997) can recognise 8-oxoG, UNG2 can recognise uracil within DNA (Slupphaug et al., 1995) and MPG can recognise multiple base

methylations (O'Brien and Ellenberger, 2004), including 3meA, 7meG and 3meG.

BER glycosylases can be categorised into two distinct classes; the monofunctional enzymes that possess solely glycosylase activity, converting the damaged base to an abasic (AP) site, or the bifunctional enzymes that possess both glycosylase and lyase activity, and are able to cleave the DNA backbone after AP site generation. Monofunctional glycosylases include UNG2 and MPG, whereas OGG1 is an example of a bifunctional enzyme (Bjorâs et al., 1997). AP sites generated by monofunctional glycosylases are then cleaved by the nuclease APE-1 to generate a nick 5' of the site (Marenstein et al., 2004; Mol et al., 2000; Wilson et al., 1995). At this point, these BER-processed SSBs are resolved in a similar manner to spontaneous SSBs (Figure 1.3).

1.3.3 SSB repair

PARP1 is the major sensor for SSBs, both those that arise by direct breakage of the DNA backbone and those that are produced through the action of BER. PARP1 can bind to, and become activated by DNA SSBs, allowing it to ADP-ribosylate itself and other proteins, including histones, at the break. The long, branched ADP-ribose chains have two functions – firstly to relax chromatin at the site of the break in order to facilitate repair, and secondly to act as a scaffold for the recruitment of further repair proteins to the break. One such protein is XRCC1, a key SSBR protein that is able to bind to PAR, and is recruited to SSBs through its PAR-binding BRCT1 domain (Breslin et al., 2015; El-Khamisy et al., 2003; Hanzlikova et al., 2016; Masson et al., 1998). XRCC1

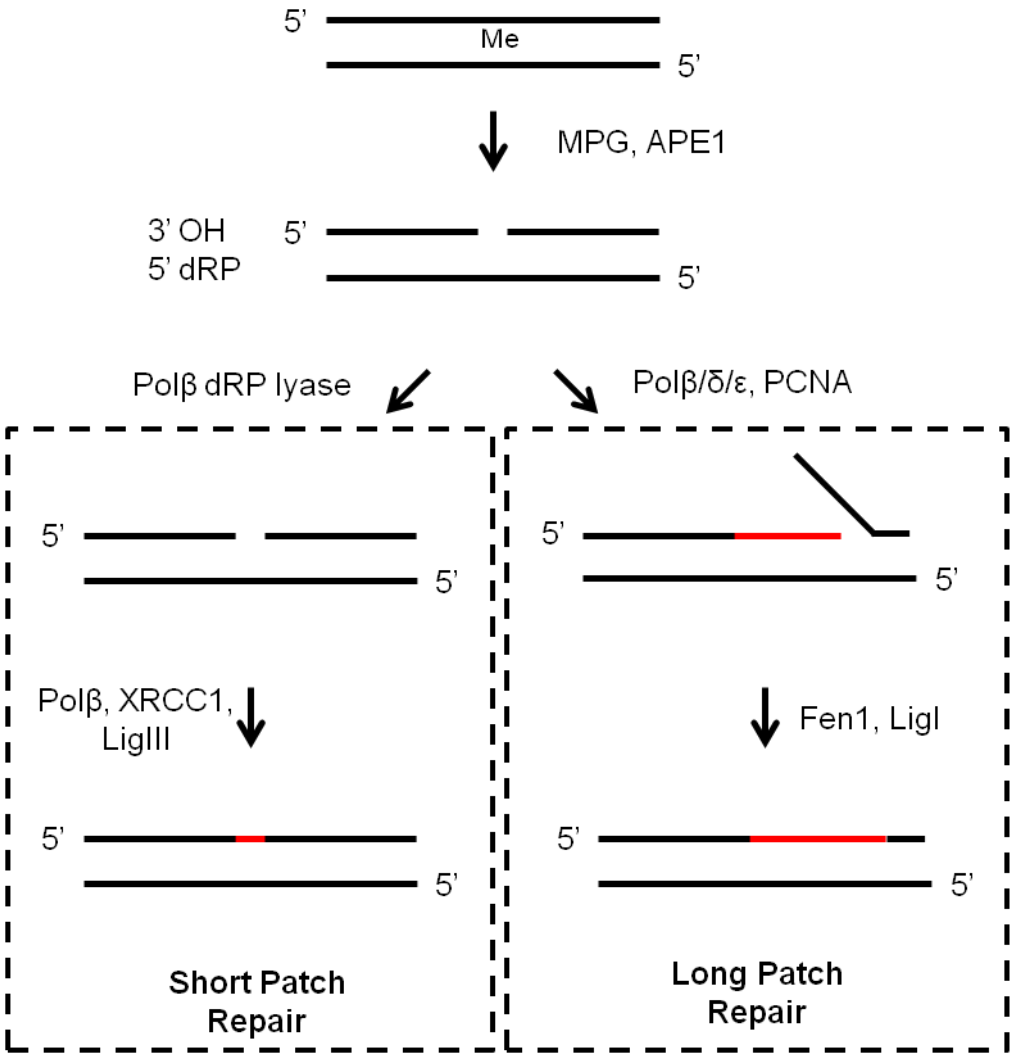


Figure 1.3: Summary of the BER/SSBR machinery in the repair of a methylated base. Methylated bases are recognised by the mono-functional glycosylase MPG, which generates an abasic (AP) site. This is cleaved by APE1 to produce a nick in the DNA backbone. This can be resolved through short patch repair, with the 5' dRP terminus processed by the dRP lyase activity of Polβ, before gap filling by Polβ and strand ligation by the XRCC1-LigIII complex. Alternatively, this can be resolved by long patch repair, where processive polymerase activity, stimulated by PCNA, displaces the 5' end of the nick. The resultant DNA flap is cleaved by Fen1, and the backbone ligated by LigI. Adapted from Caldecott 2008.

itself has no catalytic activity, but acts as a scaffold for the recruitment of a wide range of further proteins required for the completion of SSBR, including polβ (Caldecott et al., 1996; Klungland and Lindahl, 1997) and DNA ligase IIIα (Caldecott et al., 1994) as well as processing enzymes such as Aprataxin (Date et al., 2004) and PNKP (Della-Maria et al., 2012; Whitehouse et al., 2001).

Following detection of the break by PARP1, often the DNA ends require processing, as they lack the 3'-OH and 5' phosphate required for gap filling and ligation. This is true for both spontaneously arising SSBs and those generated via BER. The most common modifications for spontaneous breaks arising from ROS are 3' phosphate, which is a substrate for PNKP and 3' glycophosphate which is a substrate for the phosphodiesterase activity of APE-1. Breaks arising from the endonuclease activity of APE-1 carry 5'-dRP ends that are a substrate for processing by the N-terminus of polβ (Matsumoto and Kim, 1995), whereas those that arise from the action of bifunctional glycosylase-lyases carry 3' phosphate or 3' α,β-unsaturated aldehyde termini, which are processed by PNKP or APE-1 respectively. Additionally, SSBs which have been the subject of abortive ligation possess 5'-AMP modifications, and can be processed by the enzyme Aprataxin (Ahel et al., 2006).

Once ends have been returned to a 3'-OH and a 5' phosphate, gap filling and ligation can occur. This can take place in two distinct modes, through short-patch or long-patch repair (Frosina et al., 1996). Short-patch repair involves gap filling of a single nucleotide by polβ (Prasad et al., 1994) and ligation of the break by the XRCC1-ligase IIIα complex (Caldecott et al., 1994; Cappelli et al., 1997). Long patch repair is dependent on PCNA and involves polymerisation of 2-12 nucleotides which displace the original strand downstream of the break to

leave a flap. This is then cleaved by the nuclease FEN-1 (Kim et al., 1998; Klungland and Lindahl, 1997), before ligation by ligase I, recruited through its interaction with PCNA, to complete repair (Levin et al., 2000). However, there appears to be considerable redundancy between ligase I and ligase IIIα within SSBR (Gao et al., 2011; Simsek et al., 2011a; Sleeth et al., 2004). Long patch repair does not require processing of the 5' terminus of the break, because it is displaced by polβ activity. This means 5' ends which are not able to be processed into a 5' phosphate, such as some oxidised abasic residues (Sung and Demple, 2006), are necessarily resolved by long patch repair.

1.3.4 Roles of PARPs in SSBR

PARP1 has long been suggested to play a role in both SSBR and BER, promoting the resolution of these lesions in a number of ways. One of the major functions of the PAR chains produced by PARP1 is to facilitate the recruitment of XRCC1 to the break through its PAR-binding BRCT domain (El-Khamisy et al., 2003; Masson et al., 1998). Consistent with this, loss of PARP1 can prevent the accumulation of XRCC1 at SSBs (Godon et al., 2008). A further role of PAR is to relax chromatin at the site of the break (Poirier et al., 1982; Tulin and Spradling, 2003), and histones are one of the direct targets of ADP-ribosylation (Gibbs-Seymour et al., 2016). Chromatin relaxation by PAR may be directly due to this modification, with the highly negatively charged PAR chain altering the ability of histones to associate with DNA. Additionally, histone chaperones and chromatin-remodelling enzymes can be recruited to breaks by PAR, for example ALC1 (Ahel et al., 2009) or SMARCA5 (Smeenk et al., 2013).

However, the functional importance of PARP1 has also been challenged, with studies reporting conflicting requirements for PARP1 activity to accelerate strand ligation after SSB induction (Fisher et al., 2007; Ström et al., 2011). Furthermore, PARP1 is dispensable for *in vitro* reconstitutions of BER and SSBR, indicating it does not have a core enzymatic role in the process (Klungland and Lindahl, 1997; Pascucci et al., 2002). Nevertheless, both mouse and human cells depleted of PARP1 show sensitivity to SSB-inducing and base damaging agents, implying a functional significance of losing PARP1 activity in the resolution of these lesions (Fisher et al., 2007; Masutani et al., 2000a; Trucco et al., 1998).

Residual ADP-ribosylation detected in cells lacking PARP1 following exposure to DNA damaging agents encouraged the search for additional PARPs (Johansson, 1999; Shieh et al., 1998). PARP2 was soon identified, and proposed to have roles in both BER and SSBR (Amé et al., 1999). Mice lacking PARP2 are sensitive to radiation (Ménissier de Murcia et al., 2003a), and mouse cells lacking PARP2 are unable to efficiently repair alkylation damage (Schreiber et al., 2002). However, loss of PARP2 in human cells does not affect strand ligation rates (Fisher et al., 2007), although redundancy between PARP1 and PARP2 , at least during development, is implied by the embryonic lethality of *PARP1*$^{-/-}$*PARP2*$^{-/-}$ mice (Ménissier de Murcia et al., 2003a). Indeed, a recent study identified overlapping roles of PARP1 and PARP2 in recruiting XRCC1 to chromatin following H_2O_2 treatment (Hanzlikova et al., 2016). Loss of either PARP individually had no significant effect on XRCC1 recruitment, but in the absence of both PARPs almost no XRCC1 could be detected bound to chromatin following DNA damage. Interestingly, this relationship was not

reflected in strand ligation rates, with loss of PARP2 having no effect, even in the absence of PARP1. The reasons for the apparent disconnect between XRCC1 recruitment and strand ligation rates is not yet fully understood. Other groups have suggested PARP2 may have separate functions from PARP1, as it is activated *in vitro* most strongly by gap and flap-like structure that occur at later points during SSBR/BER (Kutuzov et al., 2013a; Langelier et al., 2014). Additionally, recruitment of PARP2 to sites of laser damage occurs after PARP1, further suggesting their roles may, at least to some extent, be distinct (Mortusewicz et al., 2007). The precise role of PARP2 in SSBR and BER, to what extent it can compensate for the loss of PARP1 and the nature of its unique functions in this process are all uncertain.

More recently, PARP3 has also been suggested to play a role in SSBR, as PARP3 can be strongly activated by 5’ phosphorylated nicks, binding them through its WGR domain (Langelier et al., 2014). Avian DT40 cells lacking PARP3 show sensitivity to ionising radiation (IR), which induces a complex array of DNA damage including SSBs and DSBs (Grundy et al., 2016). Interestingly, they also show a strand ligation defect in an alkaline comet assay following IR. Due to the fact that both SSBs and DSBs contribute to the comet tail in this assay, this observation could be attributable to a defect in DNA DSBR, in which PARP3 has been shown to function (Beck et al., 2014; Rulten et al., 2011). However, other cell lines carrying a DNA DSB repair defect do not show a reduction in strand ligation, whilst cells lacking PARP1 do, indicating that defective SSBR is likely responsible for the comet defect, and implicating PARP3 in this process. However, the precise function of PARP3 in this context, and how it might integrate with the roles of PARP1 and PARP2 in SSBR/BER,

is uncertain. It should also be noted avian cells lack a homologue of PARP2, so whether PARP3 plays a role in SSBR in human cells remains to be determined.

1.4 Repair of DNA DSBs

1.4.1 Sources of DNA DSBs

DNA double strand breaks are less common than SSBs, but unrepaired DSBs have far more serious consequences to a cell; a single unrepaired DSB at the onset of S-phase can lead to improper chromosome segregation and genome instability (Jackson, 2002). DNA DSBs can form following exposure to ionising radiation or certain DSB-inducing agents such as bleomycin or phleomycin. Double strand breaks can also form as a consequence of replication forks encountering other forms of damage which interfere with its progression. The repair of replication-associated forms of damage will be discussed in detail in section 1.5.

Programmed DSBs are also introduced during a number of normal cellular processes. These are typically tightly controlled, but if these processes become dysregulated, unscheduled DSBs can arise. One process which utilises DSBs is DNA topology manipulations by topoisomerase II enzymes. These proteins can relieve DNA supercoiling and separate catenanes by breaking both strands of the DNA simultaneously, before quickly religating them. Inhibition of topoisomerase II, for example by etoposide, leads to the formation of protein-linked DBSs. Another example of a process that utilises programmed DSBs is V(D)J recombination to generate antibody and T-cell receptor variants. The process joins together alternative gene segments using many components of the non-homologous end joining (NHEJ) DSBR pathway.

1.4.2 DNA DSBR pathways

Cells possess multiple repair pathways for DNA DSBs, which work through distinct mechanisms to repair these lesions. Arguably the simplest repair pathway, NHEJ or classical-NHEJ (c-NHEJ), simply religates the two broken end of the DSB together without a template (Figure 1.4, left panel). For this reason, NHEJ is considered an error-prone repair pathway. In contrast, homologous recombination (HR) functions during S- and G2- phases of the cell cycle to resolve DSBs by using homologous DNA as a template, making this an error-free repair pathway (Figure 1.5). The third pathway is known as alternative-NHEJ (alt-NHEJ) and is severely error prone (Figure 1.4, right panel). Extensive use of this pathway often leads to the introduction of mutations and chromosomal translocations.

1.4.3 Non-homologous end joining

In order for NHEJ to take place, the DNA ends of the DSB must be bound by a heterodimer of Ku70/80 (Feldmann et al., 2000; Walker et al., 2001). These proteins form a toroidal ring though which the DNA end can pass, allowing its translocation onto the DNA. DNA-PK$_{cs}$ is then recruited to the break, binding Ku and displacing it from the DNA terminus (Yoo and Dynan, 1999). This activates the kinase activity of DNA-PK, allowing it to phosphorylate a broad range of targets. These include DNA-PK itself (Douglas et al., 2002, 2007; Meek et al., 2007), as well as other NHEJ factors (Wang et al., 2004) and additional cellular targets to facilitate repair (Stiff et al., 2004). The autophosphorylation of DNA-PK has been shown to facilitate its release from DNA ends, potentially to allow access of processing and ligation machineries to the termini (Block et al., 2004; Uematsu et al., 2007).

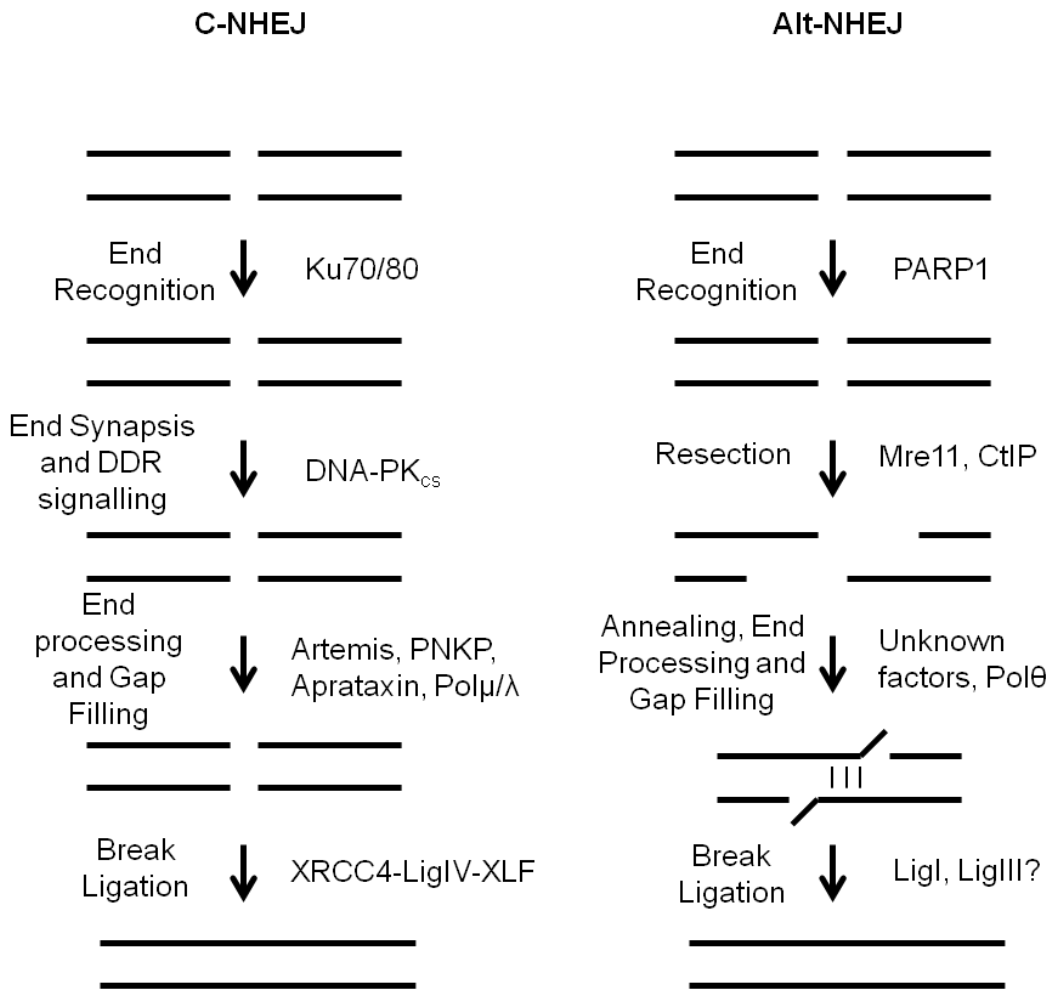


Figure 1.4: Summary of the c-NHEJ and alt-NHEJ machinery in the repair of a DNA DSB. In c-NHEJ, DNA ends are recognised by a Ku70/80 heterodimer, before subsequent binding of DNA-PK$_{cs}$, allowing activation of DNA-PK activity, and signalling through the DDR. Ends are processed by a variety of factors, including Artemis, Aprataxin and PNKP, and gaps are filled by Polμ and Polλ. The break is sealed by the XRCC4-LigIV-XLF complex. In alt-NHEJ, DNA ends are recognised by PARP1, leading to the recruitment of Mre11 to the break site. Mre11, in concert with other nucleases, facilitates end-resection at the break, revealing microhomologies across the break that can anneal. Following processing and gap filling, the break can be sealed by LigIII or LigI. Adapted from Deriano and Roth 2013.

DNA-PK$_{cs}$ is also capable of dimerisation, and this activity has been shown to be able to bridge DNA ends, bringing them into close proximity before relegation (Cary et al., 1997; DeFazio et al., 2002; Graham et al., 2016; Hammel et al., 2010).

The next step of NHEJ is end processing, in order to return the DNA ends to a 3'-OH and a 5' phosphate ready for ligation. Some of the processing enzymes are shared between NHEJ and SSBR, for example PNKP (Chappell et al., 2002; Coquelle et al., 2011; Garces et al., 2011; Karimi-Busheri et al., 2007) and Aprataxin (Ahel et al., 2006; Clements et al., 2004). Other enzymes are unique to NHEJ, such as the nuclease Artemis which is thought to aid NHEJ through the limited degradation of difficult ends, for example a terminal 3'-phosphoglycolate (Povirk et al., 2006). Polymerases μ and λ perform gap filling functions to produce blunt DNA ends (Fan and Wu, 2004; Mahajan et al., 2002). Ligation of the DNA can then occur, carried out by the XRCC4-Ligase IV-XLF complex (Ma et al., 2004). XRCC4 and XLF also interact to form a helical protein filament that can bridge the two DNA ends (Andres et al., 2012; Hammel et al., 2011). Another XRCC4-like protein called PAXX contributes to repair through its interaction with Ku and promotes the assembly of NHEJ factors onto chromatin (Ochi et al., 2015). Following successful repair of DSBs by NHEJ, Ku70/80 dimers become topologically trapped on the intact DNA molecule, and require a ubiquitin-mediated process for their removal (Brown et al., 2015; Postow et al., 2008).

1.4.4 Roles of PARPs in non-homologous end joining

PARP3 can be activated by DNA DSBs and functions to accelerate the kinetics of NHEJ, underscored by the fact cells deficient in PARP3 display sensitivity to DSB inducing agents. This was first identified to be through recruitment of APLF to the breaks via its PBZ domain (Rulten et al., 2011). APLF possesses nuclease activity as well as functioning as a histone chaperone, and works in concert with PARP3 to promote retention of XRCC4 at sites of damage. Later reports have identified a role for PARP3 in the recruitment and/or retention of Ku at DSBs, helping to limit resection and commit the break to repair via NHEJ (Beck et al., 2014).

The potential role of PARP1 in NHEJ is more controversial. PARP1 has been identified to interact with Ku (Galande and Kohwi-Shigematsu, 1999) and DNA-PK (Ruscetti et al., 1998), and bring about a rearrangement of the structure of DNA-PK bound to DNA ends (Spagnolo et al., 2012), but the functional importance of these observations is unclear. Recently, a novel mechanism by which PARP1 affects NHEJ has been suggested, through the PAR-dependent recruitment of the histone remodeler CHD2 (Luijsterburg et al., 2016). CHD2 helps to relax chromatin and support the deposition of histone H3.3, promoting repair through NHEJ. However, other groups have found no defect in the repair of breaks by NHEJ in the absence of PARP1 (Yang et al., 2004), and although mice lacking PARP1 have altered antibody responses, they are able to carry out V(D)J recombination, which relies on NHEJ for break repair (Ambrose et al., 2009). These inconsistencies may exist because PARP1 only contributes to NHEJ-mediated repair at a subset of breaks, or those induced in particular

chromatin environments. In any case, further work will be required to fully define the contribution of PARP1 to NHEJ.

1.4.5 Homologous recombination

DNA DSBs can also be repaired through homologous recombination when a sister chromatid is available for use as a template, during S- or G2- phases of the cell cycle. The first step of HR involves recognition and binding of the DSB ends by the Mre11-Rad50-Nbs1 (MRN) complex. This complex has important roles in signalling of the DDR and triggering cell cycle checkpoints, through the activation of the downstream kinase ATM (Uziel et al., 2003). The MRN complex recruits inactive dimers of ATM to the site of the break, and facilitates their autophosphorylation at S1981 (Bakkenist and Kastan, 2003), as well as several other sites (Kozlov et al., 2006). These modifications cause dissociation of the ATM dimers into their active monomeric form (Bakkenist and Kastan, 2003), and allows the triggering of the DDR and phosphorylation of up to 700 downstream targets (Bensimon et al., 2010; Matsuoka et al., 2007). One of these targets is serine 139 on the histone variant H2AX which is phosphorylated by ATM to form γH2AX at the site of the break (Burma et al., 2001). This site is also a target for other phosphatidylinositol 3-kinase-related kinases (PIKKs) including ATR (Ward and Chen, 2001) and DNA-PK (Stiff et al., 2004). The modification then spreads up to several megabases along the chromatin adjacent to the break (Rogakou et al., 1999), through a process mediated by the protein MDC1. This factor is able to bind γH2AX and recruit the MRN complex, resulting in more local ATM activation and further γH2AX formation (Chapman and Jackson, 2008; Lou et al., 2006; Lukas et al., 2004; Stucki et al., 2005; Uziel et al., 2003). γH2AX plays key roles in retention of

repair factors in the vicinity of the break (Paull et al., 1998), and mice lacking H2AX show sensitivity to DNA damage and impaired recruitment of damage factors to nuclear foci (Celeste et al., 2002).

Additionally, Mre11 possesses both endonuclease and exonuclease activity, and participates in the resection of the DNA ends to generate long 3' overhangs required for HR-mediated repair (Buis et al., 2008; Paull and Gellert, 1999; Shibata et al., 2014). Additional nucleases also contribute to this resection, including Exo1 and Dna2 (Nimonkar et al., 2008, 2011). Resection is co-ordinated by the protein CtIP, which interacts with a large number of DDR proteins, including the MRN complex (Sartori et al., 2007). CtIP possesses endonuclease activity which is required for processing of a subset of breaks with 'dirty' ends, whilst the non-catalytic roles of CtIP in regulating resection are relevant for HR more generally (Makharashvili et al., 2014). BRCA1, and its obligate partner BARD1 (Brzovic et al., 2001; Wu et al., 1996), also contribute to resection by interacting with phosphorylated CtIP through its BRCT domain (Wong et al., 1998; Yu et al., 1998), and with the MRN complex (Zhong et al., 1999). BRCA1 also ubiquitinates CtIP via its E3 ligase RING domain (Yu et al., 2006), and damage induced CtIP foci are compromised in the absence of BRCA1 E3 ligase activity. However, CtIP is also able to function independently of BRCA1, as loss of the CtIP-BRCA1 interaction does not detectably affect resection rates (Polato et al., 2014).

Following resection, the 3' ssDNA overhangs are coated with the heterotrimeric ssDNA-binding protein RPA, to form an RPA filament. This RPA filament is then replaced with a filament of the key recombinase Rad51. Formation of a Rad51 filament is facilitated by the Rad51 loader BRCA2 (Yuan et al., 1999), able to

bind Rad51 through its BRC repeats (Chen et al., 1998; Wong et al., 1997) and load it onto RPA-coated ssDNA. Rad51 paralogs, including Rad51B, Rad51C, XRCC2 and XRCC3 also contribute to this process (Suwaki et al., 2011). BRCA1 also facilitates Rad51 loading independently of its roles in resection, by interacting with PALB2 via its coiled coil domain (Sy et al., 2009). BRCA2 is then recruited to the site of the DSB through its interaction with PALB2 (Xia et al., 2006; Zhang et al., 2009). Whilst Rad52 is a key recombinase loader in yeast, which lack BRCA2, the functional importance of human Rad52 in Rad51 loading remains uncertain (Jensen et al., 2010; Rijkers et al., 1998).

Once the formation of the Rad51 filament is complete, it can perform a homology search, to find a sequence similar to that within the Rad51 filament. When a homologous sequence is found, strand invasion can occur, where the 3' overhang invades into the duplex of the homologous sequence in the sister chromatid, displacing the complementary strand to from a displacement loop (D-loop). The 3' end of the invading strand can then be extended by polymerase δ or ε using the homologous template.

At this point, there are several possible avenues for repair to be completed, resulting in either crossover or non-crossover products. If repair is completed through the DSBR or dHJ pathway, the second 3' overhang that did not invade base pairs with homologous sequence on the D-loop. This strand can also be extended, and the backbone sealed, generating a double Holliday junction (dHJ) structure where the two sister chromatids are covalently linked. These structures mostly undergo dissolution by a complex of BLM and Topoisomerase IIIα, resulting in non-crossover products (Wu and Hickson, 2003). Any remaining dHJ structures are resolved through cleavage of the structure by

endonucleases, either in a symmetrical fashion by GEN1 (Chan and West, 2015; Ip et al., 2008; Rass et al., 2010), or in an asymmetrical fashion by the action of Mus81/Eme1 (Chen et al., 2001; Ciccia et al., 2003) and Slx1/Slx4 (Fekairi et al., 2009; Muñoz et al., 2009; Svendsen et al., 2009). Resolution of dHJ structures using endonucleases can give rise to both crossover and non-crossover products, which may explain why dissolution, which does not generate crossover products, is the favoured pathway in mitotic cells. The existence of multiple redundant mechanisms for dHJ resolution reflects how deleterious these structures can be if present at the onset of mitosis, leading to chromosome mis-segregation, formation of anaphase bridges and severe chromosome instability (Sarbajna et al., 2014).

As an alternative to the DSBR pathway, synthesis-dependent strand annealing (SDSA) can also occur to repair DSBs. After invasion of the Rad51 filament and DNA synthesis from the template, the invading strand is ejected from the D-loop, and re-anneals with the 3' overhang of the other side of the DSB. Further DNA synthesis and can then occur, followed by ligation, resulting in the formation on non-crossover products, and avoiding the formation of any Holliday junction intermediates (Figure 1.5).

An additional repair mode, single-strand annealing (SSA) can occur if the break is flanked by repeats (Bhargava et al., 2016). Resection will reveal these homologous repeats either side of the break, which can then anneal. The 3' overhanging flaps are cleaved, and the intervening DNA synthesised and ligated, resulting in a deletion of the DNA between the repeats.

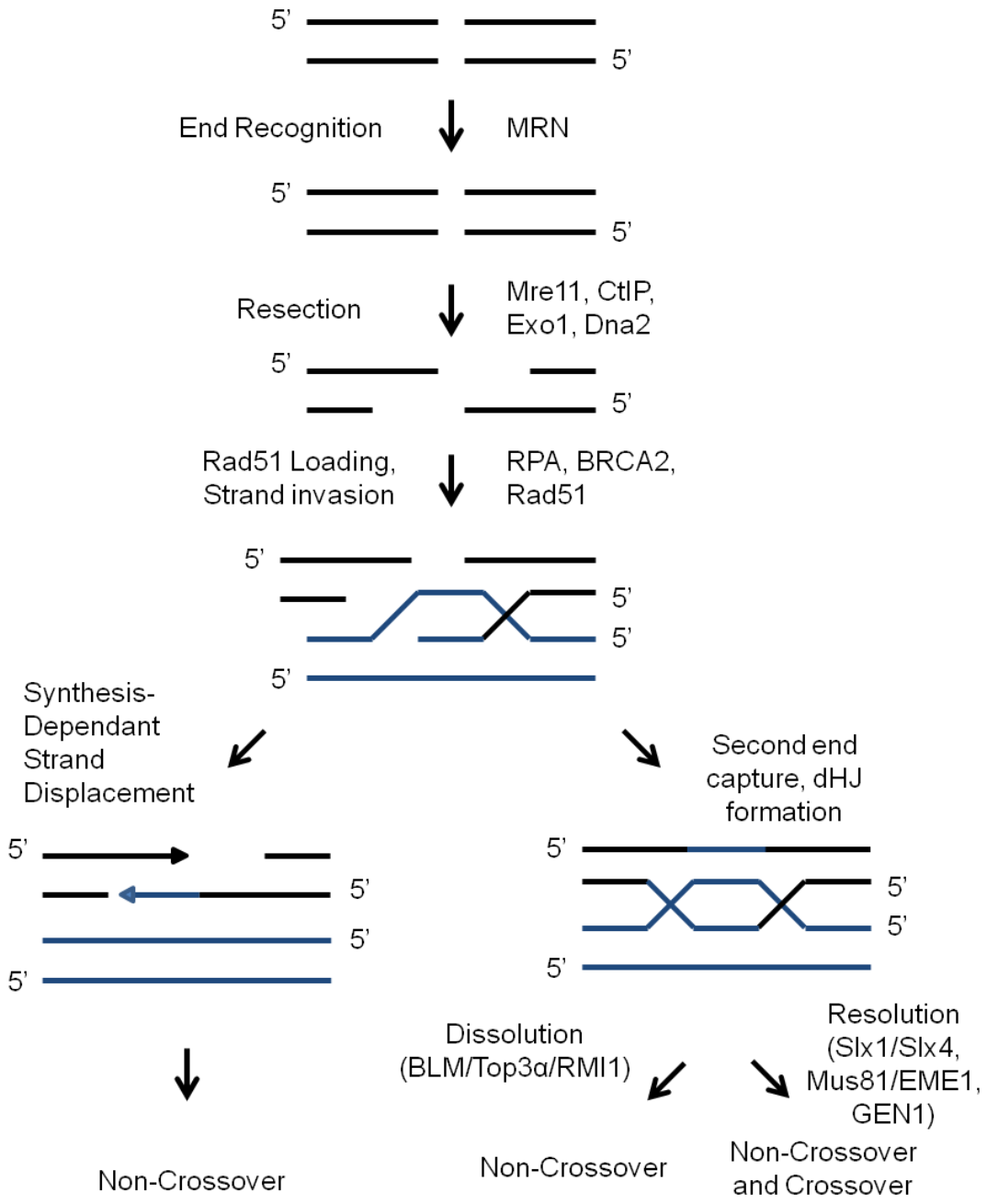


Figure 1.5: Summary of the HR machinery in the repair of a two-ended DNA DSB. During HR-mediated DSB repair, DNA ends are recognised by the MRN complex. DNA end resection, mediated by Mre11, along with Exo1, Dna2 and CtIP, produces 3' ssDNA overhangs. These are coated with RPA, before being loaded with Rad51 by a complex of BRCA2/PALB2. This Rad51 nucleofilament undergoes strand invasion into a homologous sequence, allowing DNA synthesis from this new template. If this invading strand is then ejected, it can anneal with the 3' overhang on the other side of the break, allowing DNA synthesis and ligation to repair to break. This is known as synthesis-dependent strand annealing. Alternatively, if the second 3' overhang pairs with the strand displaced by the strand invasion step (D loop), formation of a double Holliday junction can occur. These structures can undergo dissolution by a complex of BLM/Top3α/RMI1, or be resolved through nucelolytic cleavage by Slx1/Slx4, Mus81/EME1 or GEN1.Adapted from Jasin and Rothstein 2013.

SSA is independent of Rad51, as no stand invasion is required, but is highly mutagenic as the sequence between the repeats is lost.

Homologous recombination can also act upon one ended DSBs through break induced replication (BIR) (Malkova and Ira, 2013). One ended DSBs can form when a replication fork collapses or encounters a SSBs. This DNA end is resected, loaded with Rad51, and allowed to invade into homologous sequence in the sister chromatid. The D-loop that forms is then used to setup a unidirectional replication fork, allowing the resumption of DNA synthesis.

1.4.6 Roles of PARPs in homologous recombination

The role of PARP1 in HR repair of canonical DNA DSBs remains contentious, with initial work finding no defect in the repair of DSBs by HR in the absence of PARP1 (Yang et al., 2004). Since then, a number of groups have suggested that PARP1 may influence resolution of breaks through HR. Some evidence indicates a negative role of PARP1 in HR, for example PARP1 modifies BRCA1 in its DNA binding domain, promoting its binding to RAP80. Loss of this modification leads to increased HR repair of I-SceI induced DSBs and elevated chromosome rearrangements after IR exposure (Hu et al., 2014). Other work has identified a positive role for PARP1 in HR. For example PARP1 and Timeless are able to interact, and depletion of PARP1 prevents the recruitment of Timeless to site of DNA damage and leads to decreased levels of HR-mediated repair (Xie et al., 2015). Furthermore, the OB-folds of BRCA2 can bind PAR, and early recruitment of BRCA2 to laser damage can be prevented by PARP inhibitor treatment (Zhang et al., 2015). Finally, the BRCT domains of the BRCA1 partner BARD1 are also able to bind PAR, and treatment with

PARP inhibitors can prevent the rapid accumulation of BRCA1 to DNA damage (Li and Yu, 2013). These studies link ADP-ribosylation to the recruitment of core HR proteins to sites of DNA damage. However overall, contrasting reports make it difficult to build a clear picture of how PARP1 affects HR repair of DSBs. Note this is distinct from the potential contributions of PARPs in regulating HR at sites of replication-associated damage, which will be discussed in section 1.5.

PARP14 has been identified to play a role in the HR pathway, with depletion of this factor leading to reduced HR-mediated repair of I-SceI induced DSBs, and sensitivity to the DSB inducing agent bleomycin. Interestingly, in the absence of PARP14 cells show persistent Rad51 foci following camptothecin exposure (Nicolae et al., 2015). This suggests the role of PARP14 lies downstream of Rad51 filament formation, potentially mediating strand invasion or Rad51 filament disassembly.

1.4.7 Alternative-NHEJ

A third pathway for repairing DSBs, called alternative-NHEJ, was originally identified as a ‘backup’ pathway active in the absence of core components of the c-NHEJ pathway, firstly in yeast (Boulton and Jackson, 1996; Wilson et al., 1997) and later in human cells (Verkaik et al., 2002; Wang et al., 2003). The exact components and mechanism of alt-NHEJ are poorly defined, but its repair products frequently feature characteristic deletions, meaning it is considered a highly error-prone repair pathway. Indeed, use of alt-NHEJ in the absence of c-NHEJ leads to increased frequency of chromosome rearrangements and translocations (Difilippantonio et al., 2000; Ferguson et al., 2000; Zhang and

Jasin, 2010), indicating alt-NHEJ causes significant genome instability, and may contribute to tumorigenesis (Bentley et al., 2004; Sharpless et al., 2001). Microhomologies are often present at repair sites, leading to alt-NHEJ also being referred to as microhomology-mediated end-joining (MMEJ). However, the presence of microhomologies is not strictly required, possibly reflecting the idea that there could be multiple sub-pathways of alt-NHEJ, some more dependent on microhomologies than others.

Alt-NHEJ often requires limited resection at the break, and the nucleases Mre11 (Rass et al., 2009; Xie et al., 2009) and CtIP (Zhang and Jasin, 2010) have been implicated in the pathway. It is hypothesised that short-range resection by these factors reveals microhomologies, which can base pair to facilitate alt-NHEJ. Following end processing, trimming and gap filling, the DNA ends can be ligated. Whilst LigIII and XRCC1 were able to reconstitute alt-NHEJ activity *in vitro* (Audebert et al., 2004; Della-Maria et al., 2011), loss of either LigIII or XRCC1 does not prevent end-joining activity in cells (Boboila et al., 2012), even in the absence of c-NHEJ. Loss of LigI alone was also unable to prevent end-joining activity, but loss of both together abrogated alt-NHEJ induced chromosomal translocations (Simsek et al., 2011b), suggesting redundancy between these ligases in alt-NHEJ. Recently Polθ has been identified as another alt-NHEJ factor, able to facilitate alt-NHEJ *in vitro* by stabilising microhomology-mediated synapsis of DNA ends by overhang extension (Kent et al., 2015). Furthermore, cells lacking both c-NHEJ and Polθ show decreased chromosomal translocations and telomere fusions, both hallmarks of alt-NHEJ (Ceccaldi et al., 2014). Interestingly, cells lacking Polθ

display an increased reliance on HR, suggesting HR and alt-NHEJ may compete for the resolution of some lesions (Ceccaldi et al., 2014).

1.4.8 Roles of PARPs in alternative-NHEJ

PARP1 has been identified as the key sensor for the engagement of alt-NHEJ, through its ability to bind DSB ends. Indeed inhibition of PARP1 is able to sensitise DNA-PK deficient cells to DSB-inducing agents (Audebert et al., 2004), and PARP1 depletion can abrogate the joining of DSBs in the absence of Ku (Wang et al., 2006). PARP1 activity at these ends helps the recruitment of the MRN complex (Haince et al., 2008), initiating the resection required for the progression of alt-NHEJ. Competition between Ku and PARP1 at DSB ends has been proposed to regulate the choice between c-NHEJ and alt-NHEJ (Wang et al., 2006), with the high abundance and affinity of Ku for DSB ends potentially explaining the bias towards c-NHEJ in wild-type cells.

1.5 Cellular response to replication stress

1.5.1 Sources of replication stress

Replication stress occurs when the normal progression of a replication fork is disrupted, and can develop as a result of both endogenous and exogenous factors. Endogenous causes of replication stress include difficult to replicate regions of the genome such as common fragile sites (CFS), collisions with the transcription machinery or the expression of oncogenes. Exogenous sources of replication stress can come from multiple DNA damaging agents, which can induce a wide range of lesions that can disrupt the progression of a replication fork, including SSBs, base damage, and inter-strand crosslinks. Agents which

are able to inhibit replicative polymerases, trap topoisomerases onto DNA or deplete cellular dNTP pools also all result in replication stress.

1.5.2 Tolerance and resolution of replication stress

Numerous mechanisms exist for cells to overcome replication stress and accurately replicate the entire genome, but they generally share the common feature of activation of the DNA damage response through ATR signalling. Activation of ATR leads to the stimulation of Chk1 activity and triggering of the intra-S checkpoint (Liu et al., 2000), preventing the firing of new replication origins and stabilising replication forks until the source of the stress is removed. Failure to do so leads to unstable replication forks and the accumulation of strand breaks (Brown and Baltimore, 2003). ATR activation relies on the formation of ssDNA, which is created as replicative helicases unwind duplex DNA once the polymerase has stalled (Byun et al., 2005). This ssDNA is bound by the ssDNA binding protein RPA to form a filament, which interacts with the ATR interacting partner ATRIP, bringing ATR to the site of the damage (Zou and Elledge, 2003). Simultaneously, RPA interacts with Rad17, which can then load the 9-1-1 checkpoint clamp (Bermudez et al., 2003; Ellison and Stillman, 2003). TopBP1 is then brought to the proximity of the RPA through its interaction with the 9-1-1 complex, allowing it to stimulate ATR kinase activity (Kumagai et al., 2006; Ohashi et al., 2014).

If the lesion causing the replication stress cannot be removed in a timely manner, numerous mechanisms exist to allow the continuation of DNA replication. Possibly the simplest involves the activation of cryptic or dormant origins of replication, which can approach the stalled replication fork from the

opposite direction and fuse with it, this facilitating the completion of replication (Blow et al., 2011; Yekezare et al., 2013).

Some lesions, such as damaged bases or thymidine-dimers that form as a result of exposure to ultraviolet light (UV), cause polymerase stalling because the base adducts cannot be accommodated into the active site of the replicative polymerase (Byun et al., 2005). Translesion synthesis (TLS) involves the swapping of the replicative polymerase with a range of TLS-polymerases, which are lower fidelity but able to tolerate and polymerise past a variety of lesions, allowing the continuation of DNA synthesis (Prakash et al., 2005). Alternatively, template switching can occur, using the newly synthesised daughter strand as a temporary template to allow replication past the blockage (Giannattasio et al., 2014). As both of these methods rely on repair of the original stalling lesion after the completion of replication, they are collectively known as post-replication repair (PRR) pathways (Gao et al., 2017). Ubiquitination of PCNA plays a key role in the regulation of these pathways (Hoege et al., 2002; Stelter and Ulrich, 2003).

Replication fork reversal has also been suggested to be a mechanism thorough which stalled forks are protected and repaired. This is a process where a canonical three-way replication fork is converted into a four-way junction, with the newly synthesized strands annealing together. This can potentially stabilise forks in a number of ways, by limiting the formation of ssDNA, by allowing template switching to bypass a lesion, and by placing a lesion back into a dsDNA context to allow normal repair mechanisms to resolve it. Originally identified in prokaryotes, the physiological relevance of these structures to eukaryotic replication has been contentious. However, recent advances have

allowed visualisation of reversed forks from eukaryotes by electron microscopy. This has revealed that reversed forks form in response to a wide variety of fork stalling agents (Zellweger et al., 2015), and thus may represent a ubiquitous physiological response to replication stress. The factors required for the formation of reversed replication forks are not fully understood, but numerous parts of the HR machinery are involved in the process, including Rad51, BRCA1 and BRCA2. There are also numerous helicases which are able to catalyse fork regression *in vitro*, including BLM, WRN, HLTF, FANCM, ZRANB3, SMARCAL1, and Fbh1 (Bétous et al., 2012; Ciccia et al., 2012; Fugger et al., 2015; Gari et al., 2008; Kile et al., 2015; Machwe et al., 2006; Ralf et al., 2006). Many of these enzymes are also able to catalyse the reverse reaction of fork restoration, along with another helicase RecQ1 (Berti et al., 2013), which also participates in this process. The exact contributions of these helicases to this process *in vivo* are still being uncovered.

Limited resection, mediated by Mre11 and Dna2, appears to be important for the resolution of damaged replication forks (Buis et al., 2008; Hashimoto et al., 2010; Thangavel et al., 2015). BRCA2 and Rad51 have important roles in protecting stalled forks from over-resection and ensuring their stability (Hashimoto et al., 2010; Schlacher et al., 2011). Indeed, the roles of BRCA2 in replication fork stability can be separated from those in DSBR. A mutation in the C-terminal Rad51 binding domain can abrogate fork protection mediated by BRCA2, whilst not affecting HR repair of canonical DSBs (Schlacher et al., 2011). Another large protein, BOD1L, also contributes to the protection of stalled replication forks from excessive resection by shielding Rad51 filaments from disassembly by the anti-recombinogenic helicases BLM and Fbh1 (Higgs

et al., 2015). Exactly how the roles of these proteins in preventing excessive resection interface with the formation of reversed replication forks remains unclear.

If a replication fork remains stalled for an extended period of time, it can collapse and form a one-ended DSB. This may be due to the inherent instability of a stalled replication fork, or may involve processing by specific nucleases to bring about collapse (Hanada et al., 2007). A similar structure might arise when a replication fork encounters an unrepaired SSB, leading to replicative run-off. Once a one-ended DSB has formed, it is resolved by the HR machinery through a process of BIR (as described above).

1.5.3 Roles of PARPs in the cellular response to replication stress

PARP1 has been recognised to contribute to the resolution of stalled/collapsed replication forks, with cells lacking PARP1 showing sensitivity to the fork stalling agent hydroxyurea (HU) (Yang et al., 2004). Subsequent work identified a role of PARP1 in recruiting the nuclease Mre11 to stalled replication forks to facilitate repair. In the absence of PARP1, replication fork stalling was elevated after HU exposure, whilst formation of Mre11, RPA and Rad51 foci were all decreased, indicating resection is compromised without PARP1 signalling at sites of replication stress (Bryant et al., 2009). However, PARP1 has also been linked to the protection of stalled replication forks, with PARP inhibitor treatment leading to the over-resection of stalled forks after HU exposure (Ying et al., 2012). Furthermore, PARP1 has been implicated in the formation of reversed forks. The absence of PARP1, but not other parts of the SSBR machinery, can

significantly reduce the formation of reversed forks after treatment with the topoisomerase inhibitor camptothecin (Ray Chaudhuri et al., 2012). Later work identified that RecQ1 can interact with PAR, and this interaction decreases its ability to restore reversed replication forks in response to camptothecin (Berti et al., 2013). Thus PARP1 stabilises reversed replication forks by constraining the activity of RecQ1 upon these structures, preventing premature restoration of the fork. Intriguingly, stabilising reversed replication forks would be predicted to limit resection at a stalled fork, contrasting with the identified role of PARP1 in Mre11 recruitment and the promotion of resection at these structures. How these multifaceted roles of PARP1 combine to contribute to the cellular tolerance to replication stress, and interface with the roles of other DNA-dependent PARPs is unclear.

There has also been a suggestion that alt-NHEJ mediated by Polθ and PARP1 can contribute to the repair of stalled/collapsed replication forks, in competition with HR, even in wild-type cells. Cells lacking Polθ show sensitivity and increased fork stalling in response to HU, along with elevated formation of Rad51 foci (Ceccaldi et al., 2014). In the absence of HR, cells rely on Polθ-mediated repair to maintain genome stability in response to a variety of genotoxic agents, supporting the idea of HR and alt-NHEJ both contributing to the resolution of stalled replication forks.

Finally PARP10 contributes to the cellular response to replication stress by facilitating TLS. PARP10 can interact with ubiquitinated-PCNA through its N-terminal PIP box, and cells depleted of PARP10 show decreased cellular survival and increased mutation rates in response to UV exposure. These phenotypes cannot be rescued with a catalytically dead mutant of PARP10,

indicating its MARylation activity is relevant to its repair roles, although its substrates remain unknown (Nicolae et al., 2014).

1.6 The synthetic lethal relationship between PARPs and HR

1.6.1 Discovery of synthetic lethality and mechanistic models

Small molecule inhibitors of PARPs have gained general recognition for their ability to specifically kill certain types of tumours, most famously those deficient in homologous recombination, exploiting the concept of synthetic lethality. This phenomenon was first identified in *Drosophila melanogaster*, where the loss of two genes in combination resulted in inviability (DOBZHANSKY, 1946), whilst loss of either gene individually was tolerated. The presence of a synthetic lethal relationship between PARP inhibitors (PARPi) and HR-deficient tumours has resulted in the PARPi olaparib receiving Food and Drug administration (FDA) and European Medicines Agency (EMA) approval for use as a single agent against ovarian cancers defective in BRCA1 or BRCA2. Subsequently the FDA has also approved the use of a second PARP inhibitor, rucaparib, against similar tumours. This is significant given approximately to 10% of all breast cancers (Malone et al., 2000) and 15% of all ovarian cancers (Pal et al., 2005) are attributed to mutations in one of these two genes.

Two papers published in 2005 first introduced the fact that BRCA mutant cells were hypersensitive to PARPi (Bryant et al., 2005; Farmer et al., 2005), showing up to 1000-fold killing as compared to BRCA competent cells. Both of these studies suggested models whereby inhibition of PARP1 leads to defective

SSBR and an accumulation of unrepaired SSBs. Upon collision with an active replication fork, these SSBs are converted to one-ended DSBs, normally repaired via HR. However, in the absence of BRCA genes, HR is defective and these lesions cannot be resolved, resulting in cell death.

Whilst attractive, a number of subsequent experiments brought elements of this model into question. Firstly, no detectable SSBs accumulate following cellular exposure to PARP inhibitors (Gottipati et al., 2010). Furthermore, depletion of additional components of the SSBR machinery, is unable to recapitulate the specific killing of BRCA mutant cells seen when PARP1 is depleted or inhibited (Patel et al., 2011).

An alternate mechanism was based upon the finding that exposure to PARP inhibitors results in the ‘trapping’ of PARP1 and PARP2 onto chromatin following DNA damage (Murai et al., 2012). This may be due to the lack of automodification activity which normally triggers PARP release from DNA. Indeed, introducing mutations into domain interfaces important for the activation of PARP1 can prevent its DNA-dependent PARylation activity, and lead to prolonged accumulation of PARP1 onto damaged DNA (Steffen et al., 2014). It was suggested that lesions with trapped PARP occluding them may be difficult to repair due to the inaccessibility of the DNA ends, and thus rely more heavily on HR-mediated repair. Data supporting the idea that trapping contributes to synthetic lethality includes the fact PARP inhibition often elicits stronger effects than PARP ablation (Bryant et al., 2005; Farmer et al., 2005; Ström et al., 2011), and the efficacy of some PARP inhibitors correlates with their ability to trap PARPs, not the ability to inhibit PARylation activity (Murai et al., 2012, 2014). Furthermore, knockdown of PARP1 is able to abrogate the toxic effects

of olaparib, indicating that PARPi does more than simply prevent PARP catalytic activity (Bajrami et al., 2014).

A final alternate model proposes that PARP1 could regulate additional HR-independent pathway(s) that contribute to DNA repair, such that in the absence of PARP activity and BRCA proteins, no viable repair route remains for certain forms of DNA damage. Indeed, in the absence of BRCA1/2, or other HR proteins, PARP activity is elevated, indicating additional damage being channelled through PARP-dependent repair mechanisms (Gottipati et al., 2010). Interestingly, inhibition or depletion of components of the c-NHEJ pathway is able to rescue the sensitivity and elevated mutation frequency of BRCA2 null cells exposed to PARPi (Patel et al., 2011). This indicates that illegitimate engagement of c-NHEJ drives synthetic lethality in the absence of PARPs and HR. Given PARP1 and Ku can compete for DNA DSB ends (Wang et al., 2006), this suggests the ability of PARP1 to engage these lesions and influence pathway choice may be crucial for cellular survival in the absence of HR.

Whilst the exact mechanism driving synthetic lethality between HR-deficient cells and PARP inhibitors remains to be elucidated, it should be noted that each of the models presented above are not mutually exclusive. A combination of loss of PARP catalytic function, in SSBR or other repair pathways, and PARP trapping at lesions could combine to bring about the remarkably potent killing of HR-defective cells by PARPi.

1.6.2 Mechanisms of resistance to PARPi

One issue with PARP inhibitors in the clinic is the emergence of cancer cells with resistance to the therapy. This can occur through multiple mechanisms, the most obvious of which is the reversion of the BRCA mutation, leading to tumours which are resistant to treatment (Norquist et al., 2011; Sakai et al., 2008; Swisher et al., 2008). This form of resistance has been observed in PARPi-insensitive metastases in the clinic (Barber et al., 2013). Potential additional mechanisms have been identified in genetic mouse models, for example upregulation of the p-glycoprotein (Pgp) efflux transporter, for which olaparib is a substrate (Henneman et al., 2015). Interestingly, this form of resistance could be overcome by using the Pgp inhibitor tariquidar, or by using AZD2461, a PARPi with low affinity for Pgp. A third resistance mechanism involves loss of 53BP1 in cells lacking BRCA1, which partially reactivates HR and abrogates cellular sensitivity to PARPi (Jaspers et al., 2013). This is consistent with previously reported interplay between 53BP1 and BRCA1 in regulating DSB repair pathway choice (Daley and Sung, 2014; Gupta et al., 2014). Intriguingly, reduced 53BP1 expression is seen most often in BRCA-associated breast cancers, and this correlates with lower metastasis-free survival, indicating the potential clinical relevance of this mechanism of resistance (Bouwman et al., 2010). Finally, loss of PARP1 expression can also alleviate the toxicity of PARP inhibition to DNA methylating agents, presumably because PARP1 can no longer be trapped at sites of DNA damage (Liu et al., 2009).

1.6.3 Specificity and further uses of PARPi

Both of the PARP inhibitors currently licensed for clinical use are NAD^+ mimetics, and bind in the catalytic domain of PARP1. As this domain is conserved across the entire PARP superfamily, it is perhaps unsurprising that these agents show activity against numerous other PARP proteins. Olaparib and rucaparib have been shown to inhibit and trap PARP2 in an analogous manner to PARP1 (Murai et al., 2012, 2014). Furthermore, these drugs also are able to bind to numerous other PARP catalytic domains, including PARP3, 4, 5a, 5b, 10, 12, 15 and 16 (Wahlberg et al., 2012). How the effects of these inhibitors on the other members of the PARP superfamily might potentiate or undermine the efficacy of PARP inhibitors, or mediate their side effects, is currently unknown.

Finally, recent work has raised the possibility of PARP inhibitors being effective against tumours beyond BRCA1/2 deficient breast and ovarian cancers, for example olaparib has promising activity in phase II clinical trials against metastatic prostate cancers with DNA repair defects (Mateo et al., 2015). Thus with proper patient stratification and tumour genotyping, PARPi may have wider uses in oncology than their current applications.

1.7 Aims

Whilst the biological roles of PARPs has been a subject of intense research focus, much remains to be understood in how these enzymes contribute to the DDR. Each of PARP1, PARP2 and PARP3 have been implicated in the resolution of DNA SSBs, but what precise roles of these enzymes play in the repair process, how their different functions might be distinct or overlap, and to

what extent they can compensate for each other are all uncertain. Similarly in the cellular response to replication stress, PARP1 has been shown to promote resolution of stalled/collapsed replication forks, but how this integrates with the other functions of PARP1 and indeed potential contributions of PARP2 and PARP3 is uncertain. Furthermore, how these observations might interface with the recently uncovered roles of PARPs in replication fork reversal is not understood. Finally PARP inhibitors that target multiple PARPs are currently exploited to selectively kill tumours carrying BRCA1/2 mutations. However, the mechanism of this toxicity is not fully understood, and the precise complement of PARPs which must be targeted to achieve maximal efficacy of these agents is unknown

Therefore, the aims of this thesis were to firstly better understand the individual functions of PARPs within the DNA damage response, with a primary focus on the potential roles of PARP1, PARP2 and PARP3 in human BER/SSBR. Secondly, I wished to establish the nature of the relationship between these PARPs in the repair of base damage/SSBs, for example whether in the absence of one PARP, cells become more reliant on the function of another PARP. Thirdly I sought to assess the contribution of these PARPs to the efficacy of PARP inhibitors in killing HR-deficient cells. Finally, I aimed to search for novel DDR-factors that show a synthetic lethal relationship with the loss of specific PARPs, to gain insight into the mechanism of this process and potentially widen the applications of synthetic lethal strategies with PARPs in the clinic.

2. Materials and Methods

2.1 Materials

2.1.1 Buffers

DNA loading dye

0.25 % Bromophenol blue

40 % Sucrose

Phosphate Buffered Saline (PBS)

10 mM phosphate buffer

2.7 mM KCl

137 mM NaCl

(pH 7.4)

PBS-T

As above, supplemented with 0.05 % Tween-20

TBS-T

2.48 mM Tris-Cl

137 mM NaCl

(pH 7.4)

0.2 % Tween-20

SDS-PAGE Running Buffer

25 mM Tris-Cl

192 mM glycine

0.1 % SDS

SDS-Page Transfer Buffer

50 mM Tris-Cl

384 mM glycine

20% methanol

SDS-PAGE Transfer Buffer (semi-dry)

48 mM Tris-Cl

39 mM glycine

20 % methanol

0.375 % SDS

SDS Loading Buffer

25 mM Tris-Cl (pH 6.8)

10 % glycerol

0.125 % bromophenol blue

2% SDS

80 mM DTT

TAE

40 mM Tris-Cl

1 mM EDTA

20 mM acetic acid

(pH 8.2)

DNA Extraction Buffer

10 mM Tris-Cl pH 8.0

1 mM EDTA

25 mM NaCl

200 µg.mL proteinase K

Chromatin Extraction Buffer 1

10 mM Tris-Cl pH 7.5

150 mM NaCl

1.5 mM $MgCl_2$

340 mM sucrose

10 % glycerol

1 mM DTT

Protease Inhibitor Cocktail (Sigma-Aldrich)

0.1 % Triton-X 100

Chromatin Extraction Buffer 2

3 mM EDTA

0.2 mM EGTA

1 mM DTT

Protease Inhibtor Cocktail (Sigma-Aldrich)

Sucrose Buffer

10 mM Tris-Cl pH 7.5

20 mM KCl

250 mM sucrose

2.5 mM $MgCl_2$

Protease Inhibitor Cocktail (Sigma-Aldrich)

0.3 % Triton-X 100

NETN150

50 mM Tris-Cl pH 8.0

150 mM NaCl

2 mM EDTA

0.5 % NP-40

2.5 mM $MgCl_2$

Protease Inhibitor Cocktail (Sigma-Aldrich)

25 U/mL Benzonase nuclease

Click Reaction Buffer

100 mM Tris-Cl pH 8.0

4 mM $CuSo_4$

50 mM sodium ascorbate

20 µM azide dye

LB Agar

1 % bactotryptone

0.5 % yeast extract

85 mM NaCl

1.5 % Agar

LB broth

1 % bactotryptone

0.5 % yeast extract

85 mM NaCl

2.2 Methods

2.2.1 Cell culture and generation of CRISPR-mediated parpΔ cells

U2OS cells were cultured in DMEM supplemented with 10% FBS and 1% penicillin/streptomycin. DLD1 cells ($BRCA2^{-/+}$ and $BRCA2^{-/-}$), were a kind gift of F. Esashi (Dunn School of Pathology, Oxford) and were cultured in RPMI supplemented with 10% FBS and 1% Penicillin/Streptomycin. Flp-In T-Rex HT1080 cells expressing FE-PALB2 were also a kind gift of F. Esashi (Dunn School of Pathology, Oxford), and were cultured in DMEM as above, further supplemented with 10 µg/mL blasticidin and 100 µg/mL hygromycin. Expression of FE-PALB2 was induced with 5 µg/mL doxycyclin (Sigma-Aldrich) for 24 hours. All cell lines were maintained between 10 and 80 % confluency and split every 2-3 days. U2OS cell identity was verified by STR profiling (Eurofins cell line authentication service).

For siRNA-mediated knockdown, cells were transfected with 50 nM total siRNA using Dharmafect-1 (Dharmacon), transfected again after 24 hours, then allowed to recover for 48 hours before use. siRNA pools containing four

different siRNA sequences were obtained from Dharmacon, either ON-Target Plus (PARP2-16, Rad52, BLM, Fbh1) or siGenome (XRCC1). The relevant non-targeting siRNA pools were used for negative controls.

For the generation of CRISPR-mediated knockout cell lines, gRNA sequences were designed using the MIT CRISPR design tool (http://crispr.mit.edu/), and cloned into vector pX462 or pX462v2. Cells were transfected with the relevant gRNA constructs using Turbofect (Dharmacon) according to manufacturer's instructions, then selected with 2, 3 or 4 μg/mL puromycin for 24 hours, before being plated at low density. After 10-14 days growth, clonal colonies were isolated and expanded for screening.

Cell lines lacking PARP1 or PARP2 were screened by Western blotting of whole cell extracts for the absence of the relevant protein. Cells transfected with gRNAs targeting PARP3 were screened by PCR using primers flanking the gRNA target site, to identify cell lines containing insertions or deletions. Genomic DNA extracts were generated by resuspending cells in DNA extraction buffer and heating to 65 °C for 30 minutes, then 95 °C for 2 minutes. PCR was performed using PCRBIO Taq polymerase (PCR Biosystems) according to the manufacturer's instructions.

Candidate cell lines containing gene disruptions were further verified by Western blotting and PCR across the gRNA target sites. Products from these PCR reactions, using PCRBIO HIFI polymerase (PCR Biosystems), were cloned into pJet1.2 (ThermoFisher) according to manufacturer's instructions and subjected to Sanger sequencing (Source Biosciences), to confirm the presence of frameshift mutations. *parp1*Δ*parp2*Δ cells were generated by

disrupting PARP1 in a *parp2*Δ background. *parp1*Δ *parp3*Δ cells were generated by disrupting PARP3 in a *parp1*Δ background. *parp1*Δ*parp2*Δ*parp3*Δ cells were generated by disrupting PARP2 in a *parp1*Δ*parp3*Δ background.

2.2.2 Protein extract preparation and Western blotting

Whole cell extracts were prepared by washing cells in PBS before boiling in 1x SDS loading buffer for 5 minutes.

Nuclear extracts were prepared by washing cells in PBS before resuspending in sucrose buffer and incubation on ice for 5 minutes. Nuclei were pelleted by centrifugation at 1800 g, before resuspension in NETN150 buffer and incubation on ice for 30 minutes. Protein concentration was determined by Bradford assay.. Extracts were diluted to the appropriate concentration, before boiling for 5 minutes in 1x SDS loading buffer.

Chromatin extracts were prepared by washing cells in PBS, before resuspending in chromatin extraction buffer 1 and incubation on ice for 10 minutes. Following centrifugation at 18,000 xg, the pellet was resuspended in chromatin extraction buffer 2, and incubated on ice for 30 minutes. Samples were centrifuged again at 18,000 g, and the pellet resuspended in 1x SDS loading buffer and boiled.

Protein extracts were analysed by SDS-polyacrylamide gel electrophoresis (SDS-PAGE), run alongside a prestained protein ladder (PageRuler Plus, Fermaentas) on single percentage gels at 150 V. Proteins were transferred to PVDF membranes (Millipore, 0.45 µm pores) at 250 mA for 2 hours, or by semi-dry blotting (BioRad TransBlot Turbo) according to manufacturer's instructions. Following blocking in 5 % milk in TSB-T for 30 minutes, cells were incubated in

primary antibody overnight at 4 °C. After three washes in TSB-T, membranes were incubated in 5 % milk in TSB-T containing the appropriate secondary antibody diluted to 1:10,000 for 1 hour. Following further extensive TSB-T washing, membranes were incubated in ECL reagent (Millipore), before being visualised on autoradiographic film (GE Healthcare Life Sciences).

Primary antibodies used in this work are detailed as follows:

Antibody	Species	Source	Dilution (WB)	Dilution (IF)
PARP1	Mouse, monoclonal	Bio-Rad, MCA1522G	1:1000	
PARP2	Mouse, monoclonal	Enzo, ALX-804-639L	1:1000	
PARP3	Rabbit, polyclonal	A gift of F. Dantzer	1:1000	
PARP10	Rabbit, polyclobal	Novus Biologicals, NB100-2157	1:1000	
XRCC1	Mouse, monoclonal	Abcam, ab1838	1:1000	
Actin	Goat, polyclonal	Santa Cruz, SC-1615	1:1000	
γH2AX	Mouse, monoclonal	Millipore, JBW301		1:1000
Rad51	Rabbit, polyclonal	A gift of F. Esashi, 7946		1:1000
RPA32	Rabbit, polyclonal	Bethyl, A300-244A		1:1000
RPA32 S4/8	Rabbit, polyclonal	Bethyl, A300-245A	1:1000	
GFP	Mouse, monoclonal	Roche, 11814460001	1:1000	
Poly(ADP-ribose)	Protein linked to rabbit Fc domain	Millipore, MABE1031		1:1000

Rad52	Rabbit, polyclonal	Genetex, 5H9	1:1000	
BLM	Rabbit, polyclonal	Calbiochem, DR1034	1:1000	
H3	Goat, polyclonal	Abcam	1:2000	
Fbh1	Mouse, monoclonal	Abcam, ab58881	1:100	

Secondary antibodies used in this work are detailed as follows:

Antibody	Species	Source	Dilution
Anti-Rabbit HRP	Goat	DAKO	1:10,000
Anti-Mouse HRP	Rabbit	DAKO	1:10,000
Anti-Goat HRP	Rabbit	DAKO	1:10,000
Anti-Rabbit FITC	Mouse	DAKO	1:80
Anti-Mouse TRITC	Rabbit	DAKO	1:80

2.2.3 Clonogenic survival assays

Cells were detached with trypsin and counted on a haemocytometer, before plating 400 cells into each well of a 6-well plate. The following day, cells were exposed to inhibitors or DNA damaging agents, before extensive washing in PBS and recovery in fresh media for 10-14 days. Cells were fixed in 100% methanol for 20 minutes at -20 °C, then stained with 0.5% Crystal Violet (Sigma Aldrich) for 20 minutes. Colonies of more than 50 cells were scored as viable, and the survival percentage calculated relative to the untreated cells. For MMS (Sigma-Aldrich), hydrogen peroxide (Sigma-Aldrich) or phleomycin (Sigma-Aldrich) treatments, cells were exposed to the indicated concentrations of the agent for 1 hour before washing and recovery in fresh media. In experiments

combining these treatments with PARP inhibitors, cells were pre-treated with olaparib (Cambridge Bioscience) or rucaparib (Cambridge Bioscience) for 1 hour before DNA damage, and for 24 hours following DNA damage exposure. For clonogenic survival assays using Rad51 inhibitors, cells were exposed to B02 (Sigma), with or without olaparib or DNA-PKi (Nu7441, Tocris Bioscience), for 48 hours.

2.2.4 Immunofluorescence

Cells were detached by trypsin and counted on a haemocytometer, before plating $1x10^5$ cells/mL onto glass coverslips. The following day, cells were exposed to DNA damaging agents and 1 μM EdU (Sigma) for 1 hour, and after extensive washing in PBS allowed to recover in fresh media as appropriate. Where necessary, cells were pre-extracted in 0.5% Triton-X 100 for 5 minutes at 4 °C. Cells were then fixed in 4% paraformaldehyde at 4 °C for 20 minutes, and permeabilised in 0.5% Triton-X 100 for 5 minutes at 4 °C. Coverslips were then blocked in 3% BSA in PBS-T for 30 minutes. EdU was labelled by incubating cells in Click reaction buffer for 30 minutes. Following washing in PBS, cells were incubated with primary antibody diluted in 3% BSA for 2 hours at room temperature, in the dark. Coverslips were washed 3 times in PBS-T, and incubated in the appropriate fluorescently-labelled secondary antibody, diluted to 1:80 in 3% BSA for 1 hour, at room temperature in the dark. Finally, following further PBS-T washing, cells were mounted on slides in Vectasheild containting DAPI (Vector Laboratories). Samples were visualised using a Zeiss IX70 microscope, through a 10x or 100x oil-immersion objective lens. Each experiment was independently repeated at least three times, with a total of at least 100 cells analysed per condition. Images were processed in ImageJ.

2.2.5 Alkaline comet assays

The method was modified from a previously described procedure to detect DNA strand breaks and alkali labile sites[53, 54]. Cells were diluted to a concentration of $1x10^5$ / ml in PBS. The cell suspension was mixed with an equal volume of warm 2% agarose solution (Type VII). 500 μl of the suspension was spread evenly onto poly-lysine coated slides that are pre-coated with 0.3% agarose (Type 1). For cell lysis, the slides were soaked in 0.3 M NaOH/1 M NaCl/0.1% N-lauroylsarcosine, pH 11.5 in the dark for 1 hour followed by two 30 minute washes in 0.3 M NaOH, 2 mM EDTA. Slides were electrophoresed at 75 mA for 30 minutes in the same buffer at pH 11.5. Following electrophoresis slides were flooded with neutralisation buffer (Tris-Cl pH 7.5) for 30 minutes. Slides were dried overnight in the dark, and subsequently rehydrated in distilled water for 30 minutes in the dark. Slides were stained with SYBR gold (1:10,000 in water) for 20 minutes and then rinsed in water before leaving to dry overnight. The percentage DNA in the tail and Olive moment were determined using OpenComet. The area and mean pixel intensity of the head and the tail of the comets were measured to determine the percentage DNA in the tail for the individual cell. For each experimental sample 300 cells per time point (from duplicate slides) were analysed and the mean Olive Moment was determined.

2.2.6 Screen to identify novel DDR factors that display a synthetic lethal relationship with PARP loss

Cells were reversed transfected with QIAGEN siRNA pools targeting 580 genes linked to the DNA damage response. Each pool contained 4 individual siRNAs, and QIAGEN allstars non-targeting and death controls were included in each

plate. A total of 0.05 µL/well Dharmafect-1 was used to transfect cells with a final concentration of 10 nM siRNA in 96-well plate. Liquid handling was performed on a JANUS automated workstation. The following day, the cells were rescued in fresh media, and allowed to grow for 6-8 days. Cell viability was assessed by the addition of 200 µL of 10 µg/mL resazurin and incubation at 37 °C for 1 hour. Fluorescence was determined on a plate reader ($560_{ex}/590_{em}$ nm). Fluorescence readouts were used to calculate Z-scores for each siRNA pool, and identify potential hits. Z-scores and Pearson's correlation coefficients were calculated using the standard formulae.

2.2.7 Statistical analysis

Statistical significance was determined using a two-tailed Student's t-test and is indicated as: NS, not significant; * $p < 0.05$; ** $p<0.01$; *** $p<0.001$.

3. Generation and characterisation of cell lines disrupted for DNA-dependent PARPs

3.1 Introduction

3.1.1 PARP1, PARP2 and PARP3 function in the DNA damage response

The addition of poly(ADP-ribose) (PAR) to proteins has long been understood to be a post-translational modification which contributes to the DNA damage response. Early reports identified a drop in cellular NAD^+ after various forms of DNA damage (Campagnari et al., 1966), and later an accumulation of PAR chains in damaged cells (Berger et al., 1979). PARP1, an enzyme specifically activated by damaged DNA structures and capable of catalysing the synthesis of PAR chains was subsequently identified (Alkhatib et al., 1987). Loss or inhibition of this enzyme results in sensitivity of cells to DNA damage, confirming the important role of PARP1 in the DNA damage response (Durkacz et al., 1980; Trucco et al., 1998).

However, residual ADP-ribosylation activity is apparent in cells derived from PARP1 knockout mice after exposure to base damage (Amé et al., 1999), indicating additional PARPs beyond PARP1 may exist. These observations led to the identification of PARP2, an enzyme which could also catalyse the formation of PAR following activation by damaged DNA structures. Whether PARP2 is responsible for the residual PAR formed in PARP1 deficient cells has not been formally assessed. Nevertheless, PARP2 knockout mice showed a delay in the ligation of strand breaks following exposure to base damaging

agents, indicating a functional role of PARP2 independent of PARP1 (Schreiber et al., 2002). However, redundancy between PARP1 and PARP2 is implied by the embryonic lethality of PARP1$^{-/-}$/PARP2$^{-/-}$ double knockout mice, which die at the onset of gastrulation (Ménissier de Murcia et al., 2003a). The inability to isolate mice or cell lines devoid of both PARP1 and PARP2 has hampered investigations into their relationship in the DDR, resulting in an incomplete understanding of how these enzymes function together to facilitate DNA repair.

PARP3 has been identified as another DNA-dependent PARP, initially shown to be activated by blunt dsDNA ends (Rulten et al., 2011). This led to the discovery of a role for PARP3 in the DNA DSB repair pathway NHEJ by promoting the retention of Ku and APLF at breaks (Beck et al., 2014; Boehler et al., 2011; Rulten et al., 2011). More recently, PARP3 has also been suggested to have a role in DNA SSB repair, as it is strongly activated by 5' phosphorylated nicks *in vitro*, and avian cells lacking PARP3 show delays in the ligation of SSBs induced by ionising radiation (Grundy et al., 2016). However, these cells lack a homologue of PARP2, making comparisons with human SSBR difficult.

3.1.2 Additional members of the PARP superfamily function in the DNA damage response

Homology searches using the sequence of the conserved PARP catalytic domain of PARP1 have identified a number of additional PARPs in the human genome. The PARP superfamily is currently composed of 17 members (Gibson and Kraus, 2012). Considerable work has been invested in trying to understand

the function of these additional PARPs, with three of them, PARP9, PARP10 and PARP14, also being identified to function in the DDR.

PARP9 plays a role in DNA DSBR (Yan et al., 2013), with cells depleted of this protein displaying delayed kinetics of repair of IR induced breaks. The macrodomain of PARP9 binds to PAR, which recruits PARP9 to sites of damage, subsequently promoting the localisation of 53BP1 to the break (Yan et al., 2013). PARP10 has been suggested to function in translesion DNA synthesis, and interacts with ubiquitinated PCNA via both a PIP domain and ubiquitin-binding motif. Cells depleted of PARP10 show sensitivity to agents which induce replication stress and display hallmarks of genome instability (Nicolae et al., 2014). PARP14 has a role in the restart of stalled replication forks, with cells depleted of this factor demonstrating sensitivity to agents that induce replication stress, including HU and aphidicolin. These cells also display a reduced efficiency of HR, and persistent Rad51 foci, implying a role for PARP14 in HR (Nicolae et al., 2015).

Interestingly, none of these PARPs have been identified to recognise or be activated by damaged DNA, meaning their mechanism of involvement in DNA repair may be distinct from the DNA-dependent PARPs. Indeed PARP9 is catalytically inactive, and instead acts as a scaffold protein, localising to damage through it PAR-binding macrodomain and promoting the recruitment of other factors to the break (Yan et al., 2013). PARP14 also possesses a macrodomain, suggesting it may also function in concert with other PARPs (Nicolae et al., 2015). Whilst the catalytic activity of PARP10 appears to be important for its DNA damage roles, how its ADP-ribosyltransferase activity is regulated, and which factors are modified by PARP10 remains unknown

(Nicolae et al., 2014). It is conceivable that additional members of the PARP superfamily may also have DDR roles that are as yet uncharacterised.

3.1.3 Aims

Despite extensive work examining the roles of individual PARPs in the DDR, very little is known about how these PARPs function in relation to one another. Investigation into the relationship between PARP1 and PARP2 has been hampered by the embryonic lethality of double knockout mice. Whilst recent work has identified a role of PARP3 in SSBR in avian cells, whether this function is preserved in human cells, and how it relates to the roles of PARP1 and PARP2 in this process, remains unexplored. Therefore, the aim of this chapter is to characterise the nature of the redundancy between the PARP1, PARP2 and PARP3 in the resolution of SSBs and base damage. I used CRISPR-Cas9 genome editing to generate human cell lines disrupted for these PARPs alone and in combination, and assessed the sensitivity profiles of these cell lines to various DNA damaging agents. Furthermore I considered whether any additional PARPs beyond PARP1, PARP2 and PARP3 could also function in the resolution of these lesions.

3.2 Results

3.2.1 Generation and verification of *parp1Δ*, *parp2Δ* and *parp3Δ* cell lines

In order to assess the relationship between the different DNA-dependent PARPs, I decided to use CRISPR-Cas9 genome editing to disrupt these genes in different combinations in U2OS cells. I then used these cell lines to assess

the impact of loss of specific PARPs on survival to various forms of DNA damage. This approach has advantages over using siRNA or shRNA, where protein depletion is unlikely to be complete. The use of CRISPR allows an assessment of phenotypes in defined genetic backgrounds.

Initially, I generated PARP1, PARP2 and PARP3 single knockouts using a ‘double nickase’ CRISPR strategy, to reduce the potential for off-target binding of guideRNAs (gRNAs) to produce additional mutations in our cell lines. The basis of this technique is to generate two sets of closely spaced CRISPR gRNAs for each required gene disruption, and co-transfect cells with both, along with a mutant D10A Cas9 which can only cleave one strand of the DNA at the target site. Thus each gRNA will introduce only a SSB at any off-target sites where it binds, which will be repaired in an error free manner by the SSBR machinery. At the target site, however, the two closely spaced SSBs will form a DSB, allowing repair by the error-prone c-NHEJ or alt-NHEJ pathways, and the introduction of frameshift indels to disrupt the desired gene.

Pairs of closely spaced gRNAs were designed targeting exons of PARP1, PARP2 and PARP3. Numerous design considerations impacted on the selection of both the targeted exon and the exact sequence of the gRNAs. These included predicted off-target gRNA binding sites, the position of the exon within the gene and any alternative splice forms of the target gene. In general, one would wish to minimise off target sites, disrupt in as early an exon as possible to prevent potential expression of truncated protein fragments, and make disruptions in constitutive exons so all protein isoforms are disrupted.

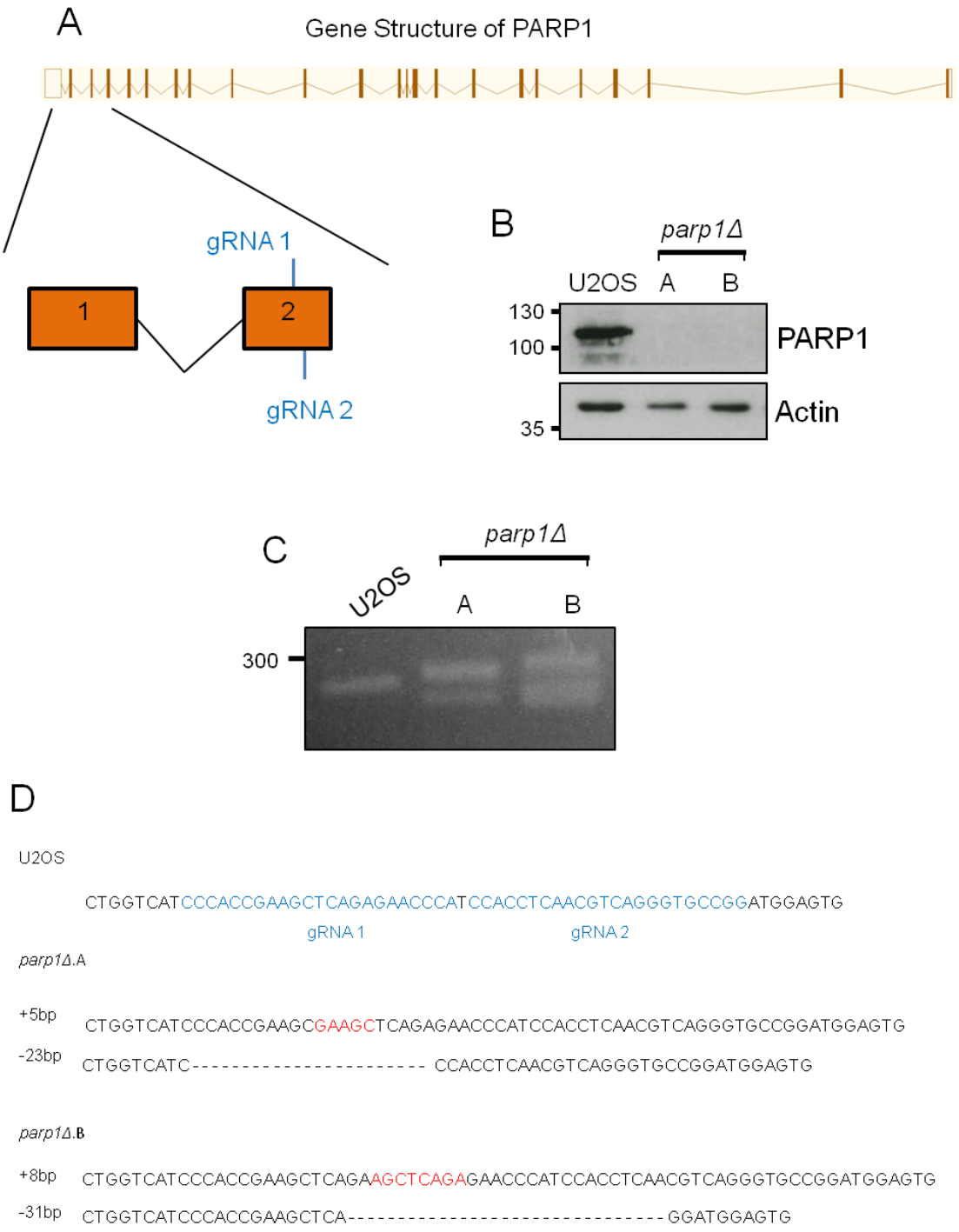
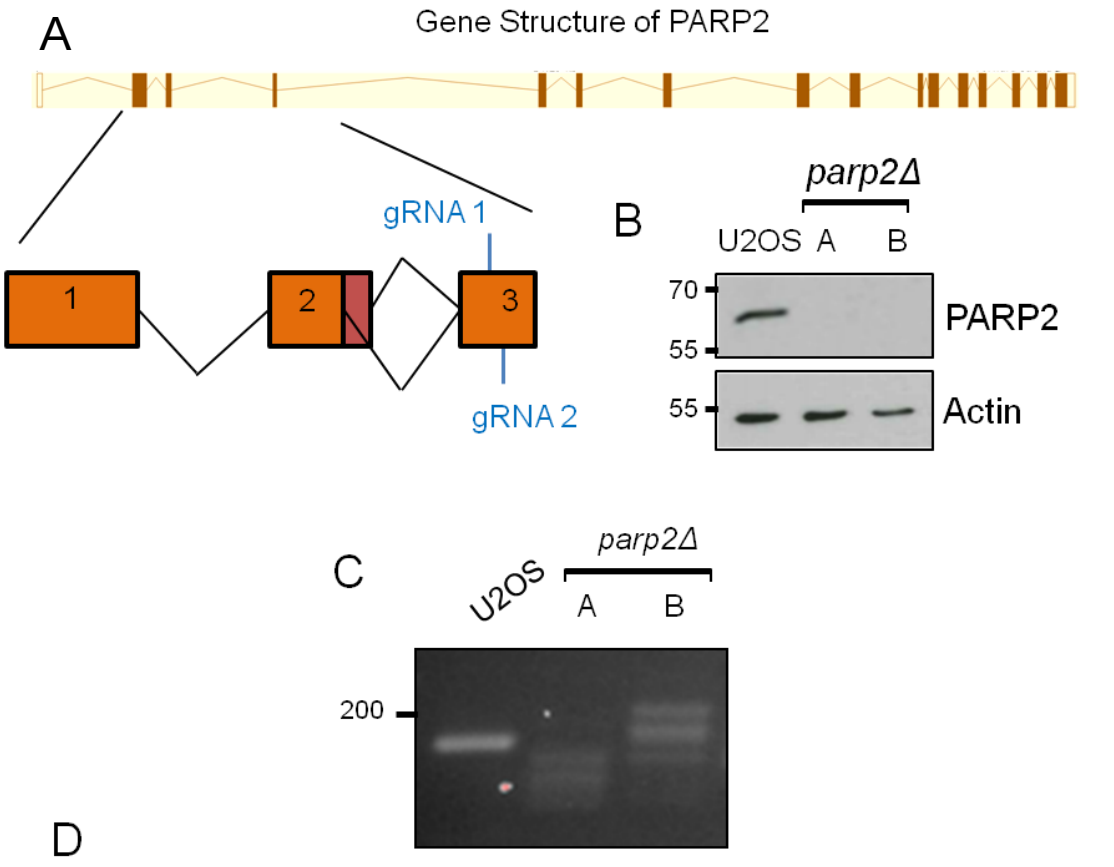


Figure 3.1: Generation and verification of *parp1Δ* cell lines A. The exon structure of PARP1. Exons are indicated by solid rectangles, introns by the connecting lines. Early exons are expanded, and the position of gRNAs is indicated by blue lines. **B.** Whole cell extracts were prepared from U2OS and two independent *parp1Δ* cell lines, and Western blotting performed with the indicated antibodies. **C.** PCR was performed across the CRISPR targeted locus within the PARP1 gene in U2OS and two *parp1Δ* cell lines, and the products analysed by agarose gel electrophoresis. **D.** Sanger sequencing of PCR products from **C** confirms they produce frameshift mutations and disrupt expression of PARP1. Wild-type sequence (U2OS) is shown with gRNA sites marked in blue. Red bases indicate insertions, dashes indicate deletions, and green bases indicate substitutions. Uppercase indicates exonic sequence.

The gRNAs were designed and cloned in collaboration with Dr. Andrew Bassett of the Oxford Genome Engineering Centre, using the MIT CRISPR design tool (http://crispr.mit.edu/). This tool identifies suitable gRNA sites, and scores them based on predicted off-target binding sequences within the human genome. gRNAs were designed within the first few suitable exons of each gene, before the highest scoring gRNA pairs were selected and cloned into the vector pX462. This contains the correct sequence context for gRNA expression, as well as Cas9n (D10A) and a puromycin resistance cassette for the selection of successfully transfected cells. The two best scoring pairs of gRNAs were tested by high-resolution melting analysis (performed by A. Bassett, data not shown), to verify their ability to cleave at the target site *in vivo*. The highest scoring pair of gRNAs that showed detectable activity by HRMA were selected for use in the generation of knockout cell lines.

PARP1 has only one known isoform, and gRNA sites with detectable activity via HRMA were found in exon 2 (Figure 3.1 A). PARP2 has 2 splice isoforms, one full length, and a variant missing 36 bp from the 3' end of exon 2. In order to disrupt both isoforms, gRNAs were designed targeting either exon 1 or exon 3. A pair of gRNAs with detectable activity was found in exon 3 (Figure 3.2 A). PARP3 also has two splice isoforms, one including and one excluding a short coding sequence on exon 1. An active pair of gRNAs was produced in exon 2, downstream of these alternative spicing events (Figure 3.3 A).

The resulting pairs of plasmids were transfected into U2OS cells and selected with puromycin for 24 hours. This is long enough to enrich for successfully transfected cells, but not so long that chromosomal integration of the plasmids might be encouraged. Following this selection, cells were plated at low density



D

U2OS

ctatctgtctttcctcagAATCTGTGAAGGCCTTGCTGTTAAAGGGCAAAGCTCCTGTGGACCCAGAG

parp2Δ.A gRNA 1 gRNA 2

-31bp ctatccgtctttcctcagAATCTGTGAAGG----------CCCAGAG

-40bp ctatctgtctttcctcagAATCTGT----------GAG

-46bp ctatctgtctt----------TGGACCCAGAG

-50bp ctatctgtctttcctc----------AG

parp2Δ.B

+8bp ctatctgtctttcctcagAATCTGTGAAGGCCTTGCTGTTAAAGGGCAAAGCTGCAAAGCTCCTGTGGACCCAGAG

+1bp ctatctgtctttcctcagAATCTGTGAAGGGCAAAGCTCGTGAAGGGCAAAGCTCCTGTGGACCCAGAG

-14bp ctatctgtctttcctcagAATCTGTG----------AAAGGGCAAAGCTCCTGTGGACCCAGAG

Figure 3.2: Generation and verification of *parp2Δ* cell lines A. The exon structure of PARP2. Exons are indicated by solid rectangles, introns by the connecting lines. Early exons are expanded, and red sections indicate alternatively spliced regions. Position of gRNAs is indicated by blue lines. **B.** Whole cell extracts were prepared from U2OS and two independent *parp2Δ* cell lines, and Western blotting performed with the indicated antibodies. **C.** PCR was performed across the CRISPR targeted locus within the PARP2 gene in U2OS and two *parp2Δ* cell lines, and the products analysed by agarose gel electrophoresis **D.** Sanger sequencing of PCR products from **C** confirms they produce frameshift mutations or affect the splice site and disrupt expression of PARP2. Wild-type sequence (U2OS) is shown with gRNA sites marked in blue. Red bases indicate insertions, dashes indicate deletions, and green bases indicate substitutions. Uppercase indicates exonic sequence and lower case indicates intronic sequence.

and allowed to form colonies, which were isolated to form clonal cell populations. These clones were screened for the absence of the appropriate PARP by Western blotting for PARP1 and PARP2 (data not shown). In the case of PARP3, where detection of the protein by Western blotting is difficult, I screened for potential *parp3Δ* cell lines using PCR around the gRNA binding sites, to identify potential indels within the PARP3 gene in each clone (data not shown).

Once candidate cell lines lacking PARP1, PARP2 and PARP3 were obtained, loss of the protein was confirmed by further Western blotting (Figure 3.1 B, 3.2 B and 3.3 B), and the presence of indels in the gene verified by PCR across the targeted region (Figure 3.1 C, 3.2 C and 3.3 C). However, the presence of indels, and lack of any visible wild-type size band, is not proof that the gene is truly disrupted. The indel must be a frameshift, meaning all downstream sequence in the gene will be read in the incorrect frame, and quickly lead to a premature STOP codon and complete loss of expression. Alternatively, the deletion could span an exon-intron boundary and affects the splice site. If at the 3' splice site, this would lead to exon skipping, and also potentially introduce a frameshift into the gene.

To confirm our cell lines lacking detectable protein expression did indeed contain indels predicted to disrupt protein expression, I cloned the products of the PCR reaction across the gRNA target site into a blunt ended cloning vector pJet1.2, and then subjected them to Sanger sequencing. This allowed us to fully characterise the genotype of each cell line, and confirm the loss of expression of PARP1, PARP2 and PARP3 in the appropriate cell lines.

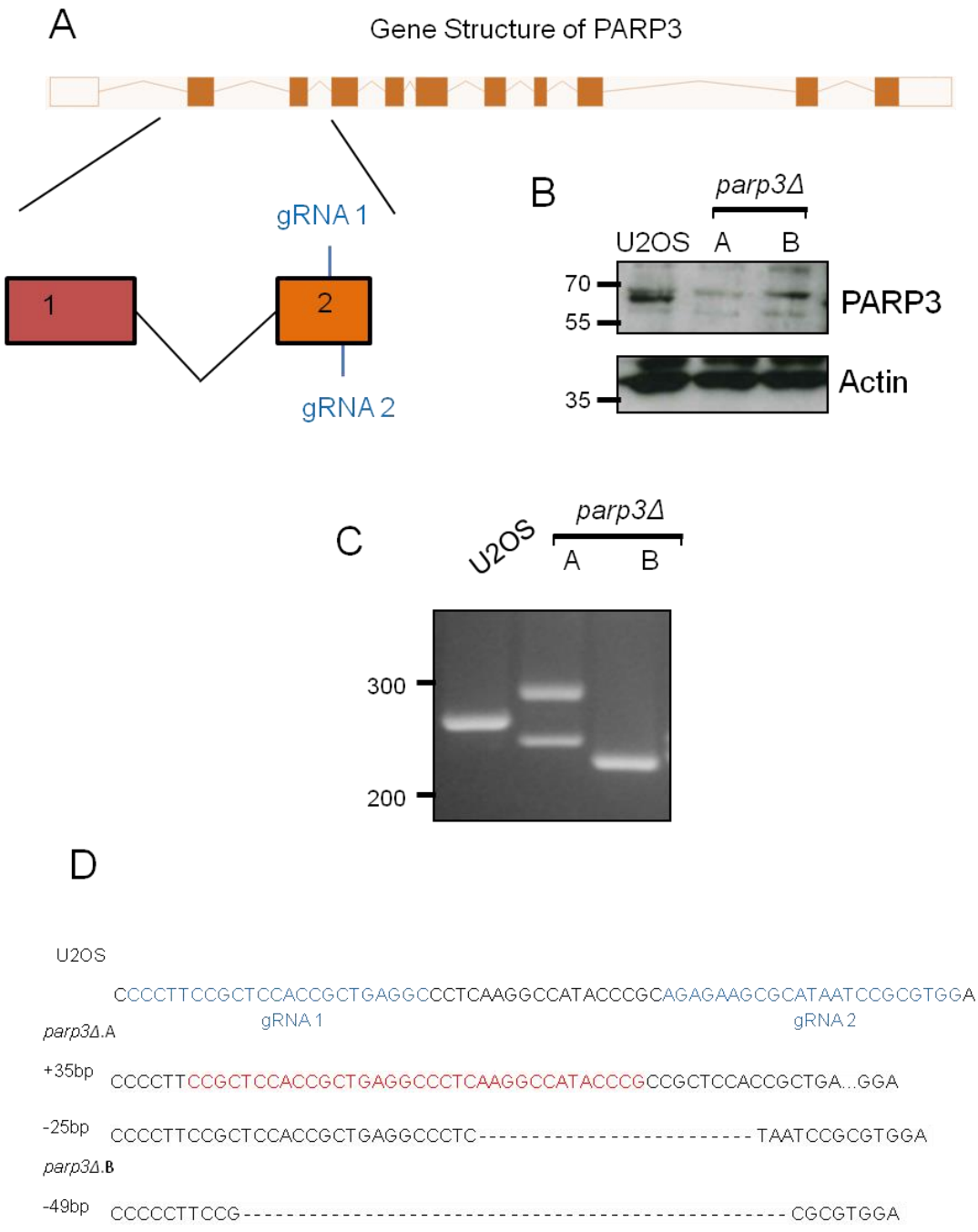


Figure 3.3: Generation and verification of *parp3Δ* cell lines A. The exon structure of PARP3. Exons are indicated by solid rectangles, introns by the connecting lines. Early exons are expanded, and red sections indicate alternatively spliced regions. Position of gRNAs is indicated by blue lines. **B.** Whole cell extracts were prepared from U2OS and two independent *parp3Δ* cell lines, and Western blotting performed with the indicated antibodies. **C.** PCR was performed across the CRISPR targeted locus within the PARP3 gene in U2OS and two *parp3Δ* cell lines, and the products analysed by agarose gel electrophoresis **D.** Sanger sequencing of PCR products from **C** confirms they produce frameshift mutations or affect the splice site and disrupt expression of PARP3. Wild-type sequence (U2OS) is shown with gRNA sites marked in blue. Red bases indicate insertions, dashes indicate deletions, and green bases indicate substitutions. Uppercase indicates exonic sequence.

Each of the *parp1Δ* cell lines carry a pair of mutations, either an insertion of 5 bp and a deletion of 23 bp, or an insertion of 8 bp and deletion of 31 bp (Figure 3.1 D). All of these indels produce frameshift mutations, and are wholly contained within exon 2. The *parp2Δ* cell lines carry multiple indels, as evidenced by the numerous visible bands for each line (Figure 3.2 D). Indeed *parp2Δ*.A carries four deletions, two of 31 bp and 40 bp which produce frameshifts with exon 3, and two larger deletions, of 46 bp and 50 bp, which disrupt the invariant AG at the 3' splice site of intron 2. This would be predicted to cause skipping of the entire 71 bp of exon 3, causing the rest of the gene to be out of frame. In contrast, *parp2Δ*.B carries two insertions and a deletion, all of which give rise to frameshifts within the exon. The *parp3Δ* cell lines have either a 35 bp insertion and 25 bp deletion, or a 49 bp deletion, all of which are entirely within exon 2, and all of which give rise to frameshifts (Figure 3.3 D).

3.2.2 DNA damage sensitivity profiles of *parp1Δ, parp2Δ and parp3Δ* cell lines

Having generated and verified cell lines disrupted for PARP1, PARP2 and PARP3, I next wished to establish the sensitivity profiles of cells lacking these PARPs to different DNA damaging agents. If cells lacking certain PARPs show sensitivity to particular forms of DNA damage, this could indicate that they are functioning in a particular repair pathway. Sensitivity profiles of cell lines can be determined using a clonogenic survival assay.

Consistent with previous studies using siRNA (Ma et al., 2012; Trucco et al., 1998) I observe an enhanced sensitivity of *parp1Δ* cells, over and above that of wild-type U2OS cells, to the base methylating agent methyl methanesulfonate

(MMS) and to the single strand break inducing agent H_2O_2 (Figure 3.4 A and B). In contrast, the CRISPR-derived *parp2Δ* cells are not overtly sensitivity to MMS or H_2O_2 (Figure 3.7 B and 3.9), indicating U2OS cells do not rely on the presence of PARP2 for the resolution of these lesions. Recent work on PARP3 identified a role in c-NHEJ (Rulten et al., 2011), and consistent with this I observe a sensitivity of *parp3Δ* cells to the DSB-inducing agent phleomycin (Figure 3.4 C), but not to the base methylating agent MMS (Figure 3.12 A).

3.2.3 Additional PARP(s) function in the absence of PARP1 in response to MMS

The aim of this chapter is to characterise the redundancy between PARPs in the DNA damage response. Whilst *parp1Δ* cells show sensitivity to MMS, *parp2Δ* and *parp3Δ* cells are able to tolerate this agent equally well as parental U2OS cells. However, these observations do not exclude the possibility that PARP2 or PARP3 could function in the absence of PARP1 to protect cells from MMS induced damage. This could either be through direct redundancy with PARP1, or by promoting resolution of lesions through alternate PARP1-independent repair pathways.

In order to extend this analysis to the redundancy between PARPs I decided to take advantage of the PARP inhibitor olaparib, which can inhibit multiple members of the PARP superfamily, including PARP1, PARP2 and PARP3 (Wahlberg et al., 2012). I reasoned that if additional PARPs were contributing to cellular survival in the absence of PARP1, treatment with PARP inhibitors would further sensitise *parp1Δ* cells to DNA damaging agents. To test this hypothesis, I pre-treated *parp1Δ* cells with olaparib, and assessed cell

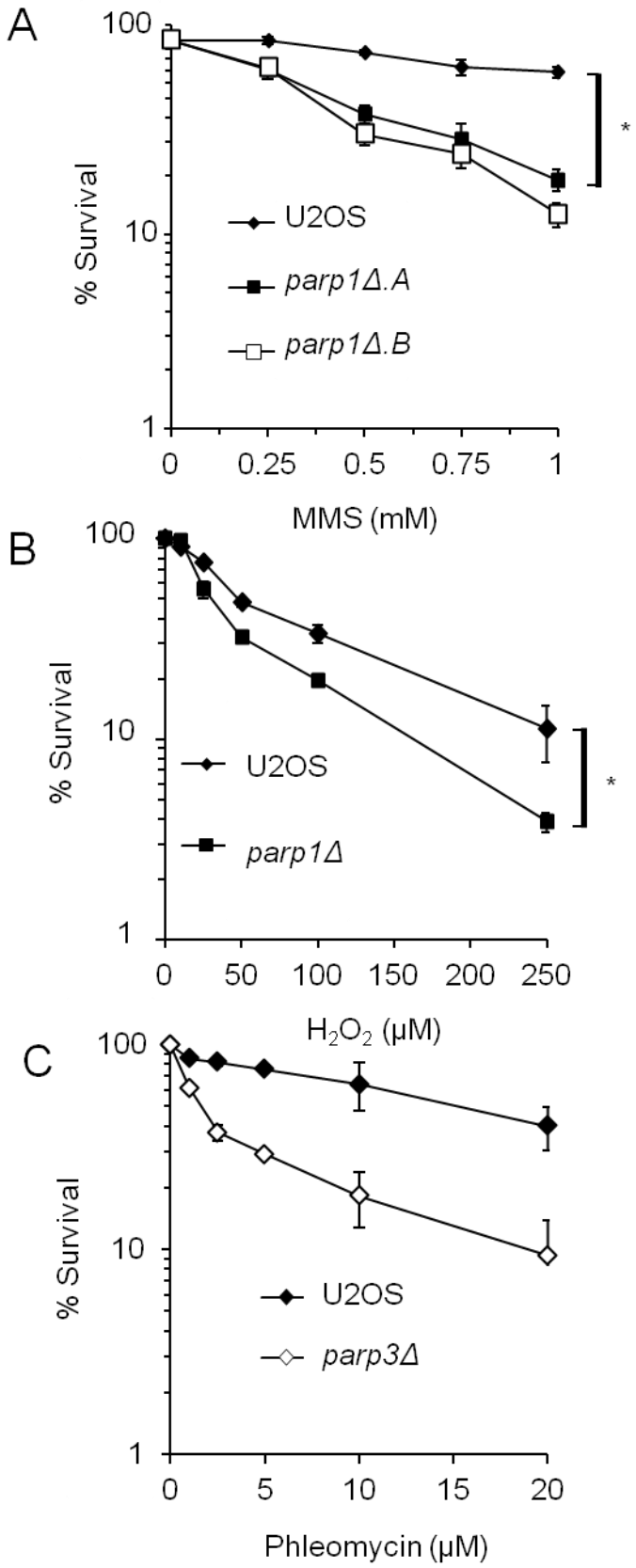


Figure 3.4: Sensitivity profiles of *parp1Δ* and *parp3Δ* cell lines to various DNA damaging agents A. U2OS and *parp1Δ* cells were exposed to MMS and cell survival assessed by clonogenic assay. **B.** U2OS and *parp1Δ* cells were exposed to H_2O_2 and cell survival assessed by clonogenic assay. **C.** U2OS and *parp3Δ* cells were exposed to phleomycin and cell survival assessed by clonogenic assay. Error bars indicate the standard error of the mean between three independent experiments.

viability following exposure to MMS. A substantial additional sensitisation of *parp1Δ* cells to MMS in the presence of olaparib is apparent, indicating that additional PARP(s) may indeed be functioning in the absence of PARP1 to promote cellular survival to base damage (Figure 3.5 A).

To further confirm that additional PARPs are functioning in the absence of PARP1, I assessed the induction of ADP-ribosylation using immunofluorescence. ADP-ribosylation can be visualised by staining cells with an anti-(poly-ADP) ribose binding reagent, composed of a recombinant PAR-binding domain fused to a rabbit antibody Fc domain. Staining cells with this reagent after exposure to MMS, followed by quantification of the nuclear fluorescence signal provides a measure of PAR induction. In U2OS cells, a robust ADP-ribosylation response can be detected after a one hour exposure to MMS. Consistent with PARP1 functioning in the cellular response to MMS, this signal is significantly reduced in *parp1Δ* cells (Figure 3.5 B). Importantly however, a modest induction of ADP-ribosylation can still be detected, providing further evidence of another PARP beyond PARP1 signalling in response to MMS-induced lesions.

3.2.4 PARP1 and PARP2 share overlapping roles in response to base damage

Given the previously suggested roles for PARP2 in responding to base damage, alongside the fact olaparib can strongly inhibit the activity of PARP2, I hypothesised PARP2 may be functioning in *parp1Δ* cells to promote cellular

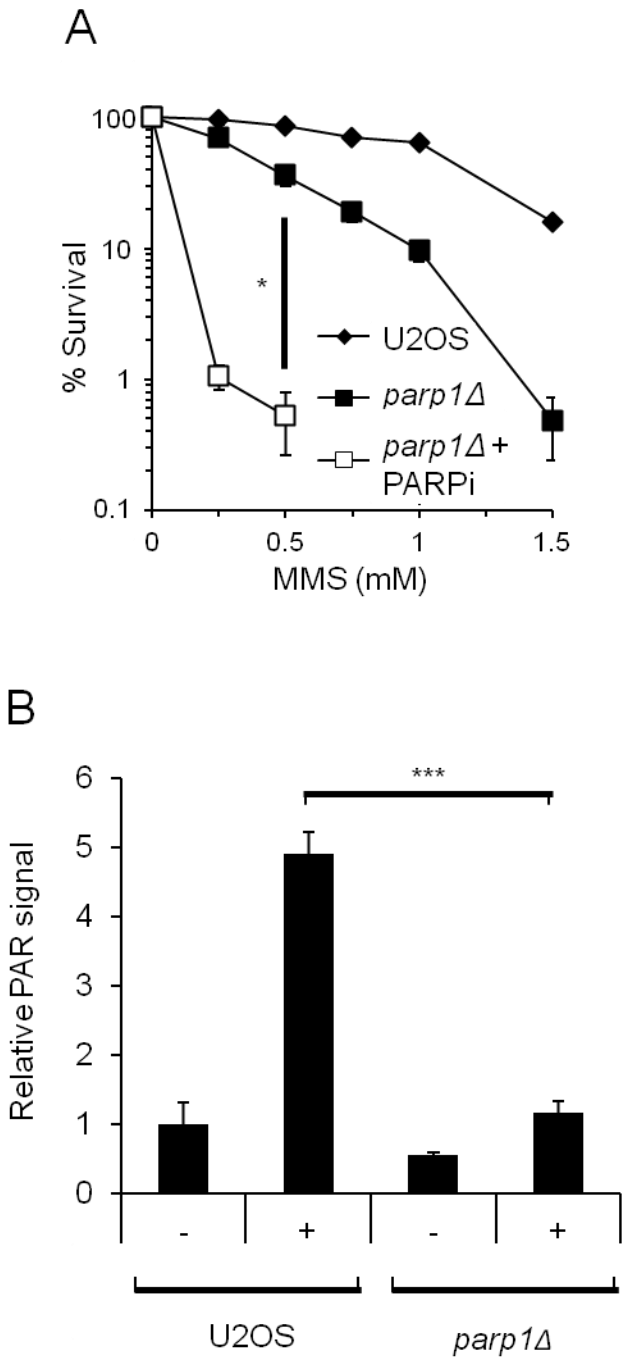
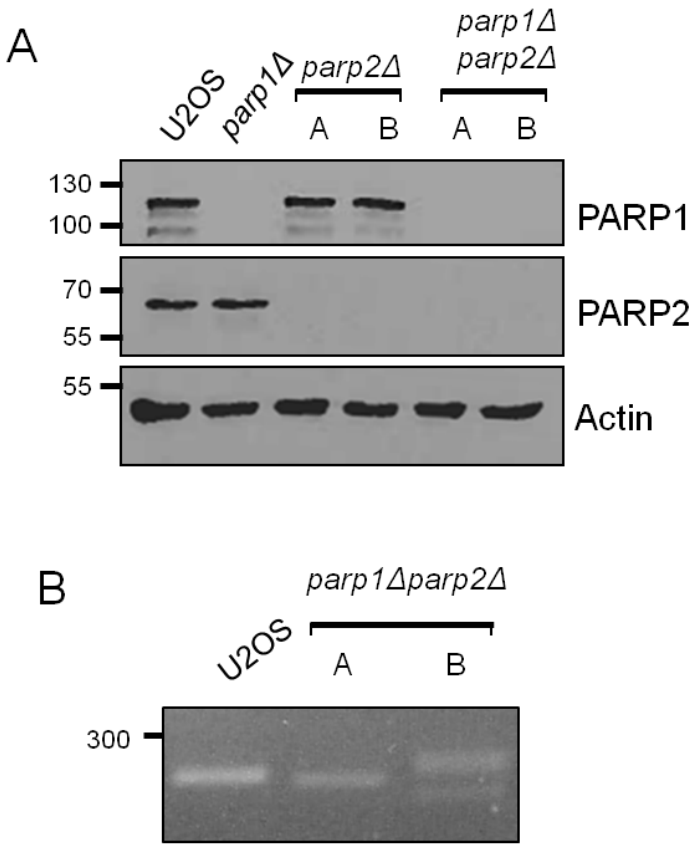


Figure 3.5: Additional PARPs function in response to MMS in the absence of PARP1 A. U2OS and *parp1Δ* cells, with or without 10 μM olaparib (PARPi) exposure, were exposed to MMS and cell survival assessed by clonogenic assay. **B.** U2OS and *parp1Δ* cells, were left untreated (-) or exposed to 1.5 mM MMS for 1 hour, and ADP-ribosylation was assessed by immunofluorescence. Error bars indicate the standard error of the mean between three independent experiments.



C

U2OS

GCTGGTCATCCCACCGAAGCTCAGAGAACCCATCCACCTCAACGTCAGGGTGCCGGATGGAGT

parp1Δparp2Δ.A

-7bp GCTGGTCATCCCACCGAAGGTCAGGG-------CCACTCAACGTCAGGGTGCCGGATGGAGT

parp1Δparp2Δ.B

+4bp GCTGGTCATCCCACCGAAGCTAGCTCAGAGAACCCATCCACCTCAACGTCAGGGTGCCGGATGGAGT

-25bp GCTGGTCATCCCA---------- TCAACGTCAGGGTGCCGGATGGAGT

Figure 3.6: Generation and verification of *parp1Δparp2Δ* cell lines
parp1Δparp2Δ cell lines were generated by disrupting PARP1 in a *parp2Δ* cell line. **A.** Whole cell extracts were prepared from U2OS, *parp1Δ, parp2Δ* and *parp1Δparp2Δ* cell lines, and Western blotting performed with the indicated antibodies. **B.** PCR was performed across the CRISPR targeted locus within the PARP1 gene in U2OS and two *parp1Δ parp2Δ* cell lines, and the products analysed by agarose gel electrophoresis **C.** Sanger sequencing of PCR products from **B** confirms they produce frameshift mutations and disrupt expression of PARP1. Wild-type sequence (U2OS) is shown with gRNA sites marked in blue. Red bases indicate insertions, dashes indicate deletions, and green bases indicate substitutions. Uppercase indicates exonic sequence.

tolerance to MMS exposure. In order to assess this possibility I generated *parp1Δparp2Δ* cell lines, where both PARP1 and PARP2 were disrupted in combination. I transfected *parp2Δ* cells with gRNAs targeting PARP1 and screened clonal colonies as before. Candidate cell lines, showing no PARP1 expression by Western blot, (Figure 3.6 A) were confirmed to be knockouts by PCR across the targeted locus (Figure 3.6 B) and subsequent sequencing. The cell line *parp1Δparp2Δ*.A had a single deletion of 7 bp, and *parp1Δparp2Δ.B* had an insertion of 4 bp and a deletion of 25 bp (Figure 3.6 C). All of these indels are within exon 2 of PARP1, and produce frameshifts to disrupt gene expression.

With *parp1Δparp2Δ* cell lines fully verified, I next tested whether PARP2 is responsible for the residual ADP-ribosylation signal that can be induced in *parp1Δ* cells by MMS (Figure 3.7 A). Whilst U2OS and *parp2Δ* cells can mount similar ADP-ribosylation responses to MMS, *parp1Δ* cells again showed reduced induction of PAR. Importantly, in the absence of both PARP1 and PARP2, no apparent induction of poly(ADP-ribose) can be detected following MMS exposure, indicating PARP2 is indeed responsible for the residual MMS-induced signal in *parp1Δ* cells.

To understand whether the presence of PARP2 is functionally important in the absence of PARP1, I assessed the survival of *parp1Δparp2Δ* cells following MMS exposure (Figure 3.7 B). Strikingly, *parp1Δparp2Δ* cells are significantly further sensitised to MMS, over and above *parp1Δ* cells. This indicates that whilst PARP2 alone is dispensable for cellular tolerance to MMS, in the absence of PARP1, the presence of PARP2 is critical for cellular survival.

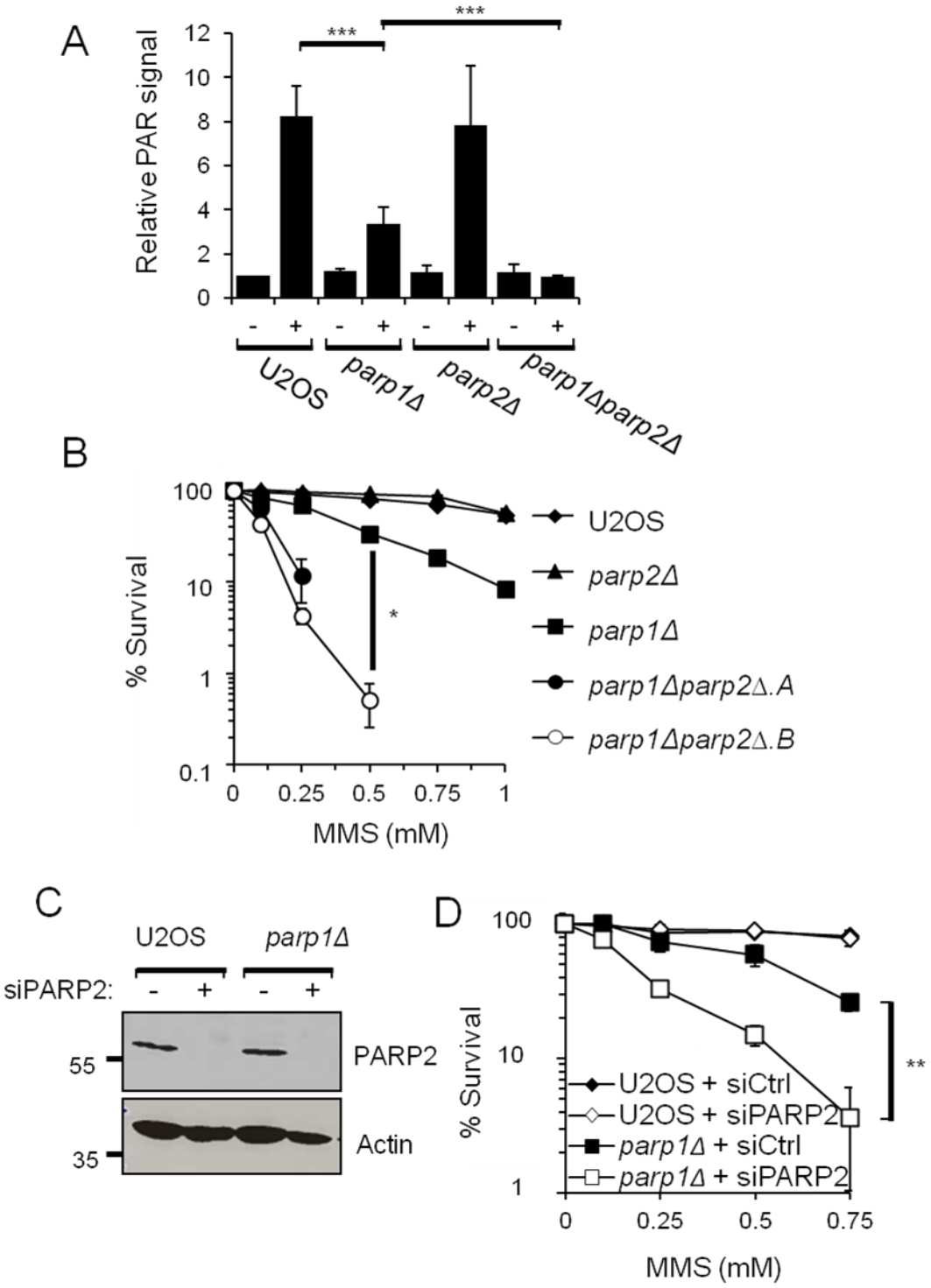


Figure 3.7: PARP1 and PARP2 show redundancy in ADP-ribosylation and cellular survival in response to MMS A. U2OS, *parp1Δ, parp2Δ or parp1Δparp2Δ* cells were left untreated (-) or exposed to 1.5 mM MMS for 1 hour, and ADP-ribosylation was assessed by immunofluorescence. Values relative to U2OS without MMS. **B.** U2OS, *parp1Δ, parp2Δ or parp1Δparp2Δ* cells were exposed to MMS and cell survival assessed by clonogenic assay. **C.** Whole cell extracts were prepared from U2OS or *parp1Δ* cells, transfected with siCtrl or siPARP2, and Western blotting performed with the indicated antibodies. **D.** U2OS or *parp1Δ* cells, transfected with siCtrl or siPARP2 were exposed to MMS and cell survival assessed by clonogenic assay. Error bars indicate the standard error of the mean between three independent experiments.

Furthermore, this result can be recapitulated by depleting PARP2 in *parp1Δ* cells using siRNA (Figure 3.7 C and D), ruling out the possibility that clonal variation or accumulated mutations in the *parp1Δparp2Δ* cell lines could be responsible for this phenotype.

3.2.5 PARP1 and PARP2 are redundant for their contribution to BER strand ligation rates

BER is a major pathway by which cells resolve the base methylations induced by MMS. PARPs accelerate BER after the formation of a nick by synthesising PAR at the site of the lesion. These PAR chains act as a scaffold for the recruitment of other repair factors to the break. Given PARP1 and PARP2 both produce ADP-ribose following MMS exposure, I considered how these different PARPs contribute to BER *in vivo*. To address this question, in collaboration with A. Olsen and P.J. McHugh, we performed alkaline comet assays on U2OS, *parp1Δ*, *parp2Δ*, and *parp1Δparp2Δ* cells following MMS exposure (Figure 3.8, performed by A. Olsen and P.J. McHugh). This assay allows direct assessment of DNA strand breaks present in a cell, calculated as a tail moment. By assessing the decay in the tail moment at time points following MMS exposure, we were able to determine the speed with which MMS induced strand breaks are resolved in these different cell lines. As expected, exposure of U2OS cells to MMS induced detectable DNA strands breaks, which were fully resolved after two hours of recovery. Interestingly, both *parp1Δ* and *parp2Δ* cells showed near identical profiles of strand break induction and recovery to wild-type cells, indicating either PARP is individually dispensable for normal BER strand ligation kinetics. In contrast, in *parp1Δparp2Δ* cells a higher level of strand

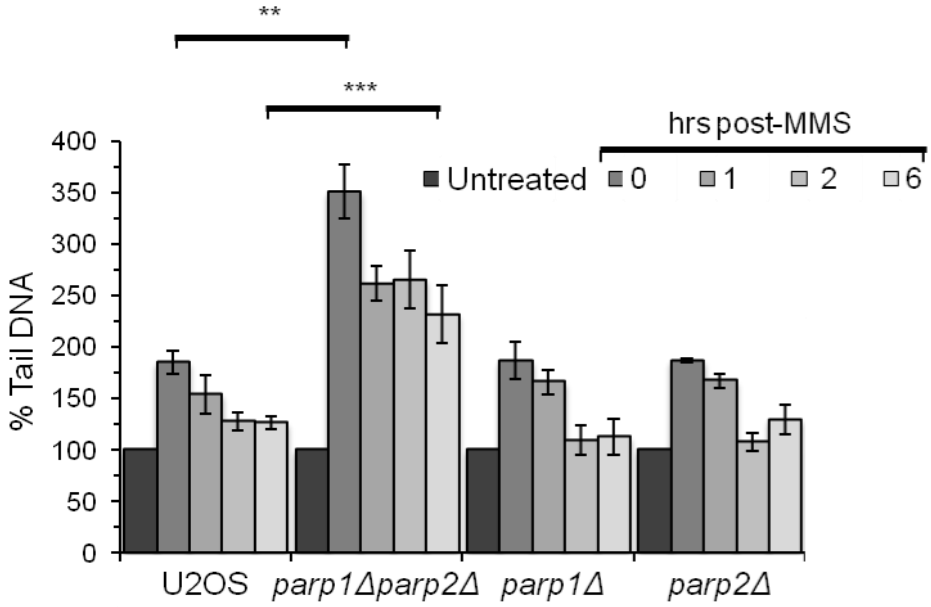


Figure 3.8: PARP1 and PARP2 are redundant for the strand ligation step of BER in response to MMS. Cells were treated with 0.25 mM MMS for 1 hour, before recovery in fresh media. Samples were taken at the indicated times post-treatment and the alkaline comet assay used to reveal strand breaks and alkali-labile sites. Comet data was normalised to the untreated sample. Error bars represent the standard deviation from at least six independent experiments.

breaks can be detected immediately after MMS treatment. The resolution of this damage is also compromised, with only approximately 40% of the stand breaks resolved after two hours of recovery, indicating that in the absence of PARP1 and PARP2 in combination, BER strand ligation is severely compromised.

3.2.6 Redundancy between PARP1 and PARP2 does not extend to H_2O_2-induced SSBs

These data indicate strong redundancy between PARP1 and PARP2 in the cellular response to MMS, including in the strand ligation step of BER. I next wished to understand whether this redundancy extended to SSBR more generally. In order to address this question, I assessed cellular survival of U2OS, *parp1Δ*, *parp2Δ*, and *parp1Δparp2Δ* cells after exposure to H_2O_2, an agent which induces SSBs directly (Figure 3.9). Interestingly, whilst *parp1Δ* cells showed sensitivity to H_2O_2, *parp1Δparp2Δ* cells were not significantly further sensitised to this agent, indicating the loss of PARP2 is dispensable for cellular survival to H_2O_2 even in the absence of PARP1. This suggests whilst there is clear redundancy between PARP1 and PARP2 in BER, this does not extend to SSBR more generally.

3.2.7 Loss of PARP3 does not affect cellular survival to MMS exposure

Whilst PARP1 and PARP2 are redundant in ADP-ribosylation, cellular survival and ligation rates following MMS exposure, this does not preclude an additional contribution of other PARPs to the cellular response to MMS. Although the lack of detectable ADP-ribosylation in *parp1Δparp2Δ* cells could be taken as

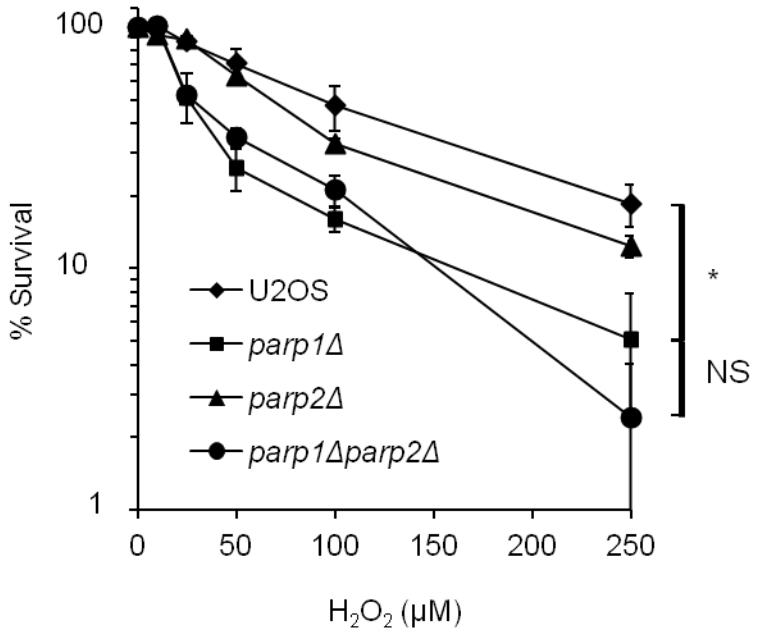


Figure 3.9: PARP1 and PARP2 do not show redundancy in cellular survival in response to H_2O_2. U2OS, *parp1Δ, parp2Δ or parp1Δparp2Δ* cells were exposed to H_2O_2 and survival assessed by clonogenic assay. Error bars indicate the standard error of the mean between three independent experiments.

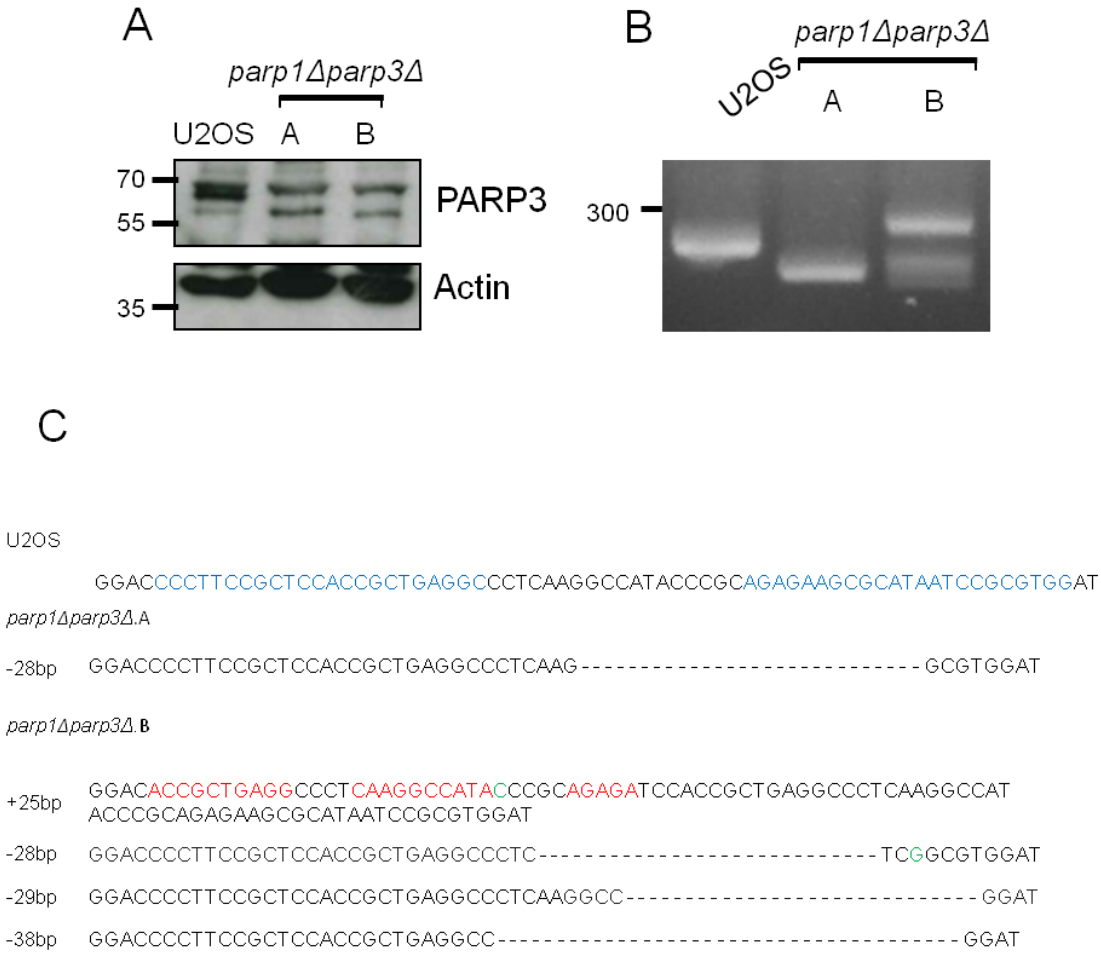


Figure 3.10: Generation and verification of *parp1Δ parp3Δ* cell lines. *parp1Δparp3Δ* cell lines were generated by disrupting PARP3 in a *parp1Δ* cell line. **A.** Whole cell extracts were prepared from U2OS and two independent *parp1Δparp3Δ* cell lines, and Western blotting performed with the indicated antibodies. **B.** PCR was performed across the CRISPR targeted locus within the PARP3 gene in U2OS and two *parp1Δparp3Δ* cell lines, and the products analysed by agarose gel electrophoresis. **C.** Sanger sequencing of PCR products from **B** confirms they produce frameshift mutations and disrupt expression of PARP3. Wild-type sequence (U2OS) is shown with gRNA sites marked in blue. Red bases indicate insertions, dashes indicate deletions, and green bases indicate substitutions. Uppercase indicates exonic sequence.

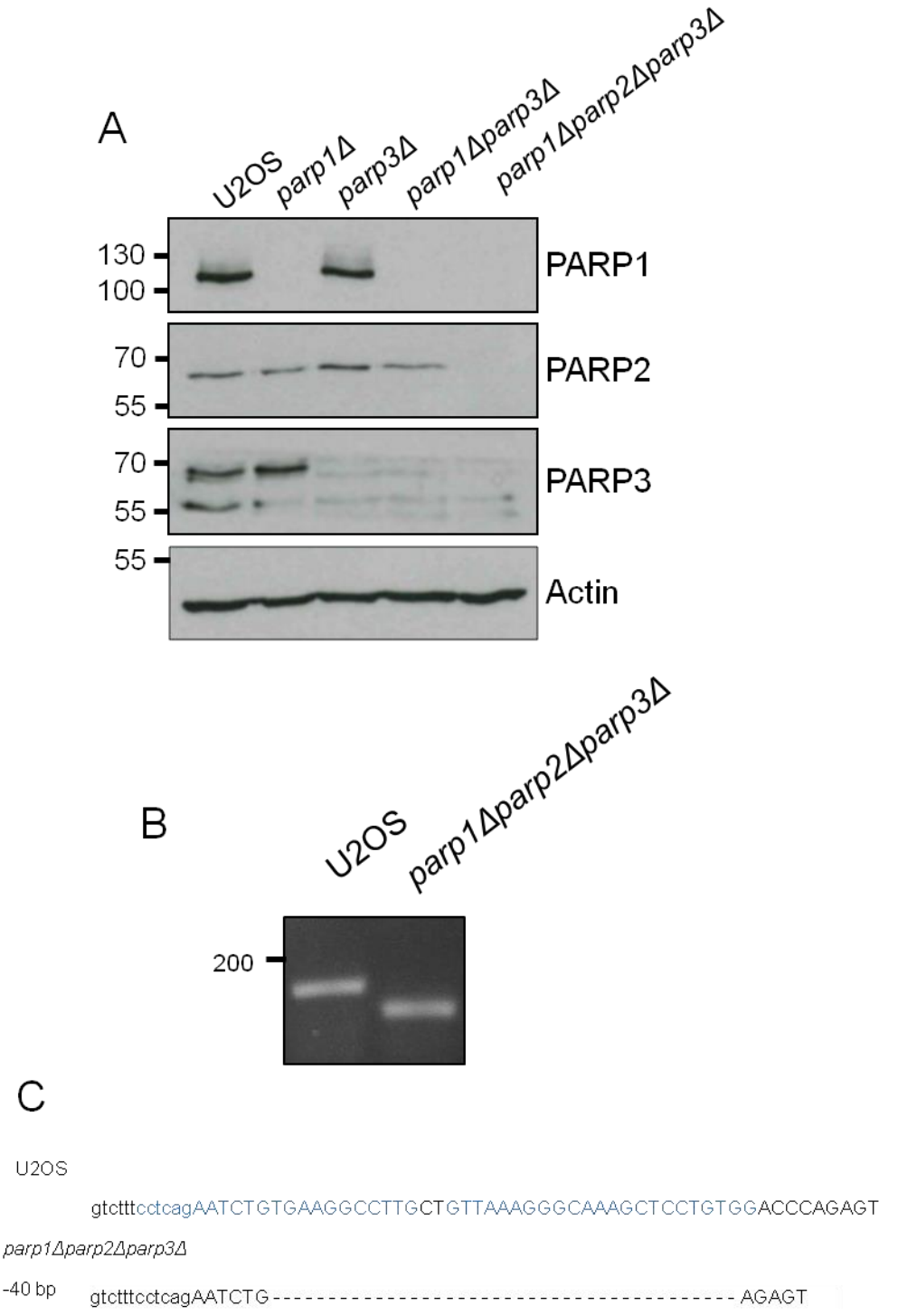


Figure 3.11: Generation and verification of *parp1Δparp2Δparp3Δ* cell lines. *parp1Δparp2Δparp3Δ* cell lines were generated by disrupting PARP2 in a *parp1Δparp3Δ* cell line. **A.** Whole cell extracts were prepared from the designated cell lines, and Western blotting performed with the indicated antibodies. **B.** PCR was performed across the CRISPR targeted locus within the PARP2 gene in U2OS and *parp1Δparp2Δparp3Δ* cell lines, and the products analysed by agarose gel electrophoresis **C.** Sanger sequencing of PCR products from **B** confirms they produce frameshift mutations and disrupt expression of PARP2. Wild-type sequence (U2OS) is shown with gRNA sites marked in blue. Red bases indicate insertions, dashes indicate deletions, and green bases indicate substitutions. Uppercase indicates exonic sequence and lowercase indicates intronic sequence.

evidence that no further PARPs are being activated by MMS, it should be noted that whilst PARP1 and PARP2 have been shown to produce long, branched poly(ADP-ribose) chains, almost all other members of the PARP superfamily are thought to either generate mono(ADP-ribose), or be catalytically inactive (Vyas et al., 2013). The binding reagent used to visualise MMS-induced PARylation in the above experiments binds only to poly(ADP-ribose). Therefore it is possible one or more mono(ADP-ribosyl)transferases are being activated in the absence of PARP1 and/or PARP2. Given PARP3 is able to be activated by 5' phosphorylated nicks *in vitro* (Langelier et al., 2014), and has been implicated in SSBR in avian cells (Grundy et al., 2016), I hypothesized it may also function in the cellular response to MMS.

In order to address this possibility, I generated *parp1Δparp3Δ* and *parp1Δparp2Δparp3Δ* cell lines by disrupting PARP3 in a *parp1Δ* cell line and PARP2 in a *parp1Δparp3Δ* cell line respectively (Figure 3.10 and 3.11). These cell lines were screened and verified as before. The loss of PARP3 in combination with PARP1 (Figure 3.12 A) or both PARP1 and PARP2 (Figure 3.12 B) made no significant difference to the survival of cells following MMS treatment. Taken together, these results indicate loss of PARP3 has no major role in promoting cellular tolerance to base damage, even in the absence of other DNA-dependent PARPs.

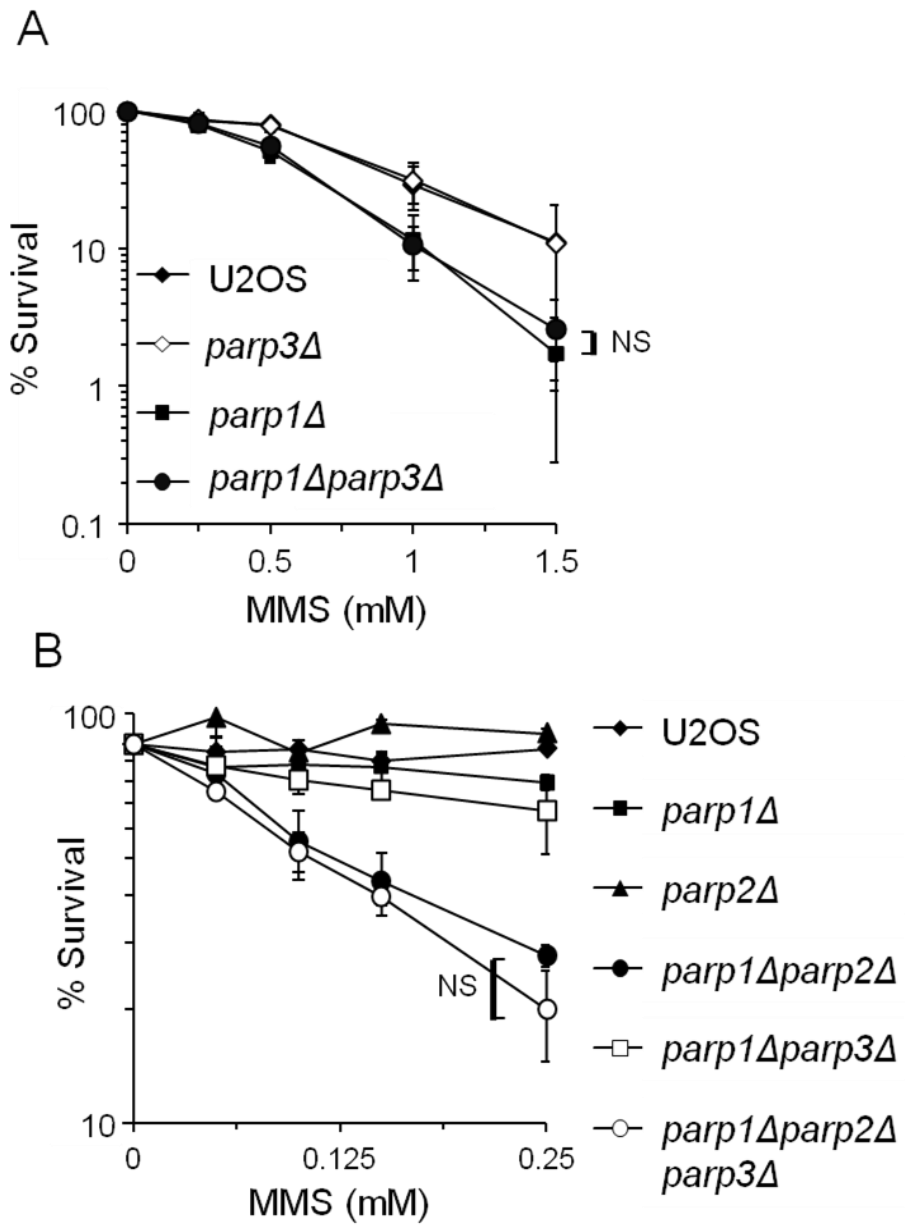


Figure 3.12: Loss of PARP3 does not affect cellular survival to MMS, regardless of the status of PARP1 and PARP2. **A.** U2OS, *parp1Δ, parp3Δ or parp1Δparp3Δ* cells were exposed to MMS and cellular survival assessed by clonogenic assay. **B**. The indicated cell lines were exposed to MMS and cellular survival assessed by clonogenic assay. Error bars indicate the standard error of the mean between three independent experiments.

3.2.8 Understanding the contribution of the PARP superfamily to the cellular response to MMS in the absence of PARP1 and PARP2

The PARP superfamily currently includes 17 members, but to date only PARP1, PARP2 and PARP3 have been shown to be specifically activated by damaged DNA structures. However, many members of the superfamily have not been extensively studied, and a number of other PARPs have recently been suggested to play roles in DNA repair. Thus it is possible that these PARPs, or other PARPs as yet unlinked to DNA repair, may also contribute to cellular resistance to MMS.

One way to assess this possibility is to utilise PARP inhibitors, a number of which have been shown to bind numerous members of the PARP superfamily outside of PARP1, PARP2 and PARP3 (Wahlberg et al., 2012). If *parp1Δparp2Δ* cells were able to be further sensitised to MMS by a PARP inhibitor, then this would indicate PARPs beyond PARP1 and PARP2 might be functioning in the cellular response to MMS. I chose to utilise two different inhibitors which have different binding profiles against the PARP superfamily. Whilst olaparib can bind to PARP1- 4, 12, 15 and 16, rucaparib can inhibit a wider profile of PARPs, including PARP 1-5b, 10, 15 and 16 (Wahlberg et al., 2012). *parp1Δparp2Δ* cells were pre-treated with these inhibitors then exposed to MMS as before. Interestingly, both inhibitors were able to increase the sensitivity of *parp1Δparp2Δ* cells to MMS by a modest but significant margin (Figure 3.13).

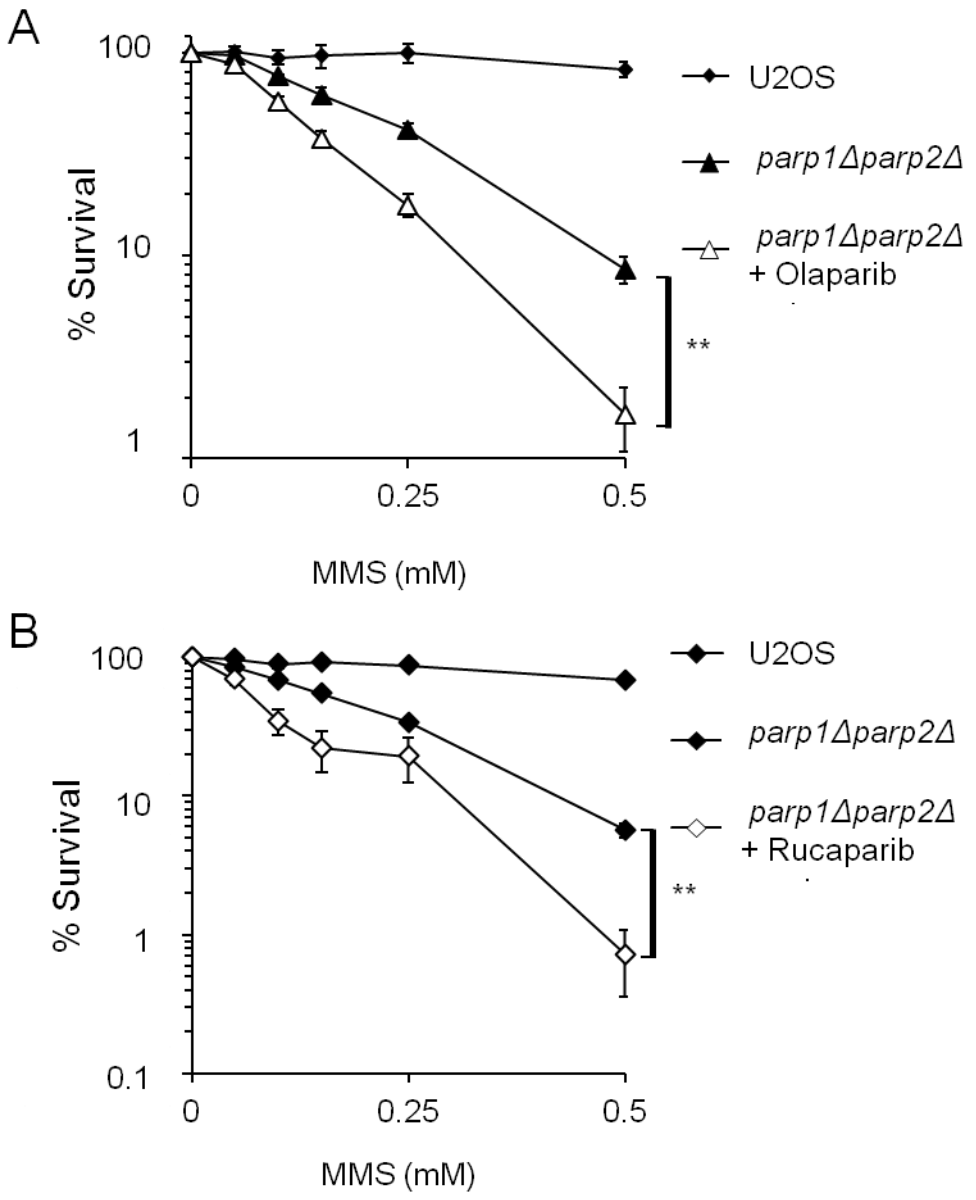


Figure 3.13: Multiple PARP inhibitors are able to further sensitise *parp1Δparp2Δ* cells to MMS. **A .**U2OS or *parp1Δparp2Δ* cells, with or without 10 μM olaparib treatment, were exposed to MMS and survival assessed by clonogenic assay. **B .**U2OS or *parp1Δparp2Δ* cells, with or without 10 μM rucaparib treatment, were exposed to MMS and survival assessed by clonogenic assay. Error bars indicate the standard error of the mean between three independent experiments.

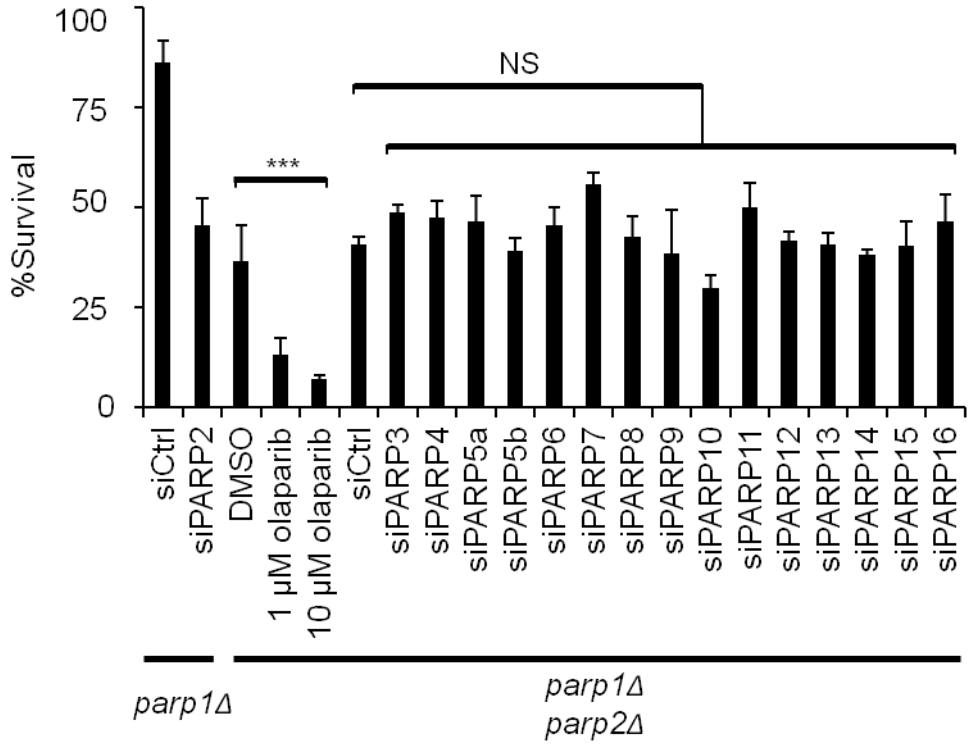


Figure 3.14: Depletion of any individual member of the PARP superfamily in *parp1Δparp2Δ* cells is unable to increase sensitivity to MMS. *parp1Δparp2Δ* cells, transfected with siCtrl, or siRNA targeting each of the remaining members of the PARP superfamily, were left untreated or exposed to 0.25 mM MMS for 1 hour, then survival was assessed by clonogenic assay. *parp1Δparp2Δ* cells treated with 1 μM or 10 μM olaparib, and *parp1Δ* cells transfected with siCtrl or siPARP2 were also included. Error bars indicate the standard error of the mean between three independent experiments.

In order to understand whether this increased sensitisation was due to the action of these inhibitors against another member of the PARP superfamily, I decided to perform a targeted siRNA screen of the all remaining annotated PARPs. *parp1Δparp2Δ* cells were transfected with siRNA targeting PARP3-PARP16, and cellular survival assessed after exposure to MMS. *parp1Δ* cells transfected with control or PARP2 siRNA were also included as a positive control for the transfection, as successful depletion of PARP2 in *parp1Δ* cells is able to increase their sensitivity to MMS (Figure 3.7 C). Whilst treatment of *parp1Δparp2Δ* cells with olaparib was able to clearly increase cellular sensitivity to MMS in this experiment, no PARP siRNA sensitised cells to the same degree (Figure 3.14).

Although not a statistically significant sensitisation, the strongest effect was seen with after depletion of PARP10, a factor that has been previously implicated in DNA damage repair through the TLS pathway (Nicolae et al., 2014). In order to confirm whether depletion of PARP10 can affect the cellular response to MMS, I assessed the sensitivity of *parp1Δparp2Δ* cells depleted of PARP10 across a wider range of MMS concentrations. I was able to verify efficient knockdown of PARP10 in these cells by Western blotting (Figure 3.15 A). However, no significant additional sensitisation of *parp1Δparp2Δ* cells was apparent after depletion of PARP10 at any of the MMS concentrations tested (Figure 3.15 B). Thus I was unable to identify any individual PARP which when depleted can further sensitise *parp1Δparp2Δ* cells to MMS.

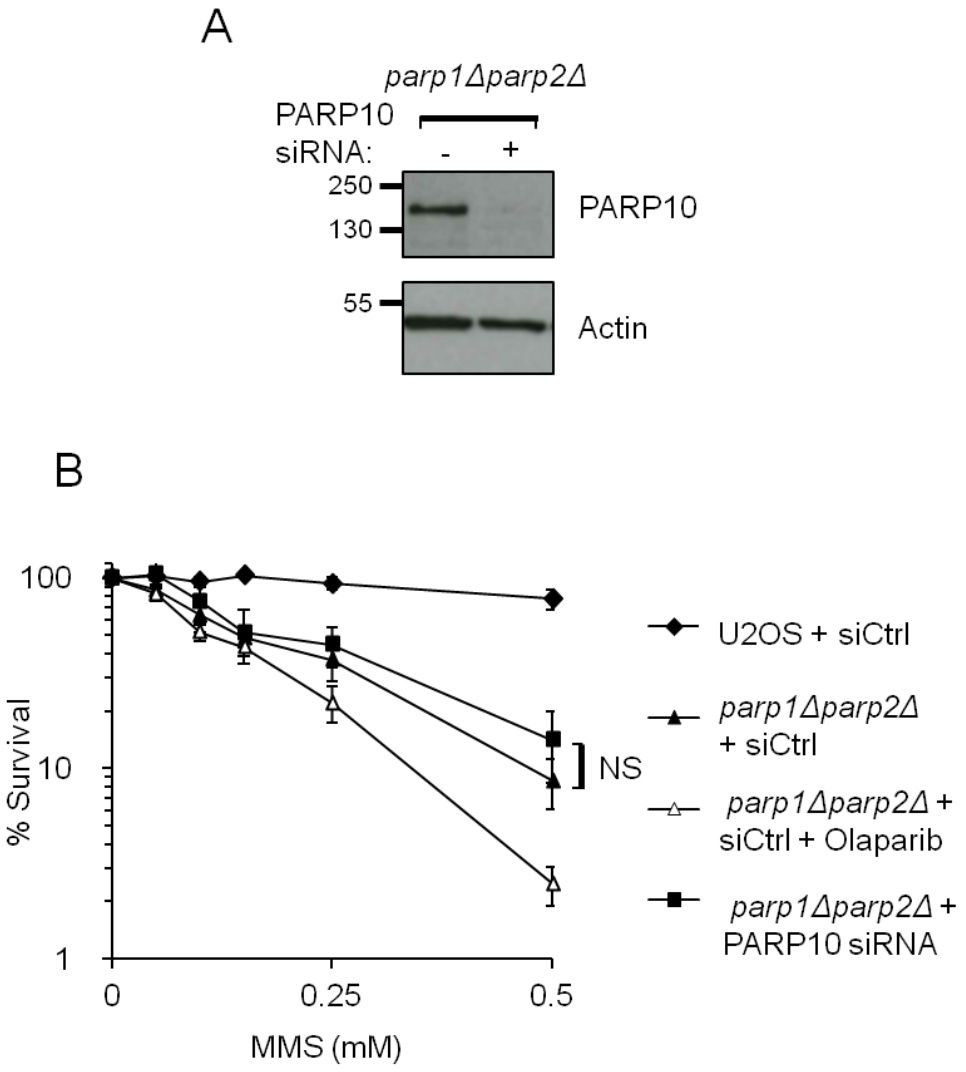


Figure 3.15: Knockdown of PARP10 does not significantly sensitise *parp1Δparp2Δ* cells to MMS. A. Whole cell extracts were prepared from *parp1Δparp2Δ* cells, transfected with siCtrl or siPARP10, and Western blotting performed with the indicated antibodies. **B.** U2OS or *parp1Δparp2Δ* cells, transfected with control or PARP10 siRNA, with or without olaparib exposure, were treated with MMS and survival assessed by clonogenic assay. Error bars indicate the standard error of the mean between three independent experiments.

3.3 Discussion

In this chapter I have examined the redundancy between PARPs in response to MMS-induced base damage. I have shown that loss of PARP1 and PARP2 in combination is able to synergistically sensitise cells to MMS, beyond the additive sensitivity of the two single mutants (Figure 3.7 B). However, this does not necessarily signify direct redundancy between PARP1 and PARP2. A relationship of this nature could indicate that the proteins play overlapping roles in a single repair pathway, so only in the absence of both is the pathway compromised and severe sensitivity observed. Alternatively, they could function in different repair pathways that both contribute to the resolution of MMS-induced damage, such that in the absence of either individual pathway repair can continue, but in the absence of both, resolution of the damage and cellular survival is compromised.

I was also able to assess the induction of ADP-ribosylation in cell lines disrupted for PARP1 and/or PARP2 alone and in combination. Consistent with previous reports (Amé et al., 1999; Hanzlikova et al., 2016), PARP1 appears to contribute the majority of the observed PAR following damage, with a significant decrease in the level of PARylation in *parp1Δ* cells (Figure 3.5 B). In contrast, *parp2Δ* cells display wild-type levels of MMS-induced PAR. This observation, taken together with the lack of an overt MMS sensitivity of *parp2Δ* cells, indicates in a wild-type context PARP2 is largely dispensable for a normal cellular response to MMS. This is in contrast to observations using mice disrupted for PARP2, which display sensitivity to IR and genomic instability following treatment with alkylating agents (Ménissier de Murcia et al., 2003b).

This could indicate different requirements for PARPs in BER between mouse and human cells. Indeed, differences in PARP biology between mice and humans have previously been identified, with PARP3 expression in bone marrow 10-fold higher in mice than rats or humans. These differences can result in functional consequences, with the tolerability of a combination therapy of PARP inhibitors and temozolomide varying between these systems (Oplustil O'Connor et al., 2016a). Nevertheless, all detectable ADP-ribosylation is lost in *parp1Δparp2Δ* cells, suggesting the hypersensitivity of *parp1Δparp2Δ* cells is due to a complete lack of MMS-induced ADP-ribosylation. Although it is not entirely clear whether the PAR chains formed by PARP1 and PARP2 are identical, no obvious differences can be seen in the length or branching when observing the chains under an atomic force microscope (Sukhanova et al., 2016).

Additionally, I assessed the ability of these different cell lines to religate strand breaks formed following MMS exposure, giving an indication of the capability of these cells to complete repair via BER (Figure 3.8). BER is the major pathway by which cells resolve the base methylations generated by MMS, and PARP1 has been proposed to function in BER once a DNA SSB has been generated by the action of APE1 on an abasic site. In this model, PARP1 binds and is activated by the SSB, ADP-ribosylating itself and other proteins at the break, and facilitating repair through the recruitment of XRCC1 (Caldecott et al., 1996; El-Khamisy et al., 2003; Masson et al., 1998). Although PARP2 has also been implicated in the resolution of base damage, its exact role remains unclear. It has been suggested that PARP2 may play a distinct role in BER downstream of PARP1, based on two lines of evidence. Firstly, recruitment of GFP-tagged

PARP2 to sites of laser damage is slower than that of GFP-PARP1, and persists longer (Mortusewicz et al., 2007). Secondly, the DNA substrates which most strongly activate PARP2 *in vitro* include gap and flap structures, which are found during the latter stages of BER (Kutuzov et al., 2013b; Langelier et al., 2014).

Our data demonstrate that a defect in BER strand ligation is only apparent in the absence of both PARP1 and PARP2, with loss of either PARP entirely dispensable for this process. This suggests a model of strict redundancy between PARP1 and PARP2 in BER, where the PAR produced by PARP2 can entirely compensate for the loss of PARP1-mediated ADP-ribosylation. However, this data is not incompatible with PARP1 and/or PARP2 also possessing additional, non-overlapping roles in other aspects of BER. Indeed, loss of PARP1 alone is sufficient to cause a increased sensitivity to MMS, despite no apparent decrease in the efficiency of BER. This could be due to additional and unique roles of PARP1 in BER that do not manifest in a comet assay defect, or due to roles of PARP1 in additional non-BER repair pathway(s) that also function in response to MMS.

Interestingly, the redundancy I observe between PARP1 and PARP2 in cellular survival in response to MMS does not extend to the direct SSB-inducing agent H_2O_2. This indicates that although PARP1 and PARP2 clearly share overlapping roles in the resolution of SSBs induced via the BER pathway, this is not true for SSBs generated directly. These observations are consistent with previous reports that loss of PARP2 does not affect strand break ligation rates in response to H_2O_2, even in the absence of PARP1 (Fisher et al., 2007; Hanzlikova et al., 2016). However, very recent work has uncovered overlapping

roles of PARP1 and PARP2 in the recruitment of XRCC1 to chromatin following H_2O_2 exposure (Hanzlikova et al., 2016). Why this redundancy is not reflected in the sensitivity or strand ligation rates of *parp1Δparp2Δ* cell lines following H_2O_2 exposure remains unclear. Nevertheless, the differences in PARP requirements for lesions induced by H_2O_2 or MMS could be due to the different chemical nature of the breaks, either generated enzymatically through BER, or produced by the direct action of H_2O_2 on the DNA backbone. Additionally, the chromatin context or local protein complement at lesions that have already been channelled through several stages of BER is likely to be different compared to those that arise at a random chromatin locus, which may impact on the requirement for different PARPs at these lesions.

I also considered the possibility that additional PARPs beyond PARP1 and PARP2 might play some role in the cellular response to MMS, either by influencing BER directly, or by promoting other pathways damage could be channelled down if BER is defective. The fact that *parp1Δparp2Δ* cells could be further sensitised by two different PARP inhibitors was suggestive of at least one additional PARP responding to MMS-induced damage (Figure 3.13). However, disrupting PARP3, even in the absence of PARP1 and PARP2, does not significantly alter the sensitivity of cells to MMS (Figure 3.12). Furthermore, depletion of any individual remaining member of the PARP superfamily by siRNA also does not recapitulate the sensitivity achieved through PARP inhibition (Figure 3.14).

There are a number of possibilities to explain these observations; firstly, the PARP inhibitors could be having effects on factors outside of the PARP superfamily which also affect the survival of cells after MMS exposure. Given

both of these agents act as NAD^+ mimetics, they could conceivably inhibit other NAD^+-dependent enzymes such as sirtuins (Chalkiadaki and Guarente, 2015). Secondly, the PARP inhibitors could be targeting an as-yet uncharacterised member of the PARP superfamily. Thirdly, the inhibitors could be affecting a combination of two or more PARPs which are redundant with one another, so depletion of individual PARPs is insufficient to phenocopy the PARP inhibitors. Finally, PARP inhibitors are known to affect PARP1 and PARP2 more profoundly than simple catalytic inhibition. Treatment of wild-type cells with PARP inhibitors and DNA damage leads to the 'trapping' of PARP1 and PARP2 at the site of the lesion, preventing normal repair and exacerbating the toxicity of the damage (Ma et al., 2012; Murai et al., 2012). Therefore in some cases, more extreme phenotypes can be seen using PARP inhibitors than by simply depleting the inhibited proteins. Although *parp1Δparp2Δ* cells lack both PARP1 and PARP2, it is possible that trapping of one or more of the remaining PARPs could account for the additional sensitivity of these cells to MMS after treatment with PARP inhibitors. This could be experimentally tested by depleting each member of the PARP superfamily in *parp1Δparp2Δ* cells and assessing whether those cells can still be sensitised to MMS by PARP inhibitors.

In summary I have identified that PARP1 and PARP2 are redundant in cellular survival, ADP-ribosylation and strand ligation rates in response to MMS, but are not redundant for cellular survival following H_2O_2 exposure. Furthermore, I was unable to identify an effect of loss of any further PARP on cellular survival in response to MMS, even in the absence of PARP1 and PARP2. However, the precise functions of PARP1 and PARP2 in BER, why *parp1Δ* cells are sensitive to MMS despite possessing no defect in strand ligation rates, and how loss of

PARP1 and PARP2 might impact on additional pathways activated in response to MMS all require further study in order to be fully addressed.

4. Understanding the roles of PARP1 and PARP2 in MMS-induced replication-associated damage

4.1 Introduction

4.1.1 Differences in the relationship between PARP1 and PARP2 in BER and SSBR

In the previous chapter, I explored the relationships between different members of the PARP superfamily in repairing MMS-induced lesions. I identified strong redundancy between PARP1 and PARP2 in cellular survival, ADP-ribosylation and BER strand ligation following MMS exposure. However, a number of observations suggest that the situation may be more complex than a simple case of redundancy between these two PARPs in BER. Firstly, *parp1Δ* cells show a significantly increased sensitivity to MMS over wild-type cells, despite the lack of any obvious defect in BER strand ligation as judged by a comet assay (Figure 3.8). Furthermore, loss of PARP2 in *parp1Δ* cells does not affect cellular survival following hydrogen peroxide exposure, which induces DNA SSBs directly (Figure 3.9). This suggests that whilst PARP1 and PARP2 are redundant in the context of BER, this does not extend more generally to SSBR. This could be due to the different circumstances in which these lesions arise. Alternatively, this could indicate that PARPs are contributing to cellular survival to MMS through additional mechanisms independently of BER.

4.1.2 MMS-induced base methylations lead to an accumulation of S-phase associated damage

MMS is a widely used model agent for inducing base damage, as it introduces a variety of methyl modifications onto DNA. The most common lesions generated by MMS are nitrogen methylations within DNA bases, for example N7-methylguanine, N3-methyladenine and N3-methylguanine (Beranek, 1990).The major way in which these lesions are repaired in mammalian cells is through the BER pathway (Meira et al., 2005). This involves recognition of damaged bases by the DNA-glycosylase MPG (O'Brien and Ellenberger, 2004), which excises the base to leave an abasic (AP) site. This AP site is recognised by the enzyme APE-1 (Marenstein et al., 2004; Mol et al., 2000; Wilson et al., 1995), which cleaves the site to generate a strand break with 3'-OH and 5'-dRP termini. Polymerase β then removes the 5'-dRP end to leave a 5' phosphate (Matsumoto and Kim, 1995), from which it polymerises the DNA. The XRCC1-LigIII complex then reseals the sugar-phosphate backbone, completing repair (Caldecott et al., 1994).

However, cellular exposure to MMS also activates DNA DSB repair pathways, including HR (Hinz et al., 2006; Nikolova et al., 2010). Indeed, MMS has previously been mischaracterised as a "radiomimetic" or "DSB-inducer" for this reason, although it lacks the ability to directly induce any type of strand break in DNA. Nevertheless, cellular exposure to MMS can physically block the progression of replication forks independently of ATM or ATR signalling (Groth et al., 2010). Multiple studies identified the formation of DSBs after MMS exposure, that have been suggested to form due to replicative run-off from BER-induced SSBs (Chlebowicz and Jachymczyk, 1979; Choy and Kron,

2002). However, later work indicated that many of these detected DSBs might be artifactual, produced during sample preparation due to the heat-labile nature of methylated DNA (Lundin et al., 2005). Therefore the exact nature of this MMS-induced replication damage was uncertain. However, recent studies have provided fresh evidence about how MMS-induced lesions affect DNA replication (Ensminger et al., 2014; Nikolova et al., 2010). After treatment with MMS, the damage marker γH2AX accumulates in foci specifically in S-phase cells, driven by ATM activation. The formation of γH2AX foci can be suppressed by disrupting early steps in BER, such as depleting MPG, the glycosylase which recognises methylated bases, indicating damaged bases *per se* do not trigger the formation of this damage (Ensminger et al., 2014). These foci can also be suppressed by preventing DNA replication with aphidicolin, demonstrating the requirement for actively moving replication forks (Ensminger et al., 2014). Downstream consequences of MMS exposure include chromatid breaks and rearrangements, hallmarks of genuine DSBs. These phenotypes, similarly to the formation of γH2AX foci, can be suppressed by depletion of MPG or treatment with aphidicolin, linking the formation of damage marked by γH2AX with serious chromosomal aberrations (Ensminger et al., 2014). Therefore it is likely that some form of DSB does form *in vivo* in response to MMS exposure, but the precise nature of this replication-associated damage is incompletely understood.

4.1.3 PARPs have been implicated in the resolution of replication-associated damage in other contexts

Interestingly, PARPs have been shown to contribute to the resolution of certain types of replication-associated damage. Fork restart kinetics were delayed in

the absence of PARP1 after HU exposure, which was later proposed to be due to compromised recruitment of the nuclease Mre11 to sites of damage (Bryant et al., 2009; Yang et al., 2004). More recently, PARP1 has also been linked to the restart of replication forks disrupted by the topoisomerase inhibitor camptothecin (Ray Chaudhuri et al., 2012; Sugimura et al., 2008), and has been suggested to stabilise reversed forks and prevent premature and aberrant restart by the helicase RecQ1(Berti et al., 2013). Intriguingly, stabilising reversed replication forks would be predicted to constrain resection, in contrast to the resection promoting activity of Mre11 recruitment. How these different activities of PARP1 are balanced at replication-associated damage, and why there are differences in how PARPs promote the resolution of HU- and camptothecin-induced replication stress is unclear. It remains possible PARPs could influence the resolution of stalled/collapsed replication forks through additional mechanisms.

The involvement of PARPs other than PARP1 in contributing to the resolution of damaged replication forks is less well established. PARP2 also functions in response to HU-induced replication stress (Bryant et al., 2009), but how these roles might interact with or compensate for PARP1 loss is uncertain. Observations made using PARP inhibitors that target both PARP1 and PARP2 has made drawing conclusions about their individual contributions difficult.

4.1.4 Aims

I have established that PARP1 and PARP2 are redundant for cellular survival and BER in response to MMS. However, MMS is able to induce the stalling and/or collapse of replication forks during S-phase. How loss of these PARPs

might affect the induction and repair of MMS-induced S-phase associated DNA damage is unknown. Therefore, the aims of this chapter are to further investigate the nature of the redundancy between PARP1 and PARP2 in response to MMS-induced base damage, with a specific focus on how loss these PARPs, alone or in combination, impacts on replication-associated damage.

4.2 Results

4.2.1 MMS induces γH2AX phosphorylation in actively replicating cells

MMS has previously been reported to cause S-phase associated damage, generated when active replication forks collide with BER intermediates (Ensminger et al., 2014). I wished to assess whether these observations were conserved in U2OS cells under our experimental conditions. Staining for γH2AX by immunofluorescence in cells after exposure to damage allows the visualisation of nuclear γH2AX foci. S-phase cells can be labelled through use of the 5-ethynyl-2'-deoxyuridine (EdU), a thymidine analogue that is stably incorporated into DNA during DNA replication. Incorporated EdU is easily labelled by conjugating it to a fluorescent azide dye using click chemistry, thus marking cells that were in S-phase at the time of EdU exposure. Combining these two techniques allows an assessment of the induction of γH2AX foci in S-phase and non S-phase (G1- or G2- phase) cells (Figure 4.1 A). U2OS cells were treated with EdU and increasing concentrations of MMS for 1 hour, before staining and quantification of the number of nuclear γH2AX foci (Figure 4.1 B). Low levels of γH2AX can be seen in EdU-negative cells in the

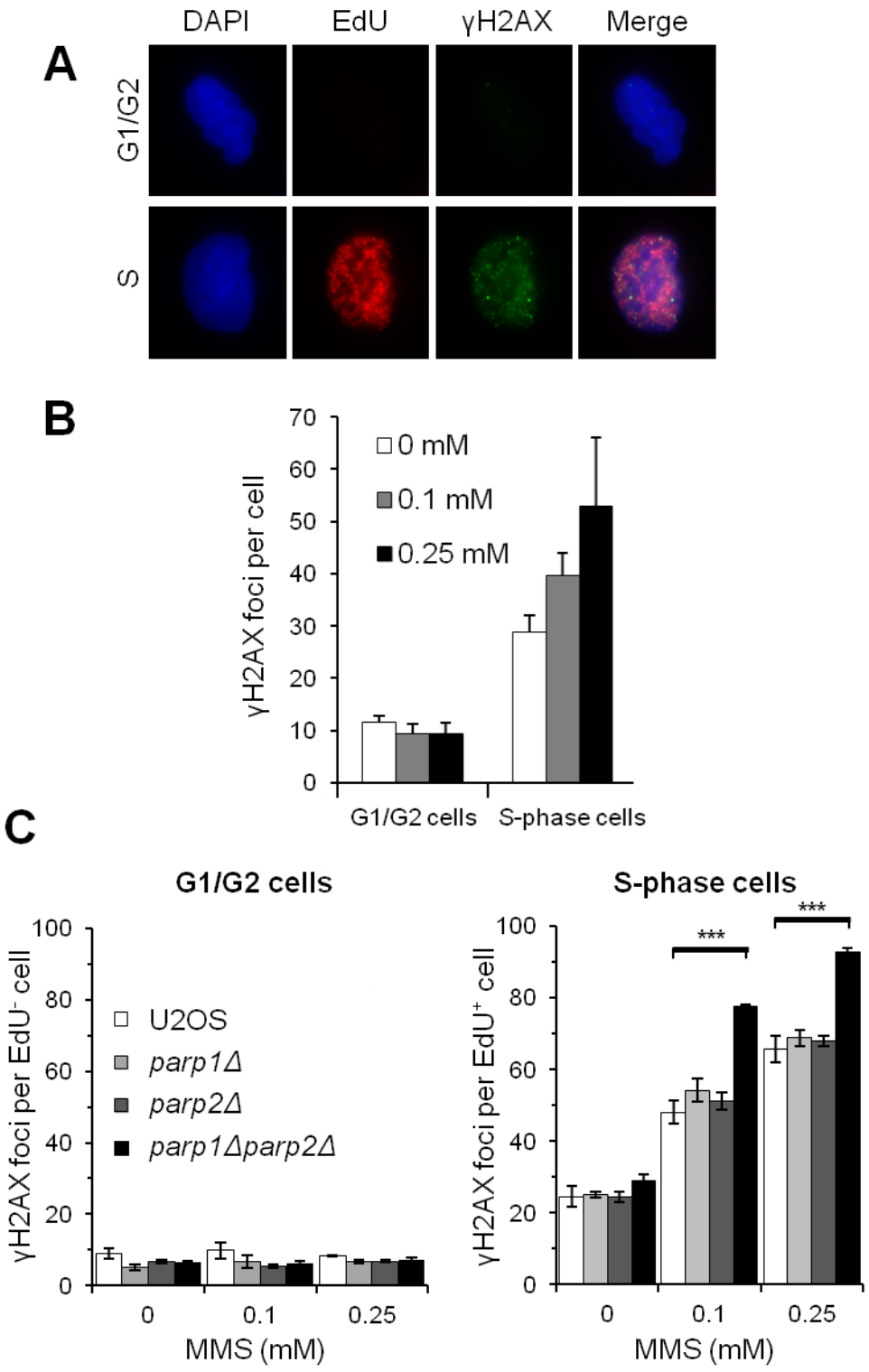


Figure 4.1: γH2AX is induced specifically in S-phase cells after treatment with MMS. **A.** U2OS cells were treated with 1 μM EdU and 0.25 mM MMS for 1 hour, before pre-extraction and fixation. EdU and γ-H2AX were detected by immunofluorescence. Representative images of EdU-positive and EdU-negative nuclei are shown. **B.** U2OS cells were treated as in **A** and following immunofluorescence γ-H2AX foci quantified in G1/G2 phase (EdU-negative) and S-phase (EdU-positive) cells. **C.** The indicated cell lines were treated as in **A** and following immunofluorescence γ-H2AX foci quantified in G1/G2 phase (EdU-negative) and S-phase (EdU-positive) cells. Error bars represent the SEM from four independent experiments.

absence of damage, and no further induction was evident upon MMS exposure. In contrast, a dose-dependent increase in γH2AX foci can be detected in EdU-positive cells after exposure to MMS, confirming this agent induces S-phase specific damage in U2OS cells.

I next wished to consider the impact of the loss of PARP1 and/or PARP2 on the induction of γH2AX in S-phase cells. I treated U2OS, *parp1Δ, parp2Δ* and *parp1Δparp2Δ* cells with EdU and increasing concentrations of MMS, and assessed γH2AX foci in EdU-positive S-phase cells (Figure 4.1 C). As before, I observe a dose dependent induction of γH2AX foci in S-phase cells, with no induction in EdU-negative cells. The profile of γH2AX induction in *parp1Δ* and *parp2Δ* cells is very similar to that observed in U2OS cells. However, in the *parp1Δparp2Δ* cells, there is a significant increase in the number of γH2AX foci induced by MMS as compared to U2OS cells.

4.2.2 Resolution of MMS-induced γH2AX foci is compromised in the absence of PARP1 and PARP2

PARPs have been identified to play a role in the resolution of stalled/collapsed replication forks in response to both HU and camptothecin. Given MMS can cause the formation of similar replication-associated damage, I wished to understand the potential contributions of PARP1 and PARP2 to the resolution of these lesions. I treated U2OS, *parp1Δ, parp2Δ* and *parp1Δparp2Δ* cells with EdU and MMS as before, but then assessed γH2AX foci at times following removal of MMS (Figure 4.2 A, B). At 12 hours after MMS addition, EdU-positive U2OS cells have resolved the majority of the MMS-induced γH2AX foci. Whilst *parp2Δ* cells show almost identical kinetics of repair to wild type

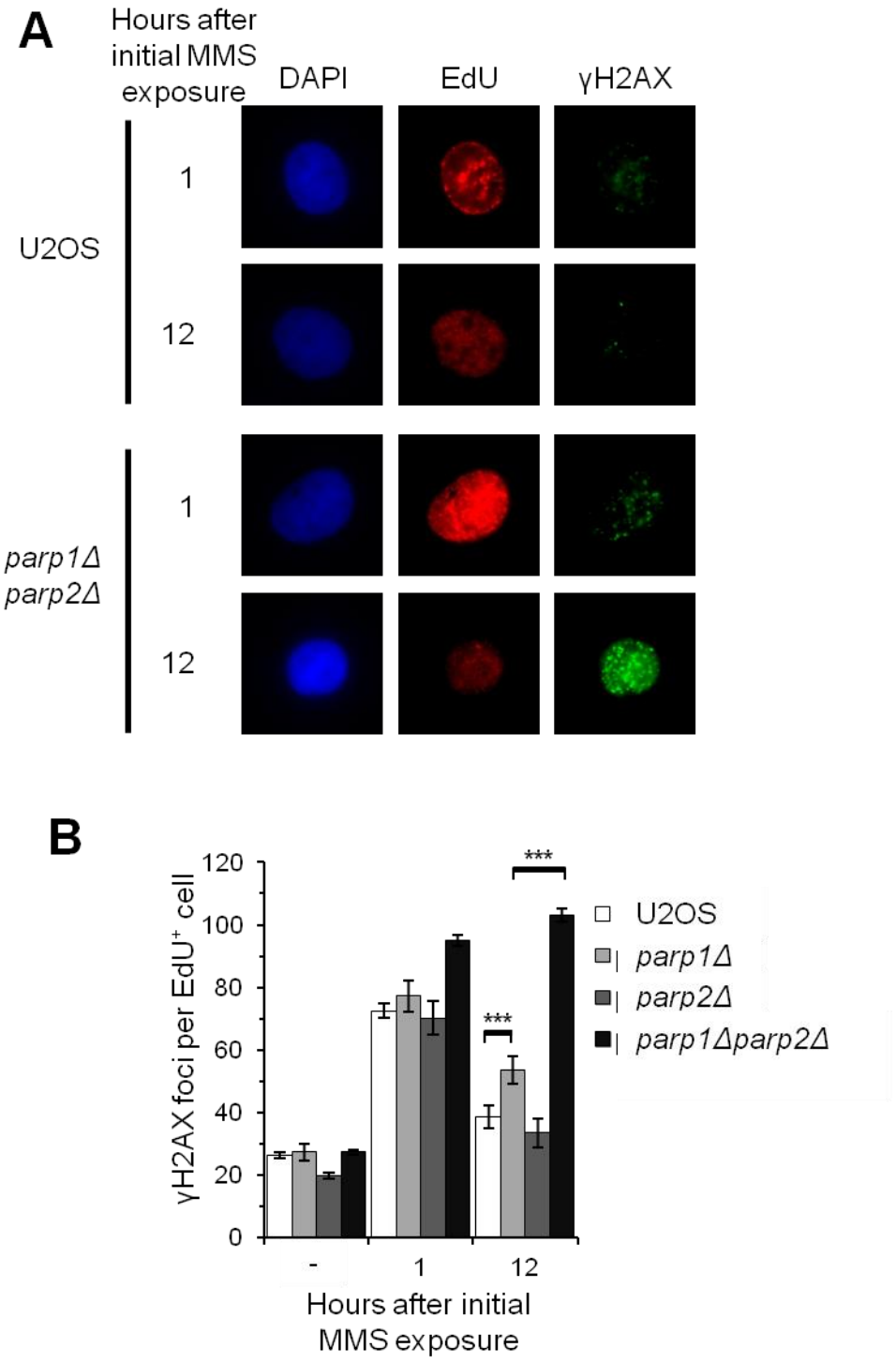


Figure 4.2: γH2AX foci persist in *parp1Δparp2Δ* cells up to 12 hours after MMS exposure. **A.** U2OS or *parp1Δparp2Δ* cells were treated with 1 μM EdU and 0.25 mM MMS for 1 hour, before recovery in fresh media. Times indicated show hours since addition of EdU and MMS. EdU and γ-H2AX were detected by immunofluorescence. Representative images of EdU-positive are shown. **B.** The indicated cell lines were treated as in **A** and following immunofluorescence γ-H2AX foci quantified in EdU-positive cells. Error bars represent the SEM from four independent experiments.

cells, *parp1Δ* cells show a mild but significant delay in the resolution of this damage. Strikingly however, *parp1Δparp2Δ* cells show no decay of γH2AX foci, indicating repair of this DNA damage is severely compromised in the absence of both PARP1 and PARP2.

One explanation for this could be that a BER defect in the absence of PARP1 and PARP2 leads to elevated levels of S-phase associated damage, which subsequently requires a longer time for repair. Alternatively, this could imply an additional role of PARP1 and/or PARP2 in pathway(s) which resolve this damage, and in their absence γH2AX foci persist due to loss of these BER-independent PARP functions. In order to distinguish between these two possibilities, I decided to disrupt BER in a PARP independent manner, by depleting cells of the key SSBR/BER protein XRCC1 (Figure 4.3 A), and assessing how this might impact on the formation and resolution of MMS-induced γH2AX foci. Knockdown of XRCC1 is sufficient to elicit a BER ligation defect and cellular sensitivity in response to MMS (Brem and Hall, 2005). This makes depletion of XRCC1 a suitable tool to assess the interplay between BER and replication-associated damage following MMS exposure.

Upon depletion of XRCC1 a modest increase in the induction of γH2AX foci can be detected in EdU-positive cells immediately following treatment with MMS (Figure 4.3 B). However, by 12 hours following the addition of MMS, the majority of these foci have been resolved even in the absence of XRCC1, in stark contrast to the situation in *parp1Δparp2Δ* cells. This demonstrates that XRCC1 does not contribute to the repair of this MMS-induced replication associated damage. Furthermore, this implies that the kinetics of resolution of γH2AX foci are not strongly impacted by a BER defect, suggesting PARP1

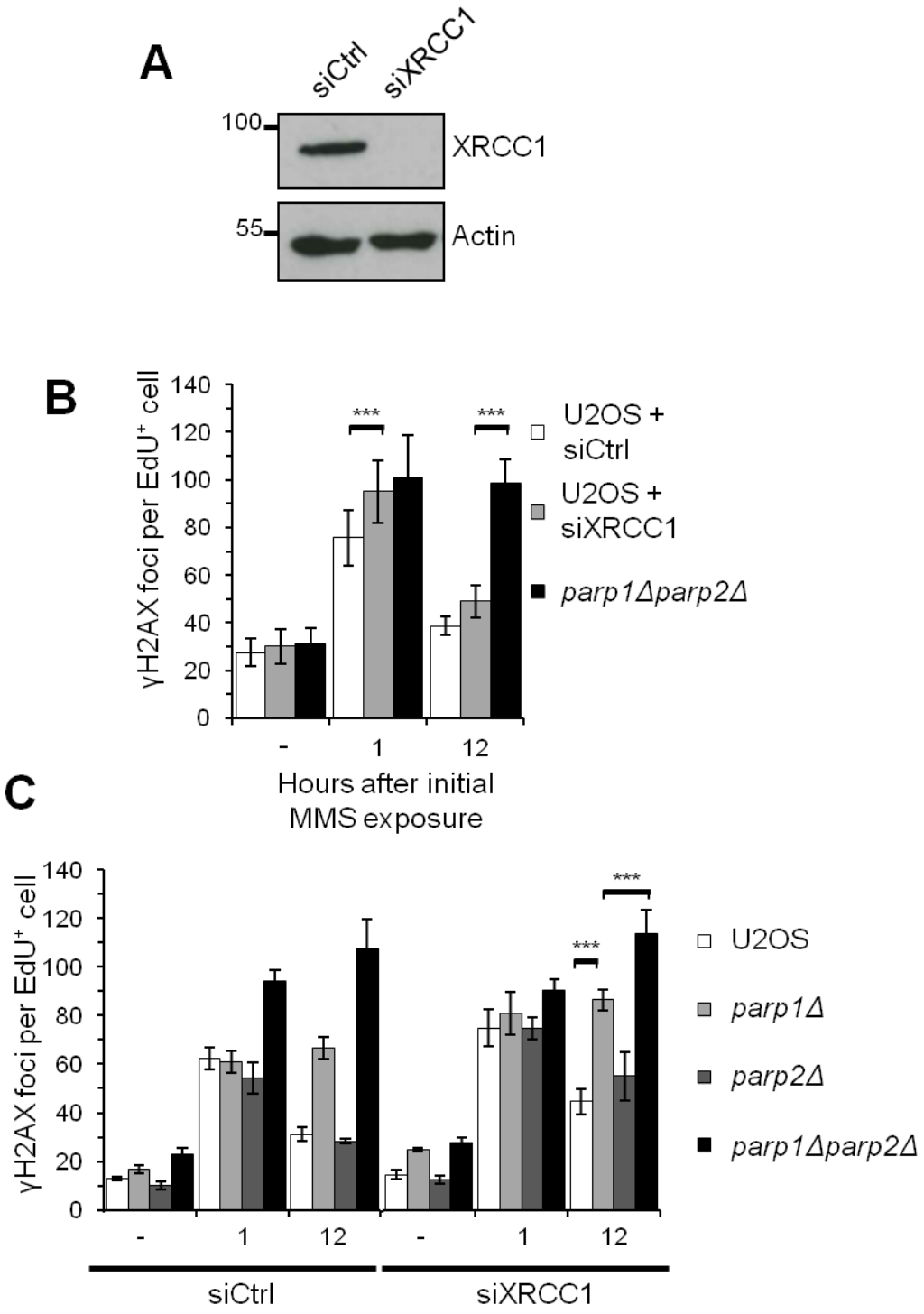


Figure 4.3: PARP1 and PARP2 also contribute to the resolution of MMS induced lesions independently of BER. **A.** Whole cell extracts were produced from U2OS cells transfected with siCtrl or siXRCC1, and Western blotting performed with the indicated antibodies. **B.** U2OS cells transfected with siCtrl or siXRCC1, or *parp1Δparp2Δ* cells were treated with 1 μM EdU and 0.25 mM MMS for 1 hour, before recovery in fresh media. Times indicated show hours since addition of EdU and MMS. EdU and γ-H2AX were detected by immunofluorescence, and the number of γH2AX foci quantified in EdU-positive cells. **C.** The indicated cell lines were transfected with siCtrl or siXRCC1 and treated as in **B**. Times indicated show hours since addition of EdU and MMS. EdU and γ-H2AX were detected by immunofluorescence, and the number of γH2AX foci quantified in EdU-positive cells. Error bars represent the SEM from at least three independent experiments.

and/or PARP2 play a BER-independent role in the resolution of MMS-induced S-phase associated damage.

These data are consistent with PARP1, PARP2 or both contributing to the resolution of MMS-induced γH2AX foci that accumulate in S-phase cells in the absence of functional BER. In order to understand which combination of these PARPs is required for this repair, I depleted XRCC1 in U2OS, *parp1Δ, parp2Δ* and *parp1Δparp2Δ* cells and assessed the resolution of MMS-induced γH2AX foci (Figure 4.3 C). By depleting XRCC1, each cell line will be defective for BER, allowing an analysis of the non-BER contributions of each PARP to induction and decay of γH2AX foci. In the absence of XRCC1, *parp1Δ* cells show a significant delay in the resolution of γH2AX foci. Although XRCC1 depleted *parp2Δ* cells display comparable kinetics of γH2AX decay to XRCC1 depleted U2OS cells, *parp1Δparp2Δ* cells depleted of XRCC1 show a persistence of these foci above that seen in XRCC1 depleted *parp1Δ* cells. This indicates that whilst PARP1 alone contributes to the resolution of MMS-induced S-phase associated damage to some extent, redundancy between PARP1 and PARP2 is also evident in this context.

4.2.3 HR is engaged in response to MMS in U2OS cells

I next wished to establish which pathway(s) PARP1 and PARP2 were contributing to, in order to facilitate the resolution of S-phase associated damage. Given the γH2AX foci that form in replicating cells after exposure to MMS are generated as a consequence of active replication forks colliding with BER intermediates, I reasoned they are likely to represent one-ended DSBs or collapsed replication forks. Therefore I considered whether DSB repair

pathways might be engaged to deal with this damage in U2OS cells, and whether they might be compromised in the absence of PARPs.

HR has previously been identified to contribute to the resolution of damage following MMS exposure, with both yeast and human cells compromised for HR showing sensitivity to this agent (Krogh and Symington, 2004; Nikolova et al., 2010). Therefore, I considered the possibility HR could function to repair the S-phase associated γH2AX foci induced after MMS exposure in U2OS cells. A core component of the HR pathway is the formation of Rad51 filaments that function to stabilise stalled/collapsed replication forks and facilitate their restart. Therefore to assess the engagement of HR in response to MMS, I exposed U2OS cells to MMS and EdU, allowed cells to recover, then stained for Rad51 and labelled the incorporated EdU. Rad51 foci clearly form in response to MMS exposure (Figure 4.4 A), peaking in EdU-positive cells at 6 hours after MMS addition (Figure 4.4 B), demonstrating HR is engaged in U2OS cells in response to MMS.

I next wished to understand how loss of function of HR might affect the resolution of MMS-induced γH2AX foci, by using a small molecule Rad51 inhibitor, B02, to disrupt HR-mediated repair (Huang et al., 2012). In order to verify the efficacy of B02 in U2OS cells, I confirmed that it was able to prevent the formation of Rad51 foci after the induction of cellular DSBs with phleomycin (Figure 4.4 C). I then exposed cells to MMS and B02 in combination, and assessed the consequence on the recovery of γH2AX foci (Figure 4.4 D). Whilst B02 treatment does not significantly affect the formation of γH2AX foci immediately after MMS treatment, it prevents their decay,

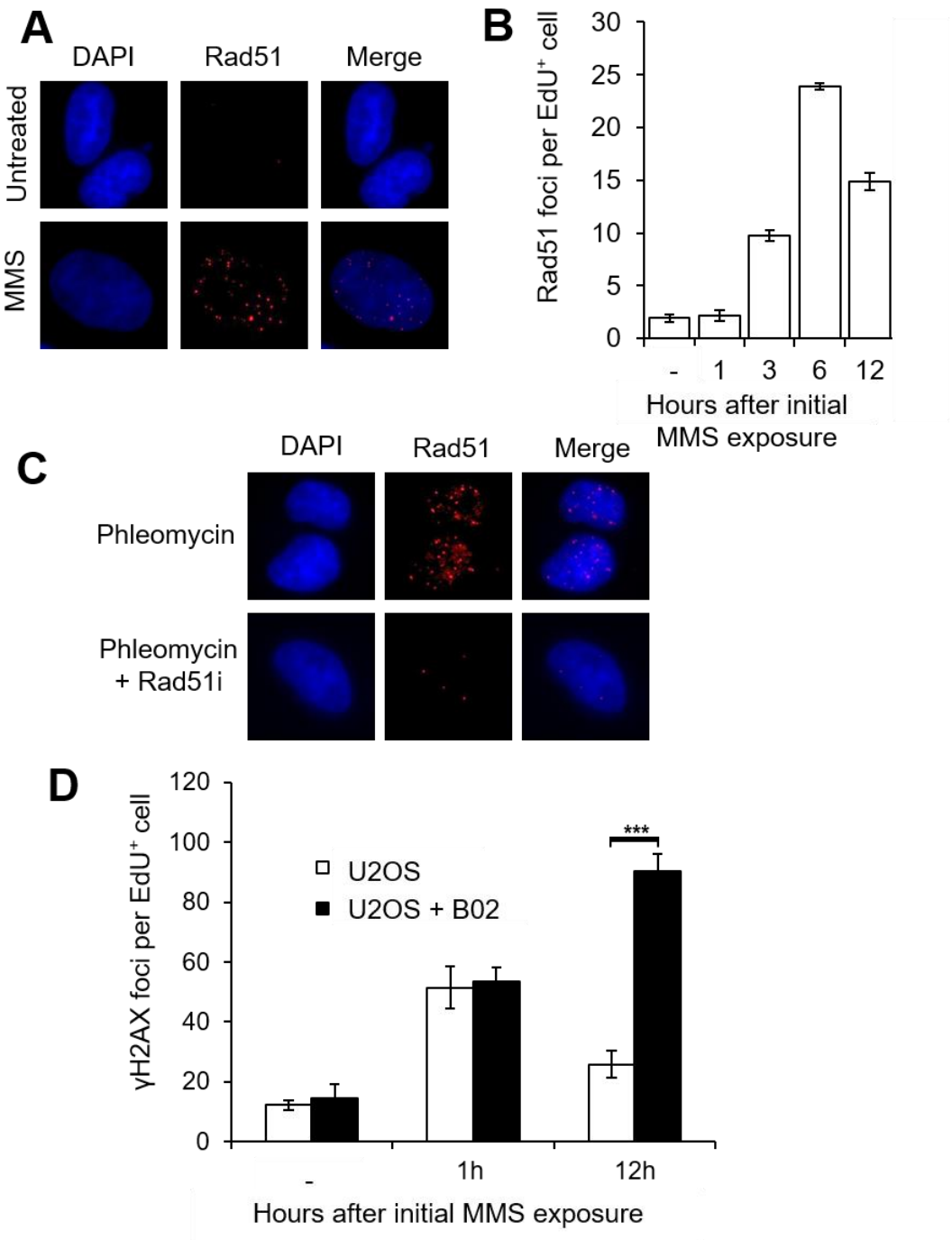


Figure 4.4: HR is engaged in response to MMS induced damage in S-phase cells. A. U2OS cells were treated with 1 μM EdU and 0.5 mM MMS for 1 hour, before recovery in fresh media for 5 hours. EdU and Rad51 were detected by immunofluorescence. Representative images of EdU-positive nuclei are shown. **B.** U2OS cells were treated with 1 μM EdU and 0.5 mM MMS for 1 hour, before recovery in fresh media. Times indicated show hours since addition of EdU and MMS. EdU and Rad51 were detected by immunofluorescence, and the number of Rad51 foci quantified in EdU-positive nuclei. **C.** U2OS cells, with or without 30 μM B02 exposure, were treated with 300 μM phleomycin for one hour before recovery in fresh media containing B02 as appropriate. Cells were fixed 6 hours after phleomycin addition, and stained for Rad51. Images taken by G. Driscoll. **D.** U2OS cells, with or without B02 exposure, were treated as in B. Times indicated show hours since addition of EdU and MMS. EdU and Rad51 were detected by immunofluorescence, and the number of Rad51 foci quantified in EdU-positive nuclei. Error bars represent the SEM from three independent experiments.

resulting in a striking accumulation of γH2AX foci 12 hours after MMS exposure (Figure 4.4 D). Thus loss of proper functioning of HR in the absence of PARP1 and PARP2 could be a potential explanation the persistent γH2AX foci apparent in these cells after MMS exposure.

4.2.4 In the absence of PARP1 and PARP2, Rad51 nucleofilament formation is compromised

Given that HR is engaged in response to MMS damage in U2OS cells, I next wished to examine whether loss of PARP1 and/or PARP2 affected the accumulation of Rad51 foci after MMS exposure. Therefore, I assessed the formation of Rad51 foci in our *parpΔ* cell lines at various times after MMS exposure (Figure 4.5 A, B). Both *parp1Δ* and *parp2Δ* cells showed robust induction of Rad51 foci up to 6 hours after MMS treatment. However, whilst the Rad51 foci in U2OS or *parp2Δ* cells had decayed 12 hours after MMS exposure, those in the *parp1Δ* background persisted. This suggests delayed resolution of damage, or additional damage being channelled through Rad51-dependent repair routes in these cells. However, *parp1Δparp2Δ* cells displayed only a modest induction of Rad51 foci after MMS exposure, in stark contrast to the high levels of γH2AX these cells accumulate in the hours after MMS exposure (Figure 4.2). Together, these data suggest *parp1Δparp2Δ* cells have problems generating and/or maintaining Rad51 nucleofilaments at sites of MMS-induced damage.

Disruption of BER has previously been identified to affect the engagement of HR following MMS exposure (Brem et al., 2008). In order to more clearly

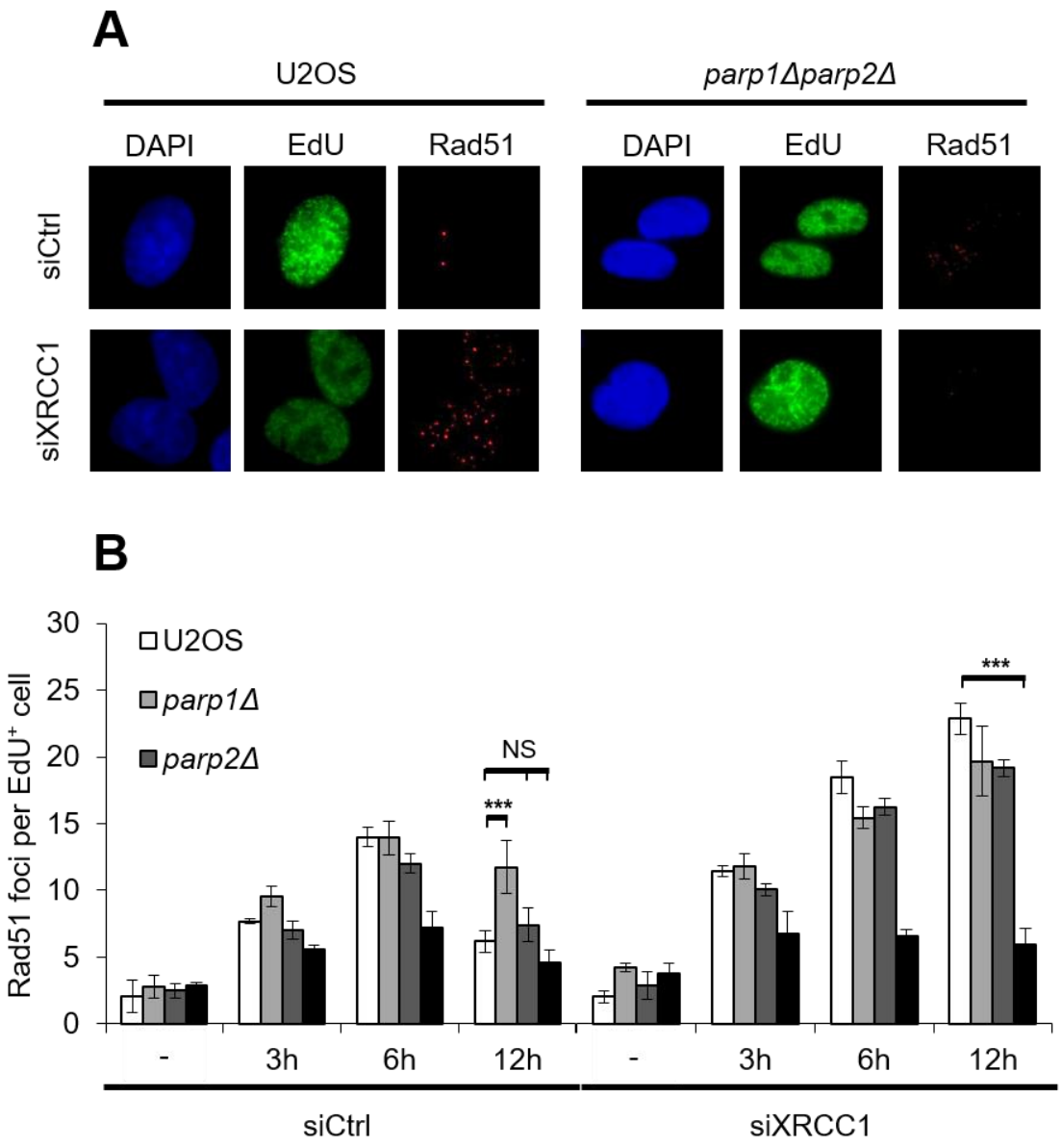


Figure 4.5: The formation of Rad51 foci are compromised in the absence of PARP1 and PARP2. A. The indicated cell lines transfected with siCtrl or siXRCC1, were treated with 1 μM EdU and 0.5 mM MMS for 1 hour, before recovery in fresh media. EdU and Rad51 were detected by immunofluorescence. Representative images of cells 12 hours after MMS and EdU addition are shown. **B.** The indicated cell lines, transfected with siCtrl or siXRCC1, were treated as in **A**. Times indicated show hours since addition of EdU and MMS. EdU and Rad51 were detected by immunofluorescence, and the number of Rad51 foci quantified in EdU-positive nuclei. Error bars represent the SEM from three independent experiments.

separate the roles of PARPs in Rad51-mediated repair from the potential effects of compromised BER on the use of HR, I assessed the formation of Rad51 foci in *parpΔ* cells after knockdown of XRCC1. This allows the disruption of BER in each cell line and a clearer assessment of the impact of loss of PARPs to Rad51 nucleofilament formation (Figure 4.5 A, B). U2OS cells depleted of XRCC1 accumulate elevated levels of Rad51 foci that continue to persist up to 12 hours after MMS treatment, indicating that in the absence of functional BER, additional damage is channelled through HR. In both *parp1Δ* and *parp2Δ* cells depleted of XRCC1, comparable numbers of Rad51 accumulate as compared to XRCC1 depleted U2OS cells. Strikingly, accumulation of these foci is compromised in XRCC1 depleted *parp1Δparp2Δ* cells, confirming Rad51-mediated repair is disrupted in the absence of PARP1 and PARP2 in combination.

Given the absence of PARP1 and PARP2 compromises the formation of Rad51 foci following MMS exposure, I might expect inhibitors able to target both of these PARPs to be able to elicit similar effects. Olaparib has been shown to strongly bind both PARP1 and PARP2 (Wahlberg et al., 2012), so I assessed the effects of olaparib exposure on the accumulation of Rad51 foci in U2OS cells transfected with control or XRCC1 siRNA (Figure 4.6). Whilst knockdown of XRCC1 was able to significantly increase the formation of Rad51 foci in EdU-positive cells, exposure to olaparib did not give rise to a similar increase. Furthermore, treatment with olaparib was able to suppress the elevated level of Rad51 foci formed in XRCC1 depleted cells. Therefore use of a PARP inhibitor is able to phenocopy a *parp1Δparp2Δ* cell line in compromising the formation of Rad51

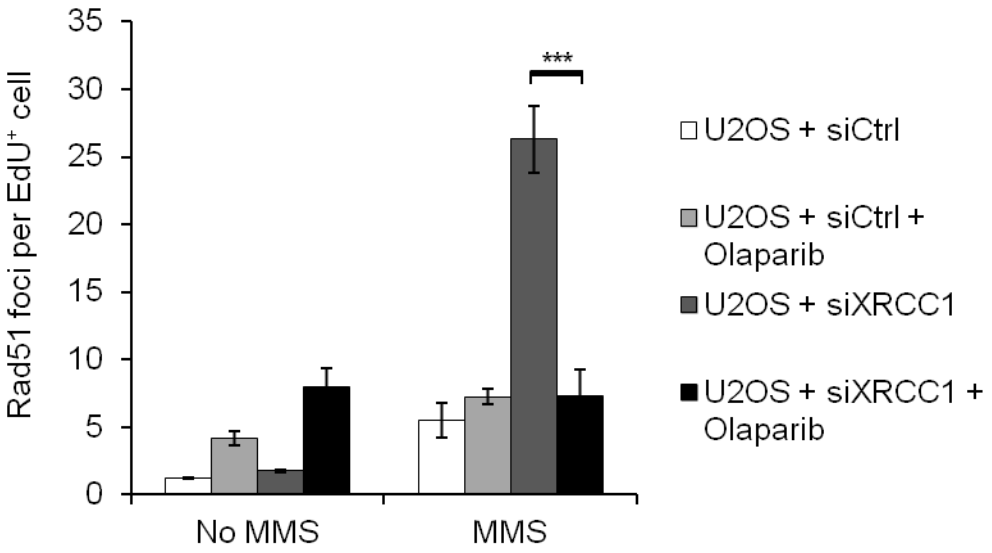


Figure 4.6: The formation of Rad51 foci are compromised by treatment with PARP inhibitors. U2OS cells, transfected with siCtrl or siXRCC1, with or without 10 μM Olaparib exposure, were treated with 1 μM EdU and 0.5 mM MMS for 1 hour, before recovery in fresh media. Cells were fixed 12 hours after addition of EdU and MMS. EdU and Rad51 were detected by immunofluorescence, and the number of Rad51 foci quantified in EdU-positive nuclei. Error bars represent the SEM from three independent experiments.

foci induced by MMS exposure. Taken together, these data indicate that PARP1 and PARP2 facilitate the resolution of MMS-induced replication-associated damage independently of BER, by promoting Rad51-dependent repair.

4.3 Discussion

MMS is able to induce replication-associated damage during S-phase, but how loss of PARPs might impact on the generation and repair of this damage was unclear. Therefore, during this chapter, I have assessed how loss of PARP1 and/or PARP2 affects the formation and resolution γH2AX foci induced by MMS. Consistent with previous reports (Ensminger et al., 2014; Nikolova et al., 2010), I was able to detect γH2AX foci formation specifically in S-phase cells, but not G1- or G2-phase cells, immediately after MMS exposure (Figure 4.1). Whilst loss of PARP1 or PARP2 individually has no effect on the induction of γH2AX foci, disruption of both PARPs together results in elevated levels of these foci. This is most likely attributable to these cells being compromised for the strand ligation step of BER, meaning BER intermediates accumulate following MMS exposure. This leads to more collisions between replication forks and these intermediates, and consequently more S-phase associated damage. Consistent with this interpretation, loss of XRCC1, another key protein in the strand ligation step of BER, also leads to elevated γH2AX foci at early time points following MMS exposure. Furthermore, no additive accumulation of γH2AX foci is apparent in *parp1Δparp2Δ* cells depleted of XRCC1 (Figure 4.3), providing additional evidence that their functions lie in the same pathway in this context.

I also assessed the ability of cells to resolve MMS-induced γH2AX following a recovery period after damage induction (Figure 4.2). U2OS cells are clearly able to resolve these γH2AX foci, with the number of foci approaching untreated levels 12 hours after MMS exposure. Whilst *parp1Δ* cells show a mild delay in the resolution of this damage, *parp1Δparp2Δ* cells show a striking persistence of these foci. This observation, taken together with the fact cells depleted of XRCC1 show normal kinetics of repair, indicates PARP1 and/or PARP2 play additional BER-independent roles in the resolution of this S-phase associated damage. Whilst *parp1Δ* cells depleted of XRCC1 show a significant delay in the resolution of γH2AX foci, *parp1Δparp2Δ* cells are further compromised in their ability to repair this damage, demonstrating both PARP1 and PARP2 contribute to the resolution of this damage (Figure 4.3). Thus PARP1 and PARP2 are required for two distinct but related aspects of the repair of methylated DNA bases. Firstly, through accelerating DNA strand ligation during BER, and secondly through promoting the resolution of replication-associated damage arising when replication forks collide with BER intermediates.

I next wished to understand in which repair pathway(s) PARP1 and PARP2 might function in order to facilitate repair of this damage. S-phase associated γH2AX foci formed after MMS exposure are ATM-dependent, and give rise to chromatid breaks and rearrangements, indicating they may represent genuine DSBs (Ensminger et al., 2014). Furthermore, cells lacking core HR factors are sensitised to MMS exposure (Nikolova et al., 2010). Indeed, in U2OS cells Rad51 clearly form in response to MMS, and inhibition of HR leads to a striking persistence of MMS-induced γH2AX foci (Figure 4.4). This suggests not only

that HR is engaged in response to these lesions, but also that its function is critical for the proper resolution of this damage.

U2OS cells depleted of XRCC1 accumulate high levels of Rad51 foci, which persist up to 12 hours post-exposure, demonstrating that in the absence of fully functional BER, additional damage is resolved through HR-dependent repair (Figure 4.5). Interestingly, *parp1Δ* cells also display persistent Rad51 foci, despite no BER defect being apparent in a comet assay (Figure 3.8). This suggests these cells are deficient in another repair pathway that competes with HR, in the absence of which more damage is channelled through Rad51-dependent repair. Alternately, *parp1Δ* cells could carry a mild BER defect which cannot be detected in a comet assay, but does manifest itself in increased Rad51 foci following MMS exposure. Both *parp1Δ* and *parp2Δ* cell lines depleted of XRCC1 accumulate similarly high levels of Rad51 foci to U2OS cells, indicating that either PARP individually is dispensable for a robust increase in HR- mediated repair. In contrast, *parp1Δparp2Δ* cells show only a modest accumulation of Rad51 foci following MMS exposure, despite the fact these cells are not competent for BER, and accumulate high levels of DNA damage marked by γH2AX. Indeed when XRCC1 is depleted in these cells, it becomes clear that Rad51 foci accumulation is severely compromised in the absence of PARP1 and PARP2 (Figure 4.5).

Our observations that loss or inhibition of PARPs leads to decreased formation of Rad51 foci following MMS is consistent with previous work, that reported a similar phenotype in response to HU-induced replication stress (Bryant et al., 2009). However, there are also some apparent differences in the relationship

between PARPs at MMS- and HU-induced replication damage. Loss of either PARP1 or PARP2 is sufficient to suppress HR after HU exposure, with loss of both proteins not leading to a cumulative defect (Bryant et al., 2009). This suggests unique and critical roles of both PARP1 and PARP2 within the same pathway of Rad51-dependent repair. In contrast, I observe essentially normal capacity to form Rad51 foci in the absence of either PARP1 or PARP2 alone, but a compromised formation and persistence of these foci in the absence of both PARPs together. This indicates overlapping or redundant roles of PARP1 and PARP2 in response to MMS, such that loss of either one is tolerated

. One potential explanation for this is differences in experimental setup, with the HU study using a recombination reporter assay to examine the relationship between PARP1 and PARP2, whereas here I use Rad51 foci formation. An alternative explanation could be differences in the nature of the replication damage induced by HU or MMS. HU inhibits ribonucleotide reductase and causes to cellular dNTP depletion and global replication fork stalling (Skoog and Nordenskjöld, 1971). In contrast, after MMS exposure replication forks collide with BER-intermediates, potentially leading to the rapid formation of one-ended DSBs through replicative run-off. The contrasting manner in which HU and MMS induce replication stress could underlie the differences in the PARP requirements for HR-mediated repair.

The mechanism through which PARP1 and PARP2 contribute to HR in response to MMS-induced damage is unclear, and a number of possibilities exist which could lead to decreased Rad51 foci formation in *parp1*Δ*parp2*Δ cells. PARPs may regulate resection at the sites of replication stress, as has been previously suggested for PARP1 at HU-induced stalled replication forks

(Bryant et al., 2009). Alternatively, PARPs may regulate loading of Rad51 onto DNA, either directly or through modulation of loading factors, for example BRCA2. Finally, the stability of the Rad51 nucleofilament may be compromised in the absence of PARPs, leading to their disassembly and failure to accumulate.

In this chapter, I have assessed the effect of PARP1 and PARP2 disruption on the formation and resolution of S-phase associated damage after MMS exposure. Loss of PARP1 and PARP2 in combination results in elevated formation of MMS-induced γH2AX foci in actively replicating cells, as well as a persistence of these foci after the removal of MMS. I have demonstrated these observations can be explained by a combination of a BER defect and compromised Rad51-mediated repair of lesions in the absence of PARP1 and PARP2. The mechanism by which the loss of these PARPs impacts on HR repair of these lesions will be explored in the following chapter.

5. PARP1 and PARP2 regulate Rad51 nucleofilament stability through an Fbh1-dependent mechanism

5.1 Introduction

5.1.1 Rad51 is a key player in the cellular response to replication stress

Rad51 is the central recombinase in HR that assembles into filaments on ssDNA to promote homology search, strand invasion and repair of DNA DSBs through a number of distinct sub-pathways (Jasin and Rothstein, 2013). A number of components of the HR machinery, along with Rad51, are also known to play a key role in the cellular response to replication stress (Kolinjivadi et al., 2017). Cells defective in Rad51-mediated HR are sensitive to various agents that induce replication stress and lose the ability to slow their replication forks in response to damage (Henry-Mowatt et al., 2003). Furthermore, the stalled forks that do form in this context are susceptible to hyper-resection, indicating they are in some way unprotected and vulnerable to the unscheduled action of nucleases (Schlacher et al., 2011). This has been suggested to be mediated by the ability of Rad51 to promote the formation and stability of reversed replication forks. Indeed in the absence of Rad51 reversed forks fail to form, leading to the generation of extensive ssDNA tracts at stalled forks (Zellweger et al., 2015).

If replication forks are stalled for a prolonged period of time, they can collapse, leading to the formation of detectable DSBs. Homologous recombination and

Rad51 also act to resolve these lesions (Malkova and Ira, 2013), meaning Rad51 participates in at least two independent pathways to facilitate the resolution of stalled and/or collapsed replication forks (Petermann et al., 2010).

5.1.2 Regulation of homologous recombination and Rad51 filament assembly

The tight regulation of recombination is crucial, such that it acts at appropriate times and locations to promote repair. Uncontrolled and inappropriate engagement of recombination can lead to mutations and chromosomal rearrangements, whilst disruption of the HR machinery leads to genome instability and cancer predisposition (Heyer et al., 2010). A major control point for recombination at canonical DSBs is the initiation of DNA end resection, controlled by the interplay between BRCA1, which promotes resection, and 53BP1, which represses it. This is highlighted by the observation that defective HR phenotypes in BRCA1-null cells can be reversed by loss of 53BP1(Bunting et al., 2010). 53BP1 is recruited to breaks even in G2 when HR predominates (Shibata et al., 2011), where it forms visible foci. However, 53BP1 is relocalised over time to the periphery of these foci, in a BRCA1 dependent manner, allowing limited resection to occur at the break and HR to proceed (Chapman et al., 2012). The phosphorylation of 53BP1, which governs its interactions with RIF1 and PTIP, is important for its role in limiting or preventing resection (Callen et al., 2013; Chapman et al., 2013). Once initiated, resection is performed by multiple nucleases, including Mre11, CtIP, Exo1 and Dna2 (Liu and Huang, 2016). The extent to which resection is required for the resolution of replication forks by fork reversal is unclear, but a number of nucleases have

been implicated promoting replication fork restart, including Mre11 and CtIP (Costanzo et al., 2001; Yeo et al., 2014).

BRCA2, along with its partner PALB2, is a key mediator of HR at canonical DSBs, loading Rad51 onto RPA-bound ssDNA to facilitate homology searching and strand invasion (Buisson et al., 2010; Jensen et al., 2010). BRCA2 also plays key functions in replication fork stability, protecting forks from degradation and contributing to replication fork stability (Schlacher et al., 2011). Interestingly, the BRCA2 protein is not conserved in yeast, where the loading function is carried out by Rad52 (Symington, 2002). Whilst humans also possess a Rad52 protein, it lacks Rad51 loading capabilities *in vitro* (Jensen et al., 2010), but is able to enhance strand annealing reactions (Reddy et al., 1997). Human Rad52 is known to play roles in the error prone SSA pathway (Stark et al., 2004), and contributes to BIR-mediated restart of stalled replication forks (Sotiriou et al., 2016). Recently, Rad52 has also been shown to mediate mitotic DNA synthesis (MiDAS), which helps to complete replication at common fragile sites (CFSs) and prevent anaphase bridge formation (Bhowmick et al., 2016). However, loss of Rad52 results in only mild HR phenotypes in wild-type cells (Rijkers et al., 1998), but is synthetic lethal with BRCA1 or BRCA2 mutations (Feng et al., 2011; Lok et al., 2013). This potentially indicates that Rad52 acts as a backup for BRCA functions, or mediates repair through a competing BRCA-independent pathway. Further work is required to clarify the exact role of Rad52 in this context.

Aside from the obvious importance of the assembly of Rad51 filaments, factors mediating the disassembly of these structures are also key for the proper control and functioning of HR. Numerous factors have been identified that can

disassemble Rad51 filaments *in vitro*, including the helicases BLM, Fbh1, PARI, RecQ5 and FANCJ (van Brabant et al., 2000; Bugreev et al., 2007; Hu et al., 2007; Moldovan et al., 2012; Simandlova et al., 2013; Sommers et al., 2009). The loss of BLM in humans leads to Bloom's syndrome, characterised by cellular hyper-mutation and hyper-recombination (Chaganti et al., 1974; German et al., 2007). Similarly, loss of Fbh1, PARI, or RecQ5 can result in elevated levels of Rad51 foci and recombination. Interestingly, the anti-recombinogenic activity of Fbh1 has been linked to both its helicase domain (Simandlova et al., 2013) and its ability to ubiquitinate Rad51 using its F-box domain as part of an SCF complex (Chu et al., 2015).

PARP1 influences the regulation of HR in response to a number of DNA damaging agents. The activity of PARP1 promotes the recruitment of both BRCA1 and BRCA2 to DSBs (Li and Yu, 2013; Zhang et al., 2015), although how this relates to their functions at replication-associated damage is uncertain. Furthermore, PARP1 can promote the recruitment of Mre11 to replication forks stalled by HU, facilitating efficient DNA-end resection and fork restart (Bryant et al., 2009). Finally, PARP1 has also been shown to promote the stability of reversed replication forks, preventing their premature dissolution by RecQ1 in response to camptothecin (Berti et al., 2013). How these different roles of PARP1 might interface with one another, and contribute to the resolution of MMS-induced replication associated damage is unclear.

5.1.3 Aims

In the previous chapter, I established that in the absence of PARP1 and PARP2, the formation and persistence of Rad51 foci are compromised after

MMS exposure. It is uncertain whether these Rad51 foci represent stabilised or reversed replication forks, or the action of HR to restart collapsed forks, or some combination of the two. Furthermore, it is unclear how loss of PARP1 and PARP2 leads to a decreased capability to form and maintain Rad51 foci. Numerous potential control points exist during the process of HR, including the initiation and processivity of DNA end resection, Rad51 loading and Rad51 nucleofilament stability. In this chapter, I will investigate the mechanism by which PARP1 and PARP2 promote the formation and/or stability of Rad51 foci following MMS-induced base damage.

5.2 Results

5.2.1 Resection is not compromised in the absence of PARP1 and PARP2

One way in which loss of PARP1 and PARP2 could impact on the formation of Rad51 foci is through control of resection. Limited resection, mediated by multiple nucleases, is required to reveal a 3' ssDNA overhang onto which Rad51 can be loaded to facilitate HR. Indeed PARP1 facilitates the recruitment of the nuclease Mre11 to replication forks stalled by HU, allowing resolution of these lesions (Bryant et al., 2009). If resection was also promoted or mediated through PARylation at MMS-induced replication damage, then in the absence of PARP1 and PARP2, this process would be compromised, leading to impaired formation of Rad51 foci and dysfunctional HR. One prediction of this model would be the reduced formation of RPA foci in *parp1Δparp2Δ* cells, as a downstream consequence of reduced ssDNA formation. Indeed, loss of key resection nucleases Mre11 or CtIP leads to reduced RPA and Rad51 foci

formation in response to a range of DNA damaging agents (Sartori et al., 2007; Shibata et al., 2014). Therefore, I assessed the formation of RPA foci in the different *parpΔ* cell lines after exposure to MMS (Figure 5.1 A). In U2OS cells, RPA foci accumulated in EdU positive nuclei, peaking at 6 hours after administration of MMS. The kinetics of RPA foci formation in *parp2Δ* cells were very similar to U2OS cells, whilst *parp1Δ* cells accumulated additional RPA foci that persisted up to 12 hours after MMS treatment. This could indicate a loss of fork protection and over-resection in these cells. However, taken together with the additional Rad51 foci that accumulate in *parp1Δ* cells after MMS exposure, this data implies that additional damage is channelled through HR in the absence of PARP1. Depletion of XRCC1 in U2OS cells was also able to significantly increase the formation and persistence of RPA foci in EdU positive cells 12 hours after MMS exposure (Figure 5.1 B), highlighting the increased flux of damage through HR in absence of functional BER.

Strikingly, in the absence of both PARP1 and PARP2, cells display very high levels of RPA foci, significantly more than in the absence of XRCC1 or PARP1 alone (Figure 5.1 A, B). Furthermore, *parp1Δparp2Δ* cells show elevated accumulation of S4/8 phospho-RPA32 (Figure 5.1 C), a modification catalysed by a number of PIKKs that stimulates DNA repair (Anantha et al., 2007; Liaw et al., 2011). These data suggest that resection is not compromised in *parp1Δparp2Δ* cells; in contrast loss of these factors results in over-resection and an accumulation of RPA foci following

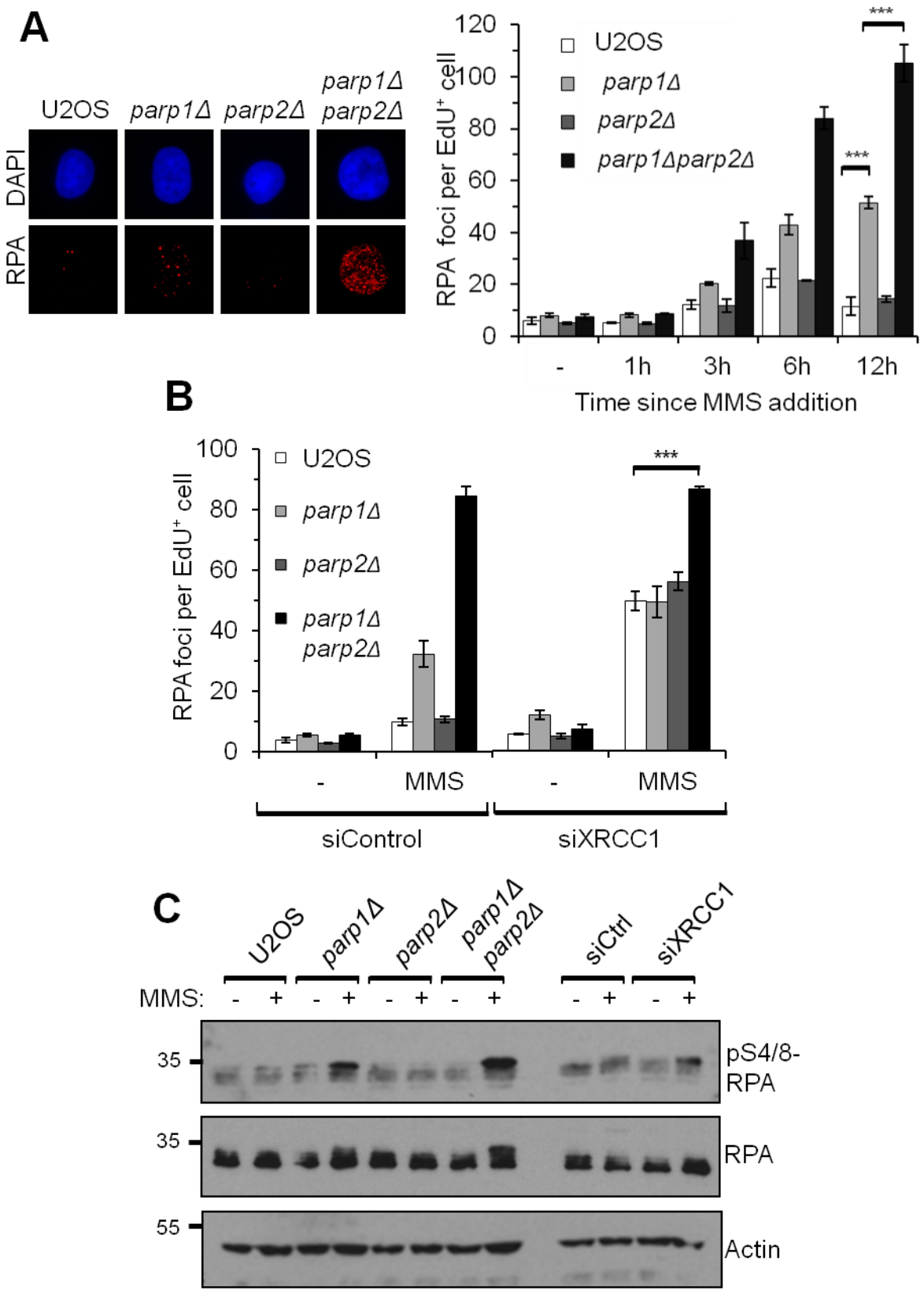

A
U2OS
parp1Δ
parp2Δ
parp1Δ parp2Δ
DAPI
RPA
RPA foci per EdU+ cell
U2OS
parp1Δ
parp2Δ
parp1Δparp2Δ
***
***
-
1h
3h
6h
12h
Time since MMS addition
B
RPA foci per EdU+ cell
U2OS
parp1Δ
parp2Δ
parp1Δ parp2Δ
***
-
MMS
-
MMS
siControl
siXRCC1
C
U2OS
parp1Δ
parp2Δ
parp1Δ parp2Δ
siCtrl
siXRCC1
MMS:
- + - + - + - + - + - +
35
pS4/8-RPA
35
RPA
55
Actin

Figure 5.1: RPA foci are elevated in *parp1Δparp2Δ* cells after MMS exposure. A. U2OS or *parp1Δparp2Δ* cells were treated with 1 μM EdU and 0.5 mM MMS for 1 hour, before recovery in fresh media. Times indicated show hours since addition of EdU and MMS. EdU and RPA-32 were detected by immunofluorescence, and quantified in EdU positive nuclei (lower panel). Representative images of EdU-positive are shown 12 hours after MMS addition (upper panel). **B.** The indicated cell lines transfected with control or XRCC1 siRNA and treated as in **A**. Following immunofluorescence, RPA foci were quantified in EdU-positive cells. **C.** The indicated cell lines were treated with 0.5 mM MMS for 1 hour, before recovery in fresh media. 12 hours after MMS addition, cells were harvested, and Western blotting of whole cell extracts carried out with the indicated antibodies. Error bars represent the SEM from three independent experiments.

MMS exposure. Therefore the function of PARP1 and PARP2 in the HR response to MMS-induced damage likely lies downstream of resection and RPA filament formation.

5.2.2 Recruitment of the BRCA2-PALB2 complex to chromatin after MMS exposure is not compromised by inhibition of PARP1 and PARP2

BRCA2/PALB2 is responsible for loading Rad51 onto RPA coated ssDNA in human cells (Yuan et al., 1999). One potential explanation for the lack of Rad51 foci forming in *parp1Δparp2Δ* cells is if PARP1 and/or PARP2 regulate the function or activity of this complex. In order to test this hypothesis, I utilised the availability of HT1080 cells containing a doxycyclin-inducible GFP-tagged PALB2 cassette (a kind gift of F. Esashi). Exposure to doxycyclin was able to clearly induce expression of GFP-tagged PALB2 (Figure 5.2 A). Recruitment of PALB2 to chromatin was apparent 6 hours after exposure to MMS (Figure 5.2 B), and this recruitment was enhanced in the presence of the PARP inhibitor olaparib. Taken together with the fact that olaparib exposure is able to suppress the additional Rad51 foci that form in XRCC1 depleted cells in response to MMS (Figure 4.6), this suggests that loss of Rad51 foci is not driven through disrupted recruitment of BRCA2/PALB2 to chromatin.

5.2.3 Rad52 does not contribute to the resolution of S-phase associated damage after MMS exposure

An additional possibility is that PARylaiton mediated by PARP1 and PARP2 could potentiate the functions of Rad52 in the resolution of MMS-induced S-phase associated damage. Whilst Rad52 in yeast carries out the core Rad51

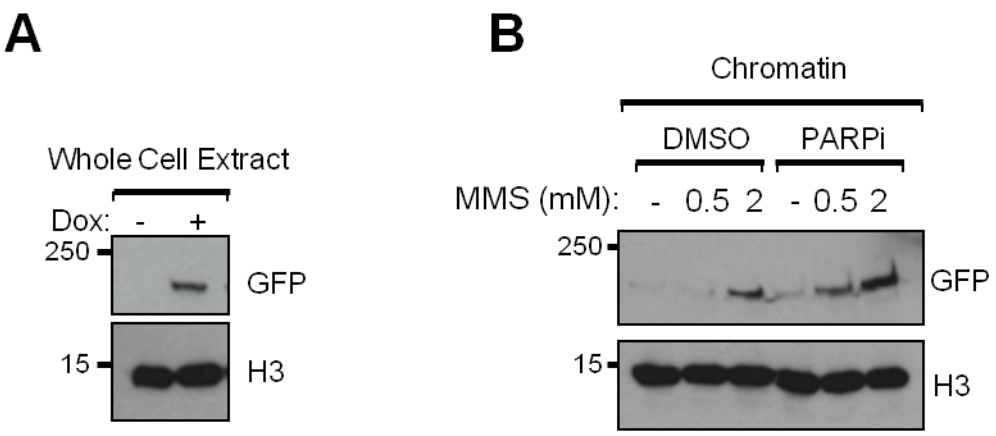


Figure 5.2: PALB2 recruitment to chromatin is not disrupted by PARPi. **A.** Flp-In T-Rex HT1080 cells containing a doxycyclin-inducible FE-PALB2 expression cassette were left untreated or exposed to 5 µg/mL doxycyclin for 24 hours. Western blotting of whole cell extracts was performed with the indicated antibodies. **B.** Flp-In T-Rex HT1080 cells expressing FE-PALB2, with or without 10 µM olaparib (PARPi) treatment, were left untreated (-) or exposed to the indicated concentrations of MMS for 1 hour before recovery in fresh media. Chromatin extracts were prepared 6 hours after MMS addition, and analysed by Western blotting with the indicated antibodies.

loading function during HR, this appears to be performed by BRCA2/PALB2 in mammals. Therefore the precise role of mammalian Rad52 in HR remains uncertain, but it has been linked to the restart of replication forks through BIR (Sotiriou et al., 2016). Furthermore, recent work has uncovered a synthetic lethal relationship between Rad52 and BRCA1/2, suggesting that Rad52 may be able to support a Rad51 loading function in the absence of BRCA proteins (Feng et al., 2011; Lok et al., 2013). Given that PARPi also has a synthetic lethal relationship with BRCA2, this raises the possibility that Rad52 and PARPs are functioning in the same pathway. In order to explore this hypothesis in the context of MMS-induced damage, I depleted cells of Rad52 to assess whether it contributes to the resolution of S-phase associated damage in some capacity (Figure 5.3 A). Depletion of Rad52 did not significantly affect cellular survival or γH2AX resolution after MMS exposure, in U2OS or *parp1Δ* cells (Figure 5.3 B, C). Depletion of Rad52 also did not affect the initial formation of Rad51 foci following MMS administration (Figure 5.3 D), and was not able to suppress the additional Rad51 foci that persist in *parp1Δ* cells. This suggests that aberrant function of Rad52 is not the cause of the compromised Rad51 foci in *parp1Δparp2Δ* cells. Interestingly, Rad51 foci persist 12 hours after MMS exposure in U2OS cells depleted of Rad52, although the implications of this result are unclear.

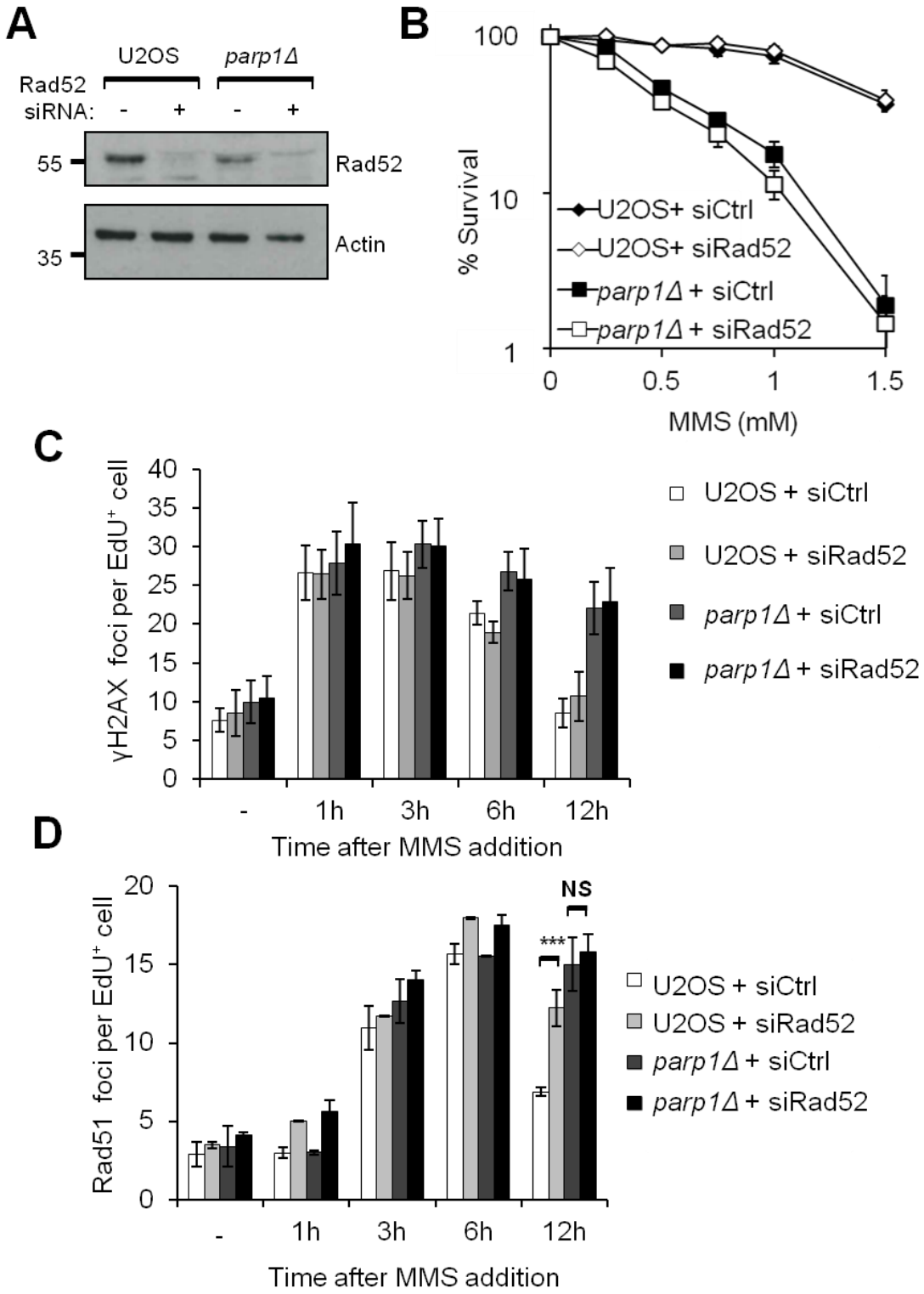


Figure 5.3: Loss of Rad52 does not affect the cellular response to MMS. **A.** Whole cell extracts were prepared from U2OS or *parp1Δ* cells transfected with siCtrl or siRad52, and Western blotting performed with the indicated antibodies.**B.** U2OS or *parp1Δ* cells, transfected with siCtrl or siRad52, were exposed to MMS and survival assessed by clonogenic assay. **C.** The indicated cell lines, transfected with siCtrl or siRad52, were treated with 1 μM EdU and 0.25 mM MMS for 1 hour, before recovery in fresh media. Times indicated show hours since addition of EdU and MMS. EdU and γ-H2AX were detected by immunofluorescence. **D.** The indicated cell lines, transfected with siCtrl or siRad52, were treated with 1 μM EdU and 0.5 mM MMS for 1 hour, before recovery in fresh media. Times indicated show hours since addition of EdU and MMS. EdU and Rad51 were detected by immunofluorescence. Error bars represent the SEM from three independent experiments.

5.2.4 Depletion of Fbh1, but not BLM, is able to rescue Rad51 foci formation in *parp1Δparp2Δ* cells

Balancing the level of HR to facilitate repair but prevent inappropriate recombination events is also a crucial element of regulation of this pathway (Kowalczykowski, 2015; Ouyang et al., 2008). Therefore, one further hypothesis is that PARPs may influence the equilibrium of pro- and anti-recombinogenic factors acting at sites of damage. In order to assess this possibility, I depleted cells of two anti-recombinogenic factors that are able to disassemble Rad51 filaments, BLM and Fbh1, and assessed Rad51 foci formation and decay in U2OS and *parp1Δparp2Δ* cells (Figure 5.4 A, B). Knockdown of BLM does not affect the formation or decay of Rad51 foci in EdU-positive U2OS or *parp1Δparp2Δ* cells following MMS treatment. In contrast, knockdown of Fbh1 causes a slight increase in the formation of Rad51 foci in U2OS cells. Strikingly however, knockdown of Fbh1 in *parp1Δparp2Δ* cells leads to significantly increased formation and persistence of Rad51 (Figure 5.4 B, C), to a similar extent as U2OS cells depleted of XRCC1 (Figure 4.6 A). Depletion of Fbh1 is also able to increase the formation and persistence of Rad51 foci in cells exposed to PARPi (Figure 5.4 D). Taken together, these data indicate that PARP1 and PARP2 function to stabilise Rad51 filaments following MMS exposure, by antagonising the activity of Fbh1.

I next considered whether depleting Fbh1 in *parp1Δparp2Δ* cells, and restoring Rad51 foci, is sufficient to rescue the sensitivity of these cells to MMS. Depletion of either Fbh1 or BLM did not significantly affect the sensitivity of *parp1Δparp2Δ* cells to MMS (Figure 5.5 A), demonstrating that restoration of

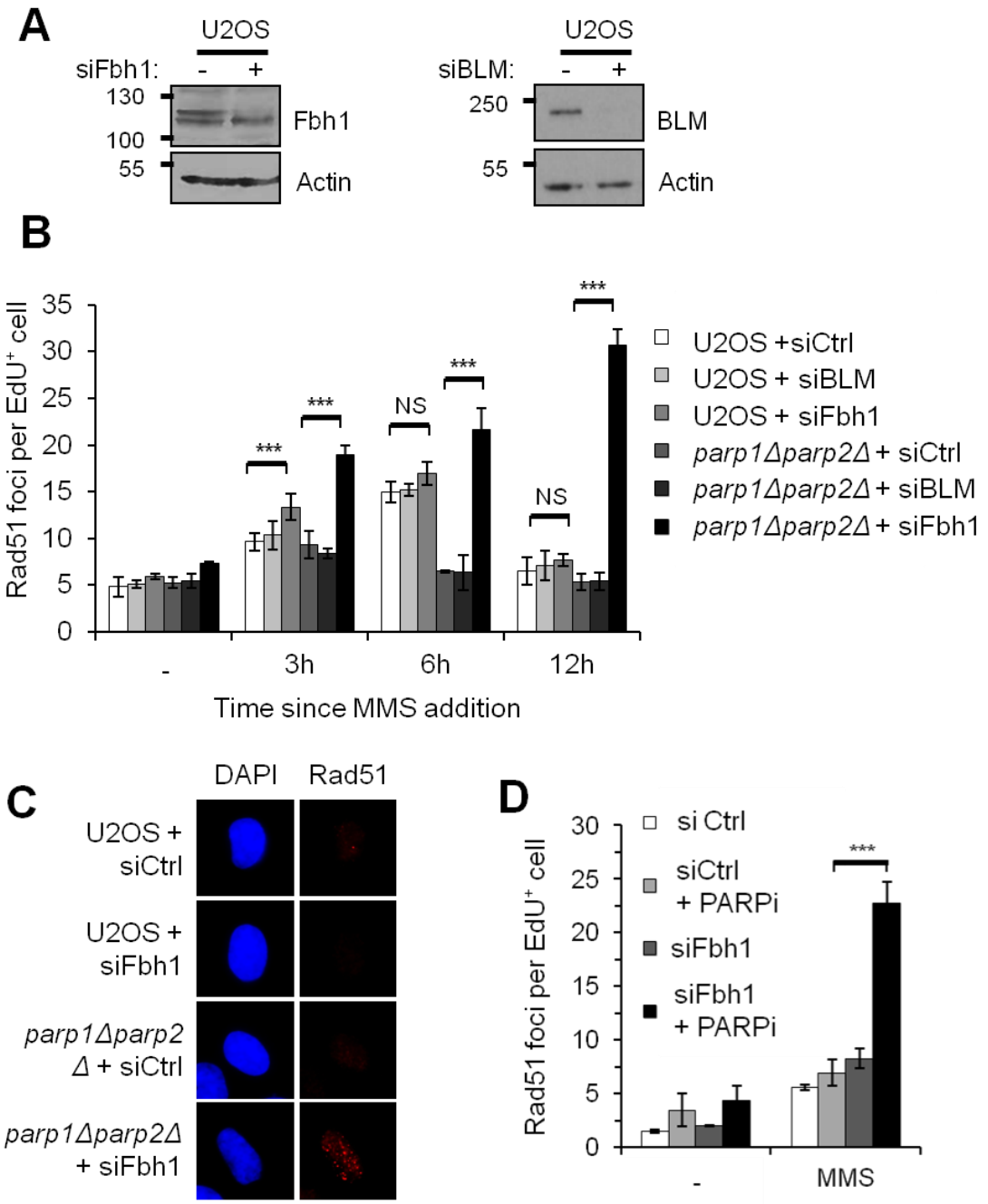


Figure 5.4: PARP1 and PARP2 promote the stability of Rad51 foci through an Fbh1-dependent mechanism. **A.** Whole cell extracts were prepared from cells transfected with siCtrl , siFbh1 or siBLM, and Western blotting performed with the indicated antibodies. **B.** The indicated cell lines, transfected with control, siBLM or siFbh1 were treated with 1 μM EdU and 0.5 mM MMS for 1 hour, before recovery in fresh media. Times indicated show hours since addition of EdU and MMS. EdU and Rad51 were detected by immunofluorescence. **C.** Representative images of Rad51 foci in EdU positive cells treated as in **B**. Images were taken 12 hours after MMS addition. **D.** U2OS cells, transfected with siCtrl or siFbh1, with or without Olaparib exposure, were treated as in **B** and Rad51 foci in EdU-positive cells analysed by immunofluorescence. Cells were fixed 12 hours after MMS and EdU addition. Error bars represent SEM from three independent experiments.

Rad51 foci alone cannot functionally compensate for PARP1 and PARP2 loss in the cellular response to MMS. Finally, I hypothesised loss of the replication-associated roles of PARP1 and PARP2 could contribute to the killing of HR-deficient cells by PARP inhibitors, and therefore that the depletion of Fbh1 could impact on the sensitivity of BRCA-null cells to these agents. In order to assess this possibility, I utilised two DLD1 cell lines which are heterozygous for, or completely lacking, functional BRCA2 (a kind gift of F. Esashi). Whilst the BRCA2 deficient cells were clearly sensitive to exposure to PARPi, loss of Fbh1 was unable to strongly affect the sensitivity these cells to olaparib (Figure 5.5 B).

5.3 Discussion

In this chapter I assessed various mechanisms by which loss of PARP1 and PARP2 could prevent the formation and/or accumulation of Rad51 foci in S-phase cells following exposure to MMS. First, I considered the possibility that PARPs could regulate resection at sites of damage, by assessing the formation and decay of RPA foci (Figure 5.1 A). Interestingly, *parp1Δparp2Δ* cells accumulate large numbers of RPA foci, suggesting that process of resection, which generates the ssDNA onto which RPA can load, is not defective. The high level of RPA foci could reflect a hyper-resection phenotype in these cells, seen when replication forks are unstable or insufficiently protected, for example in the absence of Rad51 or BRCA2 (Schlacher et al., 2011). An alternative interpretation of these data is that the elevated levels of RPA foci in *parp1Δparp2Δ* cells is simply a consequence of increased MMS-induced damage forming in cells which are not able to properly carry out BER. Indeed,

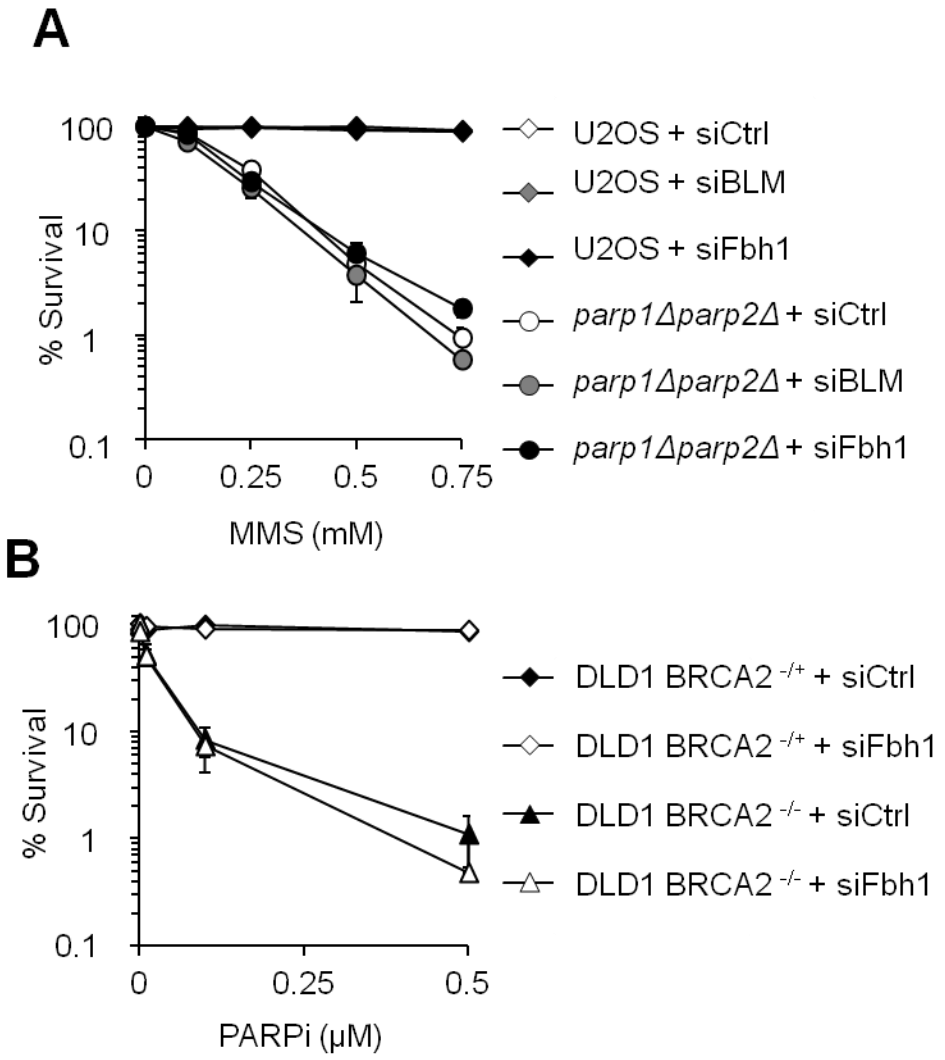


Figure 5.5: Depletion of Fbh1 does not affect the sensitivity of *parp1Δparp2Δ* cells to MMS, or the sensitivity of BRCA2-deficient cells to PARPi. A. U2OS or *parp1*Δ*parp2*Δ cells, transfected with siCtrl, siBLM or siFbh1, were exposed to MMS and survival assessed by clonogenic assay. **B.** DLD1 BRCA2 $^{-/+}$ or BRCA2 $^{-/-}$ cells, transfected with siCtrl or siFbh1, were exposed to olaparib (PARPi) and survival assessed by clonogenic assay. Error bars represent the SEM from three independent experiments.

U2OS cells depleted of XRCC1 also accumulate high levels of RPA foci following MMS treatment (Figure 5.1 B). However, *parp1Δparp2Δ* cells, whether depleted of XRCC1 or not, accumulate significantly more RPA foci than XRCC1 depleted U2OS cells, indicating that they produce more ssDNA following MMS exposure than can be attributed to a BER defect alone.

Whilst *parp1Δ* cells also show elevated formation of RPA foci, this phenotype is not as severe as in XRCC1-depleted U2OS cells. Furthermore, depletion of XRCC1 in *parp1Δ* cells results in similar levels of RPA foci as in U2OS cells depleted of XRCC1, indicating that PARP1 and XRCC1 are epistatic in regards to driving accumulation of S-phase damage that is channelled through HR. This is most likely through disruption of BER, given that both of these proteins have previously been implicated in this pathway. However, *parp1Δ* cells do not show a BER strand ligation defect in response to MMS (Figure 3.8). Conceivably, loss of PARP1 could abrogate BER in some way that does not affect strand ligation kinetics, or cause defect that is too mild to be robustly detected in an alkaline comet assay. Regardless, the large accumulation of RPA foci in *parp1Δparp2Δ* cells after MMS treatment indicates that resection is not negatively affected by the loss of PARP1 and PARP2, and cannot explain the lack of Rad51 foci in these cells. This is consistent with reports that inhibition of PARPs can lead to the destabilisation and hyper-resection of stalled replication forks (Ying et al., 2012). However, this contrasts with the roles of PARP1 and PARP2 at HU-induced replication damage, where they promote resection through the recruitment of Mre11 (Bryant et al., 2009). These differences could be due to the distinct mechanisms through which these agents induce replication stress. HU acts as a ribonucleotide reductase inhibitor, depleting

cellular dNTP pools to globally stall replicative polymerases in a cell without the immediate induction of DNA strand breaks (Skoog and Nordenskjöld, 1971). In contrast, MMS methylates DNA bases, which are subsequently resolved by the BER pathway. Replication forks can collide with BER repair intermediates and stall/collapse (Ensminger et al., 2014). If a SSB has been generated by the action of BER at the lesion, there is a risk of replicative run-off and the rapid formation of a one-ended DSB. Assessing the relationship between PARPs in promoting the resolution of replication-associated damage induced in other ways, such as camptothecin, cis-platin or UV-irradiation may provide insight into how the form of replication stress affects the mechanism through which PARPs promote its resolution.

I next assessed whether the loading of Rad51 could be defective in the absence of PARP1 and PARP2. In mammals, Rad51 is predominantly loaded onto RPA-coated ssDNA by BRCA2 and its partner PALB2. Olaparib was able to enhance the association of PALB2 with chromatin following MMS treatment, arguing against dysregulation of recruitment of the BRCA2-PALB2 complex in the absence of functional PARP1 and PARP2 (Figure 5.2). This experiment cannot exclude the possibility that direct modification of BRCA2 or PALB2 by PARPs could be required for their proper functioning, but not affect their chromatin recruitment. However, the fact that BRCA2 can successfully load Rad51 *in vitro* without any ADP-ribosylation modifications would argue against this hypothesis (Jensen et al., 2010). The additional recruitment of PALB2 to chromatin after combinatorial olaparib and MMS exposure could be explained by the additional damage that accumulates in the absence of functional BER.

I also gauged the possibility that PARPs could be regulating Rad52 to influence HR-mediated repair of MMS-induced damage. This hypothesis was based on previous observations that Rad52 contributes to BIR in mammalian cells (Sotiriou et al., 2016), along with the fact loss of Rad52 displays a synthetic lethal relationship with BRCA2 deficiency (Feng et al., 2011). Given that PARPs also display a synthetic lethal relationship with BRCA2 loss, this could indicate that PARPs and Rad52 function together in the resolution of DNA damage. However, depletion of Rad52 did not reduce the formation of Rad51 foci in U2OS cells after MMS treatment, and was not able to suppress the elevated induction and persistence of Rad51 foci in *parp1Δ* cells (Figure 5.3). Furthermore, loss of Rad52 did not affect sensitivity or γH2AX induction and decay in these cell lines after MMS exposure. Taken together, this indicates that regulation of Rad52 is not the mechanism through which PARP1 and PARP2 are promoting HR. Interestingly, U2OS cells depleted of Rad52 do show persistent Rad51 foci 12 hours after MMS exposure. This suggests that Rad52 could play a role in a pathway that competes with Rad51-dependent HR, although further work would be needed to confirm and expand on this observation.

I finally considered the possibility that in the absence of PARP1 and PARP2, factors capable of disassembling Rad51 filaments might be preventing the accumulation of Rad51 foci, so I depleted cells of two different helicases that possess this activity, BLM and Fbh1. Loss of Fbh1 did not greatly affect the response of wild-type cells to MMS, but was able to significantly increase the formation of Rad51 foci in *parp1Δparp2Δ* cells, or cells treated with PARP inhibitors (Figure 5.4). This indicates that one of the functions of PARP1 and

PARP2 in response to MMS is to somehow antagonise the anti-recombinogenic activity of Fbh1, and promote the stability of Rad51 filaments to facilitate repair. Additionally, loss of Fbh1 cannot rescue defects in Rad51 loading, for example BRCA2 loss, further suggesting that this function is not compromised by the loss of PARP1 and PARP2 (Higgs et al., 2015). The exact mechanisms of the PARP-dependent regulation of Fbh1 requires further study, but a number of options are possible to explain how this is achieved. Fbh1 could be a direct target of ADP-ribosylation by PARP1 and/or PARP2, with this modification negatively regulating its function. Similarly, Fbh1 could bind PAR or ADP-ribosylated PARP1/2 to become inactivated or sequestered to prevent its action on Rad51 filaments. A similar mechanism has been uncovered for the helicase RecQ1, which can bind PARylated PARP1 to prevent its activity on reversed replication forks (Berti et al., 2013). A more indirect mode of action is also possible, with loss of PARP1 and PARP2 altering the complement of proteins present at sites of replication-associated damage, allowing Fbh1 access to the filament. One such factor could be BOD1L, a large protein found at replication forks, which promotes replication fork stability by preventing disassembly of Rad51 foci after replication stress (Higgs et al., 2015). Knockdown of Fbh1 can also reverse the loss of Rad51 caused by depletion of BOD1L. These similarities with our observations in *parp1Δparp2Δ* cells make a potential link between PARPs and BOD1L attractive. However, depletion of BLM is also able to antagonise loss of BOD1L, whereas knockdown of BLM has no effect on Rad51 foci in *parp1Δparp2Δ* cells, suggesting differences also exist between the roles of BOD1L and PARP1/2 at replication forks (Figure 5.5). It would be interesting to understand how the loss of other helicases capable of disrupting

Rad51 filaments *in vitro*, such as RecQ5, FancJ and PARI, is able to rescue Rad51 foci formation in BOD1L-null or *parp1Δparp2Δ* cells. (Hu et al., 2007; Moldovan et al., 2012; Sommers et al., 2009),

Despite increasing the formation of Rad51 foci in response to MMS, knockdown of Fbh1 in *parp1Δparp2Δ* cells is unable to reduce cellular sensitivity to this agent. This could indicate that PARP1 and/or PARP2 also regulate additional downstream features of HR-mediated repair of stalled replication forks, such that the Rad51 foci forming in Fbh1 depleted cells are not competent to complete repair. Alternatively, the amount of damage accumulating in *parp1Δparp2Δ* cells due to their severe BER defect may simply overwhelm the capabilities of cellular DNA repair, even when Rad51 foci formation is reactivated by Fbh1 loss.

Finally, depletion of Fbh1 was also unable to robustly alter the sensitivity of BRCA2-defective cells to PARP inhibition (Figure 5.5 B). This could indicate that the roles of PARP1 and PARP2 in promoting the stability of Rad51 foci at sites of replication stress are not relevant in the context of synthetic lethality with HR-deficiency. Alternatively, it may reflect the fact that loss of Fbh1 cannot rescue BRCA2-assosciated HR defects (Higgs et al., 2015), likely because in the absence of Rad51-loading capacity, Rad51 nucleofilaments are unable to form, so modulating their stability does not impact on cellular survival.

In summary, in this chapter I have identified a novel mechanism by which PARP1 and PARP2 function redundantly to promote the stability and repair of stalled/collapsed replication forks, through antagonising the anti-recombinogenic helicase Fbh1. Therefore PARP1 and PARP2 play roles in two

independent but closely related elements of the cellular response to base alkylation. Firstly, they promote the strand ligation step of BER, and secondly they promote the stability and resolution of stalled/collapsed replication forks that have collided with BER intermediates by inhibiting Fbh1.

6. Understanding the roles of specific PARPs in the synthetic lethal relationship with HR disruption

6.1 Introduction

6.1.1 Multiple mechanisms have been proposed to explain the toxicity of PARP inhibitors to HR deficient cells

PARP inhibitors selectively kill cells with mutations in BRCA1 or BRCA2 (Bryant et al., 2005; Farmer et al., 2005). However, the mechanism by which this is achieved is unclear, with several theories being proposed. Initially, it was suggested that PARP inhibitors disrupt SSBR, leading to an accumulation of replication-associated DSBs during S-phase. These breaks require HR for effective repair, making PARPi toxic to HR-deficient cells (Bryant et al., 2005; Farmer et al., 2005). However, accumulating stand breaks are not apparent in cell treated with PARPi, drawing this model into question (Gottipati et al., 2010). Subsequently, the ability of PARP inhibitors to prevent the release of PARPs from strand breaks became evident, leading to them becoming “trapped” on the DNA (Murai et al., 2012). This led to an alternative model to explain the synthetic lethal relationship between PARPs and HR; that lesions occluded by a trapped PARP protein may be more difficult to resolve, and rely more heavily on HR for repair. Thirdly, it has been postulated that PARP-mediated pathways beyond SSBR might repair lesions in the absence of HR. Therefore, disruption of these functions could contribute to the killing of HR-defective cells. Whether some, or all of these mechanisms might contribute to the efficacy of PARPi remains an open question.

The currently available clinical PARP inhibitors were selected for their ability to inhibit the catalytic domain of PARP1. However, multiple studies using purified PARP proteins, either full length or isolated catalytic domains, have demonstrated the more general activity of these compounds against other members of the PARP superfamily (Thorsell et al., 2017; Wahlberg et al., 2012). Most notably, these inhibitors are able to strongly bind to PARP2 and PARP3, the two other DNA-dependent PARPs. Mechanistically, these PARP inhibitors act as NAD^+ mimetics, binding the catalytic domain of the PARP and preventing ADP-ribosylation activity. Given the conserved catalytic domain is present across the entire PARP family this observed lack of specificity is perhaps unsurprising. Importantly, it is possible that these additional targets of PARPi impact on the efficacy of these agents against HR-deficient tumours. PARP1 and PARP2 share some overlapping functions, such that inhibition of PARP2 may be required for maximal cellular toxicity (Hanzlikova et al., 2016; Ménissier de Murcia et al., 2003b). In contrast, PARP3 contributes to the NHEJ pathway of DSB repair (Beck et al., 2014; Rulten et al., 2011). Disruption of other components of this pathway can ameliorate the killing of HR deficient cells exposed to PARP inhibitors, suggesting that targeting PARP3 could undermine the potency of PARPi therapy (Patel et al., 2011). However, the impact of targeting these PARPs in the context of synthetic lethality with HR deficiency has not yet been explored experimentally.

6.1.2 Efforts to expand the use of clinical PARPi beyond BRCA mutant breast and ovarian cancers

Although PARPi are currently licensed for the treatment of BRCA1/2 mutant breast and ovarian cancers, numerous preclinical studies have explored the

possibility of expanding the clinical use of these agents. The most obvious way to achieve this is by searching for additional tumour types that harbour mutations in BRCA1 or BRCA2. Such mutations have been identified in prostate, pancreatic and lung cancers (Kote-Jarai et al., 2011; Leongamornlert et al., 2012; Lucas et al., 2013; Marks et al., 2008), although generally at much lower rates than the 10% of breast cancers and 15% of ovarian cancers attributed to BRCA1/2 mutations. Thus, with proper genotyping and patient stratification, PARPi may be useful for the treatment of a limited subset of these additional tumour types.

Considerable effort has also been committed to exploring the possibility of extending the applicability of PARPi beyond BRCA mutant tumours. Indeed, cells deficient in a whole range of HR proteins show sensitivity to PARPi, leading to the idea of the property of “BRCAness” (Lord and Ashworth, 2016; Turner et al., 2004). This term is used to describe tumours without germline BRCA mutations that exhibit some of the characteristics of BRCA-defective tumours, and therefore are sensitive to PARPi. One determinant of BRCAness is mutations in other known HR factors, including ATM, CHK1, CHK2, NBS1, RAD51 and CDK12 (Joshi et al., 2014; McCabe et al., 2006), all of which show sensitivity to PARPi. Whilst the prevalence of mutations in each of these genes in ovarian cancer is much lower than that of BRCA1 or BRCA2, collectively they could considerably expand the potential applications of PARPi. For example one study analysed almost 500 high-grade serous ovarian tumours, and found that whilst only 17% of cancers harboured germline BRCA mutations, up to 50% of the tumours carried a mutation that would lead to compromised HR (Bell et al., 2011). Mutations in additional HR genes beyond BRCA1/2 have

also been identified in breast cancers (Koboldt et al., 2012). It remains possible that additional unidentified factors exist that when mutated could also produce a synthetic lethal relationship with PARP inhibition or loss. The identification of such factors could widen the future clinical relevance of PARPi.

6.1.3 Aims

PARP inhibitors have demonstrated the ability to selectively kill cells with HR-deficiencies, but these compounds target multiple members of the PARP family, including PARP1, PARP2 and PARP3. How inhibition of these different PARPs impacts on the efficacy of these compounds in the clinic is unclear, and a better understanding could allow the development of more specific and potent agents, with fewer side effects. Furthermore, identification of additional genes which mediate synthetic lethality with PARP loss could provide insights into the mechanisms underlying this phenomenon, as well as widen the potential clinical applications of PARPi. Therefore, the aims of this chapter are to define the contributions of different DNA-dependent PARPs to synthetic lethality with homologous recombination deficiency, and identify novel DDR factors that show a synthetic lethal phenotype with PARP loss.

6.2 Results

6.2.1 Rad51 inhibitors can be used to chemically recapitulate synthetic lethality between PARPs and HR

The synthetic lethal strategy between PARPs and HR exploited in the clinic has been between cells genetically compromised for BRCA1/2 and exposure to PARP inhibitors. In order to investigate which PARPs are the most appropriate

to target in this strategy, I set out to develop an assay that allows us to determine the susceptibility of our established PARP knockout cell lines to HR disruption. One way to achieve this would be to use small molecule inhibitors of homologous recombination. Numerous agents have been developed for this purpose, including those targeting Mre11, RPA and Rad51. Whilst any of these compounds could be effective in this assay, I considered Rad51 inhibitors to be the most attractive, due to their ability to bind directly to Rad51 and prevent nucleofilament assembly. Thus these inhibitors may be able to closely mimic the HR defects characteristic of BRCA1/2 mutant cells, where the ability to load Rad51 onto ssDNA is compromised.

I selected two commercially available Rad51 inhibitors, B02 and RI-1, which have both been reported to prevent Rad51 foci formation and sensitise cells to a variety of DNA damaging agents (Budke et al., 2012; Huang et al., 2012). In order to test the efficacy of these inhibitors in U2OS cells, I assessed Rad51 foci formation after the induction of cellular DSBs with phleomycin in the presence of these agents (Figure 6.1 A). Whilst robust Rad51 foci could still form in the presence of 40 μM RI-1, B02 treatment was able to almost completely suppress their formation. Therefore, I selected B02 for use in the synthetic lethality assays.

To establish whether I can recapitulate synthetic lethality using B02, I treated U2OS cells with increasing concentrations of the drug for 48 hours, with or without concurrent exposure to the PARP inhibitor olaparib (Figure 6.1 B). Whilst U2OS cells without PARPi exposure showed modest sensitivity to the concentrations of B02 used, this was markedly increased by exposure to

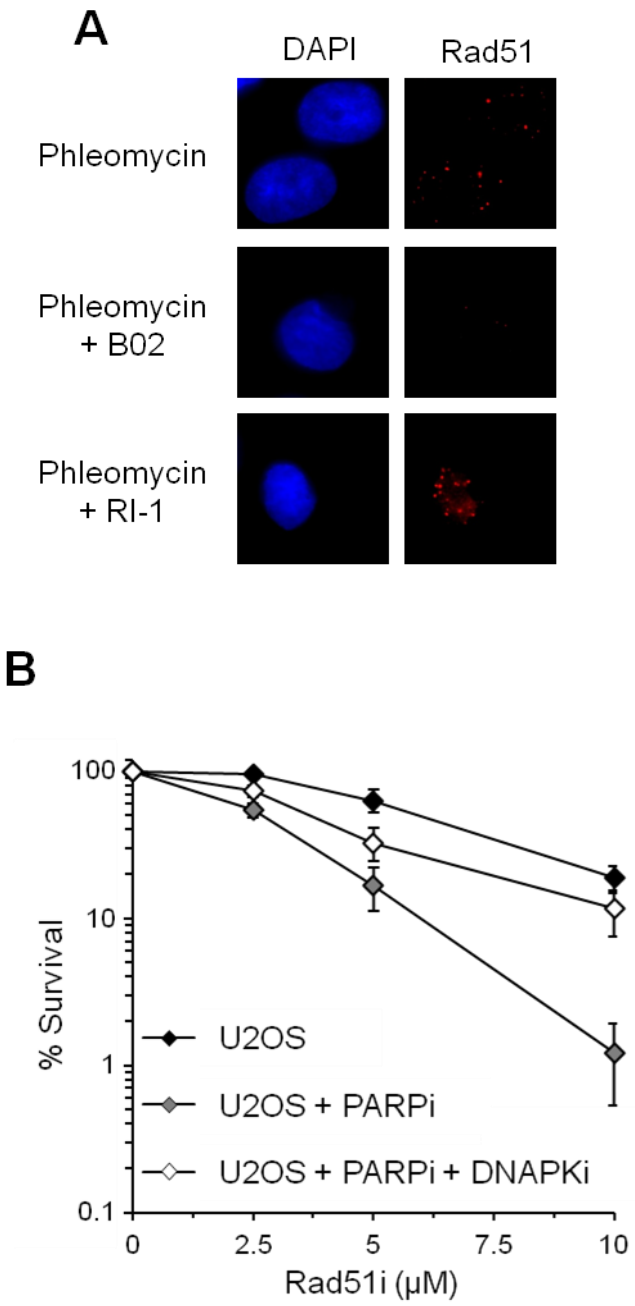


Figure 6.1: The Rad51 inhibitor B02 can prevent formation of Rad51 foci and recapitulate synthetic lethality with PARPi. **A.** U2OS cells, with or without 30 μM B02 or 40 μM RI-1 exposure, were treated with 300 μM phleomycin for one hour before recovery in fresh media containing B02 as appropriate. Cells were fixed 3 hours after phleomycin addition, and stained for Rad51. Images taken by G. Driscoll. **B.** Sensitivity profile of U2OS cell to increasing concentrations of the Rad51 inhibitor B02 with or without 10 μM olaparib (PARPi) and 5 μM Nu7441 (DNA-Pki) treatment. Error bars represent the SEM from three independent experiments.

olaparib, demonstrating that the use of Rad51 inhibitors can successfully induce synthetic lethality. Furthermore, combining olaparib treatment with exposure to a DNA-PK inhibitor can suppress the sensitivity that PARPi treated cells show towards B02 (Figure 6.1 B), an observation first made in BRCA2 mutant cells treated with PARP inhibitors (Patel et al., 2011). This indicates that the combination of B02 and olaparib drives cellular killing through the same mechanisms as in traditional models of synthetic lethality, further validating the use of B02 in this experimental context.

6.2.2 Loss of PARP1 is the key driver of synthetic lethality with HR dysfunction

In order to better understand the individual contributions of PARP1 and PARP2 to synthetic lethality with HR deficiency, I assessed the sensitivity of *parp1Δ, parp2Δ* and *parp1Δparp2Δ* cells to B02 (Figure 6.2 A). Whilst U2OS and *parp2Δ* cells showed mild sensitivity to B02, *parp1Δ* cells were additionally sensitive, demonstrating that loss of PARP1 in combination with Rad51 inhibition is toxic to cells. Interestingly, *parp1Δparp2Δ* cells were no more sensitive to B02 than *parp1Δ* cells, in stark contrast to the relationship between these PARPs in response to MMS. This indicates that the loss of PARP2 is not relevant to synthetic lethality with HR deficiency, even in the absence of PARP1.

I also wished to consider the potential impact of PARP3 on synthetic lethality, given both olaparib and rucaparib can strongly bind to its catalytic domain. However, U2OS and *parp3Δ* cells are equally sensitive to B02, demonstrating loss of PARP3 does not produce a synthetic lethal relationship

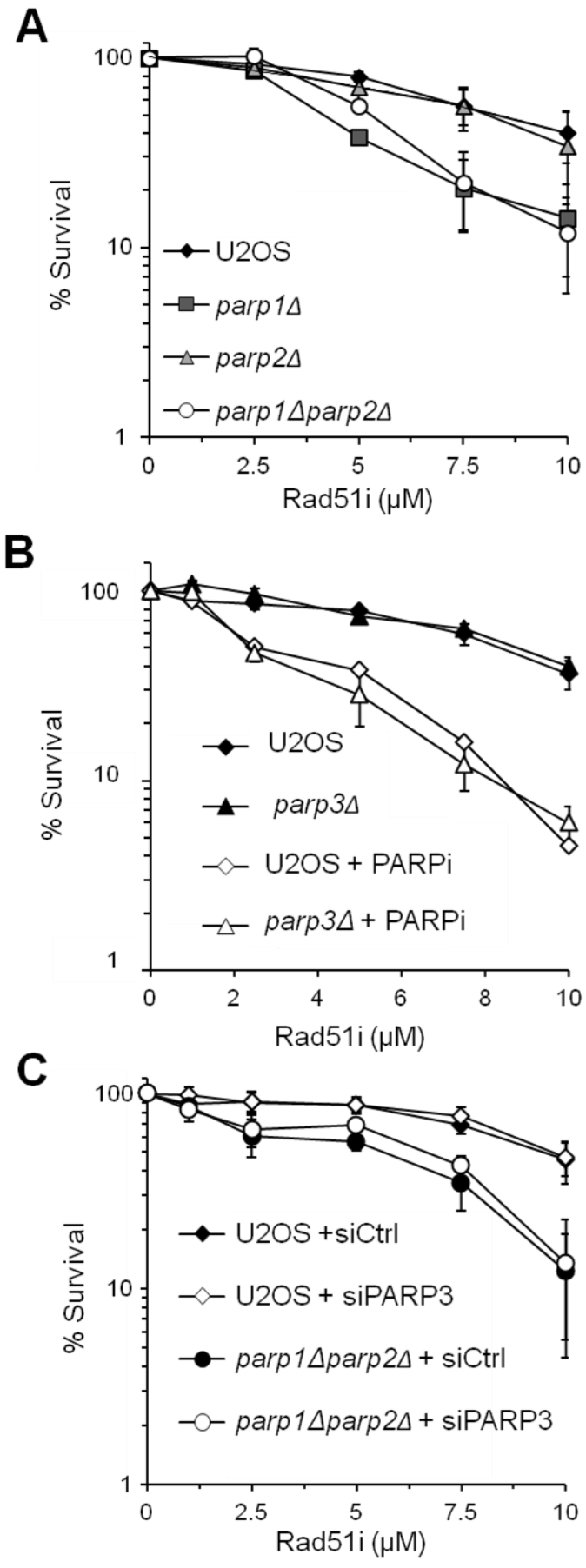

A
100
10
1
% Survival
U2OS
parp1Δ
parp2Δ
parp1Δparp2Δ
0
2.5
5
7.5
10
Rad51i (μM)
B
100
10
1
% Survival
U2OS
parp3Δ
U2OS + PARPi
parp3Δ + PARPi
0
2
4
6
8
10
Rad51i (μM)
C
100
10
1
% Survival
U2OS +siCtrl
U2OS + siPARP3
parp1Δparp2Δ + siCtrl
parp1Δparp2Δ + siPARP3
0
2.5
5
7.5
10
Rad51i (μM)

Figure 6.2: Synthetic lethality with HR-deficiency is driven by loss of PARP1, not PARP2 or PARP3. **A.** The indicated cell lines were treated with the Rad51 inhibitor B02 and survival assessed by clonogenic assay. **B.** U2OS or *parp3*Δ cells, with or without 10 μM olaparib (PARPi exposure, were treated with the Rad51 inhibitor B02 and survival assessed by clonogenic assay. **C.** U2OS or *parp1Δparp2Δ* cells, transfected with siCtrl or siPARP3, were exposed to increasing concentrations of the Rad51 inhibitor B02 and survival assessed by clonogenic assay. Error bars represent the SEM from three independent experiments.

with HR dysfunction (Figure 6.2 B). Furthermore, U2OS and *parp3Δ* cells can be equally well sensitised to B02 by olaparib exposure (Figure 6.2 B), indicating loss of PARP3 does not phenocopy other NHEJ components in suppressing the toxicity of HR deficient cell to PARPi (Patel et al., 2011). Finally, depletion of PARP3 did not affect the sensitivity of U2OS or *parp1Δparp2Δ* cells to B02 (Figure 6.2 C). Taken together, these data demonstrate the minimal impact of losing PARP3 on synthetic lethality with HR dysfunction.

6.2.3 Synthetic lethality is not wholly driven by PARP trapping or disruption of SSBR or Rad52-depedndant repair pathways

Loss of PARP2 does not affect the sensitivity of *parp1Δ* cells to HR inhibition, in stark contrast with their relationship in response to MMS. This implies disruption of BER does not drive cellular sensitivity with HR dysfunction. However, our previous observations indicate PARP2 is dispensable for the cellular tolerance of directly induced SSBs (Figure 3.9). Therefore, one hypothesis is that in the absence of PARP1, general SSBR is disrupted and this leads to toxicity with HR inhibitors. In order to assess this possibility I depleted cells of XRCC1, in order to abrogate the SSBR machinery independently of PARPs, and assessed cellular survival following B02 exposure. Depletion of XRCC1 results in elevated accumulation of both γH2AX and Rad51 foci after MMS treatment (Figure 4.3 B and 4.5 A), consistent with these cells harbouring a SSBR defect. Interestingly however, XRCC1 depleted cells are only mildly sensitive to B02 (Figure 6.3 A), indicating that SSBR disruption is not the sole determinant of the synthetic lethal relationship between PARPs and HR dysfunction.

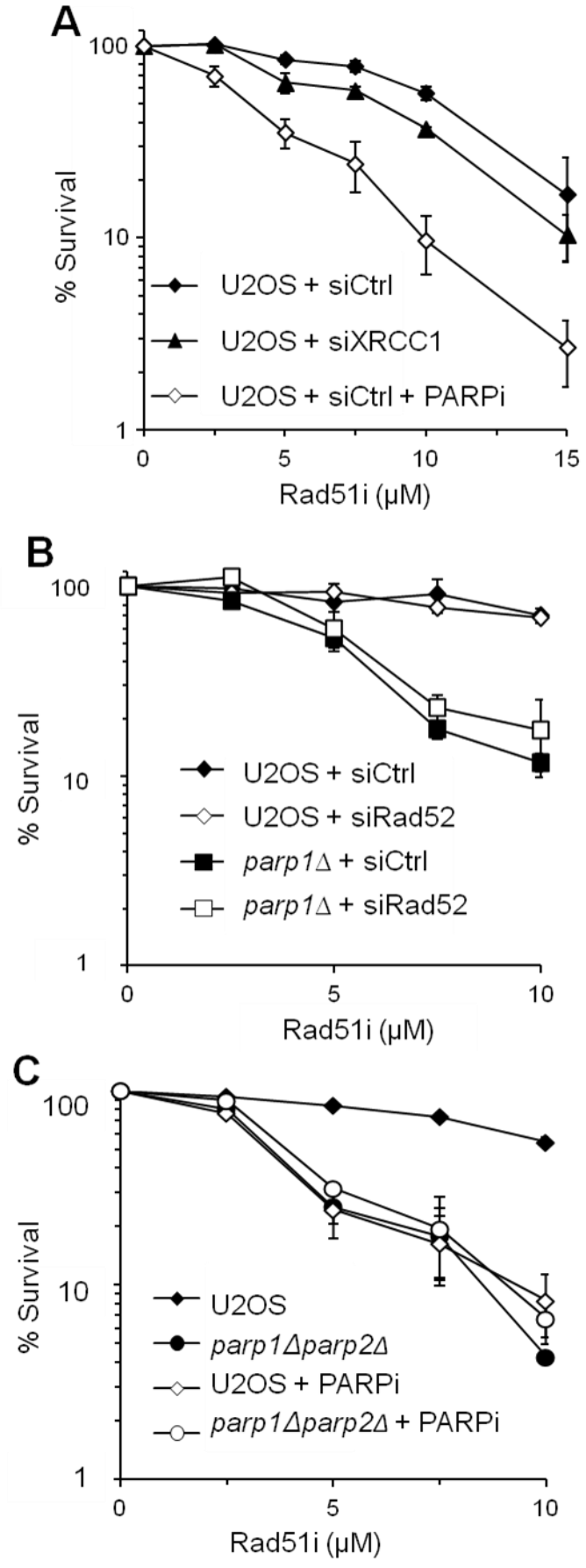

A
100
10
1
% Survival
U2OS + siCtrl
U2OS + siXRCC1
U2OS + siCtrl + PARPi
0
5
10
15
Rad51i (μM)
B
100
10
1
% Survival
U2OS + siCtrl
U2OS + siRad52
parp1Δ + siCtrl
parp1Δ + siRad52
0
5
10
Rad51i (μM)
C
100
10
1
% Survival
U2OS
parp1Δparp2Δ
U2OS + PARPi
parp1Δparp2Δ + PARPi
0
5
10
Rad51i (μM)

Figure 6.3: Synthetic lethality is not wholly mediated by SSBR-disruption, Rad52-dependent pathways, or PARP trapping. **A.** U2OS cells, transfected with siCtrl or siXRCC1, with or without 10 μM Olaparib (PARPi) exposure, were treated with the Rad51 inhibitor B02 and survival assessed by clonogenic assay. **B.** U2OS or *parp1*Δ cells, transfected with siCtrl or siRad52, were treated with the Rad51 inhibitor B02 and survival assessed by clonogenic assay. **C.** U2OS or *parp1Δparp2Δ* cells, with or without 10 μM Olaparib (PARPi) treatment, were treated with the Rad51 inhibitor B02 and survival assessed by clonogenic assay. Error bars represent the SEM from three independent experiments.

Similarly to PARPs, loss of Rad52 is toxic to cells lacking BRCA1 or BRCA2 (Feng et al., 2011; Lok et al., 2013), suggesting the possibility that PARPs may be promoting repair through a Rad52-dependent repair pathway, and that loss of this function drives cellular toxicity in the absence of HR. To investigate this option, I depleted Rad52 in U2OS and *parp1*Δ cells and assessed their sensitivity to B02 (Figure 6.3 B). Loss of Rad52 was unable to sensitise cells to B02, and did not affect the sensitivity of *parp1*Δ cells to this agent, indicating the synthetic lethal relationship between PARPs and HR is likely independent of Rad52-mediated repair pathways.

Another model of synthetic lethality proposes that the ability of PARP inhibitors to trap PARPs at sites of DNA damage is a key contributor to their toxicity to HR deficient cells. Although the fact that *parp1Δ* cells show sensitivity to B02 indicates that PARP trapping is not the only mediator of this killing, it may still potentiate the efficacy of PARPi against HR defective cells. In order to understand how trapping affected cellular sensitivity in our assay, I treated U2OS or *parp1Δparp2Δ* cells with olaparib and assessed their sensitivity to B02 (Figure 6.3 C). Olaparib treatment was unable to further sensitise *parp1Δparp2Δ* cells to B02, indicating any cellular targets of olaparib beyond PARP1 and PARP2 do not influence cellular sensitivity to Rad51 inhibitors. Furthermore, olaparib treated U2OS cells were no more sensitive to B02 than *parp1Δparp2Δ* cells without PARPi exposure. This suggests that trapping of PARP1 and/or PARP2 is not a significant contributor to the toxicity of PARP inhibitors to HR deficient cells, at least in the context of B02. Instead, loss of function of PARP1 is the major contributor to cellular killing within this assay.

6.2.4 A targeted screen of DDR factors to identify novel determinants of synthetic lethality with PARP loss

Although PARP inhibitors are currently licensed to treat BRCA1/2 mutant breast and ovarian cancers, there is sizable interest in expanding the application of these agents to other tumour types and genetic backgrounds. Furthermore, efforts are being made to develop more specific inhibitors targeting individual PARPs, in the hope that this could improve clinical outcomes and reduce side-effects (Lindgren et al., 2013a, 2013b; Steffen et al., 2013; Zhu et al., 2014). Our genetically defined *parpΔ* cell lines provide a unique opportunity to guide both of these endeavours. Therefore, I undertook a targeted siRNA screen, systematically depleting DDR factors in different *parpΔ* cells to identify novel synthetic lethal relationships with defined PARP deficiencies.

The screen was setup by transfecting U2OS, *parp1Δ*, *parp2Δ* and *parp1Δparp2Δ* cells with a custom siRNA library of 579 DDR gene targets. Following a period of 7 to 9 days of recovery, cell viability was assessed for each cell line. Comparing the survival of *parpΔ* cells with U2OS cells following depletion of a particular factor allows identification of genes that show toxicity with a specific PARP disruption (scheme summarised in Figure 6.4). This screen was performed with the help of S. Hatch and D. Ebner (Target Discovery Institute, Oxford), and optimisation of plating and transfection conditions was performed by S. Hatch (data not shown). Transfection of siRNA was optimised for loss of viability following Plk1 knockdown, whilst minimising cell death following transfection of cells with non-targeting control siRNA.

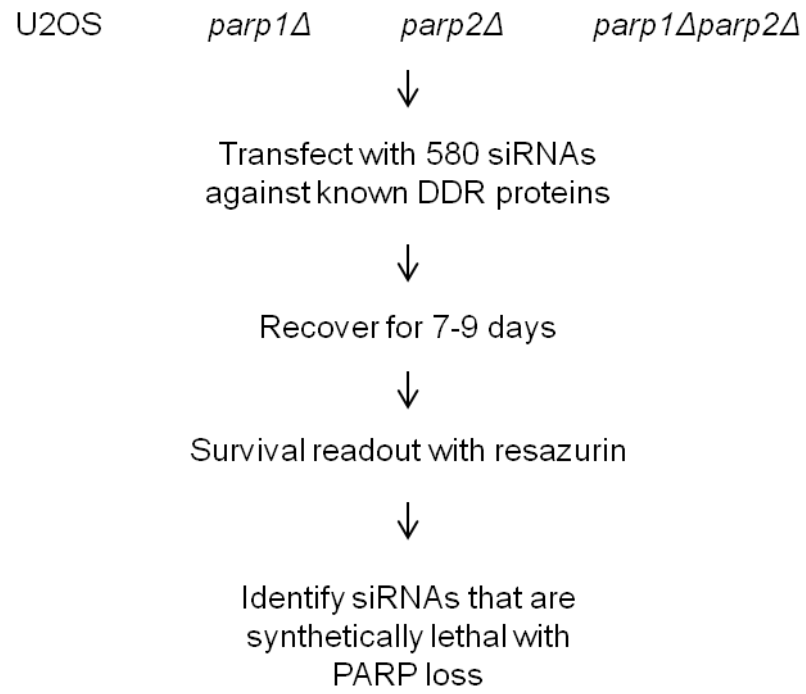


Figure 6.4: Outline of workflow for siRNA screen to identify novel DDR factors that show synthetic lethality with PARP loss. U2OS, *parp1*Δ, *parp2*Δ or *parp1*Δ*parp2*Δ cells were separately transfected with 580 siRNA pools targeting DDR factors, followed by a recovery for 7-9 days. Cell survival was assessed using a $560_{ex}/590_{em}$ nm fluorescence readout following resazurin addition. Performed with S. Hatch and D. Ebner.

6.2.5 Identification of novel factors that possess a synthetic lethal relationship with loss of PARP1 and/or PARP2

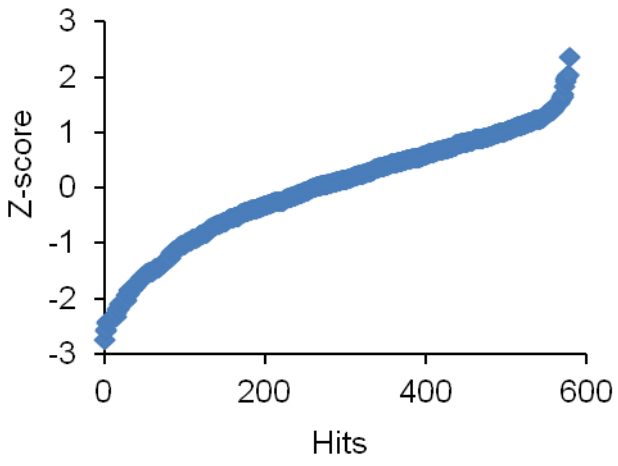
Firstly I considered the effect of depletion of each factor on U2OS cell survival, in order to understand which factors compromised cellular viability independently of PARP status. Resazurin fluorescence readouts from duplicate plates were averaged, with good agreement between replicates as judged by the Pearson correlation coefficients (Figure 6.5 A). Z-scores were calculated then ranked, to identify those genes whose knockdown is able to alter the viability of U2OS cells (Figure 6.5 B). I selected a Z-score cut-off of -1.96, as 5% of values will have a Z-score with a magnitude larger than this in a normally distributed population. 28 siRNAs produced Z-scores below -1.96, and over 80% of those have been previously annotated as essential genes (Gao et al., 2015) (Figure 6.5 B, highlighted in red).

To identify novel DDR factors that exhibit a synthetic lethal relationship with PARP loss, I calculated Z-scores for each siRNA in the *parpΔ* cell lines, and subtracted the appropriate U2OS Z-score, to generate a ΔZ score as a measure of the specific sensitisation of the *parpΔ* cells (Figure 6.6 A, B). To validate this approach, I then searched for genes confirmed to show synthetic lethality with PARP1/2 inhibition. Encouragingly, multiple factors whose depletion was previously identified to lead to synthetic lethality with PARPi were in the top 25 hits for either *parp1Δ* or *parp1Δparp2Δ* cells. These include BRCA1, ABL1, LigIV, RRM2B, Hus1, FANCD2 and MCM6 (Bajrami et al., 2014; McCabe et al., 2006).

A

Pearson correlation coefficient between replicates	
U2OS	0.91
parp1Δ	0.93
parp2Δ	0.93
parp1Δparp2Δ	0.92

B



Rank\	Gene	Z-score
1	FLJ35220	-2.73
2	NEIL2	-2.57
3	MYST1	-2.54
4	COPB2	-2.43
5	HNRNPK	-2.41
6	KIF11	-2.39
7	SNRPE	-2.38
8	PSMC4	-2.38
9	GIYD2	-2.37
10	SNRPF	-2.35
11	RPL27	-2.35
12	EIF4A3	-2.33
13	PSMA1	-2.32
14	PLK1	-2.31
15	RUVBL2	-2.31
16	RPL35	-2.25
17	CHAF1A	-2.18
18	CRIP2	-2.17
19	XAB2	-2.15
20	RPS27A	-2.09
21	INCENP	-2.09
22	COL1A2	-2.06
23	HIST2H3C	-2.05
24	APEX1	-2.05
25	HIF1AN	-2.04
26	ERCC1	-2.04
27	SETD8	-2.02
28	NUP205	-2.01

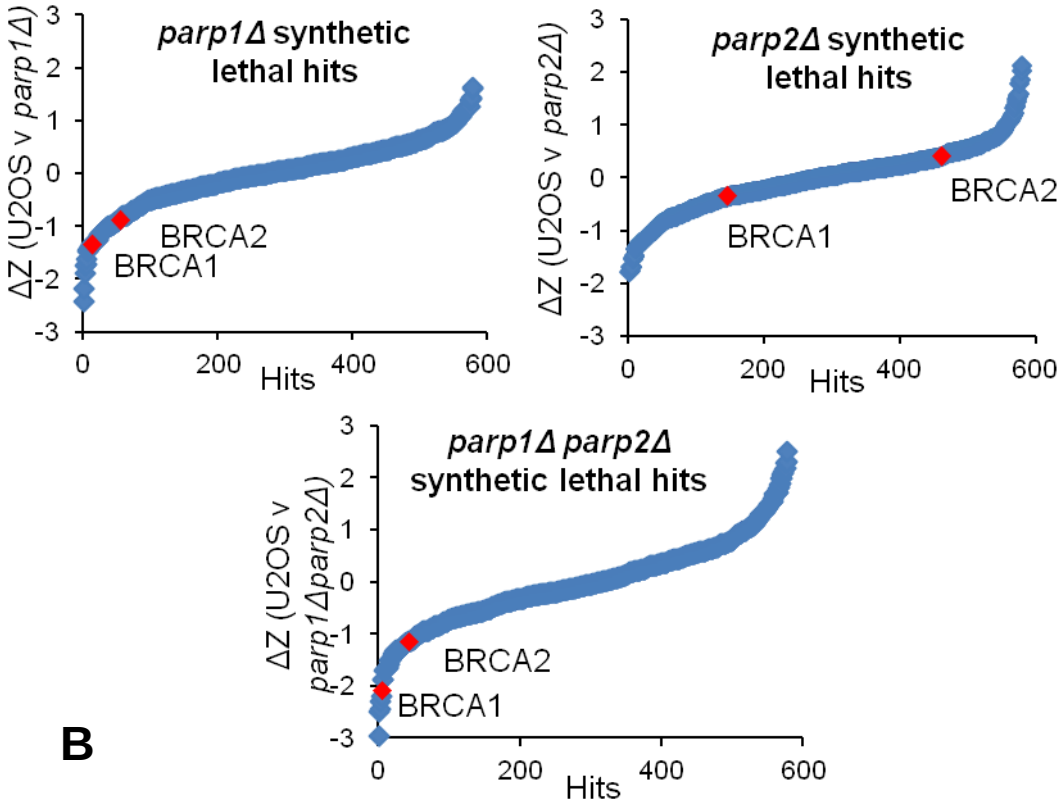
Figure 6.5: Identification of factors that compromise U2OS cell survival. **A.** The Pearson correlation coefficients between replicate plates for each cell line. **B.** Z-scores were calculated for cellular survival for each siRNA pool. A graphical representation of all hits ranked by Z-score (left panel). The top 28 hits that decreased the viability of U2OS cells are listed (right panel), Hits previously annotated as essential are marked in red. Performed with S. Hatch and D. Ebner.

To identify novel mediators of synthetic lethality with particular PARP disruptions, I again used a ΔZ score cut-off of -1.96. Whilst no factors reached this significance level for *parp2Δ* cells, two factors had ΔZ scores lower than -1.96 for *parp1Δ* cells, BRD7 and UBE2B, and there were six for *parp1Δparp2Δ* cells, UBE2B, TP73, HMGN1, TSC1, POLN and BRCA1. One hit, UBE2B, was present on both lists, highlighting its potential as a mediator of synthetic lethality.

6.3 Discussion

PARP inhibition exhibits a synthetic lethal relationship with HR dysfunction, leading to the use of a number of PARP inhibitors in the clinic to treat BRCA mutant tumours. However, given the broad activity of the currently available inhibitors, which PARPs must be targeted to facilitate efficient cellular toxicity in HR defective cells remains unclear. Our data suggests that PARP1 is the critical mediator of synthetic lethality with HR inhibition, with loss of PARP2 not affecting this phenotype, even in the absence of PARP1 (Figure 6.2 A). This is in stark contrast with the relationship between these enzymes in response to base methylation, where PARP1 and PARP2 function redundantly to potentiate cellular survival (Figure 3.7 B). Interestingly, I also fail to observe redundancy between PARP1 and PARP2 in response to hydrogen peroxide exposure (Figure 3.9), which induces oxidative damage and direct SSBs. This may represent a more physiologically relevant form of damage that cells produce endogenously through aerobic respiration. Therefore our data could be consistent with the build-up of endogenous oxidative damage in the absence of

A



B

	parp1Δ		*parp2Δ*		*parp1Δparp2Δ*	
Rank	Gene	ΔZ	Gene	ΔZ	Gene	ΔZ
1	BRD7	-2.42	STK11	-1.77	UBE2B	-2.96
2	UBE2B	-2.19	IGF1R	-1.75	TP73	-2.49
3	TET2	-1.89	OGG1	-1.68	HMGN1	-2.44
4	MMS19	-1.74	TSC1	-1.68	TSC1	-2.28
5	NUDT14	-1.73	UBE2B	-1.67	POLN	-2.19
6	RRM2B	-1.64	TP73	-1.53	BRCA1	-2.08
7	NUDT17	-1.48	C14orf169	-1.50	C9orf102	-1.88
8	JHDM1D	-1.45	POLN	-1.49	RRM2B	-1.86
9	ASPHD1	-1.44	MRE11A	-1.45	NUDT11	-1.69
10	ABL1	-1.44	EZH2	-1.33	TOP2A	-1.68
11	TSC1	-1.40	SDHC	-1.33	ILK	-1.67
12	INO80C	-1.38	ABL1	-1.32	HSP90B1	-1.67
13	BRCA1	-1.35	C9orf102	-1.28	JHDM1D	-1.66
14	AKT2	-1.35	SUPV3L1	-1.26	C14orf169	-1.65
15	NUDT11	-1.34	JMJD8	-1.24	MANF	-1.63
16	C14orf169	-1.33	HSP90B1	-1.22	CDK6	-1.59
17	HNRNPA2B1	-1.33	TOP2A	-1.21	SUPV3L1	-1.50
18	PER1	-1.30	LOC730323	-1.21	UBA52	-1.50
19	TINF2	-1.29	SUZ12	-1.19	MLLT1	-1.49
20	IFNGR2	-1.29	SUV39H1	-1.19	HUS1	-1.45
21	LIG4	-1.28	HDAC9	-1.17	LIG1	-1.43
22	JMJD7	-1.27	JMJD7	-1.17	TTF2	-1.39
23	HDAC1	-1.24	HRAS	-1.17	FANCD2	-1.39
24	SSR1	-1.18	DNMT1	-1.16	CCND1	-1.34
25	HDAC11	-1.16	TOP1	-1.15	MCM6	-1.33

Figure 6.6: Identification of factors that show a synthetic lethal relationship with PARP loss. **A.** ΔZ-scores were calculated by subtracting the U2OS Z-score from the indicated cell line's Z-score for each siRNA pool. Graphical representations of hits ranked by ΔZ-score for each cell line. The position of known synthetic lethal genes BRCA1 and BRCA2 are highlighted in red. **B.** The top 25 hits that specifically decreased the viability of *parp1Δ*, *parp2Δ* or *parp1Δparp2Δ* cells, as judged by ΔZ-score. Performed with S. Hatch and D. Ebner.

PARP1 leading to synthetic lethality with HR. However, the fact that XRCC1 depleted cells are not strongly sensitive to B02 (Figure 6.3 A) argues against SSBR/BER abrogation as the sole mechanism that drives this killing.

An additional possibility is that PARP1 regulates an alternate pathway that can contribute to the repair of the same endogenously arising lesions as HR. Indeed, our observations that *parp1Δ* cells have delayed resolution of S-phase associated γH2AX and persistent Rad51 foci following MMS exposure (Figure 4.2 B, 4.6 A) indicate that PARP1 alone regulates a Rad51-independent repair pathway. Whilst the identity of this potential pathway remains uncertain, one possibility would be that PARP1 promotes resolution of this damage through Rad52-dependent repair routes. This is particularly appealing given loss of Rad52 can elicit synthetic lethality in BRCA1 or BRCA2 mutant cells (Feng et al., 2011; Lok et al., 2013). However, loss of Rad52 was unable to influence the sensitivity of U2OS or *parp1*Δ cells to B02, indicating loss of Rad52-dependent pathways does not drive the killing of HR-deficient cells in the absence of PARP1 (Figure 6.3 B). Why Rad52 depletion does not result in sensitivity to B02 whilst being toxic to BRCA1 or BRCA2 mutant cells is not clear. One model suggests Rad52 could promote cellular survival in the absence of BRCA1/2 by acting as a secondary Rad51 loader (Lok et al., 2013). However, in the presence of B02, Rad51 nucleofilament formation will be prevented irrespective of the status of Rad51 loaders, making their presence or absence immaterial to cellular survival in this context.

Another good candidate pathway would be alt-NHEJ, which is promoted by PARP1 activity. Indeed, a Polθ dependent pathway can contribute to the repair of replication-associated damage in competition with HR following HU exposure

(Ceccaldi et al., 2014). However, transfection of U2OS cells with Polθ siRNA could not produce persistent γH2AX or Rad51 foci after MMS exposure, or sensitise U2OS cells to B02 (data not shown). Although I was unable to verify the efficiency of Polθ depletion in these cells, this could suggest that Polθ-dependent alt-NHEJ is not the pathway whose abrogation drives cellular toxicity in the absence of HR. Alternatively, PARP1 may function in a Polθ-independent sub-pathway of alt-NHEJ, or some other as yet unidentified repair route.

The ability of PARPi to trap PARP1 and PARP2 onto chromatin has also been suggested to contribute to the toxicity of these agents to HR deficient cells. Our observation that *parp1Δ* cells show sensitivity to B02 (Figure 6.2 A) demonstrates that trapping alone does not mediate this phenomenon. Moreover, olaparib treated U2OS cells are no more sensitive to B02 than *parp1Δparp2Δ* cells (Figure 6.3 C), suggesting that, in this experimental setup at least, PARP trapping is not a major contributor to the potency of PARPi against HR deficient cells.

I also hypothesised that PARP3 status could impact on the synthetic lethal relationship between PARPs and HR. Its roles in SSBR might suggest loss of PARP3 could facilitate or potentiate sensitivity to Rad51 inhibition. In contrast, its roles in NHEJ could potentially limit the efficacy of PARPi, as NHEJ has been identified to drive the killing of HR compromised cells exposed to PARPi (Patel et al., 2011). Inhibition of this pathway can reduce the sensitivity of BRCA null cells to PARPi, as well as the sensitivity of PARPi treated cells to B02 (Figure 6.1 B). However, loss of PARP3 does not affect the sensitivity of cells to B02, regardless of the presence or absence of PARPi or other DNA-dependent PARPs (Figure 6.2 B, C). This indicates loss of PARP3 has little

impact on the synthetic lethal relationship between PARPs and HR, and is consistent with the fact that AZD2461, a PARP inhibitor that does not target PARP3, can effectively cause regression of BRCA mutant tumours (Oplustil O'Connor et al., 2016b).

Overall, our data would support the future development of specific PARP1 inhibitors for treating HR defective tumours. These inhibitors should be equally as potent as the current crop of PARPi, but may have reduced side effects given the wide range of cellular processes that PARP family members mediate. For example PARP2 promotes hematopoietic stem cell survival and contributes to hepatic cholesterol regulation (Farrés et al., 2013; Szántó et al., 2014). Indeed anaemia has been a commonly reported serious adverse advent in multiple PARPi clinical trials (Kaufman et al., 2015; Ledermann et al., 2014). Therefore, by avoiding unnecessary targeting of PARP2, potential complications of PARPi treatments could be prevented. Progress towards more specific PARP1 inhibitors is already being made, as evidenced by the recent development of Zj6413 (Zhou et al., 2016). This inhibitor shows 10-fold higher potency towards PARP1 than PARP2, but is still able to cause regression of BRCA mutant tumours in xenograft models as effectively as olaparib. However, this agent is still an NAD^+ mimetic based on the same pharmacophore as current PARP inhibitors. Total discrimination between PARP1 and PARP2 using this inhibitory strategy may not be possible, given their near identical NAD^+ binding pockets. Targeting interdomain contacts within the PARP1 N-terminus that are required for the DNA-dependent activation of its catalytic activity may be an alternate route to PARP1-specific chemotherapeutics (Steffen et al., 2013, 2014).

PARPi is currently available to treat BRCA mutant breast and ovarian cancer, but there is great interest in exploring if there are wider applications of PARPi to additional tumour types, harbouring a broader range of DDR-mutations. I carried out a screen in order to identify additional DDR factors that, when depleted, can compromise cell viability in the absence of PARP1 and/or PARP2 (Figure 6.6). Cells disrupted for PARP2 did not produce any significant synthetically lethal hits, potentially reflecting the lack of sensitivity these cells display to DNA damaging agents investigated in this thesis (Figure 3.7 B, 3.9). Nevertheless, I identified six novel factors which could elicit synthetic lethality with PARP1 or PARP1/2 loss, UBE2B, PolN, BRD7, TP73, TSC1 and HMGN1. It should be noted these hits have not yet been independently validated for their ability to induce toxicity in specific PARP deficient backgrounds, meaning no firm conclusions can be drawn. Nevertheless, below I will discuss the hits and their known biological functions in the context of synthetic lethality with PARP loss.

Two of these hits have well defined roles in DNA repair pathways. PolN is an error prone A-family DNA polymerase capable of polymerising past 5S thymine glycol (Takata et al., 2006), suggesting a role in the TLS pathway. UBE2B, or Rad6B, is an E2 ubiquitin-conjugating enzyme, which in combination with the Rad18 E3 ubiquitin ligase can perform the monoubiquitination of PCNA to facilitate PRR pathways (Watanabe et al., 2004). These two hits raise the possibility of a synthetic lethal relationship between PARPs and TLS. Indeed many of the lesions which are processed by PARP-dependent BER are also capable of being tolerated during S-phase by PRR pathways, providing a potential rationale for this observation (Fu et al., 2012).

Interestingly however, both of these factors have also been shown to function in HR. Cells depleted of PolN show decreased efficiency of HR and sensitivity to the fork stalling agent HU (Moldovan et al., 2010). UBE2B promotes the degradation of HP1α after DSB induction, helping to create a chromatin environment favourable for HR repair of the break (Chen et al., 2015). Therefore the synthetic lethal relationship between these factors and PARP loss may instead be mediated through abrogation of HR. To distinguish between the potential contributions of the TLS and HR functions of these factors in promoting killing of *parp*Δ cells, one could assess their epistasis with other HR factors in the ability to induce toxicity in *parp*Δ cells.

The other four hits are less strongly associated with a particular repair pathway. Both TP73 and BRD7 are tumour suppressors that are linked to p53, which is functional in the U2OS cell lines used in the screen (Allan and Fried, 1999). TP73 is a member of the p53 family, and can support many of the tumour suppressor functions of p53. However, it is also expressed as a short isoform exhibiting dominant negative repression of the activity of the longer isoform, making understanding the implications of its depletion difficult (Candi et al., 2014). BRD7 contains a bromodomain allowing it to bind to acetylated histones, and is a component of the SWI/SNF chromatin remodelling complex. It is required for the p53-dependent activation of numerous genes, including p21 and TIGAR (Drost et al., 2010). Whilst neither BRD7 nor TP73 have been reported to be direct targets of ADP-ribosylation, p53 can be modified with PAR. Indeed, a functional interaction between p53 and PARP1 has been appreciated for many years (Kumari et al., 1998; Vaziri et al., 1997). Although the exact mechanism of this relationship is unclear, loss of PARP1 can prevent

the accumulation and activation of p53 following IR exposure (Valenzuela et al., 2002). Thus perhaps in the absence of PARP1/2 and BRD7/TP73 in combination, p53 function becomes dysregulated in a manner that triggers cell death. Furthermore, UBE2B is able to influence the cellular level of p53 through two distinct modes of action (Chen et al., 2012b). Firstly, UBE2B can mediate ubiquitination and degradation of p53 protein, but is also able to bind the p53 promoter and positively regulate transcription and mRNA levels. The fact that three hits all impact on p53 function highlights the potential importance of this protein in mediating synthetic lethality with PARP loss. Intriguingly however, loss of p53 itself did not induce synthetic lethality in the screen (ΔZ of -0.41 and +1.65 for *parp1*Δ and *parp1*Δ*parp2*Δ cells respectively). It would be interesting to assess whether p53 status affects the potential synthetic lethal relationships between PARPs and BRD7, TP73 and UBE2B.

Intriguingly, BRD7 also binds to BRCA1 and is required for some of its roles in transcriptional regulation (Harte et al., 2010). BRCA1 has been shown to negatively regulate its own promoter, allowing acute upregulation of protein levels in response to genotoxic stress (De Siervi et al., 2010). Whilst depletion of BRD7 does not significantly affect BRCA1 expression, it can reduce the expression of Rad51, providing a potential rationale for a synthetic lethal relationship with PARP1 disruption (Harte et al., 2010). Indeed the importance of the non-repair roles of BRCA1 in genomic stability has recently been highlighted. In one study, disruption of BRCA1 led to loss of the heterochromatic silencing of satellite repeats, normally maintained by the BRCA1-dependent mono-ubiquitination of histone H2A (Zhu et al., 2011a). The resulting expression of satellite RNA produced chromosomal instability and

cancer predisposition in breast tissue of *in vivo* mouse models. Meanwhile, loss of the E3 ligase function of BRCA1 does not affect its roles in HR (Reid et al., 2008). Taken together, these data suggest that loss of BRCA1 contributes to genomic instability and tumorigenesis in part through abrogation of its transcriptional and epigenetic silencing roles. Whether this also impacts on the synthetic lethal relationship with PARP abrogation remains to be fully understood.

TSC1 negatively regulates mTOR signalling, and has roles as a tumour suppressor along with its partner TSC2. Mutations in TSC1 cause the condition tuberous sclerosis complex, characterised by the development of unusual tumours called hamartomas (van Slegtenhorst et al., 1997). Interestingly, mTOR inhibitors are able to synergise with PARP inhibitors in killing BRCA-competent breast cancer cells (De et al., 2014; Mo et al., 2016). This is mediated, at least in part, by loss of expression of the HR-promoting H3K9 histone methyltransferase SUV39H1(Ayrapetov et al., 2014; Mo et al., 2016). However, loss of TSC1 causes constitutive hyper-activation of mTOR signalling (Kwiatkowski et al., 2002), making the potential mechanism of the synthetic lethal relationship between TSC1 and PARP1/2 uncertain. HMGN1 is a small non-histone chromosomal protein that can bind DNA and alter its interaction with nucleosomes. It enhances the rates of repair of UV-induced damage through modulation of chromatin compaction and architecture (Birger et al., 2003). Interestingly, HMGN1 has recently been shown to be ADP-ribosylated at S7 and S25, raising the possibility that its function may be regulated by PARPs (Bonfiglio et al., 2017). Exactly how or why this would lead to a synthetic lethal interaction with loss of PARPs is unclear.

Although preliminary, three of these hits have tumour suppressor functions; BRD7, TP73 and TSC1. Each of these have been found mutated or with dysregulated expression across a diverse set of cancers, including lung, bladder and breast tumours (Gao et al., 2016; Guo et al., 2013; Zaika et al., 2002). This raises the exciting possibility that if these synthetic lethal relationships are genuine, and hold for PARP inhibitors as well as PARP ablation, then PARPi could become an effective treatment against tumours harbouring mutations in these genes.

7. General Discussion

The aims of this thesis were to better understand how multiple PARPs function to influence DNA repair and synthetic lethality with homologous recombination deficiency. To this end, I used genome editing to generate a set of cell lines disrupted for PARP1, PARP2 and PARP3, alone and in combinations. These genetically defined *parp*Δ cell lines then allowed direct comparisons of the *in vivo* consequences of loss of different PARP combinations on the cellular response to various forms of DNA damage.

As would be predicted from the previously identified roles of PARP1 in the SSBR and BER pathways (Fisher et al., 2007; Masutani et al., 2000b), *parp1Δ* cells show sensitivity to the base methylating agent MMS as well as the SSB inducing agent hydrogen peroxide. Loss of PARP2 was able to dramatically further sensitise *parp1Δ* cells to MMS, and *parp1Δparp2Δ* cells display a severe strand ligation defect after MMS exposure that is not apparent in *parp1Δ* cells. This demonstrates that PARP1 and PARP2 function redundantly in promoting the strand ligation step of BER after base methylation. Interestingly, disruption of PARP2 did not affect the survival of *parp1Δ* cells in response to hydrogen peroxide, indicating that the redundant relationship between PARP1 and PARP2 is not conserved across the whole SSBR pathway. This is consistent with previous observations that PARP2 does not affect strand ligation rates after hydrogen peroxide treatment, even in the absence of PARP1 (Fisher et al., 2007; Hanzlikova et al., 2016). However, a recent study identified redundancy between PARP1 and PARP2 in the recruitment of XRCC1 to chromatin after hydrogen peroxide exposure (Hanzlikova et al., 2016). The fact

that cells show a strand ligation defect in response to hydrogen peroxide in the absence of PARP1, whilst still being able to support the localisation of XRCC1 to chromatin, implies additional roles of PARP1 in SSBR beyond the assembly of XRCC1 at DNA lesions. Whether these additional roles of PARP1 also function in the resolution of BER-induced breaks after MMS exposure remains unclear. Furthermore, why there are differences in the relationship between PARP1 and PARP2 in inducing sensitivity to MMS and hydrogen peroxide is also uncertain. The breaks that arise through the action of glycosylases and APE-1 in the BER pathway after MMS exposure are chemically distinct from those that arise spontaneously after hydrogen peroxide treatment, requiring different processing factors. In addition, the chromatin context, and complement of proteins already present at the lesion, is likely to differ between BER-induced and directly generated SSBs. Finally, the preference for short-patch or long-patch repair may differ between the two varieties of SSB. Any combination of these potential factors could influence the requirement for PARP1 and/or PARP2 at hydrogen peroxide and BER-induced SSBs. In any case, PARP1 and PARP2 possess overlapping roles in the promoting cellular survival and DNA strand ligation following exposure to MMS.

I further considered whether additional PARPs beyond PARP1 and PARP2 might contribute to the ability of cells to tolerate MMS exposure, given the recent identification of DDR roles for additional members of the PARP superfamily. Whilst *parp1Δparp2Δ* cells could be further sensitised to MMS by two different PARP inhibitors, loss of any of the other annotated members of the PARP family was unable to recapitulate this effect. This could be due to further redundancy between these additional PARPs, such that depletion of any

individual PARP does not cause sensitivity. Alternatively, the PARP inhibitors could be trapping one or more of the PARP family members onto DNA, in an analogous manner to PARP1 and PARP2 (Murai et al., 2012). This trapped PARP could prevent efficient repair of the lesion, despite the fact the presence of the PARP is not critical for damage resolution. Finally inhibition of some other factor(s), potentially other NAD^+-utilising enzymes such as sirtuins (Chalkiadaki and Guarente, 2015), by these PARP inhibitors could be the cause of the additional sensitivity of *parp1Δparp2Δ* cells to MMS. Further work will be required to assess these different possibilities and understand the basis of the additional sensitisation of *parp1Δparp2Δ* cells to MMS by PARPi.

I also considered the contributions of different DNA-dependent PARPs to the synthetic lethal relationship between PARPs and HR. Loss of PARP1 produces cellular sensitivity to Rad51 inhibition, whilst loss of PARP2 does not affect survival, even in the absence of PARP1. Furthermore, loss of PARP3 also does not affect cellular survival in this context, even in the absence of both PARP1 and PARP2. These data suggest that loss of PARP1 is the critical mediator of the synthetic lethal relationship with HR, and therefore support the development of specific PARP1 inhibitors for potential clinical use. Such agents may be able to reduce some of the side effects of current clinical PARP inhibitors, which could be mediated by their targeting of additional PARPs beyond PARP1. Exactly why PARP1 and PARP2 display different functional relationships with respect to sensitivity to MMS exposure and Rad51 inhibition is unclear. However, this observation implies that disruption of BER *per se* is not the driving force behind cellular killing in the absence of HR. This idea is supported by the fact knockdown of XRCC1 also cannot strongly sensitise cells to Rad51

inhibitors. Instead, our data are consistent with the synthetic lethal relationship between PARPs and HR being driven by the disruption of a solely PARP1-dependent pathway. Interestingly, a number of the observations I made whilst analysing the response of *parp1Δ* cell lines to MMS suggested that cells lacking PARP1 struggle to resolve replication-associated damage, and become more reliant on Rad51-mediated repair. If these cells are also more reliant on HR to resolve endogenously arising replication-associated damage, then this could explain their elevated sensitivity to HR inhibitors, and represent a key mechanism driving cellular toxicity in the absence of both PARP1 and HR.

I also carried out a screen to identify novel factors that display a synthetic lethal relationship with the loss of PARP1, PARP2 or both in combination. I believed this could provide novel insight into the specific functions of these PARPs, as well as potentially allowing an expansion of the repertoire of tumour mutations PARPi can be used to treat in the clinic. The depletion of any single factor was unable to significantly decrease the survival of *parp2Δ* cells as compared to U2OS cells. This potentially reflects the lack of sensitivity that *parp2Δ* cells display to forms of DNA damage tested in this work, indicating loss of PARP2 does not strongly impact on repair efficiency in the presence of PARP1. Nevertheless, I identified six novel factors that were able to specifically decrease the survival *parp1Δ* or *parp1Δparp2Δ* cells – Ube2B, PolN, BRD7, TP73, TSC1 and HMGN1. Three of these hits influence the regulation and function of the tumour suppressor p53, highlighting a potential connection between PARPs and p53. Intriguingly, altered p53 expression appears to be almost ubiquitous in BRCA1/2 mutated ovarian cancers (McAlpine et al., 2012), although what impact this observation has on the sensitivity of these tumours to

PARP inhibitors is unclear. In any case, these hits represent potential novel genes that show a synthetic lethal relationship with loss of PARP1 or PARP1/2 function. This raises the exciting possibility that tumours harbouring mutations in these genes could show sensitivity to PARPi, leading to the prospective widening of the applications of these inhibitors in the clinic.

Exposure to MMS is also able to induce replication-associated damage marked by γH2AX foci, thought to be caused by active replication forks colliding with BER intermediates (Ensminger et al., 2014). I was able to detect the induction of γH2AX foci in S-phase U2OS cells after MMS exposure, but not in G1- or G2-phase cells. Loss of XRCC1, or PARP1 and PARP2 in combination caused elevated induction of γH2AX foci in S-phase cells, whilst loss of XRCC1 in a *parp1*Δ*parp2*Δ background did not result in an additive effect. These observations are likely attributable to a BER defect, where delayed strand ligation kinetics leads to an accumulation of unrepaired strand breaks, leading to more collisions with replication forks and more S-phase associated damage. Consistent with this, loss of PARP1 alone, which did not lead to a strand ligation defect in response to MMS, also did not cause accumulation of additional γH2AX foci immediately after MMS exposure.

Following a recovery period in fresh media, U2OS cells can resolve the majority of the γH2AX-marked damage induced by MMS within 12 hours. Crucially, cells depleted of XRCC1 are also able to resolve this damage with normal kinetics, demonstrating that the pathway(s) that repair this damage are independent of SSBR/BER and XRCC1. Whilst *parp2Δ* cells repair these foci normally, both *parp1Δ* and *parp1Δparp2Δ* cells show delayed kinetics of γH2AX foci resolution, and this phenotype is markedly more pronounced in the absence of

both PARPs in combination. This pattern remains true even when each cell line is compromised for BER by depleting XRCC1. This demonstrates that whilst PARP1 has some unique role in the pathway(s) that contribute to the resolution of this damage, PARP2 is able to partially compensate for loss of PARP1 in this repair context.

Homologous recombination is known to facilitate the resolution of stalled/collapsed replication forks, and has also been shown to be activated in response to MMS (Nikolova et al., 2010). I hypothesised loss of PARP1 and/or PARP2 might impact on the function of HR in S-phase cells after MMS exposure. Indeed, treatment of U2OS cells with MMS was able to induce the formation of Rad51 foci, peaking at six hours after MMS administration. Disruption of BER by depleting cells of XRCC1 led to increased formation and persistence of Rad51 foci, suggesting that in the absence of BER, accumulating damage can be channelled through HR. In the absence of PARP1 and PARP2 however, the formation and persistence of Rad51 foci is not elevated. In contrast, it is decreased compared to U2OS cells, even in the absence of XRCC1. These observations suggest that the formation or accumulation of Rad51 foci in response to MMS is compromised in the absence of PARP1 and PARP2.

The promotion of resection, performed by the nuclease Mre11, has previously been identified as a control point for PARPs in the resolution of stalled/collapsed replication forks that form after HU exposure (Bryant et al., 2009). In order to assess whether this mechanism of control is conserved for MMS-induced replication damage, I assayed the formation and decay of RPA foci in our *parpΔ* cells. Strikingly, large numbers of RPA foci form and persist in

parp1Δparp2Δ cells after MMS exposure, demonstrating that resection and RPA loading is intact, or even enhanced, in the absence of these PARPs. Whilst consistent with reports that exposure to PARPi can cause instability of stalled replication forks (Ying et al., 2012), our observations on how PARPs contribute to the resolution of replication-associated damage differ from those made using HU. Certainly, the nature of the damaged replication forks that form after exposure to these two agents is likely to be different. HU inhibits ribonucleotide reductase, a key enzyme in the production of dNTPs, causing cellular dNTP depletion (Skoog and Nordenskjöld, 1971). This prevents replicative polymerases from being able function, leading to global replication fork stalling. After prolonged stalling, these forks can then collapse, due to nucelolytic cleavage of the fork, or the intrinsic instability of the ssDNA generated upon polymerase stalling. In contrast, the replication-associated damage that forms after MMS exposure is due to collisions between replication forks and BER-intermediates, including unrepaired SSBs (Ensminger et al., 2014). These collisions can lead to replicative run-off and the rapid formation of one-ended DSBs without additional processing. These differences could explain the discrepant mechanisms by which PARPs appear to act at these two distinct forms of replication-associated damage.

Both *parp1Δ* and XRCC1 depleted cells also show elevated formation and persistence of RPA foci following MMS exposure. Crucially however, in both of these cases, this is paired with a concomitant increase in the formation and persistence of Rad51 foci. Therefore, in these cellular contexts, this observation can be interpreted as a consequence of the increased flow of damage through the HR pathway, rather than a hyper-resection phenotype. The reason why

parp1Δ cells are channelling additional MMS-induced damage through HR is not clear. The fact that they do not display a strand ligation defect in a comet assay, combined with the observation that they do not accumulate additional γH2AX foci immediately after MMS exposure, suggests that this is not due to a BER defect. In contrast, these cells show delayed resolution of γH2AX foci, indicating that these cells struggle to resolve S-phase associated damage, despite showing robust formation of RPA and Rad51 foci. Taken together, this implies that in the absence of PARP1, either HR is disrupted downstream of Rad51 nucleofilament formation to prevent effective damage resolution, or some other pathway that competes with HR for the resolution of this damage is compromised. The best candidate for such a pathway would be alt-NHEJ, which is well understood to be dependent on PARP1 activity. Indeed there is some evidence that Polθ dependent alt-NHEJ activity can contribute to the resolution of replication-associated damage, even in wild-type cells (Ceccaldi et al., 2014). However, I was unable to recapitulate the phenotypes of MMS sensitivity, delayed γH2AX resolution or elevated Rad51 foci formation seen in *parp1Δ* cells by transfecting cells with siRNA targeting Polθ (data not shown). Whilst this suggests PARP1 does not promote Polθ-dependent repair routes in response to MMS exposure, I was also unable to verify the efficiency of endogenous Polθ knockdown, making it difficult to draw firm conclusions from these experiments. Alternatively, PARP1 may be promoting a Polθ independent alt-NHEJ sub-pathway, or some other as yet unidentified repair pathway.

However, it should be noted there is also evidence to support the idea that these phenotypes could result from a PARP1-dependent BER defect. Depletion of XRCC1 in *parp1Δ* cells does not result in an additive accumulation of RPA or

Rad51 foci after MMS exposure, as would be predicted if these proteins were functioning in independent pathways. Therefore, an alternative interpretation would be that loss of PARP1 results in a BER deficiency that does not manifest in a strand ligation defect, but still leads to some of the other phenotypes associated with BER dysfunction. These could relate back to the as yet uncharacterised unique roles of PARP1 in SSBR beyond XRCC1 recruitment as discussed above.

Given that *parp1Δparp2Δ* cells are not compromised for resection, I considered alternative mechanisms through which loss of PARPs could prevent the formation of Rad51 foci. Inhibition of PARP1 and PARP2 did not abrogate the recruitment of PALB2, part of the Rad51 loading BRCA2-PALB2 complex, to chromatin after MMS exposure. Although not conclusive proof that PARPs do not influence the function of BRCA2-PALB2 in HR, this indicates that the role of PARP1 and PARP2 is not to mediate their recruitment to sites of damage. Furthermore, depletion of Rad52 was unable to delay the resolution of γH2AX foci, or suppress the formation or persistence of Rad51 foci, after MMS exposure. This suggests that PARPs are not promoting resolution of this replication-associated damage through Rad52-dependent repair routes. Instead, I found that depletion of the anti-recombinogenic helicase Fbh1 was able to restore the formation of Rad51 foci in *parp1Δparp2Δ* or PARP inhibitor treated cells. This observation implies that Rad51 loading is competent in the absence of these PARPs, as depletion of Fbh1 cannot rescue Rad51 foci formation in BRCA1 or BRCA2 depleted cells (Higgs et al., 2015). Taken together, our data suggest that PARP1 and PARP2 function redundantly to promote the resolution of MMS-induced replication-associated damage by

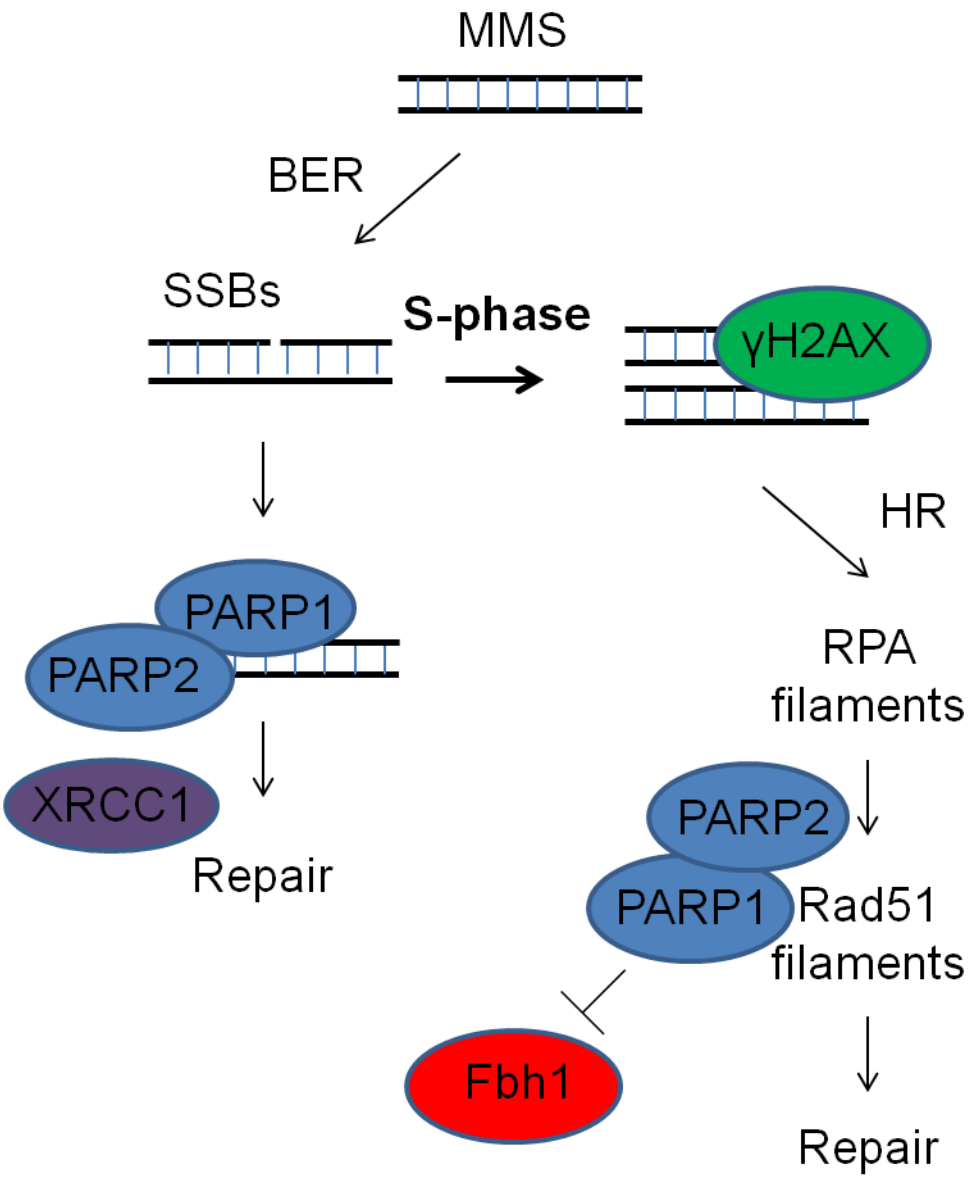


Figure 7: A model for the roles of PARP1 and PARP2 in the cellular response to MMS-induced DNA damage. PARP1 and PARP2 contribute to the resolution of MMS-induced DNA damage in two distinct ways. Firstly, they promote resolution of methylated bases by accelerating the strand ligation step of BER. Secondly, they facilitate the resolution of replication associated damage that accumulates when active replication forks collide with BER intermediates, by antagonising Fbh1 and ensuring the stability of Rad51 nucleofilaments.

protecting Rad51 filaments from dissolution by Fbh1, alongside their roles in BER (Figure 7). Interestingly, depletion of BLM, another helicase able to disassemble Rad51 filaments *in vitro*, is not able to rescue the formation of Rad51 foci in *parp1Δparp2Δ* cells. Whether this is because additional regulatory mechanisms exist to prevent inappropriate BLM activity, or BLM is unable to act on the Rad51 foci that form after MMS exposure, is uncertain. Moreover, the mechanism by which PARP1 and PARP2 facilitate the protection of Rad51 filaments from Fbh1 is unknown, with numerous potential options. This could be mediated by the direct modification of Fbh1 or Rad51 by ADP-ribosylation, or more indirectly through PARPs influencing the complement of proteins present at sites of replication stress to facilitate Rad51 filament protection. Further work will be required to uncover the precise nature of the relationship between PARP1/2 and Fbh1.

Overall, I have identified a key role of PARP1 in facilitating cell survival in the absence of functional HR, supporting the future development of PARP1-specific inhibitors. Furthermore, I have identified novel factors that could mediate synthetic lethality with PARP loss, potentially widening the applications of clinical PARP inhibitors. Finally, this work has uncovered two related but distinct roles of PARP1 and PARP2 in the cellular response to MMS-induced base methylation. Firstly, these enzymes act redundantly to enhance strand ligation in the BER pathway. Secondly, they facilitate the resolution of replication forks that have stalled or collapsed due to collisions with BER intermediates, by promoting the stability of Rad51 filaments through antagonising the activity of Fbh1.

8. References

Aguiar, R.C.T., Takeyama, K., He, C., Kreinbrink, K., and Shipp, M.A. (2005). B-aggressive lymphoma family proteins have unique domains that modulate transcription and exhibit poly(ADP-ribose) polymerase activity. J. Biol. Chem. *280*, 33756–33765.

Ahel, D., Horejsi, Z., Wiechens, N., Polo, S.E., Garcia-Wilson, E., Ahel, I., Flynn, H., Skehel, M., West, S.C., Jackson, S.P., et al. (2009). Poly(ADP-ribose)-Dependent Regulation of DNA Repair by the Chromatin Remodeling Enzyme ALC1. Science (80-.). *325*, 1240–1243.

Ahel, I., Rass, U., El-Khamisy, S.F., Katyal, S., Clements, P.M., McKinnon, P.J., Caldecott, K.W., and West, S.C. (2006). The neurodegenerative disease protein aprataxin resolves abortive DNA ligation intermediates. Nature *443*, 713–716.

Alkhatib, H.M., Chen, D.F., Cherney, B., Bhatia, K., Notario, V., Giri, C., Stein, G., Slattery, E., Roeder, R.G., and Smulson, M.E. (1987). Cloning and expression of cDNA for human poly(ADP-ribose) polymerase. Proc. Natl. Acad. Sci. U. S. A. *84*, 1224–1228.

Allan, L.A., and Fried, M. (1999). p53-dependent apoptosis or growth arrest induced by different forms of radiation in U2OS cells: p21WAF1/CIP1 repression in UV induced apoptosis. Oncogene *18*, 5403–5412.

Altmeyer, M., Messner, S., Hassa, P.O., Fey, M., and Hottiger, M.O. (2009). Molecular mechanism of poly(ADP-ribosyl)ation by PARP1 and identification of lysine residues as ADP-ribose acceptor sites. Nucleic Acids Res. *37*, 3723–3738.

Alvarez-Gonzalez, R., and Althaus, F.R. (1989). Poly(ADP-ribose) catabolism in mammalian cells exposed to DNA-damaging agents. Mutat. Res. *218*, 67–74.

Alvarez-Gonzalez, R., and Jacobson, M.K. (1987). Characterization of polymers of adenosine diphosphate ribose generated in vitro and in vivo. Biochemistry *26*, 3218–3224.

Ambrose, H.E., Willimott, S., Beswick, R.W., Dantzer, F., de Murcia, J.M., Yelamos, J., and Wagner, S.D. (2009). Poly(ADP-ribose) polymerase-1 (Parp-1)-deficient mice demonstrate abnormal antibody responses. Immunology *127*, 178–186.

Amé, J.C., Rolli, V., Schreiber, V., Niedergang, C., Apiou, F., Decker, P., Muller, S., Höger, T., Ménissier-de Murcia, J., and de Murcia, G. (1999). PARP-2, A novel mammalian DNA damage-dependent poly(ADP-ribose) polymerase. J. Biol. Chem. *274*, 17860–17868.

Anantha, R.W., Vassin, V.M., and Borowiec, J.A. (2007). Sequential and synergistic modification of human RPA stimulates chromosomal DNA repair. J. Biol. Chem. *282*, 35910–35923.

Andres, S.N., Vergnes, A., Ristic, D., Wyman, C., Modesti, M., and Junop, M. (2012). A human XRCC4–XLF complex bridges DNA. Nucleic Acids Res. *40*, 1868–1878.

Atasheva, S., Akhrymuk, M., Frolova, E.I., and Frolov, I. (2012). New PARP Gene with an Anti-Alphavirus Function. J. Virol. *86*, 8147–8160.

Audebert, M., Salles, B., and Calsou, P. (2004). Involvement of poly(ADP-ribose) polymerase-1 and XRCC1/DNA ligase III in an alternative route for DNA double-strand breaks rejoining. J. Biol. Chem. *279*, 55117–55126.

Ayrapetov, M.K., Gursoy-Yuzugullu, O., Xu, C., Xu, Y., and Price, B.D. (2014). DNA double-strand breaks promote methylation of histone H3 on lysine 9 and transient formation of repressive chromatin. Proc. Natl. Acad. Sci. U. S. A. *111*, 9169–9174.

Bai, P., Cantó, C., Oudart, H., Brunyánszki, A., Cen, Y., Thomas, C., Yamamoto, H., Huber, A., Kiss, B., Houtkooper, R.H., et al. (2011a). PARP-1 inhibition increases mitochondrial

metabolism through SIRT1 activation. Cell Metab. *13*, 461–468.

Bai, P., Canto, C., Brunyánszki, A., Huber, A., Szántó, M., Cen, Y., Yamamoto, H., Houten, S.M., Kiss, B., Oudart, H., et al. (2011b). PARP-2 regulates SIRT1 expression and whole-body energy expenditure. Cell Metab. *13*, 450–460.

Bajrami, I., Frankum, J.R., Konde, A., Miller, R.E., Rehman, F.L., Brough, R., Campbell, J., Sims, D., Rafiq, R., Hooper, S., et al. (2014). Genome-wide profiling of genetic synthetic lethality identifies CDK12 as a novel determinant of PARP1/2 inhibitor sensitivity. Cancer Res. *74*, 287–297.

Bakkenist, C.J., and Kastan, M.B. (2003). DNA damage activates ATM through intermolecular autophosphorylation and dimer dissociation. Nature *421*, 499–506.

Barber, L.J., Sandhu, S., Chen, L., Campbell, J., Kozarewa, I., Fenwick, K., Assiotis, I., Rodrigues, D.N., Reis-Filho, J.S., Moreno, V., et al. (2013). Secondary mutations in *BRCA2* associated with clinical resistance to a PARP inhibitor. J. Pathol. *229*, 422–429.

Beck, C., Boehler, C., Guirouilh Barbat, J., Bonnet, M.-E., Illuzzi, G., Ronde, P., Gauthier, L.R., Magroun, N., Rajendran, A., Lopez, B.S., et al. (2014). PARP3 affects the relative contribution of homologous recombination and nonhomologous end-joining pathways. Nucleic Acids Res. *42*, 5616–5632.

Bell, C.E., and Eisenberg, D. (1996). Crystal structure of diphtheria toxin bound to nicotinamide adenine dinucleotide. Biochemistry *35*, 1137–1149.

Bell, D., Berchuck, A., Birrer, M., Chien, J., Cramer, D.W., Dao, F., Dhir, R., DiSaia, P., Gabra, H., Glenn, P., et al. (2011). Integrated genomic analyses of ovarian carcinoma. Nature *474*, 609–615.

Bensimon, A., Schmidt, A., Ziv, Y., Elkon, R., Wang, S.-Y., Chen, D.J., Aebersold, R., and Shiloh, Y. (2010). ATM-dependent and -independent dynamics of the nuclear phosphoproteome after DNA damage. Sci. Signal. *3*, rs3.

Bentley, J., Diggle, C.P., Harnden, P., Knowles, M.A., and Kiltie, A.E. (2004). DNA double strand break repair in human bladder cancer is error prone and involves microhomology-associated end-joining. Nucleic Acids Res. *32*, 5249–5259.

Beranek, D.T. (1990). Distribution of methyl and ethyl adducts following alkylation with monofunctional alkylating agents. Mutat. Res. *231*, 11–30.

Berger, N.A., Sikorski, G.W., Petzold, S.J., and Kurohara, K.K. (1979). Association of Poly(Adenosine Diphosphoribose) Synthesis with DNA Damage and Repair in Normal Human Lymphocytes. J. Clin. Invest. *63*, 1164–1171.

Bermudez, V.P., Lindsey-Boltz, L.A., Cesare, A.J., Maniwa, Y., Griffith, J.D., Hurwitz, J., and Sancar, A. (2003). Loading of the human 9-1-1 checkpoint complex onto DNA by the checkpoint clamp loader hRad17-replication factor C complex in vitro. Proc. Natl. Acad. Sci. U. S. A. *100*, 1633–1638.

Berti, M., Ray Chaudhuri, A., Thangavel, S., Gomathinayagam, S., Kenig, S., Vujanovic, M., Odreman, F., Glatter, T., Graziano, S., Mendoza-Maldonado, R., et al. (2013). Human RECQ1 promotes restart of replication forks reversed by DNA topoisomerase I inhibition. Nat. Publ. Gr. *20*, 3–4.

Bétous, R., Mason, A.C., Rambo, R.P., Bansbach, C.E., Badu-Nkansah, A., Sirbu, B.M., Eichman, B.F., and Cortez, D. (2012). SMARCAL1 catalyzes fork regression and Holliday junction migration to maintain genome stability during DNA replication. Genes Dev. *26*, 151–162.

Bhargava, R., Onyango, D.O., and Stark, J.M. (2016). Regulation of Single-Strand Annealing and its Role in Genome Maintenance. Trends Genet. *32*, 566–575.

Bhowmick, R., Minocherhomji, S., and Hickson, I.D. (2016). RAD52 Facilitates Mitotic DNA Synthesis Following Replication Stress. Mol. Cell *64*, 1117–1126.

Bick, M.J., Carroll, J.-W.N., Gao, G., Goff, S.P., Rice, C.M., and MacDonald, M.R. (2003). Expression of the zinc-finger antiviral protein inhibits alphavirus replication. J. Virol. *77*, 11555–11562.

Birger, Y., West, K.L., Postnikov, Y. V, Lim, J.-H., Furusawa, T., Wagner, J.P., Laufer, C.S., Kraemer, K.H., and Bustin, M. (2003). Chromosomal protein HMGN1 enhances the rate of DNA repair in chromatin. EMBO J. *22*, 1665–1675.

Bjorâs, M., Luna, L., Johnsen, B., Hoff, E., Haug, T., Rognes, T., and Seeberg, E. (1997). Opposite base-dependent reactions of a human base excision repair enzyme on DNA containing 7,8-dihydro-8-oxoguanine and abasic sites. EMBO J. *16*, 6314–6322.

Block, W.D., Yu, Y., Merkle, D., Gifford, J.L., Ding, Q., Meek, K., and Lees-Miller, S.P. (2004). Autophosphorylation-dependent remodeling of the DNA-dependent protein kinase catalytic subunit regulates ligation of DNA ends. Nucleic Acids Res. *32*, 4351–4357.

Blow, J.J., Ge, X.Q., and Jackson, D.A. (2011). How dormant origins promote complete genome replication. Trends Biochem. Sci. *36*, 405–414.

Boboila, C., Oksenych, V., Gostissa, M., Wang, J.H., Zha, S., Zhang, Y., Chai, H., Lee, C.-S., Jankovic, M., Saez, L.-M.A., et al. (2012). Robust chromosomal DNA repair via alternative end-joining in the absence of X-ray repair cross-complementing protein 1 (XRCC1). Proc. Natl. Acad. Sci. *109*, 2473–2478.

Boehler, C., Gauthier, L.R., Mortusewicz, O., Biard, D.S., Saliou, J.-M., Bresson, A., Sanglier-Cianferani, S., Smith, S., Schreiber, V., Boussin, F., et al. (2011). Poly(ADP-ribose) polymerase 3 (PARP3), a newcomer in cellular response to DNA damage and mitotic progression. Proc. Natl. Acad. Sci. U. S. A. *108*, 2783–2788.

Bolton, E.C., So, A.Y., Chaivorapol, C., Haqq, C.M., Li, H., and Yamamoto, K.R. (2007). Cell- and gene-specific regulation of primary target genes by the androgen receptor. Genes & Dev. *21*, 2005–2017.

Bonfiglio, J.J., Fontana, P., Zhang, Q., Colby, T., Gibbs-Seymour, I., Atanassov, I., Bartlett, E., Zaja, R., Ahel, I., and Matic, I. (2017). Serine ADP-Ribosylation Depends on HPF1. Mol. Cell *65*, 932–940.e6.

Boulton, S.J., and Jackson, S.P. (1996). Identification of a *Saccharomyces cerevisiae* Ku80 homologue: roles in DNA double strand break rejoining and in telomeric maintenance. Nucleic Acids Res. *24*, 4639–4648.

Bouwman, P., Aly, A., Escandell, J.M., Pieterse, M., Bartkova, J., van der Gulden, H., Hiddingh, S., Thanasoula, M., Kulkarni, A., Yang, Q., et al. (2010). 53BP1 loss rescues BRCA1 deficiency and is associated with triple-negative and BRCA-mutated breast cancers. Nat. Publ. Gr. *17*.

van Brabant, A.J., Ye, T., Sanz, M., German, J.L., Ellis, N.A., and Holloman, W.K. (2000). Binding and Melting of D-Loops by the Bloom Syndrome Helicase †. Biochemistry *39*, 14617–14625.

Brem, R., and Hall, J. (2005). XRCC1 is required for DNA single-strand break repair in human cells. Nucleic Acids Res. *33*, 2512–2520.

Brem, R., Fernet, M., Chapot, B., and Hall, J. (2008). The methyl methanesulfonate induced S-phase delay in XRCC1-deficient cells requires ATM and ATR. DNA Repair (Amst). *7*, 849–857.

Breslin, C., Hornyak, P., Ridley, A., Rulten, S.L., Hanzlikova, H., Oliver, A.W., and Caldecott, K.W. (2015). The XRCC1 phosphate-binding pocket binds poly (ADP-ribose) and is required for XRCC1 function. Nucleic Acids Res. *43*, 6934–6944.

Brown, E.J., and Baltimore, D. (2003). Essential and dispensable roles of ATR in cell cycle arrest and genome maintenance. Genes Dev. *17*, 615–628.

Brown, J.S., Lukashchuk, N., Sczaniecka-Clift, M., Britton, S., le Sage, C., Calsou, P., Beli, P., Galanty, Y., and Jackson, S.P. (2015). Neddylation Promotes Ubiquitylation and Release of Ku from DNA-Damage Sites. Cell Rep. *11*, 704–714.

Bryant, H.E., Schultz, N., Thomas, H.D., Parker, K.M., Flower, D., Lopez, E., Kyle, S., Meuth, M., Curtin, N.J., and Helleday, T. (2005). Specific killing of BRCA2-deficient tumours with inhibitors of poly(ADP-ribose) polymerase. Nature *434*, 913–917.

Bryant, H.E., Petermann, E., Schultz, N., Jemth, A.-S., Loseva, O., Issaeva, N., Johansson, F., Fernandez, S., McGlynn, P., and Helleday, T. (2009). PARP is activated at stalled forks to mediate Mre11-dependent replication restart and recombination. EMBO J. *28*, 2601–2615.

Brzovic, P.S., Rajagopal, P., Hoyt, D.W., King, M.-C., and Klevit, R.E. (2001). Structure of a BRCA1-BARD1 heterodimeric RING-RING complex. Nat. Struct. Biol. *8*, 833–837.

Budke, B., Logan, H.L., Kalin, J.H., Zelivianskaia, A.S., Cameron McGuire, W., Miller, L.L., Stark, J.M., Kozikowski, A.P., Bishop, D.K., and Connell, P.P. (2012). RI-1: a chemical inhibitor of RAD51 that disrupts homologous recombination in human cells. Nucleic Acids Res. *40*, 7347–7357.

Bugreev, D. V, Yu, X., Egelman, E.H., and Mazin, A. V (2007). Novel pro- and anti-recombination activities of the Bloom's syndrome helicase. Genes Dev. *21*, 3085–3094.

Buis, J., Wu, Y., Deng, Y., Leddon, J., Westfield, G., Eckersdorff, M., Sekiguchi, J.M., Chang, S., and Ferguson, D.O. (2008). Mre11 Nuclease Activity Has Essential Roles in DNA Repair and Genomic Stability Distinct from ATM Activation. Cell *135*, 85–96.

Buisson, R., Dion-Côté, A.-M., Coulombe, Y., Launay, H., Cai, H., Stasiak, A.Z., Stasiak, A., Xia, B., and Masson, J.-Y. (2010). Cooperation of breast cancer proteins PALB2 and piccolo BRCA2 in stimulating homologous recombination. Nat. Struct. Mol. Biol. *17*, 1247–1254.

Bunting, S.F., Callén, E., Wong, N., Chen, H.-T., Polato, F., Gunn, A., Bothmer, A., Feldhahn, N., Fernandez-Capetillo, O., Cao, L., et al. (2010). 53BP1 Inhibits Homologous Recombination in Brca1-Deficient Cells by Blocking Resection of DNA Breaks. Cell *141*, 243–254.

Burma, S., Chen, B.P., Murphy, M., Kurimasa, A., and Chen, D.J. (2001). ATM phosphorylates histone H2AX in response to DNA double-strand breaks. J. Biol. Chem. *276*, 42462–42467.

Byun, T.S., Pacek, M., Yee, M., Walter, J.C., and Cimprich, K.A. (2005). Functional uncoupling of MCM helicase and DNA polymerase activities activates the ATR-dependent checkpoint. Genes Dev. *19*, 1040–1052.

Caldecott, K.W., McKeown, C.K., Tucker, J.D., Ljungquist, S., and Thompson, L.H. (1994). An interaction between the mammalian DNA repair protein XRCC1 and DNA ligase III. Mol. Cell. Biol. *14*, 68–76.

Caldecott, K.W., Aoufouchi, S., Johnson, P., and Shall, S. (1996). XRCC1 polypeptide interacts with DNA polymerase beta and possibly poly (ADP-ribose) polymerase, and DNA ligase III is a novel molecular "nick-sensor" in vitro. Nucleic Acids Res. *24*, 4387–4394.

Callen, E., Di Virgilio, M., Kruhlak, M.J., Nieto-Soler, M., Wong, N., Chen, H.-T., Faryabi, R.B., Polato, F., Santos, M., Starnes, L.M., et al. (2013). 53BP1 Mediates Productive and Mutagenic DNA Repair through Distinct Phosphoprotein Interactions. Cell *153*, 1266–1280.

Campagnari, F., Whitfield, J.F., and Bertazzoni, U. (1966). The effect of x-irradiation on the nicotinamide adenine dinucleotides (NAD-NADH) content of rat thymocytes. Exp. Cell Res. *42*, 646–656.

Candi, E., Agostini, M., Melino, G., and Bernassola, F. (2014). How the *TP53* Family Proteins

TP63 and *TP73* Contribute to Tumorigenesis: Regulators and Effectors. Hum. Mutat. *35*, 702–714.

Cappelli, E., Taylor, R., Cevasco, M., Abbondandolo, A., Caldecott, K., and Frosina, G. (1997). Involvement of XRCC1 and DNA ligase III gene products in DNA base excision repair. J. Biol. Chem. *272*, 23970–23975.

Cary, R.B., Peterson, S.R., Wang, J., Bear, D.G., Bradbury, E.M., and Chen, D.J. (1997). DNA looping by Ku and the DNA-dependent protein kinase. Proc. Natl. Acad. Sci. U. S. A. *94*, 4267–4272.

Ceccaldi, R., Liu, J.C., Amunugama, R., Hajdu, I., Primack, B., Petalcorin, M.I.R., O 'connor, K.W., Konstantinopoulos, P.A., Elledge, S.J., Boulton, S.J., et al. (2014). Homologous-recombination-deficient tumours are dependent on Polh-mediated repair. Nature *518*.

Celeste, A., Petersen, S., Romanienko, P.J., Fernandez-Capetillo, O., Chen, H.T., Sedelnikova, O.A., Reina-San-Martin, B., Coppola, V., Meffre, E., Difilippantonio, M.J., et al. (2002). Genomic Instability in Mice Lacking Histone H2AX. Science (80-.). *296*, 922–927.

Chaganti, R.S., Schonberg, S., and German, J. (1974). A manyfold increase in sister chromatid exchanges in Bloom's syndrome lymphocytes. Proc. Natl. Acad. Sci. U. S. A. *71*, 4508–4512.

Chalkiadaki, A., and Guarente, L. (2015). The multifaceted functions of sirtuins in cancer. Nat. Rev. Cancer *15*, 608–624.

Chan, Y.W., and West, S. (2015). GEN1 promotes Holliday junction resolution by a coordinated nick and counter-nick mechanism. Nucleic Acids Res. *43*, 10882–10892.

Chang, P., Coughlin, M., and Mitchison, T.J. (2005a). Tankyrase-1 polymerization of poly(ADP-ribose) is required for spindle structure and function. Nat. Cell Biol. *7*, 1133–1139.

Chang, W., Dynek, J.N., and Smith, S. (2005b). NuMA is a major acceptor of poly(ADP-ribosyl)ation by tankyrase 1 in mitosis. Biochem. J. *391*, 177–184.

Chapman, J.R., and Jackson, S.P. (2008). Phospho-dependent interactions between NBS1 and MDC1 mediate chromatin retention of the MRN complex at sites of DNA damage. EMBO Rep. *9*, 795–801.

Chapman, J.R., Sossick, A.J., Boulton, S.J., and Jackson, S.P. (2012). BRCA1-associated exclusion of 53BP1 from DNA damage sites underlies temporal control of DNA repair. J. Cell Sci. *125*, 3529–3534.

Chapman, J.R., Barral, P., Vannier, J.-B., Borel, V., Steger, M., Tomas-Loba, A., Sartori, A.A., Adams, I.R., Batista, F.D., and Boulton, S.J. (2013). RIF1 is essential for 53BP1-dependent nonhomologous end joining and suppression of DNA double-strand break resection. Mol. Cell *49*, 858–871.

Chappell, C., Hanakahi, L.A., Karimi-Busheri, F., Weinfeld, M., and West, S.C. (2002). Involvement of human polynucleotide kinase in double-strand break repair by non-homologous end joining. EMBO J. *21*, 2827–2832.

Chen, D., Vollmar, M., Rossi, M.N., Phillips, C., Kraehenbuehl, R., Slade, D., Mehrotra, P. V., von Delft, F., Crosthwaite, S.K., Gileadi, O., et al. (2011). Identification of Macrodomain Proteins as Novel *O* -Acetyl-ADP-ribose Deacetylases. J. Biol. Chem. *286*, 13261–13271.

Chen, P.L., Chen, C.F., Chen, Y., Xiao, J., Sharp, Z.D., and Lee, W.H. (1998). The BRC repeats in BRCA2 are critical for RAD51 binding and resistance to methyl methanesulfonate treatment. Proc. Natl. Acad. Sci. U. S. A. *95*, 5287–5292.

Chen, S., Xu, Y., Zhang, K., Wang, X., Sun, J., Gao, G., and Liu, Y. (2012a). Structure of N-terminal domain of ZAP indicates how a zinc-finger protein recognizes complex RNA. Nat. Struct. Mol. Biol. *19*, 430–435.

Chen, S., Wang, D.-L., Liu, Y., Zhao, L., and Sun, F.-L. (2012b). RAD6 regulates the dosage of p53 by a combination of transcriptional and posttranscriptional mechanisms. Mol. Cell. Biol. *32*, 576–587.

Chen, S., Wang, C., Sun, L., Wang, D.-L., Chen, L., Huang, Z., Yang, Q., Gao, J., Yang, X.-B., Chang, J.-F., et al. (2015). RAD6 Promotes Homologous Recombination Repair by Activating the Autophagy-Mediated Degradation of Heterochromatin Protein HP1. Mol. Cell. Biol. *35*, 406–416.

Chen, X.-B., Melchionna, R., Denis, C.-M., Gaillard, P.-H.L., Blasina, A., Van de Weyer, I., Boddy, M.N., Russell, P., Vialard, J., and McGowan, C.H. (2001). Human Mus81-Associated Endonuclease Cleaves Holliday Junctions In Vitro. Mol. Cell *8*, 1117–1127.

Chlebowicz, E., and Jachymczyk, W.J. (1979). Repair of MMS-induced DNA double-strand breaks in haploid cells of *Saccharomyces cerevisiae*, which requires the presence of a duplicate genome. Mol. Gen. Genet. *167*, 279–286.

Choy, J.S., and Kron, S.J. (2002). NuA4 subunit Yng2 function in intra-S-phase DNA damage response. Mol. Cell. Biol. *22*, 8215–8225.

Chu, W.K., Payne, M.J., Beli, P., Hanada, K., Choudhary, C., and Hickson, I.D. (2015). FBH1 influences DNA replication fork stability and homologous recombination through ubiquitylation of RAD51. Nat. Commun. *6*, 5931.

Ciccia, A., Constantinou, A., and West, S.C. (2003). Identification and characterization of the human mus81-eme1 endonuclease. J. Biol. Chem. *278*, 25172–25178.

Ciccia, A., Nimonkar, A.V., Hu, Y., Hajdu, I., Achar, Y.J., Izhar, L., Petit, S.A., Adamson, B., Yoon, J.C., Kowalczykowski, S.C., et al. (2012). Polyubiquitinated PCNA Recruits the ZRANB3 Translocase to Maintain Genomic Integrity after Replication Stress. Mol. Cell *47*, 396–409.

Clements, P.M., Breslin, C., Deeks, E.D., Byrd, P.J., Ju, L., Bieganowski, P., Brenner, C., Moreira, M.-C., Taylor, A.M.R., and Caldecott, K.W. (2004). The ataxia-oculomotor apraxia 1 gene product has a role distinct from ATM and interacts with the DNA strand break repair proteins XRCC1 and XRCC4. DNA Repair (Amst). *3*, 1493–1502.

Cook, B.D., Dynek, J.N., Chang, W., Shostak, G., and Smith, S. (2002). Role for the related poly(ADP-Ribose) polymerases tankyrase 1 and 2 at human telomeres. Mol. Cell. Biol. *22*, 332–342.

Coquelle, N., Havali-Shahriari, Z., Bernstein, N., Green, R., and Glover, J.N.M. (2011). Structural basis for the phosphatase activity of polynucleotide kinase/phosphatase on single- and double-stranded DNA substrates. Proc. Natl. Acad. Sci. *108*, 21022–21027.

Costanzo, V., Robertson, K., Bibikova, M., Kim, E., Grieco, D., Gottesman, M., Carroll, D., and Gautier, J. (2001). Mre11 protein complex prevents double-strand break accumulation during chromosomal DNA replication. Mol. Cell *8*, 137–147.

Daley, J.M., and Sung, P. (2014). 53BP1, BRCA1, and the choice between recombination and end joining at DNA double-strand breaks. Mol. Cell. Biol. *34*, 1380–1388.

Dantzer, F., Giraud-Panis, M.-J., Jaco, I., Amé, J.-C., Schultz, I., Blasco, M., Koering, C.-E., Gilson, E., Ménissier-de Murcia, J., de Murcia, G., et al. (2004). Functional interaction between poly(ADP-Ribose) polymerase 2 (PARP-2) and TRF2: PARP activity negatively regulates TRF2. Mol. Cell. Biol. *24*, 1595–1607.

Dantzer, F., Mark, M., Quenet, D., Scherthan, H., Huber, A., Liebe, B., Monaco, L., Chicheportiche, A., Sassone-Corsi, P., de Murcia, G., et al. (2006). Poly(ADP-ribose) polymerase-2 contributes to the fidelity of male meiosis I and spermiogenesis. Proc. Natl. Acad. Sci. U. S. A. *103*, 14854–14859.

Date, H., Igarashi, S., Sano, Y., Takahashi, T., Takahashi, T., Takano, H., Tsuji, S., Nishizawa,

M., and Onodera, O. (2004). The FHA domain of aprataxin interacts with the C-terminal region of XRCC1. Biochem. Biophys. Res. Commun. *325*, 1279–1285.

De, P., Sun, Y., Carlson, J.H., Friedman, L.S., Leyland-Jones, B.R., and Dey, N. (2014). Doubling down on the PI3K-AKT-mTOR pathway enhances the antitumor efficacy of PARP inhibitor in triple negative breast cancer model beyond BRCA-ness. Neoplasia *16*, 43–72.

DeFazio, L.G., Stansel, R.M., Griffith, J.D., and Chu, G. (2002). Synapsis of DNA ends by DNA-dependent protein kinase. EMBO J. *21*, 3192–3200.

Della-Maria, J., Zhou, Y., Tsai, M.-S., Kuhnlein, J., Carney, J.P., Paull, T.T., and Tomkinson, A.E. (2011). Human Mre11/human Rad50/Nbs1 and DNA ligase IIIalpha/XRCC1 protein complexes act together in an alternative nonhomologous end joining pathway. J. Biol. Chem. *286*, 33845–33853.

Della-Maria, J., Hegde, M.L., McNeill, D.R., Matsumoto, Y., Tsai, M.-S., Ellenberger, T., Wilson, D.M., Mitra, S., and Tomkinson, A.E. (2012). The Interaction between Polynucleotide Kinase Phosphatase and the DNA Repair Protein XRCC1 Is Critical for Repair of DNA Alkylation Damage and Stable Association at DNA Damage Sites. J. Biol. Chem. *287*, 39233–39244.

Difilippantonio, M.J., Zhu, J., Chen, H.T., Meffre, E., Nussenzweig, M.C., Max, E.E., Ried, T., and Nussenzweig, A. (2000). DNA repair protein Ku80 suppresses chromosomal aberrations and malignant transformation. Nature *404*, 510–514.

DOBZHANSKY, T. (1946). Genetics of natural populations; recombination and variability in populations of Drosophila pseudoobscura. Genetics *31*, 269–290.

Douglas, P., Sapkota, G.P., Morrice, N., Yu, Y., Goodarzi, A.A., Merkle, D., Meek, K., Alessi, D.R., and Lees-Miller, S.P. (2002). Identification of in vitro and in vivo phosphorylation sites in the catalytic subunit of the DNA-dependent protein kinase. Biochem. J. *368*, 243–251.

Douglas, P., Cui, X., Block, W.D., Yu, Y., Gupta, S., Ding, Q., Ye, R., Morrice, N., Lees-Miller, S.P., and Meek, K. (2007). The DNA-Dependent Protein Kinase Catalytic Subunit Is Phosphorylated In Vivo on Threonine 3950, a Highly Conserved Amino Acid in the Protein Kinase Domain. Mol. Cell. Biol. *27*, 1581–1591.

Drost, J., Mantovani, F., Tocco, F., Elkon, R., Comel, A., Holstege, H., Kerkhoven, R., Jonkers, J., Voorhoeve, P.M., Agami, R., et al. (2010). BRD7 is a candidate tumour suppressor gene required for p53 function. Nat. Cell Biol. *12*, 380–389.

Dunstan, M.S., Barkauskaite, E., Lafite, P., Knezevic, C.E., Brassington, A., Ahel, M., Hergenrother, P.J., Leys, D., and Ahel, I. (2012). Structure and mechanism of a canonical poly(ADP-ribose) glycohydrolase. Nat. Commun. *3*, 878.

Durkacz, B.W., Omidiji, O., Gray, D.A., and Shall, S. (1980). (ADP-ribose)n participates in DNA excision repair. Nature *283*, 593–596.

El-Khamisy, S.F., Masutani, M., Suzuki, H., and Caldecott, K.W. (2003). A requirement for PARP-1 for the assembly or stability of XRCC1 nuclear foci at sites of oxidative DNA damage. Nucleic Acids Res. *31*, 5526–5533.

Ellison, V., and Stillman, B. (2003). Biochemical characterization of DNA damage checkpoint complexes: clamp loader and clamp complexes with specificity for 5' recessed DNA. PLoS Biol. *1*, E33.

Ensminger, M., Iloff, L., Ebel, C., Nikolova, T., Kaina, B., and Löbrich, M. (2014). DNA breaks and chromosomal aberrations arise when replication meets base excision repair. J. Cell Biol. *206*, 29–43.

Erener, S., Hesse, M., Kostadinova, R., and Hottiger, M.O. (2012). Poly(ADP-ribose)polymerase-1 (PARP1) controls adipogenic gene expression and adipocyte function. Mol. Endocrinol. *26*, 79–86.

Fan, W., and Wu, X. (2004). DNA polymerase lambda can elongate on DNA substrates mimicking non-homologous end joining and interact with XRCC4-ligase IV complex. Biochem. Biophys. Res. Commun. *323*, 1328–1333.

Farmer, H., McCabe, N., Lord, C.J., Tutt, A.N.J., Johnson, D.A., Richardson, T.B., Santarosa, M., Dillon, K.J., Hickson, I., Knights, C., et al. (2005). Targeting the DNA repair defect in BRCA mutant cells as a therapeutic strategy. Nature *434*, 917–921.

Farrés, J., Martín-Caballero, J., Martínez, C., Lozano, J.J., Llacuna, L., Ampurdanés, C., Ruiz-Herguido, C., Dantzer, F., Schreiber, V., Villunger, A., et al. (2013). Parp-2 is required to maintain hematopoiesis following sublethal γ-irradiation in mice. Blood *122*, 44–54.

Fekairi, S., Scaglione, S., Chahwan, C., Taylor, E.R., Tissier, A., Coulon, S., Dong, M.-Q., Ruse, C., Yates, J.R., Russell, P., et al. (2009). Human SLX4 is a Holliday junction resolvase subunit that binds multiple DNA repair/recombination endonucleases. Cell *138*, 78–89.

Feldmann, E., Schmiemann, V., Goedecke, W., Reichenberger, S., and Pfeiffer, P. (2000). DNA double-strand break repair in cell-free extracts from Ku80-deficient cells: implications for Ku serving as an alignment factor in non-homologous DNA end joining. Nucleic Acids Res. *28*, 2585–2596.

Feng, Z., Scott, S.P., Bussen, W., Sharma, G.G., Guo, G., Pandita, T.K., and Powell, S.N. (2011). Rad52 inactivation is synthetically lethal with BRCA2 deficiency. Proc. Natl. Acad. Sci. U. S. A. *108*, 686–691.

Ferguson, D.O., Sekiguchi, J.M., Chang, S., Frank, K.M., Gao, Y., DePinho, R.A., and Alt, F.W. (2000). The nonhomologous end-joining pathway of DNA repair is required for genomic stability and the suppression of translocations. Proc. Natl. Acad. Sci. U. S. A. *97*, 6630–6633.

Fisher, A.E.O., Hochegger, H., Takeda, S., and Caldecott, K.W. (2007). Poly(ADP-ribose) polymerase 1 accelerates single-strand break repair in concert with poly(ADP-ribose) glycohydrolase. Mol. Cell. Biol. *27*, 5597–5605.

Frosina, G., Fortini, P., Rossi, O., Carrozzino, F., Raspaglio, G., Cox, L.S., Lane, D.P., Abbondandolo, A., and Dogliotti, E. (1996). Two pathways for base excision repair in mammalian cells. J. Biol. Chem. *271*, 9573–9578.

Fu, D., Calvo, J.A., and Samson, L.D. (2012). Balancing repair and tolerance of DNA damage caused by alkylating agents. Nat. Rev. Cancer *12*, 104–120.

Fugger, K., Mistrik, M., Neelsen, K.J., Yao, Q., Zellweger, R., Kousholt, A.N., Haahr, P., Chu, W.K., Bartek, J., Lopes, M., et al. (2015). FBH1 Catalyzes Regression of Stalled Replication Forks. Cell Rep. *10*, 1749–1757.

Galande, S., and Kohwi-Shigematsu, T. (1999). Poly(ADP-ribose) polymerase and Ku autoantigen form a complex and synergistically bind to matrix attachment sequences. J. Biol. Chem. *274*, 20521–20528.

Gamble, M.J., and Fisher, R.P. (2007). SET and PARP1 remove DEK from chromatin to permit access by the transcription machinery. Nat. Struct. Mol. Biol. *14*, 548–555.

Gao, F., Luo, H., Zhang, C.-T., and Zhang, R. (2015). Gene Essentiality Analysis Based on DEG 10, an Updated Database of Essential Genes. In Methods in Molecular Biology (Clifton, N.J.), pp. 219–233.

Gao, G., Guo, X., and Goff, S.P. (2002). Inhibition of Retroviral RNA Production by ZAP, a CCCH-Type Zinc Finger Protein. Science (80-.). *297*, 1703–1706.

Gao, Y., Katyal, S., Lee, Y., Zhao, J., Rehg, J.E., Russell, H.R., and McKinnon, P.J. (2011). DNA ligase III is critical for mtDNA integrity but not Xrcc1-mediated nuclear DNA repair. Nature *471*, 240–244.

Gao, Y., Wang, B., and Gao, S. (2016). BRD7 Acts as a Tumor Suppressor Gene in Lung Adenocarcinoma. PLoS One *11*, e0156701.

Gao, Y., Mutter-Rottmayer, E., Zlatanou, A., Vaziri, C., and Yang, Y. (2017). Mechanisms of Post-Replication DNA Repair. Genes (Basel). *8*, 64.

Garces, F., Pearl, L.H., and Oliver, A.W. (2011). The Structural Basis for Substrate Recognition by Mammalian Polynucleotide Kinase 3′ Phosphatase. Mol. Cell *44*, 385–396.

Gari, K., Decaillet, C., Delannoy, M., Wu, L., and Constantinou, A. (2008). Remodeling of DNA replication structures by the branch point translocase FANCM. Proc. Natl. Acad. Sci. *105*, 16107–16112.

German, J., Sanz, M.M., Ciocci, S., Ye, T.Z., and Ellis, N.A. (2007). Syndrome-causing mutations of the BLM gene in persons in the Bloom's Syndrome Registry. Hum. Mutat. *28*, 743–753.

Di Giammartino, D.C., Shi, Y., and Manley, J.L. (2013). PARP1 represses PAP and inhibits polyadenylation during heat shock. Mol. Cell *49*, 7–17.

Giannattasio, M., Zwicky, K., Follonier, C., Foiani, M., Lopes, M., and Branzei, D. (2014). Visualization of recombination-mediated damage bypass by template switching. Nat. Struct. Mol. Biol. *21*, 884–892.

Gibbs-Seymour, I., Fontana, P., Rack, J.G.M., and Ahel, I. (2016). HPF1/C4orf27 Is a PARP-1-Interacting Protein that Regulates PARP-1 ADP-Ribosylation Activity. Mol. Cell *62*, 432–442.

Gibson, B.A., and Kraus, W.L. (2012). New insights into the molecular and cellular functions of poly(ADP-ribose) and PARPs. Nat. Rev. Mol. Cell Biol. *13*, 411–424.

Godon, C., Cordelières, F.P., Biard, D., Giocanti, N., Mégnin-Chanet, F., Hall, J., and Favaudon, V. (2008). PARP inhibition versus PARP-1 silencing: different outcomes in terms of single-strand break repair and radiation susceptibility. Nucleic Acids Res. *36*, 4454–4464.

Gomez, M., Wu, J., Schreiber, V., Dunlap, J., Dantzer, F., Wang, Y., and Liu, Y. (2006). PARP1 Is a TRF2-associated Poly(ADP-Ribose)Polymerase and Protects Eroded Telomeres. Mol. Biol. Cell *17*, 1686–1696.

Gottipati, P., Vischioni, B., Schultz, N., Solomons, J., Bryant, H.E., Djureinovic, T., Issaeva, N., Sleeth, K., Sharma, R.A., and Helleday, T. (2010). Poly(ADP-Ribose) Polymerase Is Hyperactivated in Homologous Recombination-Defective Cells. Cancer Res. *70*, 5389–5398.

Graham, T.G.W., Walter, J.C., and Loparo, J.J. (2016). Two-Stage Synapsis of DNA Ends during Non-homologous End Joining.

Groth, P., Ausländer, S., Majumder, M.M., Schultz, N., Johansson, F., Petermann, E., and Helleday, T. (2010). Methylated DNA Causes a Physical Block to Replication Forks Independently of Damage Signalling, O6-Methylguanine or DNA Single-Strand Breaks and Results in DNA Damage. J. Mol. Biol. *402*, 70–82.

Grundy, G.J., Polo, L.M., Zeng, Z., Rulten, S.L., Hoch, N.C., Paomephan, P., Xu, Y., Sweet, S.M., Thorne, A.W., Oliver, A.W., et al. (2016). PARP3 is a sensor of nicked nucleosomes and monoribosylates histone H2BGlu2. Nat. Commun. *7*, 12404.

Guetg, C., Scheifele, F., Rosenthal, F., Hottiger, M.O., and Santoro, R. (2012). Inheritance of Silent rDNA Chromatin Is Mediated by PARP1 via Noncoding RNA. Mol. Cell *45*, 790–800.

Guo, Y., Chekaluk, Y., Zhang, J., Du, J., Gray, N.S., Wu, C.-L., and Kwiatkowski, D.J. (2013). *TSC1* involvement in bladder cancer: diverse effects and therapeutic implications. J. Pathol. *230*, 17–27.

Gupta, A., Hunt, C.R., Chakraborty, S., Pandita, R.K., Yordy, J., Ramnarain, D.B., Horikoshi, N.,

and Pandita, T.K. (2014). Role of 53BP1 in the regulation of DNA double-strand break repair pathway choice. Radiat. Res. *181*, 1–8.

Haince, J.-F., McDonald, D., Rodrigue, A., Déry, U., Masson, J.-Y., Hendzel, M.J., and Poirier, G.G. (2008). PARP1-dependent kinetics of recruitment of MRE11 and NBS1 proteins to multiple DNA damage sites. J. Biol. Chem. *283*, 1197–1208.

Hammel, M., Yu, Y., Mahaney, B.L., Cai, B., Ye, R., Phipps, B.M., Rambo, R.P., Hura, G.L., Pelikan, M., So, S., et al. (2010). Ku and DNA-dependent Protein Kinase Dynamic Conformations and Assembly Regulate DNA Binding and the Initial Non-homologous End Joining Complex. J. Biol. Chem. *285*, 1414–1423.

Hammel, M., Rey, M., Yu, Y., Mani, R.S., Classen, S., Liu, M., Pique, M.E., Fang, S., Mahaney, B.L., Weinfeld, M., et al. (2011). XRCC4 protein interactions with XRCC4-like factor (XLF) create an extended grooved scaffold for DNA ligation and double strand break repair. J. Biol. Chem. *286*, 32638–32650.

Hanada, K., Budzowska, M., Davies, S.L., van Drunen, E., Onizawa, H., Beverloo, H.B., Maas, A., Essers, J., Hickson, I.D., and Kanaar, R. (2007). The structure-specific endonuclease Mus81 contributes to replication restart by generating double-strand DNA breaks. Nat. Struct. Mol. Biol. *14*, 1096–1104.

Hanzlikova, H., Gittens, W., Krejcikova, K., Zeng, Z., and Caldecott, K.W. (2016). Overlapping roles for PARP1 and PARP2 in the recruitment of endogenous XRCC1 and PNKP into oxidized chromatin. Nucleic Acids Res. *45*, gkw1246.

Harte, M.T., O'Brien, G.J., Ryan, N.M., Gorski, J.J., Savage, K.I., Crawford, N.T., Mullan, P.B., and Harkin, D.P. (2010). BRD7, a subunit of SWI/SNF complexes, binds directly to BRCA1 and regulates BRCA1-dependent transcription. Cancer Res. *70*, 2538–2547.

Hashimoto, Y., Chaudhuri, A.R., Lopes, M., and Costanzo, V. (2010). Rad51 protects nascent DNA from Mre11-dependent degradation and promotes continuous DNA synthesis. Nat. Struct. Mol. Biol. *17*, 1305–1311.

Hatakeyama, K., Nemoto, Y., Ueda, K., and Hayaishi, O. (1986). Purification and characterization of poly(ADP-ribose) glycohydrolase. Different modes of action on large and small poly(ADP-ribose). J. Biol. Chem. *261*, 14902–14911.

Henneman, L., van Miltenburg, M.H., Michalak, E.M., Braumuller, T.M., Jaspers, J.E., Drenth, A.P., de Korte-Grimmerink, R., Gogola, E., Szuhai, K., Schlicker, A., et al. (2015). Selective resistance to the PARP inhibitor olaparib in a mouse model for BRCA1-deficient metaplastic breast cancer. Proc. Natl. Acad. Sci. *112*, 8409–8414.

Henry-Mowatt, J., Jackson, D., Masson, J.-Y., Johnson, P.A., Clements, P.M., Benson, F.E., Thompson, L.H., Takeda, S., West, S.C., and Caldecott, K.W. (2003). XRCC3 and Rad51 modulate replication fork progression on damaged vertebrate chromosomes. Mol. Cell *11*, 1109–1117.

Heyer, W.-D., Ehmsen, K.T., and Liu, J. (2010). Regulation of Homologous Recombination in Eukaryotes. Annu. Rev. Genet. *44*, 113–139.

Higgs, M.R., Reynolds, J.J., Winczura, A., Blackford, A.N., Borel, V., Miller, E.S., Zlatanou, A., Nieminuszczy, J., Ryan, E.L., Davies, N.J., et al. (2015). BOD1L Is Required to Suppress Deleterious Resection of Stressed Replication Forks. Mol. Cell *59*, 462–477.

Hinz, J.M., Tebbs, R.S., Wilson, P.F., Nham, P.B., Salazar, E.P., Nagasawa, H., Urbin, S.S., Bedford, J.S., and Thompson, L.H. (2006). Repression of mutagenesis by Rad51D-mediated homologous recombination. Nucleic Acids Res. *34*, 1358–1368.

Hoege, C., Pfander, B., Moldovan, G.-L., Pyrowolakis, G., and Jentsch, S. (2002). RAD6-dependent DNA repair is linked to modification of PCNA by ubiquitin and SUMO. Nature *419*, 135–141.

Hottiger, M.O., Hassa, P.O., Lüscher, B., Schüler, H., and Koch-Nolte, F. (2010). Toward a unified nomenclature for mammalian ADP-ribosyltransferases. Trends Biochem. Sci. *35*, 208–219.

Hu, Y., Raynard, S., Sehorn, M.G., Lu, X., Bussen, W., Zheng, L., Stark, J.M., Barnes, E.L., Chi, P., Janscak, P., et al. (2007). RECQL5/Recql5 helicase regulates homologous recombination and suppresses tumor formation via disruption of Rad51 presynaptic filaments. Genes Dev. *21*, 3073–3084.

Hu, Y., Petit, S.A., Ficarro, S.B., Toomire, K.J., Xie, A., Lim, E., Cao, S.A., Park, E., Eck, M.J., Scully, R., et al. (2014). PARP1-driven poly-ADP-ribosylation regulates BRCA1 function in homologous recombination-mediated DNA repair. Cancer Discov. *4*, 1430–1447.

Huang, F., Mazina, O.M., Zentner, I.J., Cocklin, S., and Mazin, A. V. (2012). Inhibition of Homologous Recombination in Human Cells by Targeting RAD51 Recombinase. J. Med. Chem. *55*, 3011–3020.

Ikejima, M., Noguchi, S., Yamashita, R., Ogura, T., Sugimura, T., Gill, D.M., and Miwa, M. (1990). The zinc fingers of human poly(ADP-ribose) polymerase are differentially required for the recognition of DNA breaks and nicks and the consequent enzyme activation. Other structures recognize intact DNA. J. Biol. Chem. *265*, 21907–21913.

Ip, S.C.Y., Rass, U., Blanco, M.G., Flynn, H.R., Skehel, J.M., and West, S.C. (2008). Identification of Holliday junction resolvases from humans and yeast. Nature *456*, 357–361.

Jackson, S.P. (2002). Sensing and repairing DNA double-strand breaks. Carcinogenesis *23*, 687–696.

Jackson, S.P., and Bartek, J. (2009). The DNA-damage response in human biology and disease. Nature *461*, 1071–1078.

Jankevicius, G., Hassler, M., Golia, B., Rybin, V., Zacharias, M., Timinszky, G., and Ladurner, A.G. (2013). A family of macrodomain proteins reverses cellular mono-ADP-ribosylation. Nat. Struct. Mol. Biol. *20*, 508–514.

Jankevicius, G., Ariza, A., Ahel, M., and Ahel, I. (2016). The Toxin-Antitoxin System DarTG Catalyzes Reversible ADP-Ribosylation of DNA. Mol. Cell *64*, 1109–1116.

Jasin, M., and Rothstein, R. (2013). Repair of Strand Breaks by Homologous Recombination. Cold Spring Harb. Perspect. Biol. *5*, a012740–a012740.

Jaspers, J.E., Kersbergen, A., Boon, U., Sol, W., van Deemter, L., Zander, S.A., Drost, R., Wientjens, E., Ji, J., Aly, A., et al. (2013). Loss of 53BP1 Causes PARP Inhibitor Resistance in *Brca1* -Mutated Mouse Mammary Tumors. Cancer Discov. *3*, 68–81.

Jensen, R.B., Carreira, A., and Kowalczykowski, S.C. (2010). Purified human BRCA2 stimulates RAD51-mediated recombination. Nature *467*, 678–683.

Ji, Y., and Tulin, A. V (2009). Poly(ADP-ribosyl)ation of heterogeneous nuclear ribonucleoproteins modulates splicing. Nucleic Acids Res. *37*, 3501–3513.

Johansson, M. (1999). A human poly(ADP-ribose) polymerase gene family (ADPRTL): cDNA cloning of two novel poly(ADP-ribose) polymerase homologues. Genomics *57*, 442–445.

Joshi, P.M., Sutor, S.L., Huntoon, C.J., and Karnitz, L.M. (2014). Ovarian Cancer-associated Mutations Disable Catalytic Activity of CDK12, a Kinase That Promotes Homologous Recombination Repair and Resistance to Cisplatin and Poly(ADP-ribose) Polymerase Inhibitors. Doi.org 9247–9253.

Jwa, M., and Chang, P. (2012). PARP16 is a tail-anchored endoplasmic reticulum protein required for the PERK- and IRE1α-mediated unfolded protein response. Nat. Cell Biol. *14*, 1223–1230.

Karimi-Busheri, F., Rasouli-Nia, A., Allalunis-Turner, J., and Weinfeld, M. (2007). Human Polynucleotide Kinase Participates in Repair of DNA Double-Strand Breaks by Nonhomologous End Joining but not Homologous Recombination. Cancer Res. *67*, 6619–6625.

Kaufman, B., Shapira-Frommer, R., Schmutzler, R.K., Audeh, M.W., Friedlander, M., Balmaña, J., Mitchell, G., Fried, G., Stemmer, S.M., Hubert, A., et al. (2015). Olaparib monotherapy in patients with advanced cancer and a germline BRCA1/2 mutation. J. Clin. Oncol. *33*, 244–250.

Kent, T., Chandramouly, G., McDevitt, S.M., Ozdemir, A.Y., and Pomerantz, R.T. (2015). Mechanism of microhomology-mediated end-joining promoted by human DNA polymerase θ. Nat. Struct. Mol. Biol. *22*, 230–237.

Kickhoefer, V.A., Siva, A.C., Kedersha, N.L., Inman, E.M., Ruland, C., Streuli, M., and Rome, L.H. (1999). The 193-kD vault protein, VPARP, is a novel poly(ADP-ribose) polymerase. J. Cell Biol. *146*, 917–928.

Kile, A.C., Chavez, D.A., Bacal, J., Eldirany, S., Korzhnev, D.M., Bezsonova, I., Eichman, B.F., and Cimprich, K.A. (2015). HLTF's Ancient HIRAN Domain Binds 3′ DNA Ends to Drive Replication Fork Reversal. Mol. Cell *58*, 1090–1100.

Kim, K., Biade, S., and Matsumoto, Y. (1998). Involvement of flap endonuclease 1 in base excision DNA repair. J. Biol. Chem. *273*, 8842–8848.

Kleine, H., Poreba, E., Lesniewicz, K., Hassa, P.O., Hottiger, M.O., Litchfield, D.W., Shilton, B.H., and Lüscher, B. (2008). Substrate-assisted catalysis by PARP10 limits its activity to mono-ADP-ribosylation. Mol. Cell *32*, 57–69.

Klungland, A., and Lindahl, T. (1997). Second pathway for completion of human DNA base excision-repair: reconstitution with purified proteins and requirement for DNase IV (FEN1). EMBO J. *16*, 3341–3348.

Koboldt, D.C., Fulton, R.S., McLellan, M.D., Schmidt, H., Kalicki-Veizer, J., McMichael, J.F., Fulton, L.L., Dooling, D.J., Ding, L., Mardis, E.R., et al. (2012). Comprehensive molecular portraits of human breast tumours. Nature *490*, 61–70.

Koh, D.W., Lawler, A.M., Poitras, M.F., Sasaki, M., Wattler, S., Nehls, M.C., Stoger, T., Poirier, G.G., Dawson, V.L., and Dawson, T.M. (2004). Failure to degrade poly(ADP-ribose) causes increased sensitivity to cytotoxicity and early embryonic lethality. Proc. Natl. Acad. Sci. *101*, 17699–17704.

Kolinjivadi, A.M., Sannino, V., de Antoni, A., Técher, H., Baldi, G., and Costanzo, V. (2017). Moonlighting at replication forks - a new life for homologous recombination proteins BRCA1, BRCA2 and RAD51. FEBS Lett. *591*, 1083–1100.

Kote-Jarai, Z., Leongamornlert, D., Saunders, E., Tymrakiewicz, M., Castro, E., Mahmud, N., Guy, M., Edwards, S., O'Brien, L., Sawyer, E., et al. (2011). BRCA2 is a moderate penetrance gene contributing to young-onset prostate cancer: implications for genetic testing in prostate cancer patients. Br. J. Cancer *105*, 1230–1234.

Kotova, E., Jarnik, M., and Tulin, A. V (2009). Poly (ADP-ribose) polymerase 1 is required for protein localization to Cajal body. PLoS Genet. *5*, e1000387.

Kowalczykowski, S.C. (2015). An Overview of the Molecular Mechanisms of Recombinational DNA Repair. Cold Spring Harb. Perspect. Biol. *7*, a016410.

Kozlov, S. V, Graham, M.E., Peng, C., Chen, P., Robinson, P.J., and Lavin, M.F. (2006). Involvement of novel autophosphorylation sites in ATM activation. EMBO J. *25*, 3504–3514.

Krogh, B.O., and Symington, L.S. (2004). Recombination proteins in yeast. Annu. Rev. Genet. *38*, 233–271.

Kumagai, A., Lee, J., Yoo, H.Y., and Dunphy, W.G. (2006). TopBP1 activates the ATR-ATRIP

complex. Cell *124*, 943–955.

Kumari, S.R., Mendoza-Alvarez, H., and Alvarez-Gonzalez, R. (1998). Functional interactions of p53 with poly(ADP-ribose) polymerase (PARP) during apoptosis following DNA damage: covalent poly(ADP-ribosyl)ation of p53 by exogenous PARP and noncovalent binding of p53 to the M(r) 85,000 proteolytic fragment. Cancer Res. *58*, 5075–5078.

Kutuzov, M.M., Khodyreva, S.N., Amé, J.-C., Ilina, E.S., Sukhanova, M. V., Schreiber, V., and Lavrik, O.I. (2013a). Interaction of PARP-2 with DNA structures mimicking DNA repair intermediates and consequences on activity of base excision repair proteins. Biochimie *95*, 1208–1215.

Kutuzov, M.M., Khodyreva, S.N., Amé, J.-C., Ilina, E.S., Sukhanova, M. V., Schreiber, V., and Lavrik, O.I. (2013b). Interaction of PARP-2 with DNA structures mimicking DNA repair intermediates and consequences on activity of base excision repair proteins. Biochimie *95*, 1208–1215.

Kwiatkowski, D.J., Zhang, H., Bandura, J.L., Heiberger, K.M., Glogauer, M., el-Hashemite, N., and Onda, H. (2002). A mouse model of TSC1 reveals sex-dependent lethality from liver hemangiomas, and up-regulation of p70S6 kinase activity in Tsc1 null cells. Hum. Mol. Genet. *11*, 525–534.

Langelier, M.-F., Planck, J.L., Roy, S., and Pascal, J.M. (2012). Structural basis for DNA damage-dependent poly(ADP-ribosyl)ation by human PARP-1. Science *336*, 728–732.

Langelier, M.-F., Riccio, A.A., and Pascal, J.M. (2014). PARP-2 and PARP-3 are selectively activated by 5′ phosphorylated DNA breaks through an allosteric regulatory mechanism shared with PARP-1. Nucleic Acids Res. *42*, 7762–7775.

Ledermann, J., Harter, P., Gourley, C., Friedlander, M., Vergote, I., Rustin, G., Scott, C.L., Meier, W., Shapira-Frommer, R., Safra, T., et al. (2014). Olaparib maintenance therapy in patients with platinum-sensitive relapsed serous ovarian cancer: a preplanned retrospective analysis of outcomes by BRCA status in a randomised phase 2 trial. Lancet Oncol. *15*, 852–861.

Leongamornlert, D., Mahmud, N., Tymrakiewicz, M., Saunders, E., Dadaev, T., Castro, E., Goh, C., Govindasami, K., Guy, M., O'Brien, L., et al. (2012). Germline BRCA1 mutations increase prostate cancer risk. Br. J. Cancer *106*, 1697–1701.

Levin, D.S., Mckenna, A.E., Motycka, T.A., Matsumoto, Y., and Tomkinson, A.E. (2000). Interaction between PCNA and DNA ligase I is critical for joining of Okazaki fragments and long-patch base-excision repair Results and discussion. Curr. Biol. *10*, 919–922.

Li, M., and Yu, X. (2013). Function of BRCA1 in the DNA damage response is mediated by ADP-ribosylation. Cancer Cell *23*, 693–704.

Liaw, H., Lee, D., and Myung, K. (2011). DNA-PK-dependent RPA2 hyperphosphorylation facilitates DNA repair and suppresses sister chromatid exchange. PLoS One *6*, e21424.

Lindgren, A.E.G., Karlberg, T., Ekblad, T., Spjut, S., Thorsell, A.-G., Andersson, C.D., Nhan, T.T., Hellsten, V., Weigelt, J., Linusson, A., et al. (2013a). Chemical Probes to Study ADP-Ribosylation: Synthesis and Biochemical Evaluation of Inhibitors of the Human ADP-Ribosyltransferase ARTD3/PARP3. J. Med. Chem. *56*, 9556–9568.

Lindgren, A.E.G., Karlberg, T., Thorsell, A.-G., Hesse, M., Spjut, S., Ekblad, T., Andersson, C.D., Pinto, A.F., Weigelt, J., Hottiger, M.O., et al. (2013b). PARP Inhibitor with Selectivity Toward ADP-Ribosyltransferase ARTD3/PARP3. ACS Chem. Biol. *8*, 1698–1703.

Liu, T., and Huang, J. (2016). DNA End Resection: Facts and Mechanisms. Genomics. Proteomics Bioinformatics *14*, 126–130.

Liu, Q., Guntuku, S., Cui, X.S., Matsuoka, S., Cortez, D., Tamai, K., Luo, G., Carattini-Rivera,

S., DeMayo, F., Bradley, A., et al. (2000). Chk1 is an essential kinase that is regulated by Atr and required for the G(2)/M DNA damage checkpoint. Genes Dev. *14*, 1448–1459.

Liu, X., Han, E.K., Anderson, M., Shi, Y., Semizarov, D., Wang, G., Mcgonigal, T., Roberts, L., Lasko, L., Palma, J., et al. (2009). Acquired Resistance to Combination Treatment with Temozolomide and ABT-888 Is Mediated by Both Base Excision Repair and Homologous Recombination DNA Repair Pathways. Mol Cancer Res *7*, 1686–1692.

Lok, B.H., Carley, A.C., Tchang, B., and Powell, S.N. (2013). RAD52 inactivation is synthetically lethal with deficiencies in BRCA1 and PALB2 in addition to BRCA2 through RAD51-mediated homologous recombination. Oncogene *32*, 3552–3558.

Lord, C.J., and Ashworth, A. (2016). BRCAness revisited. Nat. Rev. Cancer *16*, 110–120.

Lou, Z., Minter-Dykhouse, K., Franco, S., Gostissa, M., Rivera, M.A., Celeste, A., Manis, J.P., van Deursen, J., Nussenzweig, A., Paull, T.T., et al. (2006). MDC1 maintains genomic stability by participating in the amplification of ATM-dependent DNA damage signals. Mol. Cell *21*, 187–200.

Lucas, A.L., Shakya, R., Lipsyc, M.D., Mitchel, E.B., Kumar, S., Hwang, C., Deng, L., Devoe, C., Chabot, J.A., Szabolcs, M., et al. (2013). High prevalence of BRCA1 and BRCA2 germline mutations with loss of heterozygosity in a series of resected pancreatic adenocarcinoma and other neoplastic lesions. Clin. Cancer Res. *19*, 3396–3403.

Luijsterburg, M.S., de Krijger, I., Wiegant, W.W., Shah, R.G., Smeenk, G., de Groot, A.J.L., Pines, A., Vertegaal, A.C.O., Jacobs, J.J.L., Shah, G.M., et al. (2016). PARP1 Links CHD2-Mediated Chromatin Expansion and H3.3 Deposition to DNA Repair by Non-homologous End-Joining. Mol. Cell *61*, 547–562.

Lukas, C., Melander, F., Stucki, M., Falck, J., Bekker-Jensen, S., Goldberg, M., Lerenthal, Y., Jackson, S.P., Bartek, J., and Lukas, J. (2004). Mdc1 couples DNA double-strand break recognition by Nbs1 with its H2AX-dependent chromatin retention. EMBO J. *23*, 2674–2683.

Lundin, C., North, M., Erixon, K., Walters, K., Jenssen, D., Goldman, A.S.H., and Helleday, T. (2005). Methyl methanesulfonate (MMS) produces heat-labile DNA damage but no detectable in vivo DNA double-strand breaks. Nucleic Acids Res. *33*, 3799–3811.

Ma, Q., Baldwin, K.T., Renzelli, A.J., McDaniel, A., and Dong, L. (2001). TCDD-Inducible Poly(ADP-ribose) Polymerase: A Novel Response to 2,3,7,8-Tetrachlorodibenzo-p-dioxin. Biochem. Biophys. Res. Commun. *289*, 499–506.

Ma, W., Halweg, C.J., Menendez, D., and Resnick, M.A. (2012). Differential effects of poly(ADP-ribose) polymerase inhibition on DNA break repair in human cells are revealed with Epstein-Barr virus. Proc. Natl. Acad. Sci. U. S. A. *109*, 6590–6595.

Ma, Y., Lu, H., Tippin, B., Goodman, M.F., Shimazaki, N., Koiwai, O., Hsieh, C.-L., Schwarz, K., and Lieber, M.R. (2004). A Biochemically Defined System for Mammalian Nonhomologous DNA End Joining. Mol. Cell *16*, 701–713.

Machwe, A., Xiao, L., Groden, J., and Orren, D.K. (2006). The Werner and Bloom Syndrome Proteins Catalyze Regression of a Model Replication Fork †. Biochemistry *45*, 13939–13946.

MacPherson, L., Tamblyn, L., Rajendra, S., Bralha, F., McPherson, J.P., and Matthews, J. (2013). 2,3,7,8-Tetrachlorodibenzo-p-dioxin poly(ADP-ribose) polymerase (TiPARP, ARTD14) is a mono-ADP-ribosyltransferase and repressor of aryl hydrocarbon receptor transactivation. Nucleic Acids Res. *41*, 1604–1621.

Mahajan, K.N., Nick McElhinny, S.A., Mitchell, B.S., and Ramsden, D.A. (2002). Association of DNA polymerase mu (pol mu) with Ku and ligase IV: role for pol mu in end-joining double-strand break repair. Mol. Cell. Biol. *22*, 5194–5202.

Makharashvili, N., Tubbs, A.T., Yang, S.-H., Wang, H., Barton, O., Zhou, Y., Deshpande, R.A.,

Lee, J.-H., Lobrich, M., Sleckman, B.P., et al. (2014). Catalytic and Noncatalytic Roles of the CtIP Endonuclease in Double-Strand Break End Resection. Mol. Cell *54*, 1022–1033.

Malkova, A., and Ira, G. (2013). Break-induced replication: functions and molecular mechanism. Curr. Opin. Genet. Dev. *23*, 271–279.

Malone, K.E., Daling, J.R., Neal, C., Suter, N.M., O'Brien, C., Cushing-Haugen, K., Jonasdottir, T.J., Thompson, J.D., and Ostrander, E.A. (2000). Frequency of BRCA1/BRCA2 mutations in a population-based sample of young breast carcinoma cases. Cancer *88*, 1393–1402.

Marenstein, D.R., Wilson III, D.M., and Teebor, G.W. (2004). Human AP endonuclease (APE1) demonstrates endonucleolytic activity against AP sites in single-stranded DNA. DNA Repair (Amst). *3*, 527–533.

Marks, J.L., Golas, B., Kirchoff, T., Miller, V.A., Riely, G.J., Offit, K., and Pao, W. (2008). EGFR mutant lung adenocarcinomas in patients with germline BRCA mutations. J. Thorac. Oncol. *3*, 805.

Marsischky, G.T., Wilson, B.A., and Collier, R.J. (1995). Role of glutamic acid 988 of human poly-ADP-ribose polymerase in polymer formation. Evidence for active site similarities to the ADP-ribosylating toxins. J. Biol. Chem. *270*, 3247–3254.

Masson, M., Niedergang, C., Schreiber, V., Muller, S., Menissier-de Murcia, J., and de Murcia, G. (1998). XRCC1 is specifically associated with poly(ADP-ribose) polymerase and negatively regulates its activity following DNA damage. Mol. Cell. Biol. *18*, 3563–3571.

Masutani, M., Nozaki, T., Nakamoto, K., Nakagama, H., Suzuki, H., Kusuoka, O., Tsutsumi, M., and Sugimura, T. (2000a). The response of Parp knockout mice against DNA damaging agents. Mutat. Res. *462*, 159–166.

Masutani, M., Nozaki, T., Nakamoto, K., Nakagama, H., Suzuki, H., Kusuoka, O., Tsutsumi, M., and Sugimura, T. (2000b). The response of Parp knockout mice against DNA damaging agents. Mutat. Res. *462*, 159–166.

Mateo, J., Carreira, S., Sandhu, S., Miranda, S., Mossop, H., Perez-Lopez, R., Nava Rodrigues, D., Robinson, D., Omlin, A., Tunariu, N., et al. (2015). DNA-Repair Defects and Olaparib in Metastatic Prostate Cancer. N. Engl. J. Med. *373*, 1697–1708.

Matsumoto, Y., and Kim, K. (1995). Excision of deoxyribose phosphate residues by DNA polymerase beta during DNA repair. Science *269*, 699–702.

Matsuoka, S., Ballif, B.A., Smogorzewska, A., McDonald, E.R., Hurov, K.E., Luo, J., Bakalarski, C.E., Zhao, Z., Solimini, N., Lerenthal, Y., et al. (2007). ATM and ATR substrate analysis reveals extensive protein networks responsive to DNA damage. Science *316*, 1160–1166.

McAlpine, J.N., Porter, H., Köbel, M., Nelson, B.H., Prentice, L.M., Kalloger, S.E., Senz, J., Milne, K., Ding, J., Shah, S.P., et al. (2012). BRCA1 and BRCA2 mutations correlate with TP53 abnormalities and presence of immune cell infiltrates in ovarian high-grade serous carcinoma. Mod. Pathol. *25*, 740–750.

McCabe, N., Turner, N.C., Lord, C.J., Kluzek, K., Bialkowska, A., Swift, S., Giavara, S., O'Connor, M.J., Tutt, A.N., Zdzienicka, M.Z., et al. (2006). Deficiency in the repair of DNA damage by homologous recombination and sensitivity to poly(ADP-ribose) polymerase inhibition. Cancer Res. *66*, 8109–8115.

Meek, K., Douglas, P., Cui, X., Ding, Q., and Lees-Miller, S.P. (2007). trans Autophosphorylation at DNA-Dependent Protein Kinase's Two Major Autophosphorylation Site Clusters Facilitates End Processing but Not End Joining. Mol. Cell. Biol. *27*, 3881–3890.

Meira, L.B., Burgis, N.E., and Samson, L.D. (2005). Base excision repair. Adv. Exp. Med. Biol. *570*, 125–173.

Ménissier de Murcia, J., Ricoul, M., Tartier, L., Niedergang, C., Huber, A., Dantzer, F., Schreiber, V., Amé, J.-C., Dierich, A., LeMeur, M., et al. (2003a). Functional interaction between PARP-1 and PARP-2 in chromosome stability and embryonic development in mouse. EMBO J. *22*, 2255–2263.

Ménissier de Murcia, J., Ricoul, M., Tartier, L., Niedergang, C., Huber, A., Dantzer, F., Schreiber, V., Amé, J.-C., Dierich, A., LeMeur, M., et al. (2003b). Functional interaction between PARP-1 and PARP-2 in chromosome stability and embryonic development in mouse. EMBO J. *22*, 2255–2263.

Mo, W., Liu, Q., Lin, C.C.-J., Dai, H., Peng, Y., Liang, Y., Peng, G., Meric-Bernstam, F., Mills, G.B., Li, K., et al. (2016). mTOR Inhibitors Suppress Homologous Recombination Repair and Synergize with PARP Inhibitors via Regulating SUV39H1 in BRCA-Proficient Triple-Negative Breast Cancer. Clin. Cancer Res. *22*, 1699–1712.

Mol, C.D., Izumi, T., Mitra, S., and Tainer, J.A. (2000). DNA-bound structures and mutants reveal abasic DNA binding by APE1 DNA repair and coordination. Nature *403*, 451–456.

Moldovan, G.-L., Madhavan, M. V, Mirchandani, K.D., Mccaffrey, R.M., Vinciguerra, P., and D 'andrea, A.D. (2010). DNA Polymerase POLN Participates in Cross-Link Repair and Homologous Recombination. Mol. Cell. Biol. *30*, 1088–1096.

Moldovan, G.-L., Dejsuphong, D., Petalcorin, M.I.R., Hofmann, K., Takeda, S., Boulton, S.J., and D'Andrea, A.D. (2012). Inhibition of homologous recombination by the PCNA-interacting protein PARI. Mol. Cell *45*, 75–86.

Mortusewicz, O., Amé, J.-C., Schreiber, V., and Leonhardt, H. (2007). Feedback-regulated poly(ADP-ribosyl)ation by PARP-1 is required for rapid response to DNA damage in living cells. Nucleic Acids Res. *35*, 7665–7675.

Mueller-Dieckmann, C., Kernstock, S., Lisurek, M., von Kries, J.P., Haag, F., Weiss, M.S., and Koch-Nolte, F. (2006). The structure of human ADP-ribosylhydrolase 3 (ARH3) provides insights into the reversibility of protein ADP-ribosylation. Proc. Natl. Acad. Sci. U. S. A. *103*, 15026–15031.

Müller, S., Möller, P., Bick, M.J., Wurr, S., Becker, S., Günther, S., and Kümmerer, B.M. (2007). Inhibition of filovirus replication by the zinc finger antiviral protein. J. Virol. *81*, 2391–2400.

Muñoz, I.M., Hain, K., Déclais, A.-C., Gardiner, M., Toh, G.W., Sanchez-Pulido, L., Heuckmann, J.M., Toth, R., Macartney, T., Eppink, B., et al. (2009). Coordination of structure-specific nucleases by human SLX4/BTBD12 is required for DNA repair. Mol. Cell *35*, 116–127.

Murai, J., Huang, S.N., Das, B.B., Renaud, A., Zhang, Y., Doroshow, J.H., Ji, J., Takeda, S., and Pommier, Y. (2012). Trapping of PARP1 and PARP2 by Clinical PARP Inhibitors. Cancer Res. *72*, 5588–5599.

Murai, J., Huang, S.-Y.N., Renaud, A., Zhang, Y., Ji, J., Takeda, S., Morris, J., Teicher, B., Doroshow, J.H., and Pommier, Y. (2014). Stereospecific PARP Trapping by BMN 673 and Comparison with Olaparib and Rucaparib. Mol. Cancer Ther. *13*.

Nakano, T., Takahashi-Nakaguchi, A., Yamamoto, M., and Watanabe, M. (2014). Pierisins and CARP-1: ADP-Ribosylation of DNA by ARTCs in Butterflies and Shellfish. In Current Topics in Microbiology and Immunology, pp. 127–149.

Nicolae, C.M., Aho, E.R., Vlahos, A.H.S., Choe, K.N., De, S., Karras, G.I., and Moldovan, G.-L. (2014). The ADP-ribosyltransferase PARP10/ARTD10 Interacts with Proliferating Cell Nuclear Antigen (PCNA) and Is Required for DNA Damage Tolerance. J. Biol. Chem. *289*, 13627–13637.

Nicolae, C.M., Aho, E.R., Choe, K.N., Constantin, D., Hu, H.-J., Lee, D., Myung, K., and Moldovan, G.-L. (2015). A novel role for the mono-ADP-ribosyltransferase PARP14/ARTD8 in promoting homologous recombination and protecting against replication stress. Nucleic Acids

Res. *43*, 3143–3153.

Nikolova, T., Ensminger, M., Löbrich, M., and Kaina, B. (2010). Homologous recombination protects mammalian cells from replication-associated DNA double-strand breaks arising in response to methyl methanesulfonate. DNA Repair (Amst). *9*, 1050–1063.

Nimonkar, A. V., Ozsoy, A.Z., Genschel, J., Modrich, P., and Kowalczykowski, S.C. (2008). Human exonuclease 1 and BLM helicase interact to resect DNA and initiate DNA repair. Proc. Natl. Acad. Sci. *105*, 16906–16911.

Nimonkar, A. V., Genschel, J., Kinoshita, E., Polaczek, P., Campbell, J.L., Wyman, C., Modrich, P., and Kowalczykowski, S.C. (2011). BLM-DNA2-RPA-MRN and EXO1-BLM-RPA-MRN constitute two DNA end resection machineries for human DNA break repair. Genes Dev. *25*, 350–362.

Norquist, B., Wurz, K.A., Pennil, C.C., Garcia, R., Gross, J., Sakai, W., Karlan, B.Y., Taniguchi, T., and Swisher, E.M. (2011). Secondary somatic mutations restoring BRCA1/2 predict chemotherapy resistance in hereditary ovarian carcinomas. J. Clin. Oncol. *29*, 3008–3015.

O'Brien, P.J., and Ellenberger, T. (2004). Dissecting the broad substrate specificity of human 3-methyladenine-DNA glycosylase. J. Biol. Chem. *279*, 9750–9757.

Ochi, T., Blackford, A.N., Coates, J., Jhujh, S., Mehmood, S., Tamura, N., Travers, J., Wu, Q., Draviam, V.M., Robinson, C. V., et al. (2015). PAXX, a paralog of XRCC4 and XLF, interacts with Ku to promote DNA double-strand break repair. Science (80-.). *347*.

Ogino, H., Nozaki, T., Gunji, A., Maeda, M., Suzuki, H., Ohta, T., Murakami, Y., Nakagama, H., Sugimura, T., and Masutani, M. (2007). Loss of Parp-1 affects gene expression profile in a genome-wide manner in ES cells and liver cells. BMC Genomics *8*, 41.

Ohashi, E., Takeishi, Y., Ueda, S., and Tsurimoto, T. (2014). Interaction between Rad9–Hus1–Rad1 and TopBP1 activates ATR–ATRIP and promotes TopBP1 recruitment to sites of UV-damage. DNA Repair (Amst). *21*, 1–11.

Oka, S., Kato, J., and Moss, J. (2006). Identification and characterization of a mammalian 39-kDa poly(ADP-ribose) glycohydrolase. J. Biol. Chem. *281*, 705–713.

Oplustil O'Connor, L., Rulten, S.L., Cranston, A.N., Odedra, R., Brown, H., Jaspers, J.E., Jones, L., Knights, C., Evers, B., Ting, A., et al. (2016a). The PARP Inhibitor AZD2461 Provides Insights into the Role of PARP3 Inhibition for Both Synthetic Lethality and Tolerability with Chemotherapy in Preclinical Models. Cancer Res. *76*, 6084–6094.

Oplustil O'Connor, L., Rulten, S.L., Cranston, A.N., Odedra, R., Brown, H., Jaspers, J.E., Jones, L., Knights, C., Evers, B., Ting, A., et al. (2016b). The PARP Inhibitor AZD2461 Provides Insights into the Role of PARP3 Inhibition for Both Synthetic Lethality and Tolerability with Chemotherapy in Preclinical Models. Cancer Res. *76*, 6084–6094.

Otto, H., Reche, P.A., Bazan, F., Dittmar, K., Haag, F., and Koch-Nolte, F. (2005). In silico characterization of the family of PARP-like poly(ADP-ribosyl)transferases (pARTs). BMC Genomics *6*, 139.

Ouyang, K.J., Woo, L.L., and Ellis, N.A. (2008). Homologous recombination and maintenance of genome integrity: Cancer and aging through the prism of human RecQ helicases. Mech. Ageing Dev. *129*, 425–440.

Pal, T., Permuth-Wey, J., Betts, J.A., Krischer, J.P., Fiorica, J., Arango, H., LaPolla, J., Hoffman, M., Martino, M.A., Wakeley, K., et al. (2005). *BRCA1* and *BRCA2* mutations account for a large proportion of ovarian carcinoma cases. Cancer *104*, 2807–2816.

Di Paola, S., Micaroni, M., Di Tullio, G., Buccione, R., and Di Girolamo, M. (2012). PARP16/ARTD15 is a novel endoplasmic-reticulum-associated mono-ADP-ribosyltransferase that interacts with, and modifies karyopherin-ß1. PLoS One *7*, e37352.

Pascucci, B., Maga, G., Hübscher, U., Bjoras, M., Seeberg, E., Hickson, I.D., Villani, G., Giordano, C., Cellai, L., and Dogliotti, E. (2002). Reconstitution of the base excision repair pathway for 7,8-dihydro-8-oxoguanine with purified human proteins. Nucleic Acids Res. *30*, 2124–2130.

Patel, A.G., Sarkaria, J.N., and Kaufmann, S.H. (2011). Nonhomologous end joining drives poly(ADP-ribose) polymerase (PARP) inhibitor lethality in homologous recombination-deficient cells. Proc. Natl. Acad. Sci. U. S. A. *108*, 3406–3411.

Paull, T.T., and Gellert, M. (1999). Nbs1 potentiates ATP-driven DNA unwinding and endonuclease cleavage by the Mre11/Rad50 complex. Genes Dev. *13*, 1276–1288.

Paull, T.T., Rogakou, E.P., Yamazaki, V., Kirchgessner, C.U., Gellert, M., Bonner, W.M., and al., et (1998). A critical role for histone H2AX in recruitment of repair factors to nuclear foci after DNA damage. Curr. Biol. *10*, 886–895.

Petermann, E., Orta, M.L., Issaeva, N., Schultz, N., and Helleday, T. (2010). Hydroxyurea-Stalled Replication Forks Become Progressively Inactivated and Require Two Different RAD51-Mediated Pathways for Restart and Repair. Mol. Cell *37*, 492–502.

Peterson, F.C., Chen, D., Lytle, B.L., Rossi, M.N., Ahel, I., Denu, J.M., and Volkman, B.F. (2011). Orphan macrodomain protein (human C6orf130) is an O-acyl-ADP-ribose deacylase: solution structure and catalytic properties. J. Biol. Chem. *286*, 35955–35965.

Pogozelski, W.K., and Tullius, T.D. (1998). Oxidative Strand Scission of Nucleic Acids: Routes Initiated by Hydrogen Abstraction from the Sugar Moiety. Chem. Rev. *98*, 1089–1108.

Poirier, G.G., de Murcia, G., Jongstra-Bilen, J., Niedergang, C., and Mandel, P. (1982). Poly(ADP-ribosyl)ation of polynucleosomes causes relaxation of chromatin structure. Proc. Natl. Acad. Sci. U. S. A. *79*, 3423–3427.

Polato, F., Callen, E., Wong, N., Faryabi, R., Bunting, S., Chen, H.-T., Kozak, M., Kruhlak, M.J., Reczek, C.R., Lee, W.-H., et al. (2014). CtIP-mediated resection is essential for viability and can operate independently of BRCA1. J. Exp. Med. *211*, 1027–1036.

Postow, L., Ghenoiu, C., Woo, E.M., Krutchinsky, A.N., Chait, B.T., and Funabiki, H. (2008). Ku80 removal from DNA through double strand break–induced ubiquitylation. J. Cell Biol. *182*, 467–479.

Povirk, L.F., Zhou, T., Zhou, R., Cowan, M.J., and Yannone, S.M. (2006). Processing of 3'-Phosphoglycolate-terminated DNA Double Strand Breaks by Artemis Nuclease. J. Biol. Chem. *282*, 3547–3558.

Prakash, S., Johnson, R.E., and Prakash, L. (2005). Eukaryotic translesion synthesis DNA polymerases: specificity of structure and function. Annu. Rev. Biochem. *74*, 317–353.

Prasad, R., Beard, W.A., and Wilson, S.H. (1994). Studies of gapped DNA substrate binding by mammalian DNA polymerase beta. Dependence on 5'-phosphate group. J. Biol. Chem. *269*, 18096–18101.

Radicella, J.P., Dherin, C., Desmaze, C., Fox, M.S., and Boiteux, S. (1997). Cloning and characterization of hOGG1, a human homolog of the OGG1 gene of *Saccharomyces cerevisiae*. Proc. Natl. Acad. Sci. U. S. A. *94*, 8010–8015.

Ralf, C., Hickson, I.D., and Wu, L. (2006). The Bloom's Syndrome Helicase Can Promote the Regression of a Model Replication Fork. J. Biol. Chem. *281*, 22839–22846.

Rass, E., Grabarz, A., Plo, I., Gautier, J., Bertrand, P., and Lopez, B.S. (2009). Role of Mre11 in chromosomal nonhomologous end joining in mammalian cells. Nat. Struct. Mol. Biol. *16*, 819–824.

Rass, U., Compton, S.A., Matos, J., Singleton, M.R., Ip, S.C.Y., Blanco, M.G., Griffith, J.D., and

West, S.C. (2010). Mechanism of Holliday junction resolution by the human GEN1 protein. Genes Dev. *24*, 1559–1569.

Ray Chaudhuri, A., Hashimoto, Y., Herrador, R., Neelsen, K.J., Fachinetti, D., Bermejo, R., Cocito, A., Costanzo, V., and Lopes, M. (2012). Topoisomerase I: poisoning results in PARP-mediated replication fork reversal. Nat. Publ. Gr. *19*.

Ray Chaudhuri, A., Ahuja, A.K., Herrador, R., and Lopes, M. (2015). Poly(ADP-ribosyl) glycohydrolase prevents the accumulation of unusual replication structures during unperturbed S phase. Mol. Cell. Biol. *35*, 856–865.

Reddy, G., Golub, E.I., and Radding, C.M. (1997). Human Rad52 protein promotes single-strand DNA annealing followed by branch migration. Mutat. Res. *377*, 53–59.

Reid, L.J., Shakya, R., Modi, A.P., Lokshin, M., Cheng, J.-T., Jasin, M., Baer, R., and Ludwig, T. (2008). E3 ligase activity of BRCA1 is not essential for mammalian cell viability or homology-directed repair of double-strand DNA breaks. Proc. Natl. Acad. Sci. *105*, 20876–20881.

Rijkers, T., Van Den Ouweland, J., Morolli, B., Rolink, A.G., Baarends, W.M., Van Sloun, P.P., Lohman, P.H., and Pastink, A. (1998). Targeted inactivation of mouse RAD52 reduces homologous recombination but not resistance to ionizing radiation. Mol. Cell. Biol. *18*, 6423–6429.

Rogakou, E.P., Boon, C., Redon, C., and Bonner, W.M. (1999). Megabase chromatin domains involved in DNA double-strand breaks in vivo. J. Cell Biol. *146*, 905–916.

Rolli, V., O'Farrell, M., Ménissier-de Murcia, J., and de Murcia, G. (1997). Random mutagenesis of the poly(ADP-ribose) polymerase catalytic domain reveals amino acids involved in polymer branching. Biochemistry *36*, 12147–12154.

Rosenthal, F., Feijs, K.L.H., Frugier, E., Bonalli, M., Forst, A.H., Imhof, R., Winkler, H.C., Fischer, D., Caflisch, A., Hassa, P.O., et al. (2013). Macrodomain-containing proteins are new mono-ADP-ribosylhydrolases. Nat. Struct. Mol. Biol. *20*, 502–507.

Ruf, A., Mennissier de Murcia, J., de Murcia, G., and Schulz, G.E. (1996). Structure of the catalytic fragment of poly(AD-ribose) polymerase from chicken. Proc. Natl. Acad. Sci. U. S. A. *93*, 7481–7485.

Rulten, S.L., Fisher, A.E.O., Robert, I., Zuma, M.C., Rouleau, M., Ju, L., Poirier, G., Reina-San-Martin, B., and Caldecott, K.W. (2011). PARP-3 and APLF function together to accelerate nonhomologous end-joining. Mol. Cell *41*, 33–45.

Ruscetti, T., Lehnert, B.E., Halbrook, J., Le Trong, H., Hoekstra, M.F., Chen, D.J., and Peterson, S.R. (1998). Stimulation of the DNA-dependent protein kinase by poly(ADP-ribose) polymerase. J. Biol. Chem. *273*, 14461–14467.

Sakai, W., Swisher, E.M., Karlan, B.Y., Agarwal, M.K., Higgins, J., Friedman, C., Villegas, E., Jacquemont, C., Farrugia, D.J., Couch, F.J., et al. (2008). Secondary mutations as a mechanism of cisplatin resistance in BRCA2-mutated cancers. Nature *451*, 1116–1120.

Sarbajna, S., Davies, D., and West, S.C. (2014). Roles of SLX1-SLX4, MUS81-EME1, and GEN1 in avoiding genome instability and mitotic catastrophe. Genes Dev. *28*, 1124–1136.

Sartori, A.A., Lukas, C., Coates, J., Mistrik, M., Fu, S., Bartek, J., Baer, R., Lukas, J., and Jackson, S.P. (2007). Human CtIP promotes DNA end resection. Nature *450*, 509–514.

Saxena, A., Wong, L.H., Kalitsis, P., Earle, E., Shaffer, L.G., and Choo, K.H.A. (2002). Poly(ADP-ribose) polymerase 2 localizes to mammalian active centromeres and interacts with PARP-1, Cenpa, Cenpb and Bub3, but not Cenpc. Hum. Mol. Genet. *11*, 2319–2329.

Schlacher, K., Christ, N., Siaud, N., Egashira, A., Wu, H., and Jasin, M. (2011). Double-Strand Break Repair-Independent Role for BRCA2 in Blocking Stalled Replication Fork Degradation by

MRE11. Cell *145*, 529–542.

Schreiber, V., Amé, J.-C., Dollé, P., Schultz, I., Rinaldi, B., Fraulob, V., Ménissier-de Murcia, J., and de Murcia, G. (2002). Poly(ADP-ribose) polymerase-2 (PARP-2) is required for efficient base excision DNA repair in association with PARP-1 and XRCC1. J. Biol. Chem. *277*, 23028–23036.

Sharifi, R., Morra, R., Appel, C.D., Tallis, M., Chioza, B., Jankevicius, G., Simpson, M.A., Matic, I., Ozkan, E., Golia, B., et al. (2013). Deficiency of terminal ADP-ribose protein glycohydrolase TARG1/C6orf130 in neurodegenerative disease. EMBO J. *32*, 1225–1237.

Sharpless, N.E., Ferguson, D.O., O'Hagan, R.C., Castrillon, D.H., Lee, C., Farazi, P.A., Alson, S., Fleming, J., Morton, C.C., Frank, K., et al. (2001). Impaired nonhomologous end-joining provokes soft tissue sarcomas harboring chromosomal translocations, amplifications, and deletions. Mol. Cell *8*, 1187–1196.

Shibata, A., Conrad, S., Birraux, J., Geuting, V., Barton, O., Ismail, A., Kakarougkas, A., Meek, K., Taucher-Scholz, G., Löbrich, M., et al. (2011). Factors determining DNA double-strand break repair pathway choice in G2 phase. EMBO J. *30*, 1079–1092.

Shibata, A., Moiani, D., Arvai, A.S., Perry, J., Harding, S.M., Genois, M.-M., Maity, R., van Rossum-Fikkert, S., Kertokalio, A., Romoli, F., et al. (2014). DNA double-strand break repair pathway choice is directed by distinct MRE11 nuclease activities. Mol. Cell *53*, 7–18.

Shieh, W.M., Amé, J.C., Wilson, M. V, Wang, Z.Q., Koh, D.W., Jacobson, M.K., and Jacobson, E.L. (1998). Poly(ADP-ribose) polymerase null mouse cells synthesize ADP-ribose polymers. J. Biol. Chem. *273*, 30069–30072.

De Siervi, A., De Luca, P., Byun, J.S., Di, L.J., Fufa, T., Haggerty, C.M., Vazquez, E., Moiola, C., Longo, D.L., and Gardner, K. (2010). Transcriptional Autoregulation by BRCA1. Cancer Res. *70*, 532–542.

Simandlova, J., Zagelbaum, J., Payne, M.J., Chu, W.K., Shevelev, I., Hanada, K., Chatterjee, S., Reid, D.A., Liu, Y., Janscak, P., et al. (2013). FBH1 Helicase Disrupts RAD51 Filaments *in Vitro* and Modulates Homologous Recombination in Mammalian Cells. J. Biol. Chem. *288*, 34168–34180.

Simbulan-Rosenthal, C.M., Ly, D.H., Rosenthal, D.S., Konopka, G., Luo, R., Wang, Z.Q., Schultz, P.G., and Smulson, M.E. (2000). Misregulation of gene expression in primary fibroblasts lacking poly(ADP-ribose) polymerase. Proc. Natl. Acad. Sci. U. S. A. *97*, 11274–11279.

Simsek, D., Furda, A., Gao, Y., Artus, J., Brunet, E., Hadjantonakis, A.-K., Van Houten, B., Shuman, S., McKinnon, P.J., and Jasin, M. (2011a). Crucial role for DNA ligase III in mitochondria but not in Xrcc1-dependent repair. Nature *471*, 245–248.

Simsek, D., Brunet, E., Wong, S.Y.-W., Katyal, S., Gao, Y., McKinnon, P.J., Lou, J., Zhang, L., Li, J., Rebar, E.J., et al. (2011b). DNA ligase III promotes alternative nonhomologous end-joining during chromosomal translocation formation. PLoS Genet. *7*, e1002080.

Skoog, L., and Nordenskjöld, B. (1971). Effects of hydroxyurea and 1-beta-D-arabinofuranosyl-cytosine on deoxyribonucleotide pools in mouse embryo cells. Eur. J. Biochem. *19*, 81–89.

Slade, D., Dunstan, M.S., Barkauskaite, E., Weston, R., Lafite, P., Dixon, N., Ahel, M., Leys, D., and Ahel, I. (2011). The structure and catalytic mechanism of a poly(ADP-ribose) glycohydrolase. Nature *477*, 616–620.

Sleeth, K.M., Robson, R.L., and Dianov, G.L. (2004). Exchangeability of Mammalian DNA Ligases between Base Excision Repair Pathways. Biochemistry *43*, 12924–12930.

van Slegtenhorst, M., de Hoogt, R., Hermans, C., Nellist, M., Janssen, B., Verhoef, S., Lindhout, D., van den Ouweland, A., Halley, D., Young, J., et al. (1997). Identification of the

tuberous sclerosis gene TSC1 on chromosome 9q34. Science *277*, 805–808.

Slupphaug, G., Eftedal, I., Kavli, B., Bharati, S., Helle, N.M., Haug, T., Levine, D.W., and Krokan, H.E. (1995). Properties of a recombinant human uracil-DNA glycosylase from the UNG gene and evidence that UNG encodes the major uracil-DNA glycosylase. Biochemistry *34*, 128–138.

Smeenk, G., Wiegant, W.W., Marteijn, J.A., Luijsterburg, M.S., Sroczynski, N., Costelloe, T., Romeijn, R.J., Pastink, A., Mailand, N., Vermeulen, W., et al. (2013). Poly(ADP-ribosyl)ation links the chromatin remodeler SMARCA5/SNF2H to RNF168-dependent DNA damage signaling. J. Cell Sci. *126*, 889–903.

Smith, S., Giriat, I., Schmitt, A., and de Lange, T. (1998). Tankyrase, a poly(ADP-ribose) polymerase at human telomeres. Science *282*, 1484–1487.

Sommers, J.A., Rawtani, N., Gupta, R., Bugreev, D. V, Mazin, A. V, Cantor, S.B., and Brosh, R.M. (2009). FANCJ uses its motor ATPase to destabilize protein-DNA complexes, unwind triplexes, and inhibit RAD51 strand exchange. J. Biol. Chem. *284*, 7505–7517.

Sotiriou, S.K., Kamileri, I., Lugli, N., Evangelou, K., Da-Ré, C., Huber, F., Padayachy, L., Tardy, S., Nicati, N.L., Barriot, S., et al. (2016). Mammalian RAD52 Functions in Break-Induced Replication Repair of Collapsed DNA Replication Forks. Mol. Cell *64*, 1127–1134.

Spagnolo, L., Barbeau, J., Curtin, N.J., Morris, E.P., and Pearl, L.H. (2012). Visualization of a DNA-PK/PARP1 complex. Nucleic Acids Res. *40*, 4168–4177.

Stark, J.M., Pierce, A.J., Oh, J., Pastink, A., and Jasin, M. (2004). Genetic steps of mammalian homologous repair with distinct mutagenic consequences. Mol. Cell. Biol. *24*, 9305–9316.

Steffen, J.D., Brody, J.R., Armen, R.S., and Pascal, J.M. (2013). Structural Implications for Selective Targeting of PARPs. Front. Oncol. *3*, 301.

Steffen, J.D., Tholey, R.M., Langelier, M.-F., Planck, J.L., Schiewer, M.J., Lal, S., Bildzukewicz, N.A., Yeo, C.J., Knudsen, K.E., Brody, J.R., et al. (2014). Targeting PARP-1 Allosteric Regulation Offers Therapeutic Potential against Cancer. Cancer Res. *74*.

Stelter, P., and Ulrich, H.D. (2003). Control of spontaneous and damage-induced mutagenesis by SUMO and ubiquitin conjugation. Nature *425*, 188–191.

Stiff, T., O'Driscoll, M., Rief, N., Iwabuchi, K., Löbrich, M., and Jeggo, P.A. (2004). ATM and DNA-PK function redundantly to phosphorylate H2AX after exposure to ionizing radiation. Cancer Res. *64*, 2390–2396.

Ström, C.E., Johansson, F., Uhlén, M., Szigyarto, C.A.-K., Erixon, K., and Helleday, T. (2011). Poly (ADP-ribose) polymerase (PARP) is not involved in base excision repair but PARP inhibition traps a single-strand intermediate. Nucleic Acids Res. *39*, 3166–3175.

Stucki, M., Clapperton, J.A., Mohammad, D., Yaffe, M.B., Smerdon, S.J., and Jackson, S.P. (2005). MDC1 directly binds phosphorylated histone H2AX to regulate cellular responses to DNA double-strand breaks. Cell *123*, 1213–1226.

Sugimura, K., Takebayashi, S.-I., Taguchi, H., Takeda, S., and Okumura, K. (2008). PARP-1 ensures regulation of replication fork progression by homologous recombination on damaged DNA. J. Cell Biol. *183*, 1203–1212.

Sukhanova, M. V., Abrakhi, S., Joshi, V., Pastre, D., Kutuzov, M.M., Anarbaev, R.O., Curmi, P.A., Hamon, L., and Lavrik, O.I. (2016). Single molecule detection of PARP1 and PARP2 interaction with DNA strand breaks and their poly(ADP-ribosyl)ation using high-resolution AFM imaging. Nucleic Acids Res. *44*, e60–e60.

Sung, J.-S., and Demple, B. (2006). Roles of base excision repair subpathways in correcting oxidized abasic sites in DNA. FEBS J. *273*, 1620–1629.

Suwaki, N., Klare, K., and Tarsounas, M. (2011). RAD51 paralogs: Roles in DNA damage signalling, recombinational repair and tumorigenesis. Semin. Cell Dev. Biol. *22*, 898–905.

Svendsen, J.M., Smogorzewska, A., Sowa, M.E., O'Connell, B.C., Gygi, S.P., Elledge, S.J., and Harper, J.W. (2009). Mammalian BTBD12/SLX4 assembles a Holliday junction resolvase and is required for DNA repair. Cell *138*, 63–77.

Swisher, E.M., Sakai, W., Karlan, B.Y., Wurz, K., Urban, N., and Taniguchi, T. (2008). Secondary BRCA1 mutations in BRCA1-mutated ovarian carcinomas with platinum resistance. Cancer Res. *68*, 2581–2586.

Sy, S.M.H., Huen, M.S.Y., and Chen, J. (2009). PALB2 is an integral component of the BRCA complex required for homologous recombination repair. Proc. Natl. Acad. Sci. *106*, 7155–7160.

Symington, L.S. (2002). Role of RAD52 epistasis group genes in homologous recombination and double-strand break repair. Microbiol. Mol. Biol. Rev. *66*, 630–70, table of contents.

Szántó, M., Brunyánszki, A., Márton, J., Vámosi, G., Nagy, L., Fodor, T., Kiss, B., Virág, L., Gergely, P., and Bai, P. (2014). Deletion of PARP-2 induces hepatic cholesterol accumulation and decrease in HDL levels. Biochim. Biophys. Acta *1842*, 594–602.

Takata, K., Shimizu, T., Iwai, S., and Wood, R.D. (2006). Human DNA Polymerase N (POLN) Is a Low Fidelity Enzyme Capable of Error-free Bypass of 5 *S* -Thymine Glycol. J. Biol. Chem. *281*, 23445–23455.

Thangavel, S., Berti, M., Levikova, M., Pinto, C., Gomathinayagam, S., Vujanovic, M., Zellweger, R., Moore, H., Lee, E.H., Hendrickson, E.A., et al. (2015). DNA2 drives processing and restart of reversed replication forks in human cells. J. Cell Biol. *208*, 545–562.

Thorsell, A.-G., Ekblad, T., Karlberg, T., Löw, M., Pinto, A.F., Trésaugues, L., Moche, M., Cohen, M.S., and Schüler, H. (2017). Structural Basis for Potency and Promiscuity in Poly(ADP-ribose) Polymerase (PARP) and Tankyrase Inhibitors. J. Med. Chem. *60*, 1262–1271.

Trucco, C., Oliver, F.J., de Murcia, G., and Ménissier-de Murcia, J. (1998). DNA repair defect in poly(ADP-ribose) polymerase-deficient cell lines. Nucleic Acids Res. *26*, 2644–2649.

Tucker, J.A., Bennett, N., Brassington, C., Durant, S.T., Hassall, G., Holdgate, G., McAlister, M., Nissink, J.W.M., Truman, C., and Watson, M. (2012). Structures of the human poly (ADP-ribose) glycohydrolase catalytic domain confirm catalytic mechanism and explain inhibition by ADP-HPD derivatives. PLoS One *7*, e50889.

Tulin, A., and Spradling, A. (2003). Chromatin loosening by poly(ADP)-ribose polymerase (PARP) at Drosophila puff loci. Science *299*, 560–562.

Tuncel, H., Tanaka, S., Oka, S., Nakai, S., Fukutomi, R., Okamoto, M., Ota, T., Kaneko, H., Tatsuka, M., and Shimamoto, F. (2012). PARP6, a mono(ADP-ribosyl) transferase and a negative regulator of cell proliferation, is involved in colorectal cancer development. Int. J. Oncol. *41*, 2079–2086.

Turner, N., Tutt, A., and Ashworth, A. (2004). Opinion: Hallmarks of "BRCAness" in sporadic cancers. Nat. Rev. Cancer *4*, 814–819.

Uematsu, N., Weterings, E., Yano, K., Morotomi-Yano, K., Jakob, B., Taucher-Scholz, G., Mari, P.-O., van Gent, D.C., Chen, B.P.C., and Chen, D.J. (2007). Autophosphorylation of DNA-PK $_{CS}$ regulates its dynamics at DNA double-strand breaks. J. Cell Biol. *177*, 219–229.

Uziel, T., Lerenthal, Y., Moyal, L., Andegeko, Y., Mittelman, L., and Shiloh, Y. (2003). Requirement of the MRN complex for ATM activation by DNA damage. EMBO J. *22*, 5612–5621.

Valenzuela, M.T., Guerrero, R., Núñez, M.I., Ruiz De Almodóvar, J.M., Sarker, M., de Murcia,

G., and Oliver, F.J. (2002). PARP-1 modifies the effectiveness of p53-mediated DNA damage response. Oncogene *21*, 1108–1116.

Vaziri, H., West, M.D., Allsopp, R.C., Davison, T.S., Wu, Y.-S., Arrowsmith, C.H., Poirier, G.G., and Benchimol, S. (1997). ATM-dependent telomere loss in aging human diploid fibroblasts and DNA damage lead to the post-translational activation of p53 protein involving poly(ADP-ribose) polymerase. EMBO J. *16*, 6018–6033.

Verkaik, N.S., Esveldt-van Lange, R.E.E., van Heemst, D., Brüggenwirth, H.T., Hoeijmakers, J.H.J., Zdzienicka, M.Z., and van Gent, D.C. (2002). Different types of V(D)J recombination and end-joining defects in DNA double-strand break repair mutant mammalian cells. Eur. J. Immunol. *32*, 701–709.

Vyas, S., Chesarone-Cataldo, M., Todorova, T., Huang, Y.-H., and Chang, P. (2013). A systematic analysis of the PARP protein family identifies new functions critical for cell physiology. Nat. Commun. *4*.

Vyas, S., Matic, I., Uchima, L., Rood, J., Zaja, R., Hay, R.T., Ahel, I., and Chang, P. (2014). ARTICLE Family-wide analysis of poly(ADP-ribose) polymerase activity. Nat. Commun. *5*.

Wahlberg, E., Karlberg, T., Kouznetsova, E., Markova, N., Macchiarulo, A., Thorsell, A.-G., Pol, E., Frostell, Å., Ekblad, T., Öncü, D., et al. (2012). Family-wide chemical profiling and structural analysis of PARP and tankyrase inhibitors. Nat. Biotechnol. *30*, 283–288.

Walker, J.R., Corpina, R.A., and Goldberg, J. (2001). Structure of the Ku heterodimer bound to DNA and its implications for double-strand break repair. Nature *412*, 607–614.

Wang, H., Perrault, A.R., Takeda, Y., Qin, W., Wang, H., and Iliakis, G. (2003). Biochemical evidence for Ku-independent backup pathways of NHEJ. Nucleic Acids Res. *31*, 5377–5388.

Wang, M., Wu, W., Wu, W., Rosidi, B., Zhang, L., Wang, H., and Iliakis, G. (2006). PARP-1 and Ku compete for repair of DNA double strand breaks by distinct NHEJ pathways. Nucleic Acids Res. *34*, 6170–6182.

Wang, Y.-G., Nnakwe, C., Lane, W.S., Modesti, M., and Frank, K.M. (2004). Phosphorylation and regulation of DNA ligase IV stability by DNA-dependent protein kinase. J. Biol. Chem. *279*, 37282–37290.

Ward, I.M., and Chen, J. (2001). Histone H2AX is phosphorylated in an ATR-dependent manner in response to replicational stress. J. Biol. Chem. *276*, 47759–47762.

Watanabe, K., Tateishi, S., Kawasuji, M., Tsurimoto, T., Inoue, H., and Yamaizumi, M. (2004). Rad18 guides polη to replication stalling sites through physical interaction and PCNA monoubiquitination. EMBO J. *23*, 3886–3896.

Whitehouse, C.J., Taylor, R.M., Thistlethwaite, A., Zhang, H., Karimi-Busheri, F., Lasko, D.D., Weinfeld, M., and Caldecott, K.W. (2001). XRCC1 stimulates human polynucleotide kinase activity at damaged DNA termini and accelerates DNA single-strand break repair. Cell *104*, 107–117.

Wilson, D.M., Takeshita, M., Grollman, A.P., and Demple, B. (1995). Incision activity of human apurinic endonuclease (Ape) at abasic site analogs in DNA. J. Biol. Chem. *270*, 16002–16007.

Wilson, T.E., Grawunder, U., and Lieber, M.R. (1997). Yeast DNA ligase IV mediates non-homologous DNA end joining. Nature *388*, 495–498.

Wong, A.K., Pero, R., Ormonde, P.A., Tavtigian, S. V, and Bartel, P.L. (1997). RAD51 interacts with the evolutionarily conserved BRC motifs in the human breast cancer susceptibility gene brca2. J. Biol. Chem. *272*, 31941–31944.

Wong, A.K., Ormonde, P.A., Pero, R., Chen, Y., Lian, L., Salada, G., Berry, S., Lawrence, Q., Dayananth, P., Ha, P., et al. (1998). Characterization of a carboxy-terminal BRCA1 interacting

protein. Oncogene *17*, 2279–2285.

Wright, R.H.G., Castellano, G., Bonet, J., Le Dily, F., Font-Mateu, J., Ballare, C., Nacht, A.S., Soronellas, D., Oliva, B., and Beato, M. (2012). CDK2-dependent activation of PARP-1 is required for hormonal gene regulation in breast cancer cells. Genes Dev. *26*, 1972–1983.

Wu, L., and Hickson, I.D. (2003). The Bloom's syndrome helicase suppresses crossing over during homologous recombination. Nature *426*, 870–874.

Wu, L.C., Wang, Z.W., Tsan, J.T., Spillman, M.A., Phung, A., Xu, X.L., Yang, M.-C.W., Hwang, L.-Y., Bowcock, A.M., and Baer, R. (1996). Identification of a RING protein that can interact in vivo with the BRCA1 gene product. Nat. Genet. *14*, 430–440.

Xia, B., Sheng, Q., Nakanishi, K., Ohashi, A., Wu, J., Christ, N., Liu, X., Jasin, M., Couch, F.J., and Livingston, D.M. (2006). Control of BRCA2 Cellular and Clinical Functions by a Nuclear Partner, PALB2. Mol. Cell *22*, 719–729.

Xie, A., Kwok, A., and Scully, R. (2009). Role of mammalian Mre11 in classical and alternative nonhomologous end joining. Nat. Struct. Mol. Biol. *16*, 814–818.

Xie, S., Mortusewicz, O., Ma, H.T., Herr, P., Poon, R.Y.C., Helleday, T., Qian, C., and Qian, C. (2015). Timeless Interacts with PARP-1 to Promote Homologous Recombination Repair. Mol. Cell *60*, 163–176.

Yan, Q., Xu, R., Zhu, L., Cheng, X., Wang, Z., Manis, J., and Shipp, M.A. (2013). BAL1 and its partner E3 ligase, BBAP, link Poly(ADP-ribose) activation, ubiquitylation, and double-strand DNA repair independent of ATM, MDC1, and RNF8. Mol. Cell. Biol. *33*, 845–857.

Yang, E., Tacchelly-Benites, O., Wang, Z., Randall, M.P., Tian, A., Benchabane, H., Freemantle, S., Pikielny, C., Tolwinski, N.S., Lee, E., et al. (2016). Wnt pathway activation by ADP-ribosylation. Nat. Commun. *7*, 11430.

Yang, Y.-G., Cortes, U., Patnaik, S., Jasin, M., and Wang, Z.-Q. (2004). Ablation of PARP-1 does not interfere with the repair of DNA double-strand breaks, but compromises the reactivation of stalled replication forks. Oncogene *23*, 3872–3882.

Yekezare, M., Gomez-Gonzalez, B., and Diffley, J.F.X. (2013). Controlling DNA replication origins in response to DNA damage - inhibit globally, activate locally. J. Cell Sci. *126*, 1297–1306.

Yeo, J.E., Lee, E.H., Hendrickson, E.A., and Sobeck, A. (2014). CtIP mediates replication fork recovery in a FANCD2-regulated manner. Hum. Mol. Genet. *23*, 3695–3705.

Ying, S., Hamdy, F.C., and Helleday, T. (2012). Mre11-dependent degradation of stalled DNA replication forks is prevented by BRCA2 and PARP1. Cancer Res. *72*, 2814–2821.

Yoo, S., and Dynan, W.S. (1999). Geometry of a complex formed by double strand break repair proteins at a single DNA end: recruitment of DNA-PKcs induces inward translocation of Ku protein. Nucleic Acids Res. *27*, 4679–4686.

Yu, X., Wu, L.C., Bowcock, A.M., Aronheim, A., and Baer, R. (1998). The C-terminal (BRCT) domains of BRCA1 interact in vivo with CtIP, a protein implicated in the CtBP pathway of transcriptional repression. J. Biol. Chem. *273*, 25388–25392.

Yu, X., Fu, S., Lai, M., Baer, R., and Chen, J. (2006). BRCA1 ubiquitinates its phosphorylation-dependent binding partner CtIP. Genes Dev. *20*, 1721–1726.

Yuan, S.S., Lee, S.Y., Chen, G., Song, M., Tomlinson, G.E., and Lee, E.Y. (1999). BRCA2 is required for ionizing radiation-induced assembly of Rad51 complex in vivo. Cancer Res. *59*, 3547–3551.

Zaika, A.I., Slade, N., Erster, S.H., Sansome, C., Joseph, T.W., Pearl, M., Chalas, E., and Moll,

U.M. (2002). DeltaNp73, a dominant-negative inhibitor of wild-type p53 and TAp73, is up-regulated in human tumors. J. Exp. Med. *196*, 765–780.

Zellweger, R., Dalcher, D., Mutreja, K., Berti, M., Schmid, J.A., Herrador, R., Vindigni, A., and Lopes, M. (2015). Rad51-mediated replication fork reversal is a global response to genotoxic treatments in human cells. J. Cell Biol. *208*, 563–579.

Zhang, Y., and Jasin, M. (2010). An essential role for CtIP in chromosomal translocation formation through an alternative end-joining pathway. Nat. Publ. Gr. *18*.

Zhang, F., Ma, J., Wu, J., Ye, L., Cai, H., Xia, B., and Yu, X. (2009). PALB2 Links BRCA1 and BRCA2 in the DNA-Damage Response. Curr. Biol. *19*, 524–529.

Zhang, F., Shi, J., Bian, C., and Yu, X. (2015). Poly(ADP-Ribose) Mediates the BRCA2-Dependent Early DNA Damage Response. Cell Rep. *13*, 678–689.

Zhang, Y., Wang, J., Ding, M., and Yu, Y. (2013). Site-specific characterization of the Asp- and Glu-ADP-ribosylated proteome. Nat. Methods *10*, 981–984.

Zhong, Q., Chen, C.F., Li, S., Chen, Y., Wang, C.C., Xiao, J., Chen, P.L., Sharp, Z.D., and Lee, W.H. (1999). Association of BRCA1 with the hRad50-hMre11-p95 complex and the DNA damage response. Science *285*, 747–750.

Zhou, Q., Ji, M., Zhou, J., Jin, J., Xue, N., Chen, J., Xu, B., and Chen, X. (2016). Poly (ADP-ribose) polymerases inhibitor, Zj6413, as a potential therapeutic agent against breast cancer. Biochem. Pharmacol. *107*, 29–40.

Zhou, Y., Feng, X., and Koh, D.W. (2010). Enhanced DNA accessibility and increased DNA damage induced by the absence of poly(ADP-ribose) hydrolysis. Biochemistry *49*, 7360–7366.

Zhu, Q., Pao, G.M., Huynh, A.M., Suh, H., Tonnu, N., Nederlof, P.M., Gage, F.H., and Verma, I.M. (2011a). BRCA1 tumour suppression occurs via heterochromatin-mediated silencing. Nature *477*, 179–184.

Zhu, Y., Chen, G., Lv, F., Wang, X., Ji, X., Xu, Y., Sun, J., Wu, L., Zheng, Y.-T., and Gao, G. (2011b). Zinc-finger antiviral protein inhibits HIV-1 infection by selectively targeting multiply spliced viral mRNAs for degradation. Proc. Natl. Acad. Sci. *108*, 15834–15839.

Zhu, Z., Jin, J., Xue, N., Song, X., and Chen, X. (2014). Development and validation of high-throughput screening assays for poly(ADP-ribose) polymerase-2 inhibitors. Anal. Biochem. *449*, 188–194.

Zou, L., and Elledge, S.J. (2003). Sensing DNA damage through ATRIP recognition of RPA-ssDNA complexes. Science *300*, 1542–1548.

9. Appendices

9.1 Oligonucleotide Sequences

9.1.1 gRNA sequences

CRISPR target	gRNA sequence
PARP1	TGGGTTCTCTGAGCTTCGGTGGG
PARP1	CCACCTCAACGTCAGGGTGCCGG
PARP2	CAAGGCCTTCACAGATTCTGAGG
PARP2	GTTAAAGGGCAAAGCTCCTGTGG
PARP3	GCCTCAGCGGTGGAGCGGAAGGG
PARP3	AGAGAAGCGCATAATCCGCGTGG

9.1.2 PCR primer sequences

Gene target	PCR Primer
PARP1 Forward	GCTTCCGCTGTCTTCTTGAC
PARP1 Reverse	TCGAGGTCAAGGTCAAGGTC
PARP2 Forward	GTTTTTGATTCCCATAAAGTAGTACC
PARP2 Reverse	CATGGACTGAAGATCGGTTCC
PARP3 Forward	AAGCCCTGGGTACAGACTGA
PARP3 Reverse	GCTCCAAAACCAGAACAGAGTCC

9.2 siRNA screen dataset

Gene	Z-score (U2OS)	Z-score (*parp1Δ)*	ΔZ (*parp1Δ)*	Z-score (*parp2Δ)*	ΔZ (*parp2Δ)*	Z-score (*parp1Δ parp2Δ)*	ΔZ (parp1Δ *parp2Δ)*
FLJ35220	-2.74	-2.86	-0.12	-3.17	-0.43	-3.63	-0.89
NEIL2	-2.57	-1.81	0.76	-2.40	0.17	-1.92	0.65
MYST1	-2.55	-1.72	0.83	-1.97	0.58	-1.83	0.72
COPB2	-2.43	-2.39	0.04	-2.22	0.21	-3.04	-0.61
HNRNPK	-2.42	-2.61	-0.19	-1.85	0.56	-2.11	0.30
KIF11	-2.40	-1.78	0.62	-2.07	0.33	-3.00	-0.61
SNRPE	-2.39	-1.98	0.40	-2.00	0.39	-2.52	-0.13
PSMC4	-2.39	-2.26	0.13	-1.84	0.54	-2.79	-0.40

GIYD2	-2.37	-2.35	0.03	-2.18	0.19	-1.64	0.74
SNRPF	-2.36	-1.97	0.38	-1.97	0.39	-2.45	-0.09
RPL27	-2.35	-1.86	0.49	-2.03	0.32	-2.60	-0.25
EIF4A3	-2.33	-2.26	0.08	-2.19	0.15	-2.95	-0.61
PSMA1	-2.32	-2.02	0.30	-1.88	0.45	-2.53	-0.20
PLK1	-2.32	-2.15	0.17	-1.96	0.36	-2.84	-0.53
RUVBL2	-2.32	-2.19	0.12	-1.94	0.38	-1.72	0.60
RPL35	-2.25	-2.29	-0.03	-2.18	0.07	-2.51	-0.25
CHAF1A	-2.18	-2.18	0.00	-1.98	0.21	-2.34	-0.15
CRIP2	-2.18	-0.96	1.22	-2.18	0.00	-1.60	0.58
XAB2	-2.16	-1.98	0.17	-2.05	0.10	-2.37	-0.21
RPS27A	-2.10	-1.71	0.39	-1.78	0.32	-2.21	-0.11
INCENP	-2.10	-2.04	0.06	-1.66	0.44	-2.54	-0.44
COL1A2	-2.07	-1.65	0.42	-2.12	-0.05	-1.63	0.44
HIST2H3C	-2.06	-1.05	1.01	0.07	2.13	0.23	2.29
APEX1	-2.05	-2.00	0.06	-0.87	1.18	-1.53	0.52
HIF1AN	-2.05	-1.86	0.19	-1.94	0.11	-2.36	-0.31
ERCC1	-2.04	-1.65	0.40	-2.16	-0.11	-2.61	-0.57
SETD8	-2.03	-2.00	0.03	-2.47	-0.45	-2.71	-0.69
NUP205	-2.01	-2.16	-0.15	-1.92	0.09	-2.28	-0.27
MCM8	-1.92	-0.34	1.58	-0.87	1.06	0.16	2.09
CCT5	-1.92	-1.66	0.26	-1.80	0.12	-1.69	0.24
CCRN4L	-1.90	-1.44	0.47	-1.71	0.19	-0.63	1.27
ERCC2	-1.84	-1.65	0.19	-1.50	0.33	-1.33	0.51
RAD9A	-1.84	-1.31	0.52	-1.62	0.21	-1.63	0.21
NUDT7	-1.84	-1.55	0.29	-1.92	-0.08	-1.37	0.47
UBA52	-1.83	-2.26	-0.43	-2.85	-1.02	-3.33	-1.50
ERCC6	-1.79	-1.33	0.46	-1.19	0.60	-0.19	1.61
PRMT1	-1.79	-1.83	-0.04	-1.25	0.54	-1.83	-0.05
LOC642846	-1.78	-1.36	0.43	-0.88	0.90	-1.99	-0.21
MCM3	-1.78	-1.23	0.55	-1.87	-0.09	-1.93	-0.15
CUL3	-1.73	-0.83	0.90	-0.50	1.23	0.07	1.80
PLOD3	-1.72	-1.76	-0.04	-1.81	-0.09	-2.06	-0.34
HDAC3	-1.69	-0.90	0.79	-0.61	1.08	0.48	2.17
NTHL1	-1.69	-1.22	0.47	-1.21	0.47	-0.22	1.47
PES1	-1.68	-1.24	0.45	-1.51	0.17	-0.67	1.02
GTF2H2	-1.68	-2.33	-0.65	-1.27	0.42	-1.25	0.43
CCT4	-1.64	-1.47	0.16	-1.03	0.61	-1.12	0.52
ARID1A	-1.63	-1.79	-0.16	-0.52	1.10	-0.13	1.50
SPO11	-1.60	-1.51	0.09	-1.70	-0.10	-1.11	0.49
PTTG1	-1.60	-1.43	0.17	-0.12	1.48	-0.67	0.93
TARS	-1.60	-1.03	0.57	-0.07	1.53	0.28	1.88
SMC6	-1.57	-0.79	0.78	-0.84	0.73	-0.93	0.64
NCBP2	-1.57	-0.95	0.61	-1.43	0.13	-0.94	0.62

XRCC5	-1.55	-1.62	-0.07	-1.05	0.50	-0.75	0.80
ASPHD2	-1.54	-1.53	0.01	-1.20	0.34	-2.12	-0.57
TUBB	-1.54	-0.34	1.20	-0.88	0.65	-2.14	-0.60
C19orf40	-1.52	-1.49	0.03	-1.03	0.49	-1.71	-0.18
NDC80	-1.52	-1.27	0.25	-1.29	0.23	-1.22	0.30
HSPE1	-1.51	-1.15	0.36	-1.02	0.49	-1.54	-0.02
LEPRE1	-1.51	-0.74	0.77	-1.32	0.19	0.19	1.70
P4HA2	-1.50	-0.77	0.73	0.37	1.87	0.80	2.30
PCNA	-1.50	-1.43	0.07	-1.17	0.33	-0.72	0.78
HIST2H2AA3	-1.50	-1.76	-0.26	-2.57	-1.07	-1.63	-0.13
MCM10	-1.47	-0.99	0.48	-1.15	0.32	-1.15	0.32
BTBD12	-1.45	-0.25	1.21	-0.94	0.51	-0.52	0.93
RPA2	-1.45	-1.30	0.14	-1.34	0.11	-0.70	0.75
LOC730323	-1.44	-1.52	-0.08	-2.66	-1.21	-2.62	-1.17
KDM2A	-1.44	-1.28	0.16	-1.10	0.34	-0.12	1.32
RAD21	-1.43	-1.37	0.06	-1.24	0.19	-1.06	0.37
MLH1	-1.42	-0.91	0.51	-1.38	0.04	-1.44	-0.02
EP400	-1.41	-1.23	0.18	-1.24	0.17	-1.51	-0.10
ERCC3	-1.41	-1.39	0.02	-1.04	0.37	-1.51	-0.10
TNKS2	-1.38	-1.18	0.20	-1.50	-0.11	-0.95	0.43
RFC1	-1.36	-1.16	0.20	-1.68	-0.32	0.16	1.52
DDB1	-1.36	-0.51	0.85	-1.55	-0.19	-1.50	-0.14
FANCM	-1.33	-1.58	-0.25	-1.28	0.05	-1.35	-0.02
TOP3A	-1.32	-0.12	1.21	0.46	1.79	1.75	3.07
EME2	-1.32	-0.31	1.02	-0.83	0.49	-1.59	-0.27
RPA1	-1.30	-1.12	0.18	-1.44	-0.14	-1.12	0.18
ORC1L	-1.29	-0.40	0.89	-1.30	-0.01	-0.64	0.65
CCNH	-1.28	-0.63	0.65	0.29	1.57	0.71	1.99
FANCG	-1.27	-1.67	-0.39	0.33	1.60	0.17	1.44
VHL	-1.26	-1.29	-0.03	-0.50	0.76	-0.05	1.21
PHB	-1.26	-0.91	0.35	-0.52	0.74	-0.49	0.77
ALKBH1	-1.16	-1.40	-0.24	-1.20	-0.04	-0.80	0.36
CDC2	-1.16	-0.35	0.81	-0.88	0.28	-1.53	-0.37
TIPIN	-1.14	-1.48	-0.34	-1.44	-0.30	-0.82	0.32
ATRIP	-1.13	-0.90	0.23	-0.81	0.33	-0.77	0.37
BUB3	-1.12	0.29	1.41	-0.30	0.82	1.40	2.51
CUL1	-1.11	-1.04	0.08	-0.94	0.18	-0.54	0.58
SMARCA1	-1.11	-1.05	0.06	-0.89	0.21	0.59	1.70
CHEK1	-1.09	-0.09	1.01	-1.86	-0.76	-2.31	-1.21
CHAF1B	-1.09	-1.44	-0.34	-1.81	-0.72	-1.48	-0.39
IGF1	-1.08	-0.71	0.37	-0.81	0.27	-0.06	1.01
GADD45A	-1.06	-1.06	0.00	-0.42	0.63	0.77	1.83
JMJD7-PLA2G4B	-1.04	-1.31	-0.27	-1.04	0.01	-1.51	-0.47
KDM4B	-1.04	-0.10	0.94	-0.83	0.21	-0.30	0.73

MUTYH	-1.03	0.13	1.16	-1.76	-0.73	-0.51	0.53
TPX2	-1.02	-1.47	-0.45	-1.35	-0.33	-0.43	0.59
MCM2	-1.02	-1.42	-0.40	-0.74	0.28	-0.23	0.79
NUDT19	-1.02	-1.51	-0.49	-1.65	-0.63	-1.68	-0.67
E2F5	-1.00	-1.22	-0.22	-0.76	0.23	1.20	2.20
UBE2A	-0.99	-0.26	0.73	-0.08	0.91	1.01	2.00
ORC3L	-0.98	-1.69	-0.71	-1.44	-0.46	-1.31	-0.33
CHD4	-0.98	-0.18	0.80	-0.94	0.04	0.43	1.41
HPRT1	-0.97	-1.31	-0.34	-0.60	0.37	-0.22	0.75
SMARCD2	-0.96	-1.69	-0.72	-1.55	-0.58	-0.27	0.69
RAD51	-0.95	-0.92	0.03	-0.49	0.47	-1.27	-0.32
CHTF18	-0.95	-0.46	0.49	-0.96	-0.01	-0.33	0.62
MMP9	-0.93	-0.13	0.80	-1.22	-0.29	-1.10	-0.16
MUC1	-0.92	-0.94	-0.02	-0.93	-0.01	0.58	1.50
ALKBH8	-0.91	-1.60	-0.69	-0.55	0.36	-0.98	-0.08
SHFM1	-0.91	0.34	1.25	-0.18	0.73	-1.57	-0.67
G3BP1	-0.91	-0.94	-0.04	-1.50	-0.59	-0.94	-0.03
PPP1R1B	-0.90	-1.83	-0.92	-1.50	-0.60	-1.85	-0.95
PRDX2	-0.90	-1.90	-1.01	-1.91	-1.01	-1.12	-0.22
MSH3	-0.88	0.22	1.10	-0.50	0.38	-0.34	0.55
MSH5	-0.88	-0.47	0.41	-0.71	0.17	-0.98	-0.10
ZSWIM7	-0.87	-0.36	0.51	-0.85	0.02	-0.24	0.63
NUDT18	-0.85	-0.16	0.69	-0.75	0.10	-0.53	0.32
CKS2	-0.85	-0.95	-0.10	0.19	1.04	0.55	1.40
MLH3	-0.84	-0.72	0.12	-0.62	0.23	-0.62	0.23
BAZ2B	-0.84	-0.99	-0.15	-0.99	-0.15	0.09	0.93
EGFR	-0.83	-0.98	-0.15	-0.72	0.10	-0.26	0.56
EGLN2	-0.83	0.42	1.25	1.20	2.03	0.46	1.29
PLK4	-0.82	-0.80	0.02	-0.85	-0.03	-0.97	-0.15
KDM3A	-0.82	-0.59	0.22	-0.01	0.81	-0.46	0.35
ZBTB16	-0.81	-1.63	-0.82	-1.78	-0.97	-0.87	-0.06
BRCA2	-0.81	-1.69	-0.89	-0.40	0.40	-1.96	-1.15
JMJD8	-0.80	-1.72	-0.92	-2.05	-1.25	-1.65	-0.84
DNMT3A	-0.74	0.06	0.80	-0.18	0.56	0.25	0.99
MRPL3	-0.73	-0.91	-0.18	-0.04	0.69	0.43	1.16
MCM7	-0.73	-0.19	0.54	0.39	1.12	-1.39	-0.66
LIG3	-0.72	-0.06	0.66	-0.24	0.48	-0.71	0.01
MBD3	-0.71	-1.39	-0.69	-0.46	0.25	0.04	0.74
CENPA	-0.70	-0.54	0.17	-0.43	0.27	0.35	1.05
DCLRE1B	-0.70	-0.67	0.03	-1.40	-0.69	-0.96	-0.26
OGT	-0.69	-0.16	0.53	-0.07	0.62	-0.61	0.08
IARS	-0.68	-0.58	0.10	-0.43	0.24	-0.67	0.01
TDG	-0.68	-0.86	-0.19	-0.49	0.18	0.12	0.79
C17orf101	-0.67	-0.11	0.56	-0.87	-0.20	-0.13	0.54

RAD51AP1	-0.67	-0.62	0.05	-0.60	0.07	-0.15	0.51
BRDT	-0.66	-1.24	-0.58	-1.33	-0.66	-1.19	-0.52
NUDT5	-0.66	0.58	1.24	-0.34	0.32	-0.08	0.58
CARM1	-0.65	-0.87	-0.21	-0.77	-0.12	-0.79	-0.14
TERF2IP	-0.64	-0.42	0.22	-0.75	-0.11	1.46	2.10
KDM2B	-0.62	-1.22	-0.59	-1.02	-0.40	-1.00	-0.37
BRD4	-0.62	-0.65	-0.02	-1.15	-0.52	-1.57	-0.95
JHDM1D	-0.62	-2.08	-1.46	-1.70	-1.08	-2.28	-1.66
TOX2	-0.61	-0.49	0.12	0.55	1.16	-0.04	0.57
HAT1	-0.61	-0.34	0.27	0.15	0.76	0.29	0.89
KDM4D	-0.60	-0.10	0.50	-0.17	0.43	0.38	0.98
GTF2H5	-0.60	-1.03	-0.43	-1.63	-1.03	-1.16	-0.56
REV3L	-0.58	-0.67	-0.09	-1.05	-0.47	-1.27	-0.69
WRN	-0.57	-1.64	-1.07	-1.21	-0.64	0.47	1.05
PLOD2	-0.56	-1.49	-0.93	-1.56	-1.00	0.77	1.33
POLL	-0.55	0.02	0.57	-0.92	-0.37	-0.78	-0.23
LEPREL1	-0.55	0.83	1.38	0.83	1.38	0.48	1.02
MEN1	-0.55	-0.38	0.17	-0.54	0.01	0.87	1.41
PHF8	-0.54	-0.69	-0.15	0.00	0.54	0.13	0.67
NUDT8	-0.53	-1.56	-1.03	-1.34	-0.81	-0.89	-0.36
BTAF1	-0.53	0.25	0.79	-0.32	0.21	0.63	1.16
P4HTM	-0.53	-0.89	-0.36	-0.88	-0.35	-1.13	-0.61
NUDT17	-0.53	-2.02	-1.49	-1.63	-1.11	-0.85	-0.32
DUT	-0.53	-0.12	0.40	-1.22	-0.70	0.12	0.64
RAD18	-0.52	-0.40	0.12	-0.15	0.38	-0.47	0.05
TMEM30A	-0.52	0.12	0.64	-0.77	-0.25	0.44	0.97
ASF1A	-0.52	-0.88	-0.36	-0.73	-0.21	-0.18	0.34
UBE2I	-0.51	-0.62	-0.12	-0.85	-0.34	-1.52	-1.01
DVL3	-0.48	-0.92	-0.44	-0.43	0.04	-0.68	-0.21
DCLRE1C	-0.46	-0.18	0.29	-1.19	-0.73	-0.23	0.23
RPN1	-0.46	0.12	0.58	0.27	0.73	-0.13	0.33
HSPD1	-0.45	-0.50	-0.04	-0.03	0.42	-1.00	-0.55
CITED1	-0.44	-0.96	-0.52	-0.52	-0.07	0.45	0.89
OBFC2B	-0.44	-1.58	-1.15	-1.19	-0.75	-1.04	-0.61
HELLS	-0.43	-0.95	-0.52	-0.97	-0.54	0.29	0.72
XPA	-0.43	-0.76	-0.34	-1.10	-0.67	-0.24	0.19
LIG4	-0.42	-1.71	-1.28	-0.73	-0.31	-0.85	-0.43
HMGB2	-0.42	-1.05	-0.63	-0.15	0.28	-0.74	-0.32
MDC1	-0.42	-0.92	-0.50	-0.46	-0.04	-1.25	-0.83
ECT2	-0.41	-0.13	0.28	-1.41	-1.00	0.17	0.58
HDAC5	-0.41	0.15	0.55	-0.51	-0.10	0.57	0.98
MCM9	-0.41	0.34	0.74	-0.89	-0.48	-0.21	0.20
C14orf169	-0.40	-1.74	-1.34	-1.90	-1.50	-2.05	-1.65
SIRT5	-0.39	-0.82	-0.43	-0.39	0.00	0.10	0.49

APEX2	-0.39	0.80	1.19	0.08	0.47	0.90	1.29
ALKBH2	-0.38	-0.85	-0.47	0.37	0.75	0.81	1.20
ASPH	-0.38	-1.09	-0.71	-1.19	-0.81	-1.19	-0.81
IRS1	-0.37	-1.11	-0.74	-0.10	0.28	-0.79	-0.42
MSH2	-0.37	0.45	0.82	0.40	0.78	1.32	1.69
SSBP1	-0.37	-1.09	-0.72	-1.21	-0.84	0.37	0.74
BRCA1	-0.36	-1.72	-1.36	-0.71	-0.35	-2.45	-2.09
HIST1H2BD	-0.36	-0.68	-0.32	0.00	0.36	-0.09	0.27
TMLHE	-0.35	0.59	0.94	0.67	1.02	0.81	1.16
CDK2	-0.35	-0.35	0.00	-0.59	-0.24	0.10	0.45
ERCC4	-0.34	1.05	1.39	0.99	1.33	1.39	1.73
NUDT2	-0.34	-0.88	-0.54	-0.36	-0.02	-0.99	-0.65
SMARCA5	-0.34	0.29	0.63	1.01	1.35	0.64	0.98
PPP2R1B	-0.33	0.20	0.53	0.08	0.40	-0.12	0.20
WDHD1	-0.32	0.00	0.32	-0.21	0.11	-0.06	0.26
CDK4	-0.32	-0.10	0.22	-0.57	-0.25	-0.23	0.09
HIST2H4A	-0.31	-0.11	0.20	0.38	0.69	-0.10	0.21
BAZ1B	-0.30	0.07	0.37	0.26	0.56	0.76	1.06
CHRAC1	-0.30	-0.80	-0.50	-0.88	-0.58	0.11	0.41
PHF2	-0.29	-0.40	-0.11	0.50	0.79	-0.53	-0.24
TTF2	-0.28	-0.37	-0.08	-1.05	-0.76	-1.68	-1.39
RARA	-0.28	-0.91	-0.63	-0.53	-0.25	0.61	0.89
POLE3	-0.28	-0.57	-0.29	-0.37	-0.08	-0.51	-0.23
POLM	-0.28	0.37	0.65	-0.63	-0.35	-0.72	-0.45
SRCAP	-0.27	-0.19	0.08	-0.13	0.14	0.26	0.53
FANCI	-0.27	0.24	0.51	-0.52	-0.26	-0.87	-0.60
TREX2	-0.25	0.45	0.70	0.13	0.38	0.78	1.03
RAD52	-0.25	-0.61	-0.36	-0.89	-0.64	-0.18	0.07
CHD7	-0.25	0.95	1.20	0.74	0.99	-0.12	0.13
NEIL1	-0.24	-0.16	0.09	-0.80	-0.55	0.27	0.51
GINS2	-0.24	-0.63	-0.39	-1.26	-1.01	-0.85	-0.61
POLK	-0.24	0.72	0.97	-0.43	-0.19	0.39	0.64
CCNA1	-0.24	0.52	0.76	0.95	1.19	0.68	0.92
DNMT1	-0.24	0.53	0.76	-1.40	-1.16	-0.35	-0.11
P4HA1	-0.24	0.35	0.59	-0.49	-0.26	0.85	1.09
DMC1	-0.24	-0.24	-0.01	0.54	0.77	0.63	0.86
ARID4B	-0.23	0.58	0.81	-0.19	0.04	-1.40	-1.17
TREX1	-0.23	-0.05	0.18	-0.04	0.19	0.34	0.57
HGD	-0.23	-0.41	-0.18	-0.99	-0.76	0.27	0.51
CFDP1	-0.22	0.84	1.06	-0.35	-0.13	0.42	0.64
MRE11A	-0.20	-0.05	0.15	-1.66	-1.46	-0.37	-0.17
ARID5B	-0.20	0.30	0.50	0.59	0.79	0.89	1.09
KDM6B	-0.19	0.50	0.69	-0.53	-0.34	0.15	0.34
FTO	-0.18	-0.28	-0.10	-0.44	-0.26	-1.37	-1.18

SMARCD1	-0.18	-0.41	-0.23	-0.82	-0.63	0.26	0.44
JMJD4	-0.18	0.11	0.29	-0.80	-0.62	-0.60	-0.42
SOD1	-0.17	0.46	0.63	-0.04	0.14	0.21	0.38
ORC5L	-0.16	-0.05	0.12	0.24	0.41	1.20	1.36
TDP1	-0.16	0.68	0.84	0.57	0.73	-0.87	-0.71
RFC4	-0.15	-0.49	-0.34	-0.42	-0.27	0.34	0.49
SMARCAL1	-0.15	0.42	0.57	-0.02	0.13	-0.71	-0.56
CLSPN	-0.14	-1.07	-0.93	-0.59	-0.45	-0.91	-0.76
CLK2	-0.14	-0.58	-0.45	-0.97	-0.83	-0.82	-0.68
XRCC6	-0.14	0.30	0.43	-0.45	-0.31	0.92	1.05
RTEL1	-0.13	-0.42	-0.30	-0.06	0.07	0.81	0.94
CHD5	-0.12	-0.66	-0.54	0.38	0.49	0.29	0.40
MGMT	-0.11	-0.46	-0.35	-0.59	-0.48	0.64	0.75
NUDT14	-0.11	-1.85	-1.74	-0.61	-0.50	-0.29	-0.18
CCNA2	-0.11	-0.06	0.04	-0.03	0.08	-1.00	-0.90
NEIL3	-0.11	0.42	0.52	-0.25	-0.15	1.42	1.53
XRCC3	-0.10	0.07	0.16	-0.33	-0.23	0.55	0.65
ALKBH7	-0.09	0.10	0.19	-0.88	-0.80	-0.02	0.06
HDAC9	-0.08	-0.72	-0.64	-1.26	-1.18	0.11	0.19
OGG1	-0.07	0.96	1.04	-1.76	-1.69	-0.98	-0.91
TAPBP	-0.06	-0.32	-0.26	-0.95	-0.89	-0.24	-0.18
ARID5A	-0.06	0.44	0.49	-0.31	-0.25	0.06	0.11
NUDT4	-0.05	0.15	0.20	-0.88	-0.83	-0.60	-0.55
GTF2H3	-0.05	-0.28	-0.23	-0.83	-0.77	0.66	0.71
NUDT15	-0.04	0.90	0.95	0.57	0.62	-0.36	-0.31
SSR1	-0.04	-1.23	-1.19	0.19	0.23	0.56	0.61
HDAC8	-0.03	0.61	0.64	1.41	1.44	0.94	0.97
MRC1	-0.02	0.13	0.14	0.49	0.51	0.71	0.73
POT1	-0.01	0.24	0.25	0.09	0.10	-0.60	-0.59
RECQL4	-0.01	-0.13	-0.12	-0.25	-0.24	-1.19	-1.18
HIST3H2A	-0.01	0.81	0.82	0.39	0.40	-0.63	-0.63
RPA4	0.01	0.55	0.55	0.19	0.19	1.56	1.55
FBXO18	0.01	0.07	0.06	0.70	0.69	0.24	0.23
CCND3	0.02	0.05	0.03	-0.26	-0.28	0.15	0.13
NEK2	0.02	1.17	1.15	0.07	0.05	2.08	2.06
JMJD6	0.03	-0.12	-0.15	0.20	0.17	1.10	1.07
HR	0.03	0.55	0.52	0.28	0.25	-0.20	-0.23
ORC4L	0.03	0.43	0.40	0.34	0.30	1.72	1.69
PHF1	0.04	-0.10	-0.14	0.27	0.23	0.28	0.24
HRAS	0.04	0.34	0.30	-1.13	-1.17	0.09	0.05
TOP1	0.05	-0.25	-0.29	-1.11	-1.16	-1.20	-1.24
EXO1	0.05	0.48	0.43	-0.07	-0.12	-0.33	-0.38
MANF	0.06	-0.04	-0.10	0.25	0.19	-1.58	-1.64
RAD51L1	0.06	-0.16	-0.22	0.17	0.11	0.51	0.45

MAP2K2	0.06	0.15	0.09	0.17	0.11	0.19	0.13
RAD54L	0.06	0.40	0.34	0.52	0.46	0.00	-0.06
PAICS	0.07	-0.63	-0.70	-0.21	-0.27	-0.73	-0.80
MMS19	0.07	-1.68	-1.75	-0.12	-0.19	-0.86	-0.93
HAAO	0.07	-0.13	-0.20	-0.36	-0.43	0.12	0.05
TRIM28	0.07	-0.25	-0.33	-0.49	-0.56	-0.56	-0.63
CCNB1	0.08	0.85	0.77	0.34	0.26	0.51	0.44
TIMELESS	0.08	0.37	0.29	0.93	0.85	0.16	0.08
CHD2	0.09	1.19	1.10	0.46	0.36	1.34	1.25
RFX7	0.09	0.08	-0.01	0.42	0.33	-0.11	-0.21
PHYHD1	0.09	-0.24	-0.33	-0.81	-0.91	-0.28	-0.37
DSCC1	0.10	0.96	0.86	-0.40	-0.49	0.10	0.00
KPNA2	0.11	-0.36	-0.47	0.68	0.57	0.51	0.41
CHD8	0.11	0.79	0.68	0.23	0.12	-0.14	-0.25
NUDT3	0.11	-0.16	-0.27	0.14	0.03	0.04	-0.08
DNMT3B	0.11	-0.50	-0.61	0.14	0.03	0.40	0.28
RNF40	0.12	0.06	-0.06	-0.30	-0.42	0.12	0.00
MINA	0.12	0.75	0.63	1.15	1.03	0.21	0.09
STK11	0.13	0.10	-0.03	-1.65	-1.77	-0.57	-0.70
XRCC1	0.13	0.70	0.57	0.38	0.25	-0.49	-0.62
PIF1	0.14	-0.34	-0.47	-0.01	-0.15	-0.22	-0.36
NUDT10	0.14	0.60	0.46	0.24	0.10	0.49	0.35
GTF2H1	0.14	-0.13	-0.28	0.82	0.68	0.61	0.47
FAP	0.14	0.20	0.05	-0.72	-0.86	0.09	-0.05
POLH	0.15	-0.35	-0.49	-0.60	-0.74	0.46	0.31
PER1	0.15	-1.16	-1.31	-0.91	-1.07	0.01	-0.14
HMGA1	0.16	0.51	0.35	0.77	0.62	0.27	0.12
EGLN1	0.16	0.81	0.65	0.69	0.53	-0.22	-0.38
P4HA3	0.16	-0.31	-0.47	0.01	-0.15	0.16	0.00
HDAC4	0.16	0.83	0.67	-0.31	-0.47	0.61	0.45
C2orf60	0.17	0.49	0.32	0.69	0.52	1.49	1.31
RAD51L3	0.18	0.26	0.08	0.36	0.19	0.59	0.42
SMARCC2	0.18	0.38	0.20	0.27	0.09	0.08	-0.09
SDHC	0.18	-0.27	-0.44	-1.16	-1.34	0.03	-0.14
CDKN3	0.18	-0.34	-0.52	0.77	0.59	-0.08	-0.26
LEPREL2	0.19	-0.18	-0.37	-0.05	-0.25	-0.53	-0.72
INO80C	0.19	-1.20	-1.39	-0.13	-0.32	0.23	0.04
CDK7	0.20	0.04	-0.16	-0.34	-0.54	-0.61	-0.81
OGFOD2	0.22	0.29	0.07	-0.09	-0.31	0.53	0.31
FANCE	0.22	0.65	0.42	1.08	0.86	0.81	0.59
RPA3	0.22	0.66	0.43	0.92	0.70	1.31	1.09
ATAD5	0.23	-0.40	-0.63	-0.26	-0.48	-0.37	-0.60
PTCH1	0.23	0.18	-0.05	0.62	0.38	0.44	0.21
BRD2	0.24	0.38	0.13	-0.04	-0.28	-0.80	-1.05

TP53BP1	0.25	1.08	0.84	0.83	0.58	0.03	-0.22
CUL4B	0.25	0.59	0.35	0.20	-0.04	0.31	0.06
BRD8	0.25	0.23	-0.03	0.08	-0.17	-0.39	-0.64
ORC6L	0.25	-0.12	-0.38	-0.87	-1.12	0.03	-0.22
TSTA3	0.25	-0.28	-0.53	-0.71	-0.96	0.54	0.28
PLOD1	0.25	-0.14	-0.39	-0.15	-0.40	-0.13	-0.39
SETD7	0.26	0.18	-0.08	0.13	-0.13	0.79	0.53
FANCL	0.26	0.50	0.24	0.96	0.70	0.28	0.02
ILF2	0.26	0.02	-0.24	-0.01	-0.27	-0.88	-1.14
ASPHD1	0.26	-1.18	-1.44	-0.23	-0.49	-1.05	-1.31
PALB2	0.28	-0.23	-0.51	0.46	0.18	-0.54	-0.82
CHD1	0.29	-0.18	-0.47	0.41	0.12	-0.22	-0.51
TP53	0.29	-0.12	-0.41	0.89	0.59	1.95	1.65
CHD9	0.29	0.19	-0.11	-0.11	-0.40	-0.79	-1.08
RFX5	0.29	0.45	0.15	0.23	-0.06	-0.23	-0.52
HDAC11	0.31	-0.86	-1.17	-0.82	-1.12	-0.44	-0.74
HDAC1	0.31	-0.93	-1.24	0.93	0.62	0.89	0.58
CCNE2	0.31	0.04	-0.27	-0.59	-0.90	0.33	0.02
SMARCC1	0.32	0.62	0.31	0.94	0.63	0.92	0.61
CANX	0.34	0.42	0.08	0.54	0.20	0.06	-0.28
ERCC5	0.36	0.30	-0.06	0.41	0.05	1.03	0.67
MTHFD2	0.36	0.44	0.08	-0.01	-0.37	0.39	0.03
MECP2	0.37	-0.45	-0.82	0.00	-0.37	-0.76	-1.13
NAPRT1	0.37	0.05	-0.32	0.87	0.50	1.18	0.82
CCNB2	0.37	0.26	-0.11	0.32	-0.06	2.27	1.90
NONO	0.37	0.92	0.55	0.74	0.37	0.80	0.43
DHX58	0.38	0.99	0.61	0.01	-0.36	0.44	0.06
H2AFX	0.38	0.03	-0.35	1.04	0.66	-0.28	-0.65
KDM4C	0.38	-0.08	-0.47	0.22	-0.16	-0.56	-0.95
ARID4A	0.39	0.58	0.19	0.74	0.36	0.49	0.10
PMS1	0.39	-0.58	-0.98	-0.04	-0.43	0.38	-0.01
RAD17	0.39	0.20	-0.19	-0.50	-0.90	0.16	-0.24
SND1	0.40	0.34	-0.05	-0.33	-0.73	-0.91	-1.30
ILK	0.40	-0.51	-0.91	0.41	0.01	-1.28	-1.68
SHPRH	0.41	0.36	-0.04	0.23	-0.18	0.19	-0.22
JMJD7	0.41	-0.87	-1.28	-0.76	-1.17	0.09	-0.32
UBE2S	0.41	0.01	-0.40	-0.15	-0.56	0.17	-0.24
ARID3B	0.43	0.45	0.02	0.47	0.04	0.56	0.13
RFX4	0.43	0.86	0.43	0.77	0.34	0.64	0.21
RFX2	0.43	0.49	0.06	0.15	-0.28	-0.27	-0.70
SMC5	0.44	0.80	0.36	0.73	0.29	0.63	0.18
MCM5	0.44	0.63	0.19	0.63	0.19	0.16	-0.28
ADI1	0.44	1.36	0.91	1.22	0.78	0.31	-0.13
POLE	0.45	0.68	0.23	0.46	0.01	0.13	-0.32

FOXO1	0.45	0.03	-0.43	0.30	-0.15	0.24	-0.21
SMUG1	0.45	0.45	0.00	0.52	0.06	0.83	0.38
MBD1	0.45	-0.52	-0.97	0.14	-0.31	-0.21	-0.67
FEN1	0.46	0.45	-0.02	0.20	-0.27	-0.39	-0.85
KAT2B	0.47	0.83	0.36	1.34	0.87	1.09	0.62
ATF4	0.48	0.04	-0.43	0.18	-0.30	0.40	-0.08
PMS2L3	0.48	0.81	0.33	0.52	0.04	0.45	-0.02
CHD3	0.48	0.21	-0.26	-0.04	-0.52	-0.25	-0.73
MBD2	0.48	0.88	0.40	0.59	0.11	1.03	0.55
RECQL	0.49	0.59	0.10	0.71	0.22	0.43	-0.05
SIRT1	0.49	0.12	-0.37	0.69	0.20	0.74	0.25
MLLT3	0.49	1.13	0.64	0.77	0.28	0.69	0.20
FANCB	0.49	0.63	0.14	0.58	0.09	0.52	0.02
FANCC	0.49	0.96	0.47	0.34	-0.15	1.15	0.66
MUS81	0.50	0.11	-0.39	0.17	-0.32	-0.55	-1.04
KDM5A	0.52	0.67	0.15	0.48	-0.03	0.30	-0.22
GTF2H4	0.52	0.53	0.01	0.49	-0.03	0.04	-0.48
INO80	0.52	-0.48	-1.00	0.33	-0.19	-0.05	-0.57
JMJD1C	0.52	0.61	0.09	0.77	0.25	0.78	0.26
RAD23B	0.52	0.45	-0.07	0.48	-0.04	0.26	-0.27
RIF1	0.53	-0.56	-1.09	0.53	0.01	-0.49	-1.02
PSME2	0.53	0.89	0.36	1.03	0.50	0.87	0.33
POLG	0.53	0.46	-0.08	0.47	-0.06	0.25	-0.28
KIAA0101	0.53	0.46	-0.07	0.32	-0.21	0.28	-0.26
MSH4	0.54	1.42	0.89	1.23	0.69	0.35	-0.18
HELQ	0.54	0.77	0.23	0.88	0.34	0.78	0.24
PLK3	0.54	1.34	0.79	0.59	0.05	0.46	-0.09
TOP3B	0.55	0.86	0.32	0.72	0.17	1.89	1.34
PARP2	0.55	0.36	-0.19	0.69	0.13	0.35	-0.20
TOPBP1	0.55	-0.51	-1.06	0.43	-0.13	-0.35	-0.91
RECQL5	0.55	1.10	0.54	0.52	-0.04	0.92	0.37
NRAS	0.56	0.42	-0.13	0.52	-0.04	1.26	0.70
UBE2N	0.56	1.09	0.54	-0.29	-0.84	-0.44	-0.99
MPG	0.56	-0.31	-0.87	0.33	-0.23	0.56	-0.01
BAZ2A	0.57	-0.55	-1.11	0.01	-0.56	-0.37	-0.94
HFM1	0.58	1.08	0.50	0.05	-0.54	1.15	0.56
PDS5B	0.59	0.89	0.30	1.21	0.62	0.90	0.30
C9orf102	0.60	-0.53	-1.13	-0.69	-1.29	-1.29	-1.89
AKT1	0.60	1.08	0.48	0.95	0.35	0.41	-0.19
MNAT1	0.60	-0.56	-1.16	0.24	-0.36	-0.23	-0.83
RAD23A	0.61	0.46	-0.15	1.08	0.47	0.61	0.00
TRDMT1	0.62	0.32	-0.30	1.36	0.73	0.30	-0.33
POLI	0.62	0.59	-0.04	0.91	0.28	0.64	0.01
PAFAH1B3	0.63	0.84	0.21	0.40	-0.23	0.70	0.07

NUDT12	0.64	-0.19	-0.82	0.27	-0.36	-0.48	-1.11
MAD2L2	0.64	0.69	0.05	0.62	-0.02	0.85	0.21
FANCA	0.64	0.31	-0.33	1.23	0.59	1.04	0.40
BRD3	0.64	1.48	0.83	1.45	0.81	0.37	-0.27
ARID3A	0.64	0.01	-0.64	0.53	-0.12	0.02	-0.63
MRPS12	0.64	0.69	0.04	0.90	0.25	0.51	-0.13
KDM6A	0.65	0.68	0.03	1.14	0.48	1.33	0.68
PHYH	0.66	0.13	-0.52	0.90	0.24	0.22	-0.44
PRDX4	0.67	1.29	0.62	0.16	-0.50	0.34	-0.33
AKT2	0.67	-0.68	-1.35	-0.03	-0.69	-0.23	-0.90
KDM5C	0.67	2.29	1.62	1.63	0.95	0.55	-0.12
POLD1	0.67	0.40	-0.27	0.62	-0.06	-0.18	-0.85
ERCC8	0.68	1.55	0.87	1.13	0.45	1.75	1.07
TET3	0.68	1.14	0.46	1.23	0.55	0.99	0.31
KIN	0.68	0.71	0.03	1.22	0.54	0.90	0.22
MAPK1	0.68	0.90	0.21	0.72	0.04	0.15	-0.54
SMARCA2	0.69	1.05	0.36	0.91	0.21	1.04	0.35
KDM5B	0.70	1.46	0.76	0.86	0.16	1.13	0.43
TOP2B	0.70	0.23	-0.47	-0.15	-0.85	-0.23	-0.93
SOX4	0.71	1.34	0.63	1.23	0.52	1.45	0.74
RAD51C	0.71	0.90	0.18	0.74	0.03	0.56	-0.15
FOXO3	0.71	0.90	0.19	1.00	0.28	1.13	0.41
TRAF4	0.72	0.33	-0.39	0.07	-0.64	-0.24	-0.96
KDM4A	0.72	0.29	-0.43	0.11	-0.61	0.11	-0.61
KDM5D	0.72	1.12	0.40	0.82	0.10	0.67	-0.04
IGF1R	0.72	0.95	0.23	-1.03	-1.75	0.49	-0.23
NHEJ1	0.72	0.93	0.21	0.41	-0.32	1.04	0.31
CCNB3	0.73	1.14	0.42	0.40	-0.33	0.91	0.19
ALKBH5	0.74	0.50	-0.24	0.62	-0.11	0.89	0.15
PDS5A	0.75	0.36	-0.38	1.03	0.29	0.75	0.00
PTEN	0.75	0.82	0.06	0.89	0.13	0.47	-0.28
TLK1	0.76	0.45	-0.31	0.67	-0.09	0.61	-0.15
UNG	0.76	0.83	0.07	1.65	0.89	0.20	-0.56
HDAC10	0.79	1.10	0.31	0.08	-0.71	0.42	-0.37
ORC2L	0.79	1.86	1.07	0.88	0.09	0.81	0.01
BAZ1A	0.80	0.53	-0.26	0.62	-0.18	0.15	-0.65
APTX	0.80	0.99	0.19	0.93	0.13	0.59	-0.21
SMARCD3	0.80	1.16	0.36	0.92	0.12	1.35	0.55
MCM4	0.81	0.67	-0.14	1.09	0.28	-0.03	-0.84
PMS2	0.81	1.14	0.32	1.01	0.19	0.66	-0.16
CCND1	0.81	0.20	-0.62	-0.14	-0.95	-0.53	-1.34
RAD50	0.81	0.53	-0.29	0.57	-0.24	0.41	-0.41
NUDT22	0.82	1.10	0.28	1.00	0.18	1.18	0.36
RBBP8	0.83	0.31	-0.52	0.89	0.07	0.37	-0.46

EME1	0.83	1.17	0.34	1.42	0.59	1.68	0.86
POLQ	0.83	0.86	0.04	0.97	0.14	0.36	-0.47
RFX3	0.83	0.80	-0.03	0.68	-0.15	0.41	-0.42
ABL1	0.84	-0.60	-1.44	-0.49	-1.33	-0.40	-1.24
BRIP1	0.84	0.74	-0.10	0.61	-0.23	0.07	-0.77
CBX3	0.84	1.07	0.23	1.03	0.19	1.27	0.43
TET1	0.85	0.51	-0.34	0.46	-0.39	0.51	-0.33
KIF2C	0.85	0.83	-0.02	1.04	0.19	0.63	-0.22
GEN1	0.86	0.29	-0.57	0.52	-0.34	0.01	-0.84
KDM3B	0.86	1.28	0.43	1.89	1.04	0.84	-0.01
CHD6	0.86	0.83	-0.03	1.09	0.22	0.97	0.11
ACD	0.87	-0.12	-0.99	0.18	-0.68	-0.17	-1.04
PRKDC	0.89	1.11	0.23	0.65	-0.24	0.52	-0.36
EZH2	0.89	0.56	-0.32	-0.45	-1.34	0.54	-0.34
ASF1B	0.89	0.64	-0.25	1.12	0.24	2.19	1.30
PPP2R5C	0.89	1.38	0.49	0.97	0.08	0.93	0.04
RBM4	0.89	0.80	-0.09	0.87	-0.01	0.71	-0.18
RAD1	0.89	0.83	-0.06	0.53	-0.36	-0.04	-0.93
FANCF	0.89	1.31	0.41	1.06	0.17	0.80	-0.10
INSR	0.90	1.10	0.20	1.42	0.52	1.01	0.11
CITED2	0.90	0.09	-0.81	1.14	0.24	0.60	-0.30
SSX1	0.90	-0.24	-1.14	0.13	-0.77	-0.19	-1.09
MLL	0.90	1.78	0.88	1.44	0.54	0.69	-0.21
RPL13	0.90	1.13	0.23	0.91	0.00	0.74	-0.16
NUDT1	0.91	1.11	0.21	0.43	-0.48	1.49	0.58
PTMA	0.92	0.11	-0.80	0.59	-0.32	-0.32	-1.23
ATR	0.92	1.44	0.52	0.83	-0.09	0.06	-0.86
IGF2	0.92	1.31	0.39	1.13	0.21	1.28	0.36
RDM1	0.93	0.91	-0.02	0.95	0.02	1.69	0.76
PLK2	0.93	0.88	-0.05	0.61	-0.32	0.14	-0.78
AHCY	0.93	-0.01	-0.94	0.24	-0.69	-0.03	-0.96
CHEK2	0.93	1.16	0.23	1.25	0.32	0.88	-0.05
EGLN3	0.94	1.03	0.09	0.92	-0.01	0.80	-0.13
OGFOD1	0.95	-0.07	-1.01	0.65	-0.30	1.06	0.11
HMGB1	0.95	0.55	-0.40	0.78	-0.17	0.40	-0.55
XRCC4	0.96	1.25	0.29	0.75	-0.21	1.26	0.30
HDAC2	0.96	0.39	-0.57	0.65	-0.31	1.00	0.04
RMI1	0.98	1.36	0.38	0.82	-0.17	0.93	-0.05
NBN	0.99	1.48	0.49	1.47	0.48	1.33	0.34
PPP3CA	0.99	0.91	-0.08	0.66	-0.33	0.51	-0.48
DDB2	0.99	1.61	0.62	1.64	0.65	1.49	0.50
TLK2	0.99	1.01	0.02	1.47	0.48	1.20	0.20
HLTF	1.00	1.41	0.41	0.77	-0.23	0.66	-0.34
MBD4	1.00	0.92	-0.08	1.21	0.21	-0.15	-1.15

H2AFZ	1.00	0.78	-0.22	1.15	0.14	0.53	-0.47
TOP2A	1.00	0.52	-0.48	-0.22	-1.22	-0.68	-1.68
ALKBH3	1.01	0.24	-0.77	1.57	0.56	1.24	0.23
SMARCA4	1.01	1.03	0.02	1.03	0.02	0.34	-0.67
UBE2V2	1.02	0.44	-0.58	0.29	-0.73	0.25	-0.76
PPP1R14C	1.02	0.76	-0.26	0.90	-0.12	0.82	-0.20
PPARG	1.02	0.03	-1.00	0.43	-0.59	1.54	0.52
TINF2	1.02	-0.27	-1.30	0.44	-0.59	0.49	-0.54
XRCC2	1.03	1.11	0.09	1.06	0.04	0.67	-0.36
RAD54L2	1.04	1.21	0.17	1.27	0.23	0.53	-0.52
KDELR2	1.05	0.95	-0.10	0.58	-0.47	0.86	-0.19
POLB	1.06	1.00	-0.05	1.00	-0.05	0.14	-0.92
PNKP	1.06	1.58	0.52	1.29	0.23	0.86	-0.20
PARP1	1.06	0.88	-0.18	1.15	0.09	0.63	-0.43
CITED4	1.07	1.30	0.23	1.59	0.52	1.02	-0.06
FANCD2	1.07	0.70	-0.38	1.71	0.63	-0.32	-1.39
BRD7	1.08	-1.35	-2.43	0.29	-0.79	-0.20	-1.28
TGIF1	1.09	1.05	-0.04	1.59	0.50	-0.03	-1.12
XPC	1.09	0.96	-0.13	1.21	0.12	1.04	-0.05
NUDT9	1.10	0.91	-0.19	1.33	0.23	0.82	-0.28
ACLY	1.11	0.96	-0.15	1.16	0.05	0.87	-0.24
SMARCB1	1.12	0.88	-0.23	0.74	-0.37	0.17	-0.95
NUDT11	1.12	-0.22	-1.34	0.44	-0.68	-0.58	-1.70
SUPV3L1	1.12	0.28	-0.84	-0.15	-1.27	-0.38	-1.51
HSPBAP1	1.13	1.05	-0.08	1.20	0.07	0.87	-0.26
MAD1L1	1.13	0.94	-0.19	1.39	0.26	0.84	-0.29
TAL1	1.13	0.77	-0.36	1.29	0.16	0.75	-0.38
SUZ12	1.14	0.48	-0.66	-0.06	-1.20	1.58	0.44
UBE2B	1.15	-1.05	-2.20	-0.52	-1.67	-1.82	-2.97
DCLRE1A	1.15	0.90	-0.25	1.00	-0.15	0.46	-0.69
RFX1	1.16	1.05	-0.11	1.50	0.35	1.25	0.09
SUV39H1	1.16	0.91	-0.25	-0.03	-1.19	-0.15	-1.31
CETN2	1.16	1.27	0.10	0.40	-0.76	0.58	-0.58
MCM6	1.17	1.38	0.21	0.66	-0.50	-0.17	-1.34
BRD1	1.18	1.60	0.42	0.87	-0.31	0.02	-1.16
PIR	1.19	1.54	0.35	0.91	-0.28	0.74	-0.45
SUV39H2	1.19	1.13	-0.07	0.60	-0.60	1.13	-0.06
CUL4A	1.19	0.93	-0.26	1.02	-0.17	0.05	-1.14
CDYL	1.20	1.54	0.35	1.21	0.01	1.24	0.04
LDHA	1.20	1.10	-0.10	1.02	-0.18	0.21	-0.99
BRD9	1.21	0.90	-0.31	1.06	-0.15	0.49	-0.72
TSC1	1.21	-0.19	-1.40	-0.47	-1.69	-1.07	-2.29
REV1	1.23	0.20	-1.03	1.31	0.08	0.46	-0.77
JARID2	1.23	0.15	-1.08	0.97	-0.26	1.85	0.62

POLN	1.23	0.81	-0.43	-0.26	-1.50	-0.96	-2.19
ALKBH6	1.24	0.45	-0.79	1.28	0.04	1.27	0.04
RRM2B	1.24	-0.40	-1.64	0.58	-0.66	-0.63	-1.87
SMARCAD1	1.24	2.30	1.06	1.18	-0.06	1.61	0.37
UTY	1.24	1.05	-0.19	1.20	-0.04	1.15	-0.09
MYL4	1.25	1.94	0.70	1.00	-0.25	0.67	-0.57
RFX6	1.26	1.22	-0.03	1.41	0.15	0.27	-0.98
ARID1B	1.26	1.97	0.72	1.78	0.52	1.77	0.51
TERF2	1.26	1.12	-0.14	0.38	-0.88	0.32	-0.94
SMARCE1	1.26	1.34	0.07	1.38	0.12	0.89	-0.37
TTRAP	1.29	0.17	-1.12	1.42	0.12	1.17	-0.12
HUS1	1.30	0.34	-0.96	1.43	0.13	-0.15	-1.45
ZDHHC17	1.32	1.47	0.15	1.66	0.34	2.12	0.80
CCND2	1.34	1.19	-0.15	1.21	-0.13	0.23	-1.11
MSH6	1.35	1.65	0.31	1.66	0.32	2.27	0.93
BBOX1	1.36	0.89	-0.47	1.02	-0.34	0.05	-1.31
POLE4	1.37	1.69	0.31	1.77	0.39	0.97	-0.40
POLS	1.38	0.54	-0.84	1.32	-0.06	0.85	-0.53
HNRNPA2B1	1.38	0.05	-1.33	1.15	-0.23	0.10	-1.28
ADO	1.39	1.66	0.27	0.96	-0.43	0.69	-0.69
DOT1L	1.39	1.16	-0.23	1.09	-0.30	0.73	-0.67
BLM	1.40	1.73	0.33	1.30	-0.10	0.77	-0.62
ALKBH4	1.42	0.65	-0.77	0.69	-0.73	0.56	-0.86
NME1	1.44	1.21	-0.23	0.68	-0.75	0.66	-0.78
CDK6	1.45	0.55	-0.90	0.91	-0.54	-0.14	-1.59
HMGXB4	1.49	0.68	-0.81	1.35	-0.14	0.85	-0.64
HDAC6	1.51	1.20	-0.30	1.61	0.10	1.10	-0.40
CSNK2A1	1.51	1.57	0.06	0.99	-0.53	0.90	-0.61
CCNE1	1.53	1.09	-0.44	1.44	-0.10	1.21	-0.33
MLLT1	1.53	1.89	0.35	1.85	0.31	0.04	-1.50
EHMT1	1.56	0.80	-0.77	0.99	-0.58	0.92	-0.65
IFNGR2	1.58	0.29	-1.29	1.30	-0.28	0.87	-0.71
CDO1	1.64	1.16	-0.48	1.36	-0.27	0.79	-0.84
LIG1	1.65	0.84	-0.81	0.97	-0.68	0.21	-1.44
JMJD5	1.66	1.27	-0.39	1.48	-0.18	1.44	-0.21
TET2	1.69	-0.20	-1.89	1.24	-0.46	0.38	-1.31
HMGN1	1.83	0.84	-0.99	1.54	-0.30	-0.62	-2.45
ATM	1.94	1.15	-0.79	1.42	-0.52	0.63	-1.31
HSP90B1	1.99	1.27	-0.72	0.77	-1.22	0.31	-1.68
HDAC7	2.03	1.23	-0.81	1.67	-0.36	2.09	0.05
TP73	2.05	1.02	-1.03	0.51	-1.54	-0.44	-2.50
RAD54B	2.06	1.61	-0.44	1.05	-1.01	1.38	-0.67
HP1BP3	2.36	2.65	0.29	1.92	-0.44	1.35	-1.01